TRANSPORTATION RESEARCH RECORD 962

Bridge Maintenance Management, Corrosion Control, Heating, and Deicing Chemicals

TRB
TRANSPORTATION RESEARCH BOARD
NATIONAL RESEARCH COUNCIL
WASHINGTON, D.C. 1984

Transportation Research Record 962
Price $11.80
Editor: Scott C. Herman
Compositor: Joan G. Zubal
Layout: Betty L. Hawkins

mode
1 highway transportation

subject areas
25 structures design and performance
32 cement and concrete
40 maintenance

Transportation Research Board publications are available by ordering directly from TRB. They may also be obtained on a regular basis through organizational or individual affiliation with TRB; affiliates or library subscribers are eligible for substantial discounts. For further information, write to the Transportation Research Board, National Research Council, 2101 Constitution Avenue, N.W., Washington, D.C. 20418

Printed in the United States of America

Library of Congress Cataloging in Publication Data
National Research Council. Transportation Research Board.
Bridge maintenance management, corrosion control, heating, and deicing chemicals.

(Transportation research record; 962)
1. Bridges–Maintenance and repair–Addresses, essays, lectures.
I. National Research Council (U.S.). Transportation Research Board. II. Series.

TE7.H5	no. 962	380.5 s	84-25469
[TG315]		[624'.28]	
ISBN 0-309-03718-2		ISSN 0361-1981	

Sponsorship of Transportation Research Record 962

GROUP 2–DESIGN AND CONSTRUCTION OF TRANSPORTATION FACILITIES
Robert C. Deen, University of Kentucky, chairman

Concrete Section
Robert E. Philleo, Consulting Engineer, chairman

Committee on Performance of Concrete
Charles F. Scholer, Purdue University, chairman
Philip D. Cady, Theodore R. Cantor, W. P. Chamberlin, Kenneth C. Clear, James R. Clifton, Glenn William De Puy, Ludmila Dolar-Mantuani, Bernard Erlin, John W. Figg, Richard H. Howe, Stella L. Marusin, Katharine Mather, Richard C. Meininger, Richard C. Mielenz, Roger P. Northwood, V. Ramakrishnan, Richard Karl Smutzer, David Stark, Hollis N. Walker, Richard D. Walker

GROUP 3–OPERATION AND MAINTENANCE OF TRANSPORTATION FACILITIES
D. E. Orne, Michigan Department of Transportation, chairman

Committee on Structures Maintenance
Jimmy D. Lee, North Carolina Department of Transportation, chairman
Robert N. Kamp, Byrd, Tallamy, MacDonald & Lewis, secretary
John J. Ahlskog, Robert M. Barnoff, Roland H. Berger, Alfred G. Bishara, William G. Byers, A. J. Dunn, Ian J. Dussek, Nicholas M. Engelman, Ray W. James, Eldon D. Klein, Robert H. Krier, David G. Manning, Wallace T. McKeel, Jr., Richard J. Posthauer, Jack W. Roberts, George P. Romack, Steven J. Shecter, Arunprakash M. Shirole, Charles V. Slavis, Lloyd M. Smith, Marilyn H. Tobey, Robert G. Tracy, Alden L. West

Committee on Winter Maintenance
L. David Minsk, U.S. Army CRREL, chairman
Robert R. Blackburn, Francis H. Carr, Jr., John C. Cook, Robert A. Crawford, Henri De Lannoy, William E. Dickinson, Joseph J. Difabio, Robert C. Donnaruma, Charles E. Dougan, Karl H. Dunn, Henry W. Farrell, Gerald P. Fitzgerald, Brice E. Horwell, John G. Irving, Edward J. Kehl, James F. Kelley, Henry W. Kirchner, Byron N. Lord, Warren M. Reeves, T. Ray Ringer, Ronald D. Tabler, Ross G. Wilcox

Committee on Corrosion
Carl F. Crumpton, Kansas Department of Transportation, chairman
Hans H. Arup, Kenneth J. Boedecker, Jr., E. J. Breckwoldt, Kenneth C. Clear, Seymour K. Coburn, Robert H. Heidersbach, Jr., Richard J. Kessler, Walter Kilareski, Carl E. Locke, Jr., David G. Manning, A. P. Moser, Arnold M. Rosenberg, Gary T. Satterfield, Herbert J. Schmidt, Jr., Robert G. Tracy, Frank O. Wood

Adrian G. Clary and William G. Gunderman, Transportation Research Board staff

Sponsorship is indicated by a footnote at the end of each report. The organizational units, officers, and members are as of December 31, 1983.

Notice: The Transportation Research Board does not endorse products or manufacturers. Trade and manufacturers' names appear in this Record because they are considered essential to its object.

Contents

Addresses of Authors

Aggour, M. S., Department of Civil Engineering, University of Maryland, College Park, Md. 20742
Apostolos, John A., Office of Transportation Laboratories, California Department of Transportation, 5900 Folsom Boulevard, P.O. Box 19128, Sacramento, Calif. 95819
Bhuyan, Sam, CWA Walker, Inc., 2121 Hudson Avenue, Kalamazoo, Mich. 49008
Bukovatz, John E., Bureau of Materials and Research, Kansas Department of Transportation, 2300 Van Buren Street, Topeka, Kans. 66611
Cady, Philip D., Department of Civil Engineering, Pennsylvania State University, 212 Sackett Building, University Park, Pa. 16802
Clear, K. C., Kenneth C. Clear, Inc., 9 Rheims Court, Sterling, Va. 22170
Crumpton, Carl F., Bureau of Materials and Research, Kansas Department of Transportation, 2300 Van Buren Street, Topeka, Kans. 66611
Eck, Ronald W., Department of Civil Engineering, West Virginia University, Morgantown, W.Va. 26506
Frascoia, Ronald I., Materials and Research Division, Vermont Agency of Transportation, 133 State Street, State Administration Building, Montpelier, Vt. 05602
Hsu, Martha T., Materials and Research Division, Maine Department of Transportation, Box 1208, Bangor, Maine 04402
Johnston, David W., Center for Transportation Engineering Studies, Department of Civil Engineering, North Carolina State University, P.O. Box 7908, Raleigh, N.C. 27695
Lee, Ron C., Department of Mechanical Engineering, University of Wyoming, University Station, Box 3295, Laramie, Wyo. 82071
Manning, D. G., Ontario Ministry of Transportation and Communications, 1201 Wilson Avenue, Downsview, Ontario M3M 1J8, Canada
Nydahl, John E., Department of Mechanical Engineering, University of Wyoming, University Station, Box 3295, Laramie, Wyo. 82071
Pell, Kynric M., Department of Mechanical Engineering, University of Wyoming, University Station, Box 3295, Laramie, Wyo. 82071
Ragab, A. M., Bechtel Power Corporation, 157040 Shady Grove Road, Gaithersburg, Md. 29659
Sack, William A., Department of Civil Engineering, West Virginia University, Morgantown, W.Va. 26506
Sackos, John T., Department of Mechanical Engineering, University of Wyoming, University Station, Box 3295, Laramie, Wyo. 82071
Schell, H. C., Ontario Ministry of Transportation and Communications, 1201 Wilson Avenue, Downsview, Ontario M3M 1J8, Canada
Shirolé, Arunprakash M., City of Minneapolis, 203 City Hall, Minneapolis, Minn. 55415
Tracy, Robert G., Tracy Materials Consultants, 5380 Holiday Terrace, Kalamazoo, Mich. 49009; formerly with CWA Walker, Inc.
Weyers, Richard E., Department of Civil Engineering, Lafayette College, 422 Alumni Hall of Engineering, Easton, Pa. 18402
White, E. J., Jr., Bureau of Bridge Design, Maryland State Highway Administration, 707 North Charles Street, Baltimore, Md. 21203
Zia, Paul, Center for Transportation Engineering Studies, Department of Civil Engineering, North Carolina State University, P.O. Box 7908, Raleigh, N.C. 27695

Level-of-Service System for Bridge Evaluation

DAVID W. JOHNSTON and PAUL ZIA

ABSTRACT

Data collected during federally mandated bridge inspections are a valuable resource. Evaluations based on these data influence levels of federal funding and determine types of funding uses. Nevertheless, the states and other owners have significant flexibility in selecting bridges for replacement and rehabilitation. Methods are needed for analyzing the data to facilitate bridge management functions and long-range planning related to replacement, rehabilitation, and maintenance. In this paper research efforts to develop methods to enhance use of North Carolina inspection data by evaluating bridges based on deficiency, as related to acceptable and desirable levels of service, are described. Methods of assigning priorities are also introduced. The long-range goal of the research is to develop a maintenance, rehabilitation, and replacement priority system with the capability of estimating future funding needs.

The establishment of a federally mandated system for bridge inspection, evaluation, and reporting (1) has provided the states with a valuable data resource. Regularly updated individual inspection reports, and especially the computerized Structure Inventory and Appraisal data file, have been essential for rapid evaluation and identification of bridges.

Three summary evaluations are made for each bridge under the federal system. The sufficiency rating, which ranges from 0 to 100 points, is calculated; the bridge is classified as structurally deficient or not, and as functionally obsolete or not. Depending on the sufficiency rating, a bridge may be eligible for federal funding for replacement or rehabilitation. However, within broad ranges of sufficiency rating (0 to 50 for replacement or rehabilitation and 50 to 80 for rehabilitation), the states may assign priorities for the order of funding.

Thus the states are faced with two related problems. First, although the data base is available and the data can be tabulated and summarized in many ways by using the National Bridge Inventory Report Generator program (2), there is a need for in-depth analysis of the data over a period of time to provide long-range bridge management information. Any one inspection cycle provides a snapshot, but not a history or a trend. Second, methods are needed for assigning priorities of bridges for replacement, rehabilitation, and maintenance.

There are both short-term and long-term possibilities. In the long term, trends accumulated from analysis of the data base over several cycles of inspection will assist in optimizing selection of bridges for maintenance, rehabilitation, and replacement. In the short term, less refinement is possible; nevertheless, priorities must be based on the degree to which a bridge is deficient in meeting public needs.

With the support of the North Carolina Department of Transportation (NCDOT), a study has been undertaken that had the following objectives:

1. Develop methods to enhance inspection data use in the management of bridge maintenance, rehabilitation, and replacement;
2. Establish a level-of-service system that can serve as a basis for evaluating the adequacy of North Carolina bridges in serving public needs;
3. Assign priorities to bridges in order of need based on level-of-service deficiency;
4. Evaluate the present cost of replacement or rehabilitation to achieve the needed levels of service;
5. Determine the impact of maintenance and deferred maintenance by task; and
6. Develop a least-cost maintenance, rehabilitation, and replacement priority system with the capability of estimating future funding needs.

The data in this paper represent a progress report on the results of efforts to achieve these objectives. Tasks incorporating the first three objectives have been completed. The approaches being used are presented at this time for the benefit of other bridge owners faced with similar problems.

NATURE OF NORTH CAROLINA BRIDGE PROBLEMS

In North Carolina there are approximately 17,300 bridges. More than 16,800 of these (97 percent) are state-maintained bridges compared with 46 percent state-maintained bridges nationwide. Thus, unlike most state-maintained inventories, which are dominated by Interstate, arterial, and collector system bridges, the NCDOT-maintained inventory is 56 percent local system bridges serving low traffic volumes. Almost 40 percent of the total inventory is located on routes with an average daily traffic (ADT) volume of less than 250 vehicles.

Approximately 65 percent of the bridges in North Carolina are classified as structurally deficient or functionally obsolete, as detailed in the following table:

Classification	No. of Bridges	Percent
Structurally deficient	5,664	34
Functionally obsolete	5,333	31
Neither	5,792	35
Total	16,789	

This relatively high percentage often evokes a public assumption of significant deterioration, but analysis of the inspection data reveals a clearer picture. Figure 1 shows the frequency of condition ratings for the deck, superstructure, and substructure. A rating of 4 (which indicates marginal condition with potential for minor rehabilitation) or less on any of these items would cause a bridge to be classified as structurally deficient. However, note that virtually all the bridges are in good to fair condition, which indicates that they have been generally well maintained.

Thus the high percentage of structurally deficient bridges is not due to condition as related to maintenance versus deterioration. As the data in the

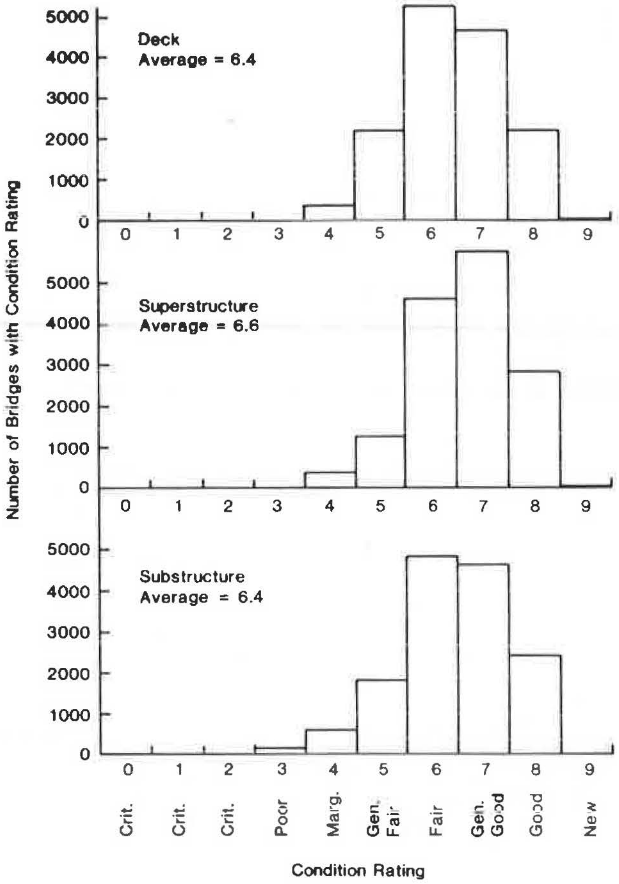

FIGURE 1 Frequency of deck, superstructure, and substructure condition ratings.

following table indicate, the principal cause for classification as structurally deficient is the rating for structural condition (note that the total does not add because it includes some multiple items):

Item	No. of Bridges
Structural condition $\leq$ 2	5,044
Deck condition $\leq$ 4	569
Superstructure condition $\leq$ 4	458
Substructure condition $\leq$ 4	838
Waterway appraisal $\leq$ 2	14
Total	5,660

The principal causes for classification as functionally obsolete, according to the data in the following table, are structural condition and deck geometry (note that the total does not add because it includes some multiple items):

Item	No. of Bridges
Structural condition $\leq$ 3	3,151
Deck geometry $\leq$ 3	3,009
Approach alignment $\leq$ 3	1,188
Underclearances $\leq$ 3	1,163
Waterway adequacy $\leq$ 3	45
Total	5,333

Some bridges are classified as deficient or obsolete for more than a single cause.

Structural condition is not a qualitative evaluation of bridge condition; rather, it is a quantitative evaluation of bridge load capacity. For many years North Carolina was a state with limited resources and yet a large geographical area. In order to provide access to rural areas, limited funds were stretched by constructing relatively narrow and low load-capacity (HS-10 and HS-15) bridges on low ADT roads. Approximately 3,600 of these bridges have timber superstructures, and many others have timber piles, which further reduce the condition rating. Thus, although many bridges have been maintained in satisfactory condition, the structural condition rating is often 1, 2, or 3, thereby causing the bridge to be deficient or obsolete.

The distribution of posted bridges versus ADT volume is given in Table 1. Although any posting due to load capacity is undesirable, it must also be recognized that low load capacities on high ADT routes (the lower left triangle of the matrix) is least acceptable. Because determination of sufficiency rating places a heavy weighting on adjusted inventory tonnage, structural condition, and width, the distribution (Table 2) of sufficiency ratings versus ADT volume is similar.

TABLE 1 ADT Versus Single-Vehicle Posting

	No. of Bridges with Single-Vehicle Posting[a] Between					
ADT	3-8	9-15	16-24	25-33	NP	Total
<250	327	2,002	2,354	668	1,220	6,571
250-499	96	647	626	388	711	2,468
500-999	55	380	443	343	802	2,023
1,000-1,999	24	160	223	222	869	1,498
2,000-3,999	6	47	82	128	1,035	1,298
>3,999	4	26	56	136	2,709	2,931
Total	512	3,262	3,784	1,885	7,346	16,789

Note: NP = not posted.
[a]Posting in tons based on operating rating.

TABLE 2 ADT Versus Sufficiency Rating

	No. of Bridges with Sufficiency Rating Between				
ADT	0-25	25-50	50-80	80-100	Total
<250	399	2,832	2,532	808	6,571
250-499	242	1,077	772	377	2,468
500-999	183	736	676	428	2,023
1,000-1,999	123	383	546	446	1,498
2,000-3,999	57	176	462	603	1,298
>3,999	65	252	1,166	1,448	2,931
Total	1,069	5,456	6,154	4,110	16,789

Under federal criteria, a large number of North Carolina bridges are eligible for replacement or rehabilitation funding. However, assigning priorities strictly on the basis of sufficiency rating does not place adequate emphasis on appropriate service in proportion to public need. The sufficiency rating places little emphasis on volume of traffic, detour length, and level of service needed on various functional systems such as arterials, collectors, and local systems. An additional system of evaluation that more directly considers these factors is needed, especially where the maintenance condition of the bridges is fair to good and the estimated bridge remaining life is relatively long. To meet this need, a level-of-service system has been developed for evaluating and assigning priorities of bridges on the basis of level-of-service deficiency.

BRIDGE LEVEL OF SERVICE

Although it might be ideal to have all existing bridges meet North Carolina Bridge Policy (3) requirements for new bridges, it is recognized that this is not financially possible. Thus a method of determining an appropriate level of service for each bridge is established herein.

There are many characteristics that can contribute to making a bridge safe, functional, and beneficial to the public. However, three easy-to-quantify characteristics most directly contribute to these needs:

1. Load capacity,
2. Clear bridge deck width, and
3. Vertical roadway underclearance and overclearance.

The level-of-service goal for each of these characteristics will vary, depending on the volume of traffic and the functional classification of the roadway. Furthermore, the goals can be set at an acceptable low level, at a desirable higher level, or at an intermediate level between these two.

[Level-of-service goals--acceptable and desirable--are defined in Tables 3, 4, and 6 for capacity, width, and vertical clearance, respectively (note that these tables are presented in a later subsection).]

Functional Classifications

North Carolina highway segments between intersections are classified according to the functional service provided by the route in meeting statewide transportation needs. Bridges are classified in the same functional system as the route carried by the bridge. The principal functional classifications are as follows.

1. Interstate and arterial systems provide moderate- to high-volume highways for travel between major points. These highways are primarily for through traffic, usually on a continuous route, and are generally the top 10 percent of the total highway system based on relative importance for statewide travel.

2. The collector system primarily provides intracounty service with shorter travel distances and generally more moderate speeds. These routes provide service to county seats and towns not on the arterial system. Routes that carry traffic from local roads to arterials are collectors.

3. The local system provides access to farms, residences, businesses, or other abutting properties. Traffic volume is low and local in nature.

The systems are further subdivided in some cases. For example, collectors are divided into major collectors and minor collectors.

Acceptable Goals

The acceptable load-capacity goals seek to provide a safe and functional level of strength to serve most vehicles expected on the route being served. The minimum acceptable level is that which would accommodate essential vehicles such as passenger cars, school buses, fire trucks, residential garbage trucks, heating oil home delivery trucks, and two-axle electrical utility line trucks on all routes.

All normal passenger cars can be accommodated within the 3-ton capacity required for an open bridge. A survey was conducted by the NCDOT Bridge Maintenance Unit to determine the weights of essential service vehicles. Inquiries to the State Department of Public Instruction indicate that the weight of loaded school buses ranges from 6 tons to a maximum of 12 tons. Fire trucks for the city of Raleigh weigh approximately 16 tons. Special permits are obtained for those in the 18- to 20-ton range. Wake County rural fire trucks are limited to 15 tons, and most do not exceed 11 or 12 tons. Residential garbage trucks in Raleigh and Wake counties are all two-axle vehicles limited to a legal weight of 15.75 tons. Commercial garbage trucks are often 3-axle or tandem vehicles with 22.5-, 25-, or 33.6-ton legal limits. Carolina Power & Light Co. line trucks generally weigh 13 tons, although there are a limited number of 18-ton tandem-axle trucks. Medical emergency vehicles weigh up to 4 or 5 tons.

Furthermore, operation of a vehicle weighing more than 15 tons requires a chauffeur's license, which would imply better operator understanding of vehicle weight and posting requirements. Based on these factors, a minimum acceptable load-capacity goal of 16 tons was established (Table 3). This level will serve all two-axle trucks and two- and three-axle buses. Higher capacities are needed for major collectors, arterials, and Interstates to serve commerce and industry with a minimum of detour. The major collector goal of 25 tons was selected to serve the needs of all 3-axle trucks, which would include many concrete and logging trucks.

TABLE 3 Bridge Capacity Goals

Road Over Functional Classification	Single-Vehicle Capacity (tons) Acceptable	Desirable
Interstate and arterial	NP	NP
Major collector	25	NP
Minor collector	16	NP
Local	16	NP

Note: NP = not posted (capacity = 33.6 tons for single vehicles).

Clear bridge deck width goals are intended to provide reasonable safety. Narrow bridges contribute to both single- and multiple-vehicle collisions as well as accidents involving pedestrians. Width needs depend on the volume of traffic (ADT) and the roadway functional classification (as an indication of traffic content and speed). The acceptable goals given in Table 4 generally correspond to bridge policy for existing bridges to remain in place when

TABLE 4 Clear Bridge Deck Width Goals for Two-Lane Routes

Road Over Functional Classification	Current ADT	Clear Width (ft) Acceptable	Desirable
Interstate and arterial	≤800	22	32
	801-2,000	24	36
	2,001-4,000	26	40
	>4,000	28	40
Major and minor collectors	≤800	20	24
	801-2,000	22	28
	2,001-4,000	24	30
	>4,000	26	30
Local	≤800	20	24
	801-2,000	22	28
	2,001-4,000	24	30
	>4,000	26	30

Note: For bridges with more than two lanes see Table 5. Width = number of lanes (lane width) + 2 (shoulder width).

the approach roadway is reconstructed. However, a width of 26 ft rather than 28 ft was accepted for local and collector systems with ADTs greater than 4,000 vehicles. Also, the current-year ADT is used for the evaluation of acceptability rather than a design-year ADT. The data in Table 4 present width goals for two-lane bridges. For bridges with other than two lanes, the width goals are calculated from the lane and shoulder dimensions given in Table 5.

Vertical roadway underclearance goals affect only those bridges that span over another roadway. Vertical roadway overclearance goals affect only those bridges such as trusses, which have overhead obstructions. The benefits of adequate vertical clearance are related to reducing detours of vehicles serving commerce and industry and detours of certain farm equipment as well as reducing collision damage. The acceptable goals given in Table 6 correspond to the minimum vertical clearance not requiring posting. At 14.0 ft, this is slightly higher than the legal maximum height of 13.5 ft in order to allow for vehicle bounce and resurfacing between inspections.

TABLE 5 Clear Bridge Deck Width Goals (lane and shoulder)

Road Over Functional Classification	Current ADT	Deck Width (ft) Acceptable Lane	Acceptable Shoulder	Desirable Lane	Desirable Shoulder
Interstate and arterial	≤800	10	1	12	4
	801-2,000	10	2	12	6
	2,001-4,000	11	2	12	8
	>4,000	11	3	12	8
Major and minor collectors	≤800	9	1	10	2
	801-2,000	9	2	11	3
	2,001-4,000	10	2	12	3
	>4,000	10	3	12	3
Local	≤800	9	1	10	2
	801-2,000	9	2	11	3
	2,001-4,000	10	2	12	3
	>4,000	10	3	12	3

TABLE 6 Bridge Vertical Underclearance Goals

Road Under Functional Classification	Underclearance (ft) Acceptable	Desirable
Interstate and arterial	14.0	16.5
Major and minor collectors	14.0	15.0
Local	14.0	15.0

Note: Bridge vertical overclearance goals for the road over functional classification shall be the same as the above values.

Desirable Goals

The desirable goals for load capacity, deck width, and vertical clearance generally correspond to North Carolina Bridge Policy for new bridge construction. Current ADT is used in the evaluation rather than design-year ADT. However, the bridge width goals have been adjusted, assuming that design-year ADT would be approximately double the current ADT.

ASSIGNING PRIORITIES BASED ON NEED

The method of assigning priorities involves calculation of deficiency points. The four major areas of deficiency to be evaluated are as follows:

Deficiency	Weighting
Single-vehicle load capacity	WC = 70
Clear bridge deck width	WW = 12
Vertical roadway underclearance or overclearance	WV = 12
Estimated remaining life	WL = 6

Within these areas, additional consideration is given to volume of traffic and length of detour.

The deficiency magnitude expressed in deficiency points (DP) (the larger the DP, the more deficient the bridge) is given by

$$DP = CP + WP + VP + LP \qquad (1)$$

where CP, WP, VP, and LP are priority points accumulated from evaluation of capacity, width, vertical clearance, and remaining life, respectively. The method for determining each of these point parameters follows.

Single-Vehicle Load Capacity Priority

Calculation of capacity priority (CP) considers the following parameters:

CG = capacity goal (tons; see Table 3),
SV = single vehicle posting (tons),
ADTO = average daily traffic of over route,
DL = detour length (miles), and
WC = capacity weighting.

User costs related to the load capacity of a bridge are generated from time lost and extra mileage accumulated during detour around a posted bridge. These costs increase essentially linearly with capacity deficiency (CG - SV), ADT, and detour length. Thus ADT and detour length are included in a linear factor (KD) in the following analysis. However, some public costs are not linear. A posted bridge is more likely to be damaged by overload. Although the overload may occur with higher frequency on a high ADT route, a single overload on a low ADT route produces similar damage. Furthermore, there is a need to provide basic service that is not directly proportional to ADT. Thus a second nonlinear factor (KA) increases with ADT but provides somewhat extra consideration for low ADT bridges and bridges with short detour lengths.

The priority is calculated as follows:

$$CP = WC \times [(CG - SV)/10] \times (0.6KA + 0.4KD) \qquad (2)$$

where

$$KA = (ADT)^{0.30}/12 \qquad (3)$$

$$KD = (DL/20) \times (ADTO/4{,}000) \qquad (4)$$

The priority is limited to the range $0 \leq CP \leq WC$. The relationships expressed by Equation 2 are shown in Figure 2.

Clear Bridge Deck Width Priority

Calculation of width priority (WP) considers the following parameters:

WG = width goal (ft; see Tables 4 and 5),
CDW = present clear deck width (ft),
ADTO = average daily traffic of over route, and
WW = width weighting.

User costs related to bridge width are associated

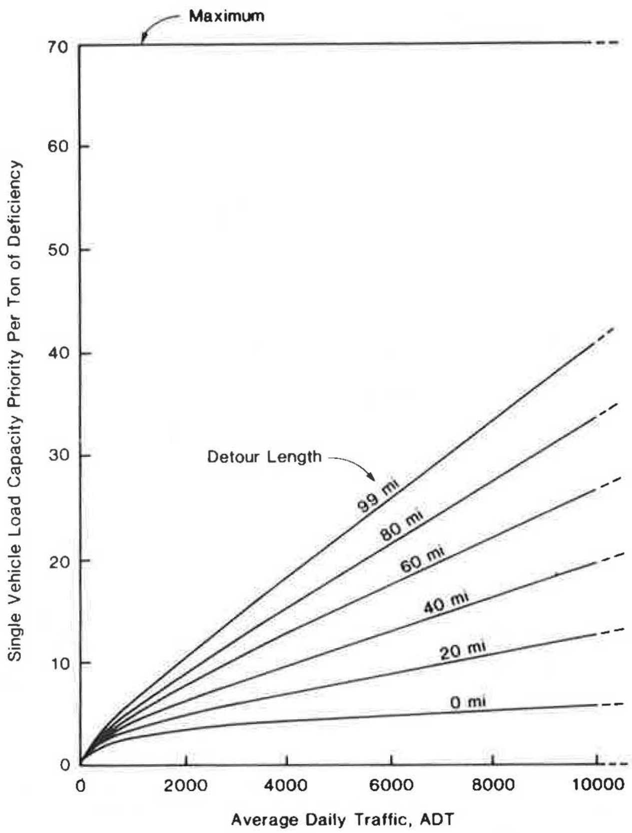

FIGURE 2 Capacity priority per ton versus ADT and detour.

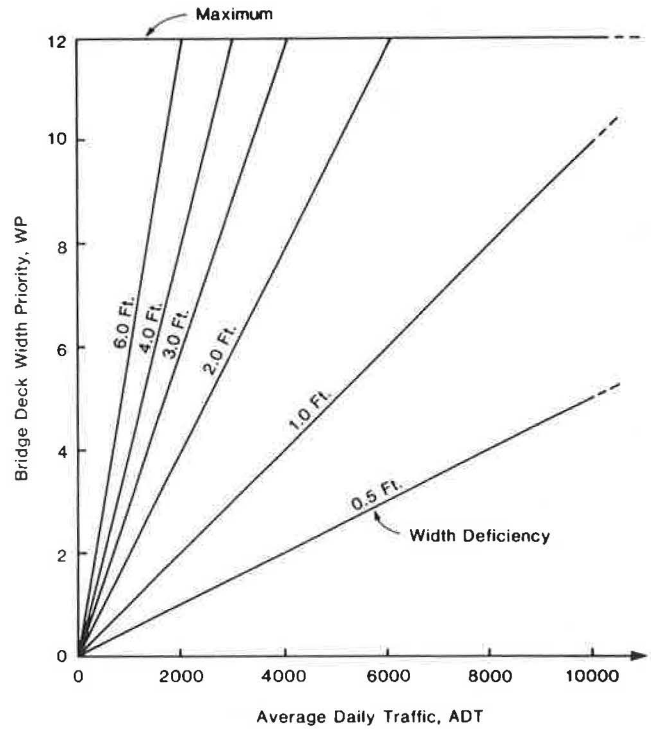

FIGURE 3 Width priority versus ADT and width deficiency.

with accidents. Narrow bridges contribute to single-vehicle collisions involving bridge elements or pedestrians and to multiple-vehicle collisions involving approaching or passing vehicles. Direct user costs include loss of life, injuries, and vehicle damage. Public costs include increased insurance premiums and bridge damage repair. The expected numbers of accidents and resulting costs would increase as a function of width deficiency (WG - CDW) and ADT. The relationship is essentially linear for both parameters. Thus width priority deficiency points (WP) should increase linearly as either ADT or width deficiency increases. No extra weighting is needed for extremely low ADT bridges because the probability of encountering other vehicles on such bridges is low. With low ADT, the usable lane width increases on an otherwise unoccupied bridge.

The width priority is calculated as follows:

$$WP = WW \times [(WG - CDW)/3] \times (ADTO/4{,}000) \quad (5)$$

The width priority factor is limited to the range $0 \leq WP \leq WW$. The relationships expressed by Equation 5 are shown in Figure 3.

Vertical Roadway Underclearance and Overclearance Priority

Calculation of vertical clearance priority (CP) considers the following parameters:

UG = underclearance goal (ft; see Table 6),
VCLU = present vertical underclearance (ft),
ADTU = average daily traffic of under route,
OG = overclearance goal (ft; see Table 6),
VCLO = present vertical overclearance (ft),
ADTO = average daily traffic of over route, and
WV = vertical clearance weighting.

User costs related to vertical clearance are associated with accident losses, detours of high clearance vehicles, and temporary detours resulting from out-of-service damaged bridges. Public costs include increased insurance premiums and bridge damage repair when accidents occur. In North Carolina vertical clearance usually involves underclearance for a grade separation. Overclearance problems are much less numerous because the inventory of through truss bridges and multiple-level bridges at interchanges is small. Nevertheless, both overclearance and underclearance contribute to user costs, and both types of clearance problems can occur simultaneously in one bridge.

The magnitude of user and public costs would increase linearly as a function of vertical clearance deficiency (UG - VCLU or OG - VCLO) and ADT. Although the length of detour has an impact on these costs, the detour length for the route under is not available in the data base. Thus detour length is not included in the evaluation.

The priority is calculated as follows:

$$VPU = WV \times [(UG - VCLU)/2] \times (ADTU/4{,}000) \quad (6)$$

$$VPO = WV \times [(OG - VCLO)/2] \times (ADTO/4{,}000) \quad (7)$$

$$VP = VPU + VPO \quad (8)$$

The priority is limited to the range $0 \leq VP \leq WV$. The relationships expressed by Equations 6 and 7 are shown in Figure 4.

Estimated Remaining Life Priority

An estimate of remaining life is made by bridge inspectors during the process of inspection. A sig-

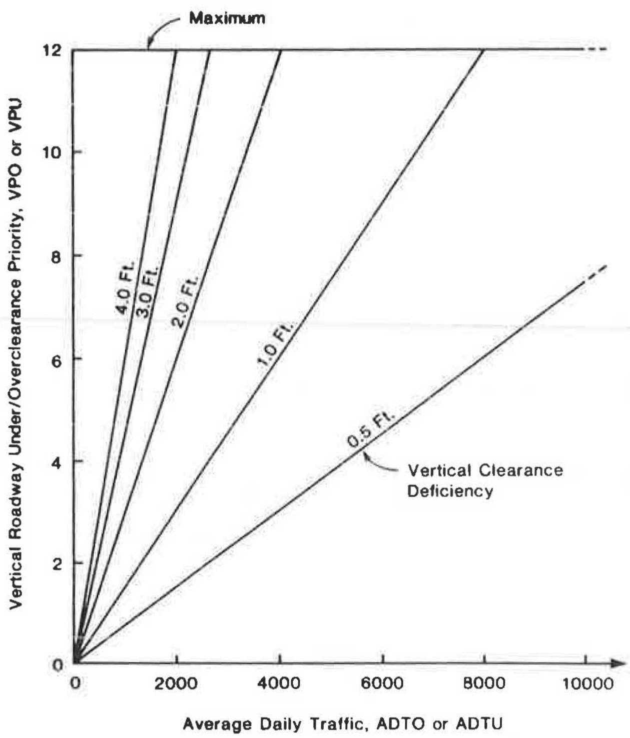

FIGURE 4 Clearance priority versus ADT and clearance deficiency.

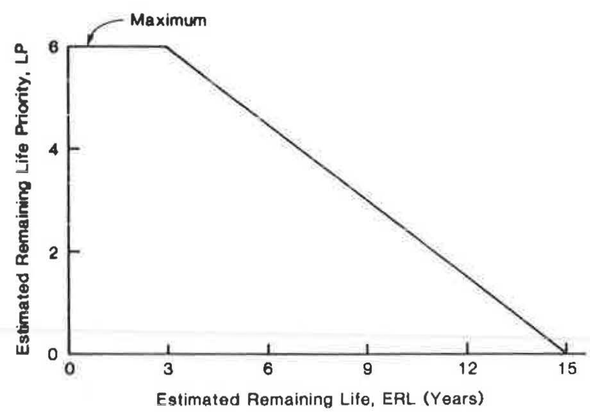

FIGURE 5 Remaining life priority versus estimated remaining life.

nificant degree of judgment is involved. Many factors appear to be considered, including condition ratings, appraisal ratings, load capacity, and age. Thus the estimate is approximate. A remaining life of less than 3 years generally indicates significant deterioration. A remaining life greater than approximately 15 years appears to indicate a generally acceptable situation. Inclusion of estimated remaining life in the analysis is intended to provide some weighting based on general condition.

The points assigned are a maximum for a remaining life of 3 years or less because the planning, funding, design, and construction process requires approximately 3 years.

Assignment of life priority (LP) considers RL = estimated remaining life (years) and WL = remaining life weighting. The priority is assigned as follows:

$$LP = WL \times \{1 - [(RL - 3)/12]\} \tag{9}$$

The priority is limited to the range $0 \leq LP \leq WL$. The relationship expressed in Equation 9 is shown in Figure 5.

ANALYSIS RESULTS

Data for each bridge from the NCDOT Structure Inventory and Appraisal Expanded File was analyzed by using the criteria and methods previously outlined. A computer program--Level of Service and Prioritization (LOSAP)--was developed to facilitate data processing. The results of the analysis are printed in various sorting formats to fit the needs of the user. An example of the analysis results based on acceptable criteria goals is presented in Table 7. The results shown are for bridges in the secondary highway system. Sample groups of output lines from the top of the output list, middle of the list, and near the bottom of the list are included. Abbreviations for the column headings are further defined in Table 8.

Sorting can be accomplished on several levels. Normally, the first level of sorting is either statewide--by system such as Interstate, primary, secondary, and so forth, or by county. The second level of sorting is by deficiency points with highest listed first. Other levels and types of sorting and limiters are used as needed.

The output printed is intended to provide the user with information that is most frequently used in evaluating the circumstances of the bridge being considered for possible replacement, rehabilitation, or maintenance. Information groupings include

1. Bridge identification numbers, location, facility carried, and Federal-Aid classification;
2. Principal bridge materials, type, condition ratings, age, and estimated remaining life;
3. Traffic volume, current capacity, width and underclearance, length, estimated replacement cost, and capacity and width goals; and
4. Deficiency points, sufficiency rating, and cost factor.

The cost factor (CF) is defined as follows,

$$CF = [\text{Replacement cost (000s)}]/(\text{Deficiency points}) = RC/DP \tag{10}$$

The maximum value is 999. This factor is an indication of the cost-to-need ratio. A low cost factor indicates a bridge whose deficiency can be eliminated for a relatively low cost. All parameters of deficiency being equal, it is generally more cost effective to replace a short bridge than a long bridge.

In examining the data sample in Table 7, note that the bridges at the top of the list are characterized by high ADT, significant load capacity and width deficiency, and low remaining life. Bridges with zero deficiency have no capacity, width, or vertical clearance deficiency and significant remaining life. Bridges with moderate deficiency points usually have moderate deficiencies. However, the deficiencies may be large when the ADT is extremely low and the detour length is extremely short.

The sources of the deficiency points accumulated versus acceptable and desirable criteria are shown in Figures 6 and 7. Most of the points are due to load-capacity deficiency because it is heavily weighted. Note, however, that in Figure 6a the number of bridges with a high number of points is small in the acceptable criteria case. The allocation of

TABLE 7 Sample LOSAP Output for Secondary Highway System and Acceptable Criteria

SY = S

	OBS	SY	BRNO	STRUCTUR	CNTY	FACILITY	FEDA	SUPMT	SM	AG	RL	DPA	SUFF	CF	LEN	ADTO	SV	CG	CDW	WG	VCLU	DL	DK	SP	SB	RC
High Deficiency	556	S	59212	10090067212U	MECK	SR1009	FAU	ST M-BM	TM	49	2	08.0	2.0	4	125	12500	9	34	20.0	28	0.0	12	4	5	4	338
	557	S	41104	164100301040	HLFX	SR1641	NFA-U	TM M-BM	TM	30	1	88.0	5.0	2	69	4000	17	34	24.0	20	0.0	5	6	6	3	199
	558	S	49	170000470490	ALMC	SR1700	FAU	ST M-DM	TM	33	3	88.0	34.5	1	31	5800	12	34	24.2	28	0.0	3	4	7	6	122
	559	S	73105	153000221050	PITT	SR1530	FAS	TM M-BM	TM	24	2	88.0	35.4	2	69	8700	12	25	24.0	26	0.0	4	5	5	5	209
	560	S	22403	186100804030	CLEV	SR1861	NFA-R	ST F-BM	TM	42	4	87.5	5.0	8	270	6700	4	16	19.5	26	0.0	4	6	4	4	673
	561	S	91100	201200401000	WAKE	SR2012	FAU	ST M-BM	TM	18	4	87.5	10.4	2	36	7200	18	34	24.0	28	0.0	4	5	5	4	133
	562	S	79083	191000630830	ROWN	SR1910	NFA-U	ST F-BM	TM	28	5	87.0	2.0	2	77	3450	6	34	19.2	26	0.0	6	6	7	5	217
	563	S	33113	134800621130	FRSY	SR1348	FAU	ST M-BM	TM	47	5	87.0	27.2	3	82	4800	19	34	22.2	28	0.0	9	7	7	7	239
Moderate Deficiency	1500	S	41058	101500300580	HLFX	SR1815	NFA-R	TM M-BM	TM	31	6	17.0	19.5	9	53	300	10	16	19.1	20	0.0	9	6	5	4	150
	1501	S	10207	274900842070	BUNC	SR2749	NFA-R	ST M-BM	RC	13	10	17.0	42.0	5	23	350	9	16	20.1	20	0.0	3	8	7	5	93
	1502	S	96054	112200760540	WILK	SR1122	NFA-R	ST TR-T	TM	21	5	16.9	21.9	10	62	40	5	16	14.9	20	0.0	6	5	6	6	167
	1503	S	42042	127900450420	HARN	SR1279	NFA-R	ST M-BM	TM	27	4	16.9	47.3	5	21	70	7	16	19.0	20	0.0	4	7	6	7	89
	1504	S	72076	154200300766	PERS	SR1542	NFA-R	TM M-DM	TM	29	8	16.9	36.5	7	35	400	10	16	19.2	20	0.0	5	6	6	6	116
	1505	S	48326	214500823260	IRED	SR2145	NFA-R	ST M-BM	RC	23	8	16.9	17.0	14	97	160	8	16	17.3	20	0.0	3	8	6	4	233
	1506	S	87000	119501000000	TRAN	SR1195	NFA-R	TM M-BM	0	31	6	16.9	40.9	5	21	330	10	16	19.1	20	0.0	2	6	7	6	89
Low Deficiency	6100	S	6175	170000151750	BEAU	SR1700	NFA-R	ST M-BM	TM	21	15	0.0	36.3	999	135	350	27	16	24.0	20	0.0	11	6	7	7	305
	6101	S	62197	201700561970	MOOR	SR2017	NFA-R	PC SLAB	ST	5	43	0.0	36.5	999	126	60	34	16	28.8	20	0.0	99	6	7	5	314
	6102	S	40120	212800491200	GUIL	SR2128	NFA-R	ST M-BM	TM	16	30	0.0	36.7	999	106	440	19	16	24.0	20	0.0	9	8	8	7	250
	6103	S	164	111300471040	ALMC	SR1113	FAS	ST M-DM	TM	34	15	0.0	36.8	999	121	780	25	25	24.0	20	0.0	6	7	7	6	278
	6104	S	78109	176700511090	ROCK	SR1767	NFA-R	ST M-BM	TM	32	20	0.0	37.0	999	90	400	17	16	22.1	20	0.0	10	7	8	8	220
	6105	S	30021	170000370210	CRNV	SR1700	NFA-R	TM M-DM	TM	19	18	0.0	37.9	999	18	320	20	16	23.9	20	0.0	6	6	5	6	84
	6106	S	8105	151100421050	BLAD	SR1511	NFA-R	PC M-BM	TM	11	18	0.0	38.3	999	91	200	19	16	28.9	20	0.0	6	7	7	7	241
	6107	S	24139	147000171390	CRAV	SR1470	NFA-R	PC SLAB	ST	11	30	0.0	38.5	999	182	500	34	16	29.3	20	0.0	30	7	7	8	431

life points is the same under both the acceptable and the desirable criteria, as shown in Figure 6b. As shown in Figure 7a, there are a large number of bridges with width deficiency, but most are either on low ADT routes or the width deficiency is not large. There is, however, a concentration of bridges with a large number of width deficiency points that should be eliminated. As shown in Figure 7b, few bridges are deficient in terms of vertical clearance when compared to the acceptable criteria.

A frequency distribution of the numbers of bridges in ranges of acceptable and desirable deficiency points is given in Table 9. A goal of the level-of-service approach would be to eventually reach a situation in which

1. The average deficiency will be virtually zero when measured against the acceptable level-of-service goals, and
2. The average deficiency when measured against the desirable goals will be allowed to fluctuate in

TABLE 8 LOSAP Output Abbreviations

Abbreviation	Definition
OBS	Output line number
SY	Highway system (S = secondary)
BRNO	Permanent bridge number
STRUCTUR	Structure number
CNTY	County
FACILITY	Facility carried
FEDA	Federal-Aid classification
SUPMT	Superstructure material and type (TM = timber, M-BM = multibeam/girder)
SM	Substructure material (ST = steel)
AG	Age
RL	Remaining life
DPA	Deficiency points (acceptable)
SUFF	Sufficiency rating
CF	Cost factor
LEN	Length
ADTO	Average daily traffic over bridge
SV	Single vehicle posting (tons)
CG	Capacity goal (tons, 34 = NP)
CDW	Clear deck width (ft)
WG	Width goal (ft)
VCLU	Vertical clearance under (ft) (0.0 if no grade separation)
DL	Detour length (miles)
DK	Deck condition rating
SP	Superstructure condition rating
SB	Substructure condition rating
RC	Replacement cost ($000s)

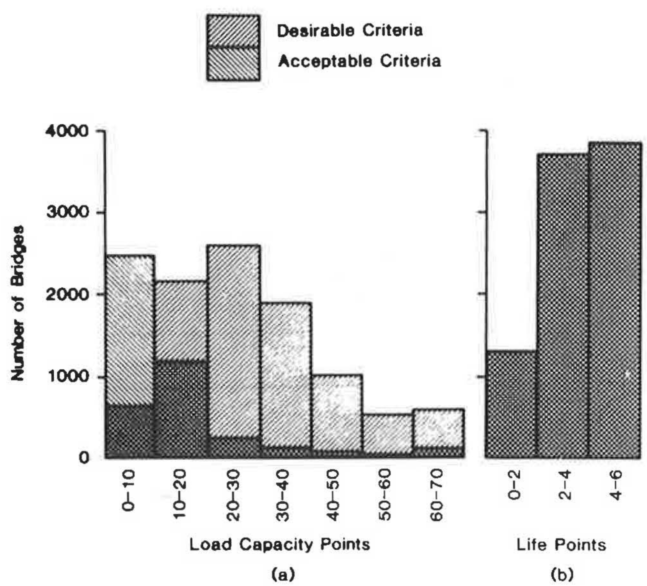

FIGURE 6 Distribution of deficiency points due to load and remaining life.

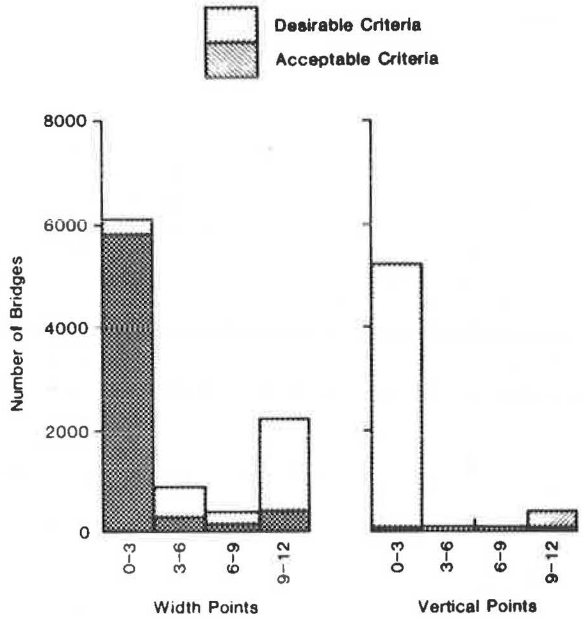

FIGURE 7 Distribution of deficiency points due to width and vertical clearance.

TABLE 9 Deficiency Point Distribution

	No. of Bridges	
Point Range	Acceptable	Desirable
DP = 0	7,026	4,131
0 < DP ≤ 10	6,595	1,821
10 < DP ≤ 20	2,309	3,150
20 < DP ≤ 30	476	2,561
30 < DP ≤ 40	165	2,132
40 < DP ≤ 50	82	1,294
50 < DP ≤ 60	48	728
60 < DP ≤ 70	31	412
70 < DP ≤ 80	26	267
80 < DP ≤ 90	30	287
90 < DP ≤ 100	1	6
Total	16,789	16,789

a manner that allows for least cost maintenance, rehabilitation, and replacement.

This recognizes that essential service must be provided with due regard to need for service. However, all bridges cannot be maintained in a new desirable condition indefinitely. Toward the end of bridge life, certain maintenance should be discontinued and some deterioration accepted before replacement, as long as essential acceptable levels of service are still provided.

CONCLUSIONS

The concept of a level-of-service system offers the following possibilities for bridge evaluation.

1. Acceptable levels of service related to essential public needs can be established in accordance with the functional classification of the highway system being carried.
2. Assigning priorities for replacement or rehabilitation can be based on the magnitude of the bridge deficiency calculated in a manner that parallels the magnitude of user costs incurred. Optimization techniques for least-cost selection among these alternatives are being developed.

Although much effort remains to achieve all the objectives desired, the directions taken to date have enhanced use of the bridge inspection data. It is recognized that special needs and situations not accounted for by the system will continue to refine the priority listing. In addition, refinement of the weightings and factors included in the level-of-service analysis is expected to continue. Nevertheless, the system is already greatly assisting in the process of identifying bridges for replacement, rehabilitation, and certain maintenance operations.

ACKNOWLEDGMENT

The research reported herein was supported by the North Carolina Department of Transportation through the Institute for Transportation Research and Education.

The authors gratefully acknowledge the valuable suggestions of M.C. Adams, J. Lee, J. Johnson, O. Reagan, G. Phillips, and N. Benson of NCDOT and W. F. Babcock of the Institute for Transportation Research and Education. Special thanks are due Eric Svendsen, research assistant in civil engineering, who assisted in the analysis development and prepared computer programs for data processing.

REFERENCES

1. Recording and Coding Guide for the Structure Inventory and Appraisal of the Nation's Bridges. FHWA, U.S. Department of Transportation, Jan. 1979.
2. National Bridge Inventory Report Generator Program Documentation. FHWA, U.S. Department of Transportation, 1980.
3. Bridge Policy. Division of Highways, North Carolina Department of Transportation, Raleigh, 1981.

Publication of this paper sponsored by Committee on Structures Maintenance.

Management of Bridge Maintenance, Repair, and Rehabilitation—A City Perspective

ARUNPRAKASH M. SHIROLÉ

ABSTRACT

The management of bridge maintenance, repair, and rehabilitation functions is discussed from the perspective of a major metropolitan city. The management objectives of the city, and the data base and cost control systems that assist the city in effectively managing the growing responsibilities in these fields, are described. Further, information concerning how routine and scheduled bridge maintenance and repair, as well as scheduled bridge rehabilitation, is planned, coordinated, and administered is also discussed.

It is widely known that a large percentage of the 567,820 bridges in the United States are in urban areas, and an even larger percentage of these bridges are under local government jurisdictions. Of the 302,775 bridges under local government jurisdictions, 165,928, or more than 50 percent, are considered to be deficient according to FHWA standards. Therefore, bridge maintenance, repair, and rehabilitation has assumed a larger dimension in local government responsibilities. In this paper the discussion centers on how Minneapolis, Minnesota, a major metropolitan city, views and manages this responsibility.

MANAGEMENT OBJECTIVES

There are 399 bridges serving the transportation needs within the city of Minneapolis. The data in Table 1 indicate the number of different bridge groups and their average ages. Based on age and condition of these bridges, the management objectives of the city are as follows:

1. Pursuant to state statutes, conduct annual maintenance inspection of 260 bridges for which the city is responsible to ensure that all repair needs and normally predictable major bridge problems are identified;
2. To provide preventive maintenance for and maintain in safe condition 176 bridges, 38,000 linear feet of bridge approaches, pier protections of six major river crossings, and 10,000 linear feet of various types of embankments and retaining walls;
3. To ensure safety of pedestrians, control snow and ice on 154 bridges, 38,000 linear feet of bridge approaches, and 28 pedestrian bridges; and
4. To do necessary major bridge repair and rehabilitation work, including work under county and state agreements.

TABLE 1 Bridge Groups and Average Age

	Bridge Group	No. of Bridges	Avg Age (years)
A	Interstate highway	70	14
B	Street over or under Interstate highway	74	17
C	River	13	55
D	Railroad	130	62
E	Creek	40	50
F	Miscellaneous	11	31
G	Pedestrian	28	17
H	Parkway	33	58
Total of C-H		255	53
Total		399	40

MANAGEMENT INFORMATION SYSTEMS

Bridge Structure Inventory and Inspection

The data in Tables 2 and 3 describe a broad range of valuable information available from the data base system. The bridge maintenance, repair, and rehabilitation or replacement decisions for the city are primarily based on the up-to-date information provided by this system. A library of more than 5,000 drawings on microfiche and periodic field measurements support and update the structure inventory.

The current formal bridge inspection program was instituted in 1971. The inspection team consists of two to four trained inspectors. A large variety of tools and equipment (such as sounding equipment, cameras, a snooper-truck, and boats) are used in the inspection process. A library of photographs, in chronological sequence, along with historical inspection records and scour studies around piers of river bridges are also maintained. When more frequent inspections are needed for some critically deficient bridges, inspections are conducted daily.

Every year structure inventory and inspection records are updated during winter months and communicated to the Minnesota Department of Transportation. The state's computer is used to maintain annual bridge structure inventory and inspection records. These records are then used to compute the FHWA's sufficiency ratings, and computer printouts are made available to the city.

Structural Capacity Ratings

Evaluation of current structural capacity of all bridges is completed at least once every 5 years. Inspection reports with current estimates of loss of sections are used for this purpose. Interim capacity ratings become necessary when accelerating deterioration or accident damage is reported in inspection reports.

Results of structural capacity ratings are promptly communicated to appropriate agencies or organizations and necessary load limit signs are posted. Typically, bridges are posted for gross weights of a truck (M-3) and truck and semitrailer combination (M-3S2). In some instances a combination of load limits and speed limits is used. The structural capacity information is updated as often as deemed necessary and promptly communicated to state and city enforcement agencies. Currently, 29 bridges

TABLE 2 Bridge Structure Inventory and Appraisal

Data Base--Part I: Section A

STRUCTURE INVENTORY AND TRAFFIC (SECTION A): (Dated______; Updated________

1. Structure Number_______; Built in_______; Remodeled in______; Owner_____
2. Inventory Route________; Over/Under________; Location___________________
3. Alternate Length_______; Impact on Travel Time_____min.;kmh (mph)_______
4. Lanes/R.R. Tracks (over)_______; (under)______; One/Two Way_____________
5. Av. Daily Traffic (ADT) on Bridge_____;Peak Hour Traffic_____;Year_______
6. Projected ADT________; For Year________; Heavy Commercial ADT___________
7. Design Load_______; Present Structural Capacity______; Posted Load Limit_
8. Approach Width: Roadway_______________; With Shoulder___________________
9. Angle Skew _____; Is Structure Flared?____; Width: Max___; Min.________
10. Minimum Clearances: Vertical: Over_______________; Under_______________
    Horizontal: Over______ (North/West;__________ (South/East)_______________
    Under_____ (North/West);__________ (South/East)_______________
11. Navigation Control: Yes/No; Vertical__________; Horizontal_______________
12. Structure Type: Main Span____________; Approach Spans___________________
13. Number of Spans: Main_______________________; Approach___________________
14. Structure Length: Total_______; Max. Span._______; Approach Spans_______
15. Widths: Roadway (curb to curb)_________; Deck (out to out)______________
    Sidewalks:_________ (North/West)_______ (South/East)_______________
16. Wearing Course and Overburden: Type(s)______; Thickness(es)______________
17. Guardrail: Type___;___ Length; Other Railings: Type_____; Length________
18. Utilities Carried, Location____
19. Joints on the Bridge: Type___________________;Length___________________
20. Lighting System____
21. Painted in____________________________; Type of Paint____________________
22. Material Inventory: Roadway_______________; Sidewalk____________________
    Substructure____________; Superstructure_______________
23. Other Features (such as safety lights):______________________________

Data Base--Part I: Sections B and C

STRUCTURE INSPECTION AND APPRAISAL (SECTION B): (Dated ___________________)

1. Deck: Overall Condition____
   Type and Extent of Deterioration____
   Repairs Needed and When____
2. Superstructure: Overall Condition____
   (Other than Type and Extent of Deterioration________________________________
   Deck) Repairs Needed and When____
3. Substructure: Overall Condition____
   Type and Extent of Deterioration_____________________________________
   Repairs Needed and When____
4. Safety Considerations: Unsafe or Hazardous Conditions______________________
   (Width, alignment, load-limits, steep grades, railings, clearances, etc.)
5. Serviceability: Drainage____
   Rideability (Roughness Coefficient)_________________________
   Lighting____
6. Condition of Paint____
7. Estimate of Remaining Life: Without (with) major repairs____(____)Years
8. Description and Estimated Cost of Major Repairs Needed and When__________

STRUCTURAL CAPACITY AND FUNCTIONAL ADEQUACY (SECTION C): (Dated___________)

1. Load Carrying Capacity____
   (Based on: Current Legal Loads______, Estimate of Deterioration________
2. Minimum Clearances: Vertical_____________; Horizontal______________________
3. Adequacy for Present and Projected Traffic________________________________
4. Waterway Adequacy and Protection (e.g., Pier or Scour Protection)_______
5. Limits for Special Permit Loads____; Wheel-Load Configuration Used______

Data Base--Part II

MAINTENANCE HISTORY AND PROJECTED FUTURE NEEDS (SECTION D): (DATED_________)

1. Chronology and a Brief Description of Major Repairs Done:_________________
   (When, what, at what cost and who made them, improvement in life expectancy)____
2. Brief Description of Minor Repairs in the Past Five Years_______________
3. Projected Future Maintenance Needs: (e.g., New Overlay)__________________

ENVIRONMENTAL AND OTHER FACTORS (SECTION E): (Dated_______________________)

1. Aesthetical Considerations (e.g., Paint, etc.)_____________________________
2. Developmental Plans and Projected Needs of the Area Served_____________

TABLE 3 Typical Bridge Inspection Data Sheet

CITY OF MINNEAPOLIS

INSPECTION

Bridges and Related Structures

Urgent____________

1. IDENTIFICATION: Bridge No.__________ Mn/DOT No.____________ Apr.__________

   Location ____

   Posted Limit____________________ Inspected By ____________ Date__________

2. CONDITION & SUGGESTED IMPROVEMENT: RATING

   Railing__________

   Curb__________

   Roadway__________

   Subsurface__________

   Sidewalk__________

   Subsurface__________

   Stringers__________

   ( )__________

   Expansion Devices__________

   Piers__________

   Abutments__________

   Walls__________

   Warning Lights__________

   Lighting__________

   Other__________

3. GENERAL CONDITION & REMARKS: __________

4. IMPROVEMENTS & REPAIRS: __________

   Estimated Cost__________ Date Needed__________

5. PLANS MADE OR OWNER NOTIFIED: __________ DATE__________

6. REPAIRS MADE: __________ DATE__________

7. CONDITION CODES: DECK______ Superstructure______ Substructure______

are posted for load limits and 4 bridges are closed to vehicular traffic.

Cost-Control System

In 1980 a new financial and accounting information system was instituted with the capability of providing up-to-date cost records for any work being done on any one of the bridges. This computer-based system uses location and activity codes. The coding system is given in Tables 4 and 5. Each bridge is identified with letters JC followed by a four-digit number. Letters PC instead of JC identify approaches for that bridge. The first two digits of the bridge number identify the bridge group it belongs to and the route system it is on. Other locations are identified by two zeros and two digits following the letters PC.

The city does all of its bridge maintenance, repair, and (some) rehabilitation work using its own forces. Therefore, the activity codes are organized in such a way that each foreman can select appropriate codes while reporting daily activities of in-

TABLE 4 Cost-Control System: Location Codes

Bridge numbers	JC 0001-JC 9999
Bridge approaches, Special locations	PC 0001-PC 9999
Bridge approaches first digit (after letters PC): zero	
PC 0001:	Bridge yard and plant
PC 0002:	Bridge division–boat dock and building
PC 0003:	Harbor lights–river bridges
PC 0004:	Mississippi River bridges (flood control)
PC 0005:	Minnehaha Creek bridges (flood control)
PC 0006:	Shingle Creek bridges (flood control)
PC 0007:	Bassetts Creek bridges (flood control)
PC 0008:	All bridges
PC 0009:	Bridge building expansion
PC 0010:	Major equipment–snooper
PC 0011:	Major equipment–pontoon boats
PC 0012:	Major equipment–pusher (tow boat) and/or barge
PC 0013-PC 0020:	Bridge–miscellaneous
PC 0021:	City Hall–bridge: office and administration
PC 0022:	Bridge yard: office and administration

dividual crews. Answers to simple questions such as "What activity?", "In which area?", and "Who did it?" help the foreman or supervisor select appropriate activity codes.

All costs related to the activity are also reported and processed by the computer on a daily basis. Therefore, this system has the capability of producing reports (on demand or periodically) of costs of each activity, budget line-item expenditures and balances (year to date), and revenues. The system serves the city as an effective tool in monitoring and controlling costs of all bridge-related activities.

BRIDGE MAINTENANCE AND REPAIR

Routine Maintenance and Repair

Routine maintenance and repair is an ongoing activity to provide preventive maintenance for and maintaining in safe condition 176 bridges, 38,000 linear feet of bridge approaches, pier protections of six major river crossings, and 10,000 linear feet of various types of embankments and walls. This activity is funded totally by general revenue and is conducted with permanent and day-labor staff.

During the spring, summer, and fall bridge crews are busy with the following types of activities:

1. Washing steel grid deck bridges;
2. Cleaning joints, beam seats, catch basins, and drains;
3. Removing sand, salt, and debris from bridge decks;
4. Welding and other structural steel repair;
5. Patch, repair, and seal spalled, cracked, and deteriorated concrete;
6. Repair accident and fire damage, emergency repairs;
7. Remove branches and debris from around piers in river and creeks; and
8. Erosion control.

During the winter months crews are kept busy in snow and ice control on 154 bridges, 38,000 linear feet of bridge approaches, and 28 pedestrian bridges. Repairs of an emergency nature and of accident damage are also conducted during this period. This activity is fully funded by general revenue and is conducted with permanent and day-labor staff.

Scheduled Major Maintenance and Repair

Scheduled major maintenance and repair is more of a nonroutine type and is based on reports of formal bridge inspections. As the annual formal inspections conclude, inspection reports and maintenance history for each bridge are reviewed. When necessary, another inspection by a senior supervisory-level engineer is scheduled, especially in cases of accelerated deterioration or serious accident damage. At this stage maintenance and repair needs of each bridge are evaluated. An annual needs statement is then prepared. Typically, the needs statement indicates type, extent, preliminary cost estimates, and urgency of maintenance or repairs needed for each bridge.

The needs statement is then reviewed with other relevant information such as the current FHWA sufficiency rating and importance of the bridge in the present and projected overall transportation needs of the area. The maintenance and repair needs are then assigned on a priority basis according to their urgency and by matching the cost estimates with pro-

TABLE 5 Cost-Control System: Activity Codes

What Activity?	In Which Area?	Who?
A. New work or replacement	A. Roadway	A. Maintenance
B. Maintenance and repair	B. Sidewalk and/or curb	B. Carpenter
C. Concrete patch	C. Railings and fences	C. Ironwork
D. Asphalt patch	D. Beams or girders	D. Cement finisher
E. Maintenance cleaning	E. Abutments	E. Painter
F. Grass cutting and weed control	F. Columns or pier bents	F. Shop repair
G. Flood control	G. Walls	G. Stock help
H. Snow and ice control	H. Embankments	H. Other
J. Routine bridge inspection	J. Miscellaneous–structural	J. Accounting staff
K. Formal bridge inspection	K. Combination of above	K. Supervisory staff
M. Soundings	M. Mowers and grass cutting equipment	M. General foreman
N. Project engineering		N. Engineers
P. Construction engineering	N. Snow and ice equipment	P. Engineering contract
Q. Structural capacity rating	P. Other equipment	
R. Administration and support services	Q. Tool storage boxes, snow trailers, and wagons	
T. Administration–office expenses	R. Salaries	
X. Rental	T. Additives–vacation, holiday, sick, and other leave	
V. Store–supplies		
W. Capital outlay	X. Additives–workman's compensation, employee injury expenses, unemployment compensation, severence pay	
	V. Unallocated	

jected availability of general revenue funds for the following year. Individual major bridge maintenance and repair is then scheduled as the bridge maintenance and repair budget for the following year is finalized. As a general rule, the FHWA sufficiency rating for those bridges on which major maintenance and repair is scheduled would range between ±50 to 80.

Typical major bridge maintenance and repair activities are as follows

1. Repair or replacement of steel stringers, beams, or steel grid panels;
2. Repair of concrete beams, columns, abutments, and walls;
3. Repair or replacement of pier protections;
4. Replacement of expansion devices;
5. Extensive repair of masonry;
6. Construction of walls for erosion protection;
7. Sidewalk and deck slab repairs and overlays;
8. Painting of structural steel; and
9. Extraordinary maintenance and repair for the state or county.

BRIDGE REHABILITATION

Rehabilitation or Replacement Decision Making

Realities of fiscal constraints are such that the city can neither think of replacing all of the aging bridges nor reasonably justify replacement options in all cases. In 1980 a Bridge Task Force was created to evaluate the bridge needs of the city and to recommend a 5-year capital improvements program. As a part of this process, bridges a with sufficiency rating between 0 and 80 are screened annually and possible candidates for rehabilitation, replacement, or rehabilitation and replacement are identified and assigned priorities based on structural condition, safety, and overall transportation needs.

Bridges that are candidates for rehabilitation or rehabilitation and replacement within the next 5-year period become the subject of an in-depth investigation. All components of the superstructure and substructure are investigated by reputed materials engineering consultants for material properties, deterioration, and their available structural capacity. A decision is then made, based on recommendations resulting from this in-depth investigation, as to whether any part or all of the bridge structure can be rehabilitated and modified to meet the future overall transportation needs of the city. Bridges that are to be scheduled for rehabilitation and replacement within the next 5-year program are recommended to the City Council as a part of the capital improvements program (CIP). Funding for this program is generally sought from municipal or county state aid, state bridge bond, or federal SBR or Resurfacing, Restoration, and Rehabilitation funds.

Scheduled Bridge Rehabilitation

Plans for scheduled rehabilitation of a bridge are either drawn in-house or by consulting engineers retained by the city. Similarly, the rehabilitation work, depending on its magnitude and complexity, is either done by using city forces or contractors. In either case, the city engineering staff supervises the construction activity.

CONCLUSION

The magnitude of problems related to maintenance, repair, and rehabilitation of bridges within the city of Minneapolis has been on the increase. However, efforts through effective management are being made to contain and limit these problems. Because of the involvement of many agencies, and as many as five railroads, delays can complicate execution of the city's policies. Therefore, cooperation among different agencies and groups that represent a variety of interests governs the success of the management efforts of the city.

Publication of this paper sponsored by Committee on Structures Maintenance.

Abridgment

Development: Deep Grooving–A Method for Impregnating Concrete Bridge Decks

RICHARD E. WEYERS and PHILIP D. CADY

ABSTRACT

Polymer impregnation of concrete can be used for the long-term protection of salt-contaminated concrete bridge decks. However, the current impregnation process requires long impregnation times and the development of new equipment. In addition, most monomers are a potential fire hazard. A laboratory investigation was performed to develop a simplified system that will reduce the impregnation time, simplify the equipment needs, and mitigate the potential fire hazards by deep grooving the concrete. The monomer used was an MMA-TMPTMA-AZO system. The laboratory results indicate that the impregnation time can be significantly reduced by optimizing the groove width, depth, and spacing. Optimum drying (by using infrared heaters) and polymerization conditions for the grooving conditions are also presented. The results of the laboratory study demonstrate the feasibility of the method and the need for a full-scale field trial to demonstrate its applicability to field conditions.

In March 1981 the U.S. General Accounting Office estimated the number of deficient bridges to be more than 100,000, with an estimated cost of $33.2 billion needed to replace or rehabilitate bridges in the United States (1). Approximately 50,000 of the deteriorated bridges and $11 to $17 billion of the cost are related to the deterioration of concrete bridge decks. The primary cause of bridge deck deterioration is the corrosion of the reinforcing steel. The corrosion of reinforcing steel in chloride-contaminated concrete is an electrochemical cell. In order for the electrochemical corrosion cell to be active in reinforced concrete, the following conditions must be present:

1. Chloride ion in excess of the threshold level must be present at the anode (corroding site),
2. Oxygen must be present at the cathode (noncorroding site),
3. Moisture must be present to take place in the reaction at both the anode and the cathode, and
4. Moisture must be present in the capillary void system to act as the conductive path between the anode and the cathode.

The corrosion reaction in concrete is an oxygen diffusion limited system. That is, the reaction can occur only as fast as oxygen can be supplied to the cathode.

Current rehabilitation methods, such as removing any deteriorated concrete and overlaying with a latex-modified concrete or applying a preformed membrane and overlaying with an asphaltic concrete, are of limited value because the corrosion cell remains active (2). However, polymer impregnation should stop the corrosion process by encapsulating the in-place chlorides, replacing the electrolyte (capillary moisture) with a dielectric material (polymer), and restricting the ingress of moisture and oxygen by partly filling the capillary void system. No corrosion current could be detected after the deep polymer impregnation of concrete that contained an active chloride-contaminated reinforcing steel corrosion cell (3).

The polymer impregnation method consists of drying the concrete to the desired depth of impregnation, impregnating the concrete with a monomer, and polymerizing the monomer in situ. To improve the present deep polymer impregnation system, several problems must be addressed, especially

1. Reducing the impregnation time,
2. Improving the drying system,
3. Simplifying the current impregnation process,
4. Understanding better the polymerizing rates, and
5. Minimizing the fire hazard.

One approach to improve the impregnation process is to cut grooves in the deck--for example, to a depth of 0.5 in. above the upper reinforcing bars--and to use the grooves as vessels to contain the monomer. After impregnation the grooves can be filled with sand and saturated with the monomer, followed by polymerization of the monomer in the entire mass. The deep grooves would thus eliminate the need for an impregnation vessel. Further, the grooves can be cut on contour lines (lines of equal elevation), thereby eliminating the problems associated with grade, cross slope, and superelevation that are encountered with the ponding method. Also, the method should reduce the impregnation time, simplify the polymerization process by eliminating the need to attach the hot-water polymerization vessel to the deck, possibly provide a more skid-resistant surface, and reduce the bridge-deck maintenance problem by upgrading the strength, freezing and thawing durability, and wear-resistant properties of the concrete. In addition, the deep-grooving method may reduce the fire hazard associated with the impregnation process by decreasing the potential flame surface area.

This study was designed to test the hypothesis that concrete bridge decks can be impregnated with an MMA monomer system by using the deep-grooving method. Thus the study addressed the following tasks:

1. Develop and optimize the deep-grooving impregnation process;
2. Optimize the gas-fired infrared (IR) drying method, considering time and energy expended;
3. Optimize the hot-water polymerization method of the MMA impregnant system, considering time and temperature; and
4. Demonstrate the deep-grooving impregnation system in the laboratory.

EXPERIMENT

Materials and Processes

The concrete mixture design used for preparing laboratory specimens was calculated in accordance with Pennsylvania Department of Transportation (PennDOT) specifications for bridge deck concrete in effect in the late 1960s and early 1970s when most of the Interstate system was being constructed.

The impregnant system selected was 100 parts methyl methacrylate (MMA) to 10 parts trimethylopropane trimethacrylate (TMPTMA) to 0.5 parts 2, 2'-azobisisobutyronitrile (AZO), by weight. The MMA system was selected because it is the most commonly used monomer system for impregnating concrete and because it exhibits the material properties needed for the long-term rehabilitation of chloride-contaminated bridge decks (3,4).

Gas-fired IR radiant heating was selected on the basis that it is currently the most efficient and practical method available for the large-scale drying of concrete bridge decks (5).

Hot-water polymerization was selected because of its simplicity and effectiveness (6).

Experimental Design

Figure 1 presents a flow diagram of the experimental design. The horizontal and vertical impregnation rates were determined to aid in the evaluation of the optimum groove spacing, width, and depth. Then the effects of groove width on the rate of impregnation were determined, and the effect of time on the optimized groove width, depth, and spacing were evaluated. The rate of polymerization and drying were investigated, and laboratory demonstrations of the deep-grooving impregnation system were performed.

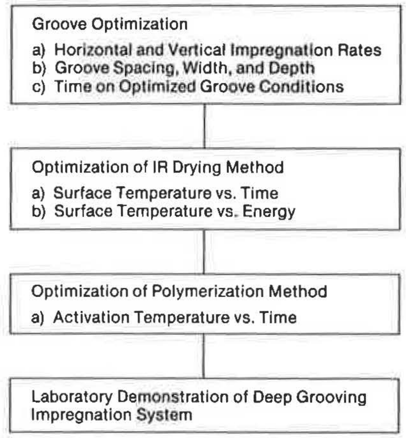

FIGURE 1 Experimental flow diagram.

RESULTS

Horizontal and Vertical Impregnation Rates

A linear-regression analysis was performed on the horizontal and vertical impregnation data. The best-fit line was obtained with the depth of penetration as the dependent variable (expressed in inches) and the square-root of time as the independent variable (expressed in hours). This shows that the data fit the Rideal-Washburn equation for fluid flow in a porous medium, as was found earlier (5). The data in the following table present the results of the linear-regression analyses and indicate that the slopes of the curves are equal:

Impregnation	Slope	Coefficient of Determination
Horizontal	0.731	0.989
Vertical	0.733	0.996

Thus the horizontal rate of impregnation is equal to the vertical

Optimization of Groove Width, Depth, and Spacing

The data presented in Table 1 indicate that as the ratio (S/G) of groove spacing (S) to impregnation depth below the groove bottom (G) (impregnation ratio, see Figure 2) increases from 1.0 at the 3-in. spacing to 1.4 at the 4-in. spacing and to 1.7 at the 5-in. spacing, the depth of impregnation midway

TABLE 1 Depths of Impregnation for Grooved Beams (groove depth 1.5 in.)

Specimen	Depth at Centerline of Groove (in.)	Depth at Centerline Between Grooves (in.)	Depth of Centerline of Groove (in.)	Depth at Pond Area (in.)	Depth Gained (in.)	Impregnation Ratio
Groove spacing = 3 in., groove width = 1.125 in., impregnation time = 24 hr						
G-9	4.5	4.5	4.5	3.625	0.875	1.0
G-10	4.625	4.5	4.625	3.5	1.125	1.0
Groove spacing = 5 in., groove width = 1.125 in., impregnation time = 24 hr:						
G-11	4.5	3.5	4.5	3.25	1.25	1.7
Groove spacing = 4 in., groove width = 1.125 in., impregnation time = 24 hr:						
G-12	4.375	3.75	4.375	3.375	1	1.4
Groove spacing = 4 in., groove width = 0.875 in., impregnation time = 24 hr:						
G-13	4.5	4.25	4.5	3.25	1.25	1.4
Groove spacing = 4 in., groove width = 0.625 in., impregnation time = 24 hr:						
G-14	4.25	4	4.25	3.25	1	1.4
Groove spacing = 2.25 in., groove width = 0.75 in., impregnation time = 16 hr:						
G-17	3.75	3.75	3.75	2.25	1.5	1.0
Groove spacing = 3 in., groove width = 0.75 in., impregnation time = 16 hr						
G-18	3.625	3.625	3.625	2.5	1.125	1.4

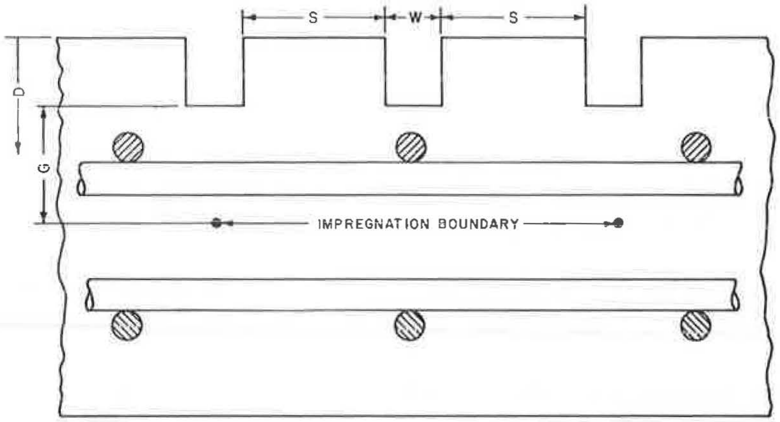

S = GROOVE SPACING G = IMPREGNATION DEPTH BELOW GROOVE BOTTOM
IMPREGNATION RATIO = S/G
D = POND IMPREGNATION DEPTH
GROOVE RATIO = G/D

FIGURE 2 Impregnation ratio and groove ratio.

between the grooves decreases for the 24-hr impregnation time. Figures 3-5 illustrate the effects of an increasing impregnation ratio. That is, as the impregnation ratio increases to greater than 1.0, the boundary of the impregnation becomes more sinuous. Also, the depth of impregnation, or the shape of the impregnation boundary, appears not to be affected by reducing the groove width from 1.125 to 0.625 in. (see Table 1).

The data in Table 1 also indicate that time has no effect on the impregnation ratio. At an impregnation ratio equal to 1.0, the boundary impregnation is straight; at 1.4 it becomes slightly sinusoidal.

The average depth gained through grooving versus surface ponding for the beams presented in Table 1 is about 1.125 in. This is about 75 percent of the groove depth. Of more interest than the depth gained, per se, is the depth of impregnation below the groove base (G) expressed in terms of the depth of impregnation by ponding (D) (groove ratio = G/D; see Figure 2). For grooved and ponded impregnation data presented in Table 1, the mean groove ratio is 0.90, with a standard deviation of 0.05. Therefore,

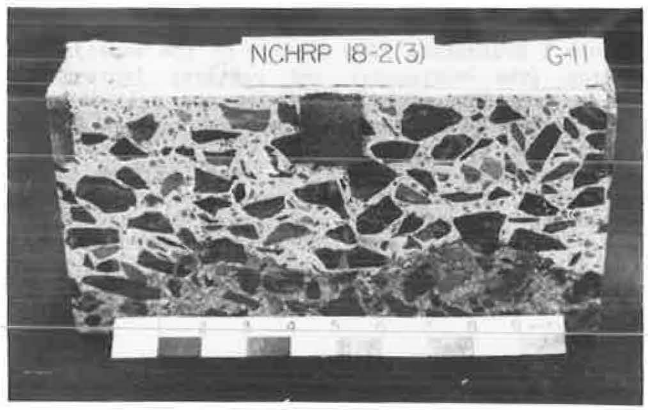

FIGURE 4 Grooved beam after polymer impregnation (impregnation time = 24 hr, groove spacing = 5 in., groove width = 1.5 in., groove depth = 1.5 in., impregnation ratio = 1.7).

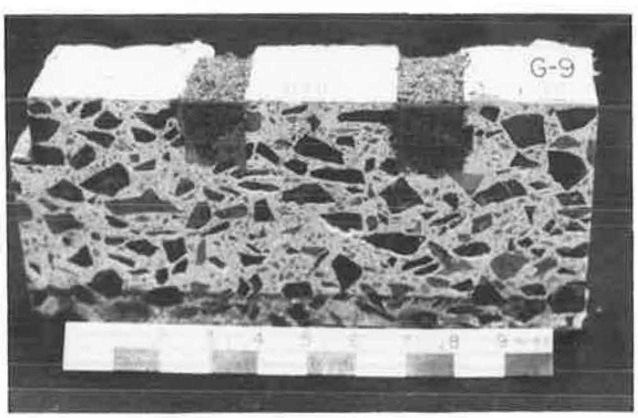

FIGURE 3 Grooved beam after polymer impregnation (impregnation time = 24 hr, groove spacing = 3 in., groove width = 1.5 in., groove depth = 1.5 in., impregnation ratio = 1.0).

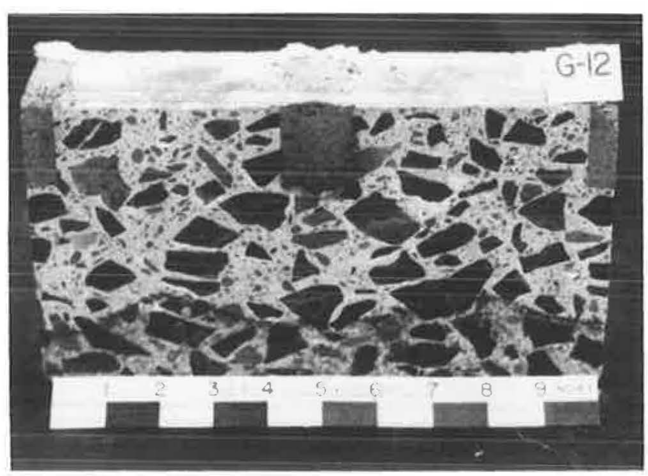

FIGURE 5 Grooved beam after polymer impregnation (impregnation time = 24 hr, grooved spacing = 4 in., groove width = 1.5 in., groove depth = 1.5 in., impregnation ratio = 1.4).

for a specified depth of 2.25 in. below the groove base, a mean depth of impregnation of 2.50 in. by ponding would be required.

For 99 percent of the time, the range of the depth of the impregnation below the groove base would be 1.93 to 2.63 in. for a mean depth of impregnation by ponding equal to 2.5 in. If the groove were cut to 0.5 in. above the reinforcing steel bars, an impregnation depth of 1.75 in. below the groove base would be required to encapsulate the upper reinforcing steel mat, assuming No. 5 bars.

Optimization of Polymerization Time

Strength data presented in Table 2 were used to determine the time for in situ polymerization of the MMA system in concrete. The data indicate that, as expected, the time for polymerization increases with decreasing activation temperatures. The time for polymerization was about 8 hr at 114°F and decreased to 1 hr at 148°F.

By using the hot-water polymerization method on the surface of a typical 8-in. concrete bridge deck slab, an equilibrium temperature of 124°F is reached in 16 hr at a 4-in. depth with the surface temperature at 208°F. Therefore, based on the strength gain data, a suggested polymerization criterion is to maintain the hot-water equilibrium temperature at about 124°F for a period of 5 hr. A total polymerization time of 21 hr is then required.

TABLE 2 Compressive Strength Gain of MMA-Impregnated Mortar Cubes as Related to Time and Activation Temperature

Time (min)	Compressive Strength (psi) at Bath Temperature (°F) 114°	122°	130°	148°
0	1,800	1,800	1,800	1,800
15	-	-	-	3,250
30	-	-	1,680	6,000
40	-	-	-	7,200
60	2,430	2,330	2,500	9,100
120	2,320	2,650	8,220	-
180	2,750	4,380	8,170	-
240	3,150	6,310	-	-
300	5,450	8,540	-	-
360	-	9,450	-	-
420	6,830	-	-	-
480	7,650	-	-	-
510	7,350	-	-	-

Optimization of IR Drying Method

The flow of heat during the heating cycle extends 12 in. beyond the heated area. To better estimate the drying energy used, the energy required to heat the area outside of the heated area was calculated and subtracted from the total energy (in pounds of propane used). Figure 6 shows the heating and drying time and energy used as a function of surface temperature.

As illustrated, the heating time (time to raise the temperature at a depth of 4 in. from ambient to 220°F) decreased and the rate of energy use increased as the surface temperature increased. However, for the drying time (heating time plus the time required for the slab to cool to 100°F) and energy used, there appears to be an optimum condition at approximately 600°F, as both functions initially decrease and then increase as the surface temperature increases.

Visual observations of the slab during the drying

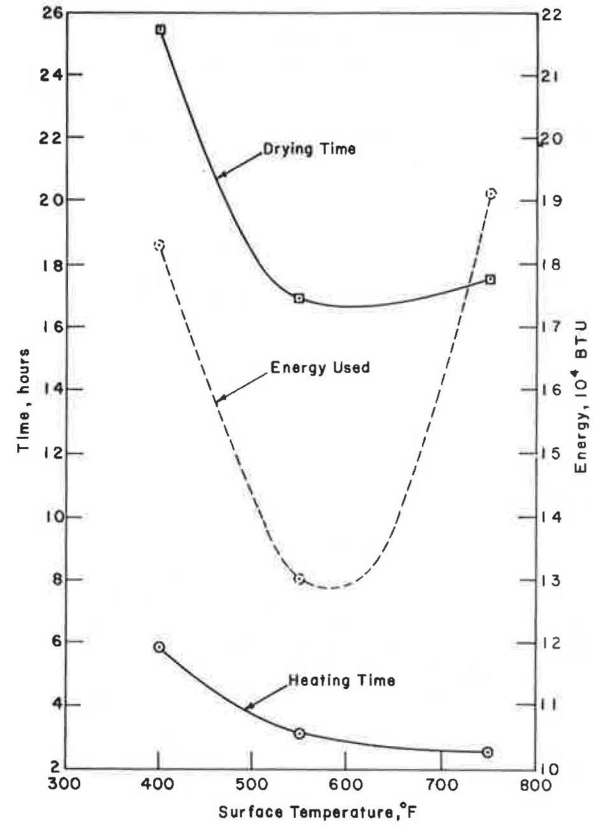

FIGURE 6 Drying and heating time and energy.

cycle indicated that the slab cracked only once during each test cycle. For all three drying tests, the crack was at the centerline of the heater at the edge of the slab, extended through the depth of the slab and 6 in. inward along a line parallel to the centerline of the heater, and ended at the outside face of the heater shield.

A microscopic survey of a polished section sawn from a core from each of the test areas showed no evidence of cracking. That is, at a magnification of 100X, no cracking was visible between the paste and aggregate, within the paste, between the paste and reinforcing, or anywhere within all three of the examined areas.

Laboratory Demonstration of Deep-Grooving Impregnation Method

A 6-ft by 6-ft by 8-in.-thick slab, designed to simulate a section of bridge deck, was constructed in the laboratory. Cores taken from the slab were impregnated for 9, 16, and 40 hr. The rate of impregnation was equal to 0.579 in. per $\sqrt{\text{hours}}$ with a correlation coefficient of determination equal to 0.997. The depth of impregnation was 2.5 in. at 16 hr and was determined to be sufficient for a required depth of impregnation of 2.25 in. with a groove ratio equal to 0.90 (0.90 x 2.5 in. = 2.25 in. = required depth of impregnation below the groove base). The groove spacing was set at 2.25 in. by using the optimum impregnation ratio of 1.00 [groove spacing = (impregnation ratio)(required depth of impregnation below the groove base)]. The optimum groove width was calculated to be 0.75 in. by using a 10 percent by volume MMA loading rate. However, the grooves were cut 0.5 in. wide because of the limitations of the saw.

The three areas dried for the optimization of the IR heating method were impregnated and polymerized by using the ponded hot-water method and the depth of impregnation was determined (see Table 3). The boundary of the impregnation was straight and the depth of impregnation was below the upper rebar mat for all three cores.

TABLE 3 Depths of Impregnations for Grooved Slab

Specimen	Depth at Center-line of Groove (in.)	Depth at Center-line Between Grooves (in.)	Depth of Center-line at Groove (in.)
S-400	3.625	3.625	3.625
S-550	3.75	3.625	3.625
S-750	4.125	4.125	4.125

CONCLUSIONS

1. It is concluded that the grooving of concrete to a depth of 1.5 in. before impregnation with an MMA system can reduce the time required for impregnation--16 hr for grooving versus 45 hr for surface ponding to obtain an impregnation depth of 3.75 in. Also, the method obviates the need for the impregnation chamber required for ponding and pressurized methods.

2. The optimum groove spacing is equal to the required depth of impregnation below the groove base.

3. The impregnation time required for the groove method can be determined from the surface pond impregnation rate by using a groove ratio of 0.90.

4. Minimum energy costs for drying before impregnation can be attained by heating for ~3 hr at a surface temperature of ~600°F. Under such conditions, cracking was not observed in the interior of the test specimens, although cracks from the nearest free edges of the slab to the edge of the heated area did occur.

5. Optimum polymerization conditions were found to be 5 hr at a steady-state temperature of 122°F, which corresponds to a conservative 21 hr of heating with a hot-water pond at a surface temperature of 208°F.

ACKNOWLEDGMENT

The authors wish to acknowledge the support of the National Cooperative Highway Research Program of the Transportation Research Board in funding the research described here as part of a larger project.

REFERENCES

1. Deteriorating Highways and Lagging Revenues: A Need to Reassess the Federal Highway Program. Report CED-81-42. U.S. General Accounting Office, March 5, 1981.
2. Y.P. Virmani. Cost Effective Rigid Concrete Construction and Rehabilitation in Adverse Environments. Project 4K, FPC Annual Progress Report. FHWA, U.S. Department of Transportation, Sept. 30, 1982.
3. J.A. Manson et al. Long-Term Rehabilitation of Salt-Contaminated Bridge Decks. NCHRP Final Report 18-2(3). TRB, National Research Council, Washington, D.C., Oct. 1982.
4. L.E. Kukacka. Concrete-Polymer Materials. Fourth Topical Report, REC-ERC-72-10 and BNL 50328. Brookhaven National Laboratory, Upton, Long Island, N.Y., Jan 1972.
5. J.A. Manson et al. Use of Polymers in Highway Concrete. NCHRP Final Report 18-2(1). TRB, National Research Council, Washington, D.C., Sept. 1975.
6. J.A. Manson et al. Use of Polymers in Highway Concrete. NCHRP Final Report 18-2(2). TRB, National Research Council, Washington, D.C., Sept. 1978.

The authors are responsible for the accuracy of the data and the conclusions and opinions.

Publication of this paper sponsored by Committee on Structures Maintenance.

Abridgment

Application: Deep Grooving—A Method for Impregnating Concrete Bridge Decks

RICHARD E. WEYERS and PHILIP D. CADY

ABSTRACT

Polymer impregnation of concrete is a long-term protection method for chloride-contaminated concrete bridge decks. The deep-grooving impregnation method significantly reduces impregnation time, simplifies equipment needs, mitigates potential fire hazards, and may provide a long-lasting and more skid-resistant surface. The procedures for impregnating a concrete bridge deck using the deep-grooving method are presented. Included are methods used to calculate the optimum groove spacing, width, and depth. An optimum drying criterion using a propane-fired infrared heater is presented. A method for determining the impregnation time and polymerization times and methods for a methyl methacrylate (MMA) monomer system are also presented. In addition, methods for filling the grooves, an estimated total time to impregnate an average bridge, and cost data are presented.

The polymer impregnation of steel-reinforced concrete bridge decks is a process that may provide long-term rehabilitation of salt-contaminated bridge decks where the corrosion of the reinforcing steel is imminent or in its initial stage. Therefore, an investigation into the cause(s) of any observed deterioration and the extent of the chloride contamination should be performed on every candidate deck. The purpose of the investigation is to determine if polymer impregnation is the proper solution to the observed deterioration problem. The investigation should include a topographic survey, half-cell potentials, level of chloride contamination, detection of delamination planes, and depth of concrete cover. In addition, cores need to be taken for petrographic examinations and for determination of the mean surface pond impregnation rate. The application of the deep-grooving impregnation method is based on laboratory results and thus necessitates the need for a full-scale field trial. The field trial procedures for the deep-grooving impregnation method are presented in this paper.

DEEP-GROOVING IMPREGNATION METHOD

The deep-grooving method of the polymer impregnation of concrete bridge decks consists of the following phases:

1. Cutting grooves on lines of equal elevation to a depth of 0.5 in. above the upper steel reinforcing bars,
2. Drying the concrete to a depth of 0.5 in. below the upper steel reinforcing mat,
3. Soak-impregnating the dried concrete by filling the grooves with the monomer, and
4. Filling the grooves with dry sand, impregnating the dry sand with the monomer, and polymerizing the impregnated mass, or filling the grooves after the polymerization of the impregnated concrete.

The optimum spacing of the grooves (distance from edge of groove to edge of groove) is to be equal to the distance from 0.5 in. above the upper steel reinforcing bars to 0.5 in. below the upper steel reinforcing mat (1). Figure 1 shows an example of spacing, where No. 5 steel reinforcing bars are used in both directions; therefore, the spacing of the grooves is equal to 2.25 in. (0.5 in. + 2 x 0.625 in. + 0.5 in.). This value is the required depth of impregnation from the bottom of the grooves. The width of the grooves is determined by dividing 10 percent of the vertical cross-sectional area of the deck to be serviced by one groove by the groove depth. The area to be serviced by the area of one groove is the depth of impregnation required (D - 0.5 + S) times the width (W + S) minus the groove area [(W) (D - 0.5)]. Groove depth will be equal to cover depth minus 0.5 in. (D - 0.5). Therefore,

$$W = \left\{ (0.10)\,[(W + S)(D - 0.5 + S) - (W)(D - 0.5)] \right\} / (D - 0.5) \qquad (1)$$

where

W = groove width (in.),
S = edge-to-edge distance between grooves (in.), and
D = cover depth (in.).

Continuing the previous example and assuming a cover depth of 2 in., the groove depth will be 1.5 in. (2 in. - 0.5 in.), and the groove width can be determined from the preceding equation:

$$W = \left\{ (0.10)\,[(W + 2.25)(2 - 0.5 + 2.25) - (W)(2 - 0.5)] \right\} / (2 - 0.5) \qquad (2)$$

from which W = 0.66 in., and the groove spacing, center-to-center, is W + S = 0.66 + 2.25 = 2.91 in.

The calculation is based on a monomer loading of 10 percent by volume (2). An estimated cost of a grooving machine to cut grooves 0.75 in. wide, 1.5 in. deep, and spaced at 3 in. center-to-center is $480,000. The machine would have a cutting width of 6 ft and would cut the grooves at a rate of about 300 yd^2/hr. The entire deck is to be grooved before the drying phase is started.

The grooved-concrete deck is to be dried with a propane-fired infrared (IR) heater with an optimum constant surface temperature of approximately 600°F (1). The concrete is to be considered dry when the temperature at a depth of 0.5 in. below the upper steel reinforcing mat is equal to 230°F (2). A 24-in.-wide area around the perimeter of the shielded drying area should be covered with insulation that has an insulating value of R-19 (1). An area of 20 x 12 ft can be dried at one time. An estimated cost of a 20 x 12-ft heater is $48,000. R-19 insulation is to be placed over the dried area during the cooling cycle. Thermocouples (two per drying area) are to be placed at a depth of 0.5 in. below

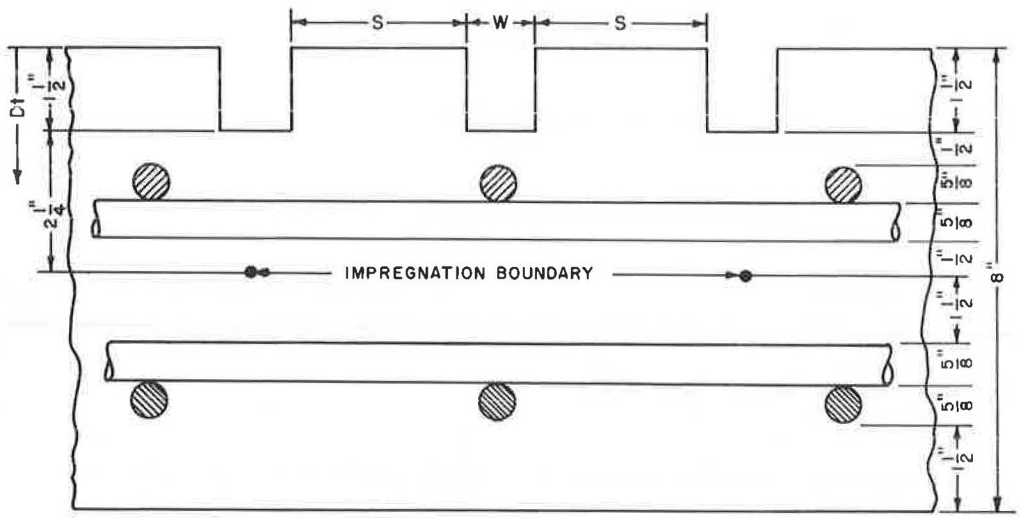

Dt = DEPTH OF POND IMPREGNATION AT TIME t IN HOURS
(0.90) (Dt) = $2\frac{1}{4}$ inches (THE REQUIRED GROOVE DEPTH OF IMPREGNATION)
GROOVE IMPREGNATION TIME = THE TIME REQUIRED FOR D(t) = $2\frac{1}{2}$ inches
GROOVE SPACING S = (1.0) (GROOVE DEPTH OF IMPREGNATION) = (1.0) ($2\frac{1}{4}$ inches)

FIGURE 1 Method for determining the groove impregnation time and groove spacing.

the upper steel reinforcing mat in order to determine when the concrete is dry and when the monomer has polymerized. The propane requirements for drying are expected to average approximately 0.331 gal/ft². Typically, 3 hr is the required heating time needed to achieve drying by using a 600°F constant surface temperature (1).

The time of soak impregnating by grooving is to be determined from the mean surface pond impregnation rate (1). As an example (Figure 1), with a required depth of impregnation of 2.25 in. below the base of the groove, the surface pond impregnation depth (D_t) would be equal to 2.25 in. ÷ 0.90 = 2.50 in. The time of impregnation would then be equal to the time required to impregnate to a depth of 2.5 in. by surface ponding, which is typically 16 hr. Approximately 3 lb of monomer is required per square foot of bridge deck [100 parts methyl methacrylate (MMA) to 10 parts trimethylopropane trimethacrylate (TMPTMA) to 0.5 parts 2,2'- azobisisobuyronitrile (AZO), by weight]. During the impregnation phase, the deck is to be covered with a 4-milthick sheet of polyethylene to reduce the evaporation rate of the monomer and the fire hazard.

After the impregnation phase, the grooves are to be filled with dry, compact, well-graded sand with 100 percent passing the No. 8 sieve and less than 2.0 percent passing the No. 200 sieve. About 4 lb of dry sand are required per square foot of deck. The sand is to be saturated with monomer and the impregnated mass polymerized by placing a polymerization vessel over the impregnated area. The vessel is to be filled with several inches of water, and the water temperature increased to about 205°F with steam. The 205°F water temperature is to be maintained with steam until the monomer is polymerized. The monomer is to be considered polymerized when the thermocouples indicate that a temperature of 122°F has been maintained for 5 hr or 130°F for 2 hr (as shown in Figure 2) at the depth of impregnation.

It is envisioned that the sides and top of the compartmentalized vessel is to be constructed of nonspark metal. The steam pipes would run through the vessel, and the bottom of the vessel would be lined with a nylon-metal laminate. The top, sides, and a 24-in.-wide area encompassing the vessel should be insulated with an insulation material with a value of R-30. Typically, it takes 16 hr to obtain a temperature of 122°F at a depth of 4 in. below the surface with hot water being maintained at about 205°F. Therefore, a conservative estimate of the time to polymerize is about 21 hr.

The total time required to impregnate a bridge deck by the grooving method is going to be dependent on site conditions. However, as an estimate, an average bridge deck that is about 40 ft wide and 216 ft long can be completed in about 10 days by using the grooving method. The estimate assumes one 20-ft lane to be completed at one time by using 1 IR heater (20 x 12 ft) and the following time requirements: 8 hr grooving, 72 hr drying, 16 hr impregnating, and 21 hr polymerizing.

As an alternative, electric blankets similar to those used for curing wax bead concrete may be used

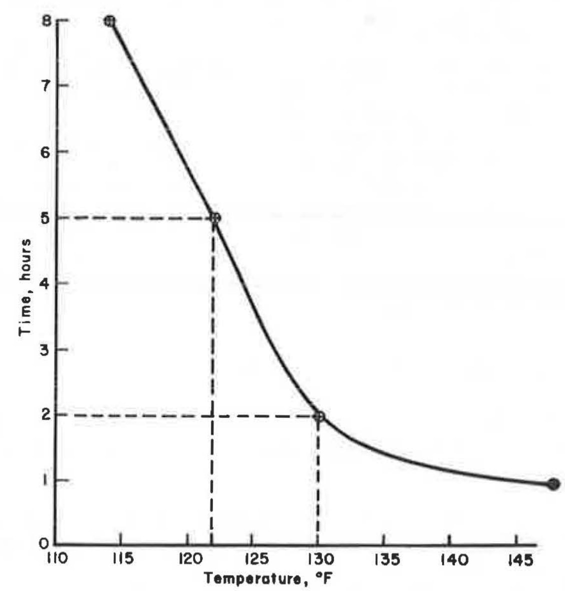

FIGURE 2 Impregnated in situ concrete polymerization time of an MMA system as a function of activation temperature.

to polymerize the MMA monomer system (3). A conservative polymerization time would be about 6 hr [4.25 hr to obtain a temperature of 130°F at a depth of 4 in., see Figure 3 (3), plus 1.75 hr]. The estimated total time required to impregnate an average bridge deck would be reduced to 8.5 days. In either approach, the grooves can either be filled with an ambient cure polymer concrete or latex-modified mortar after the polymerization process has been completed.

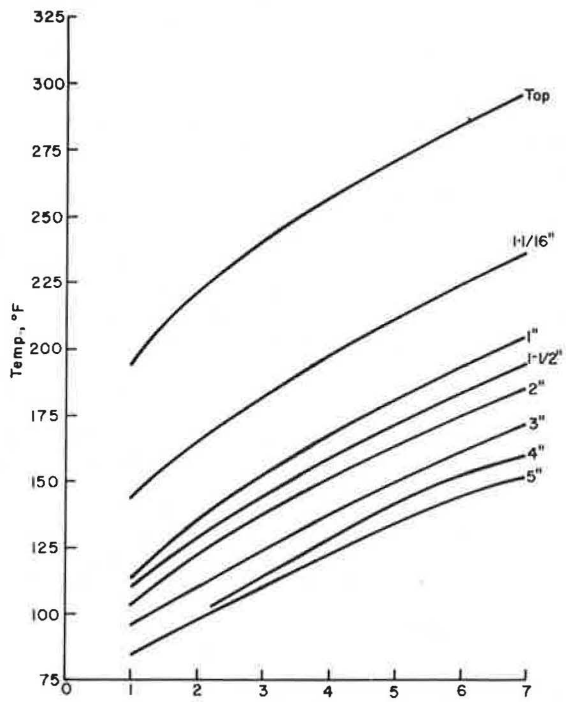

FIGURE 3 Temperature versus time at various depths by using electric heating blankets at 100 to 89 w/ft^2 *(3)*.

COST

The cost data presented are for average 1981 values (4). Road user and traffic maintenance and protection costs were not included. Although these are real and important costs, it is difficult to arrive at representative average values because these costs vary so widely, primarily in response to traffic volume. The data in Table 1 present the average 1981 costs for the deep-grooving impregnation system, present method of deck rehabilitation, deck replacement, and maintenance.

However, decisions based on initial costs or individual events will generally not result in a least-cost solution. Least-cost solutions account for all of the costs incurred over the service life of a structure, considering the time value of money. Least-cost solutions may be realized by comparing equivalent uniform annual cost for perpetual service, in the case of bridge decks, or capitalized cost (present worth of perpetual service). By using engineering economic evaluation methods with a true cost of long-term borrowing (6 percent interest factor), the capitalized cost of the current method of concrete bridge deck rehabilitation is about \$12.80/ft^2 compared with \$7.96/ft^2 for the deep-grooving impregnation method. Therefore, the deep-grooving method of impregnation offers a cost-effective solution to significant problems, and thus efforts should be extended to further develop the method through the application of full-scale field trials.

TABLE 1 Summary of Cost Data

Item, Material, or Activity	1981 Estimated Cost (\$/ft^2)
Deep-grooving impregnation system	
Deep grooving (0.75 in. x 1.5 in. deep, 3 in. center-to-center	1.00
Drying	1.06
Impregnation	0.98
Polymerization	2.29
Impregnant (MMA)	2.49
Present method of deck rehabilitation	
Scarification of sound areas of deck (0.25 in.)	0.59
Removal of deteriorated concrete and PCC[a] patch	12.89
Deck modifications (raising expansion dams, scuppers, and back walls)	0.96
Latex-modified mortar or concrete (1.5 in. thick)	3.64
Deck replacement	
Complete deck removal	11.11
New deck with epoxy-coated rebars in top mat only	13.73
Maintenance: hot-mix bituminous patching	1.18

[a]PCC = portland cement concrete.

ACKNOWLEDGMENT

The authors wish to acknowledge the support of the National Cooperative Highway Research Program of the Transportation Research Board in funding the research described here as part of a larger project.

REFERENCES

1. R.E. Weyers. Deep Grooving--A Method for Impregnating Concrete Bridge Decks. Ph.D. thesis. Department of Civil Engineering, Pennsylvania State University, University Park, 1983.
2. J.A. Manson et al. Use of Polymers in Highway Concrete. NCHRP Final Report 18-2(1). TRB, National Research Council, Washington, D.C., Sept. 1975.
3. Internally Sealed Concrete Status Report. FHWA, U.S. Department of Transportation, Feb. 1976.
4. J.A. Manson et al. Long-Term Rehabilitation of Salt-Contaminated Bridge Decks. NCHRP Final Report 18-2(3). TRB, National Research Council, Washington, D.C., Oct. 1982.

The authors are responsible for the accuracy of the data and the conclusions and opinions.

Publication of this paper sponsored by Committee on Structures Maintenance.

Cathodic Protection of Reinforced Concrete by Using Metallized Coatings and Conductive Paints

JOHN A. APOSTOLOS

ABSTRACT

Corrosion-caused distress to reinforced-concrete structures is a serious and continuing problem. A practical mitigation measure is cathodic protection of the embedded reinforcing steel. In this paper the results of an ongoing laboratory and field study that tests proprietary conductive paints and flame-spray metallizing as conductive coatings/anodes on concrete are described, and their physical characteristics, behavior, and economics as part of cathodic protection systems are also discussed. Results to date indicate that several of the paints and most of the metals tested provide adequate conductivity and bond to the concrete, but differ significantly in ease of application, toxicity, aesthetics, and economics. Of the materials tested, zinc metallizing appears to provide the most viable combination of physical characteristics and economics for cathodic protection of concrete reinforcement.

Concrete normally provides excellent protection from corrosion to embedded reinforcing steel by forming a thin, stable oxide layer on the surface of the metal. This layer acts as a barrier to further corrosion, a phenomenon known as passivation. Chloride ions can destroy this passivating oxide film and allow corrosion to proceed at a rapid rate, given an adequate supply of oxygen and moisture.

One successful method of stopping or significantly reducing the corrosion process is the introduction of direct current (dc) to the corrosion cell, but flowing in the opposite direction to the natural process. This current, delivered by an external source, blocks the normal flow of charges and thus converts the corroding area (the anode) into a noncorroding area (a cathode). This method is called cathodic protection (CP).

The first reported application of CP to aboveground reinforced concrete was by the state of California in 1959 (1), and the first application of CP to a concrete bridge deck was reported by the state of California in 1974 (2). Since then a number of agencies have revised and improved the pioneering system (3-5) and, currently, CP is considered a reliable means of controlling corrosion in the top mat of bridge deck reinforcing steel (6-10).

The pioneering system distributed CP current evenly throughout the surface of the concrete by means of a layer of coke breeze (small particles of coke, a byproduct of the petroleum industry, consisting of approximately 97 percent carbon; it is a good conductor).

More recently, considerable interest has been shown in substituting coke with conductive paints, conductive mortars, conductive (platinum-coated) wires set into cut grooves, and other materials with a combination of conductive and adhesive properties (11-13). The aim of these studies was to develop a conductive layer with the satisfactory current distribution capabilities of the coke system but improving on one or more of its disadvantages [better adhesion, use on vertical surfaces such as bridge substructures, avoiding trapped water, eliminating asphalt concrete (AC) overlays, reducing costs, and so forth].

In this paper the interim results of a study concentrating on tests and evaluation of two general types of conductive material--proprietary conductive paints and sprayed molten metals applied by the flame-spraying process--are presented. Conductive paints are applied in a conventional manner. The flame-spraying process involves melting a continuously fed metal wire by an oxygen-acetylene flame and spraying the molten metal by compressed air onto the concrete surface (14). Adhesion is achieved primarily by mechanical bond to the prepared (sandblasted) concrete surface. (It should be noted that flame spraying is one of three methods of metallizing, the other two being arc spraying, in which the wire is melted by an electric arc, and plasma spraying, in which the metal, in the form of powder, is melted in a nitrogen-oxygen or argon-hydrogen gas flame.)

Testing concentrated on the properties that have a direct influence on their suitability for CP applications: conductivity, consumption of anodes, adhesion to concrete, resistance to weathering, environmental impact, aesthetics, and economics.

The basic workplan was to select as many commercially available conductive materials (paints and metals) as practicable and perform initial laboratory testing to determine their physical characteristic and suitability. Following this initial determination, the most promising of these materials were selected and they were applied to a reinforced-concrete slab mounted in an outdoor exposure. When sufficient testing and evaluation has been performed on the slab, the most promising of the surviving candidate materials were selected and applied to a real-world structure.

Currently, the laboratory and concrete slab testing have been completed, and two candidate materials, flame-sprayed zinc and flame-sprayed Sprababbitt A, alloy have been applied to a real structure (pier 4 of the Richmond-San Rafael Bridge in San Francisco Bay) and are delivering CP current to the reinforcing steel. In this paper the findings to date are documented.

SELECTION OF MATERIALS

Review of the literature and inquiries to industry resulted in the selection of seven paints and six metals or alloys in wire form. The paints were manufactured and sold specifically for their conductivity. Several had been investigated in a previous study (11). The metals and alloys were selected on the basis of reasonable cost and availability in wire form; their expected performance as conductors of CP current was unknown, because their use in this manner had not been considered or tested before this project. The paints and metals tested are given in the following lists.

The paints tested were as follows:

1. Cho-Shield 4130--a carbon-filled latex paint (by Chomerics, Woburn, Massachusetts);
2. E-Kote 3062--an iron-filled acrylic paint (by Acme Chemicals and Insulation Company, New Haven, Connecticut);
3. E-Kote 3063--a nickel-filled acrylic paint (by Acme Chemicals and Insulation Company);
4. Electrodag 112--a graphite-filled acrylic paint (by Acheson Colloids Co., Port Huron, Michigan);
5. Konductokure--a carbon-filled concrete curing compound (by Master Builders, Cleveland, Ohio);
6. Con-Deck W-0731--a carbon-black filled latex paint (by Wescorp/DAL Industries, Inc., Mountain View, California); and
7. Con-Deck W-0735--a carbon-black filled latex paint (by Wescorp).

The metals tested were as follows:

1. Aluminum SF--a 43 alloy that contains 94 percent aluminum and 6 percent silicon (by METCO Inc., Westbury, Long Island, New York);
2. Aluminum--a 1100 commercially pure 99+ percent aluminum (by METCO);
3. 405 Bond--a clad wire, 80 percent nickel encased in a 20 percent aluminum outer sheath (by METCO);
4. Metcoloy #2--a 420 stainless steel; contains 13 percent chromium and 0.5 percent nickel (by METCO);
5. Sprababbitt A--a tin base (lead-free) babbit that contains 89 percent tin, 7.25 percent antimony, 3.5 percent copper, and 0.25 percent lead (by METCO); and
6. Zinc--commercially pure, 99+ percent zinc (by METCO).

LABORATORY TESTING

Conductivity

A series of tests was devised and performed in order to test the ability of each material to conduct CP current and to obtain an estimate of its rate of consumption. All wires were 0.125 in. nominal diameter.

Wire Consumption

All metals in wire form were tested in the circuit shown in Figure 1. A measured and weighed length of each wire was immersed in a container of salt water (3.5 percent NaCl solution by weight). The wire was partly coated with wax so that a length of 2.5 in. would be in contact with the water. An external power supply created a potential in the range of 1 to 2 V between the wire and the aluminum foil lining of the container. This caused the wire to discharge current into the water and thus consume itself. Testing was ended when a significant portion had been consumed, but before the wire broke at its thinnest point. Subsequent weighing and computations provided values for consumption rates (Table 1).

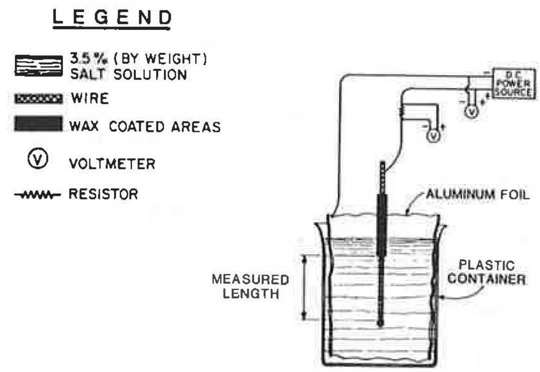

FIGURE 1 Schematic–wire consumption test.

TABLE 1 Consumption Rates of Metals in Wire Form

	Consumption Rate	
Metal	Ampere-Hours per Pound	Pounds per Ampere-Year
Aluminum SF	1,057.3	8.3
Aluminum 1100	1,115.9	7.8
405 Bond	1,184.3	7.4
Metcoloy #2	440.8	19.9
Sprababbitt A	327.0	26.8
Zinc	366.7	23.9

CP Current Delivery to Reinforced Concrete

All paints and metals were tested in the circuit shown in Figure 2. Each material was painted or sprayed in the form of stripes on the surface of all reinforced-concrete test specimens. Applied quantities were estimated, but because of the small areas involved, the precision of these values was low. The main usefulness of this test was to imitate real-life conditions (with the exception of current density) and establish whether or not some coatings (especially the metals) would lose bond or quickly develop a poorly conductive oxide layer between themselves and the concrete.

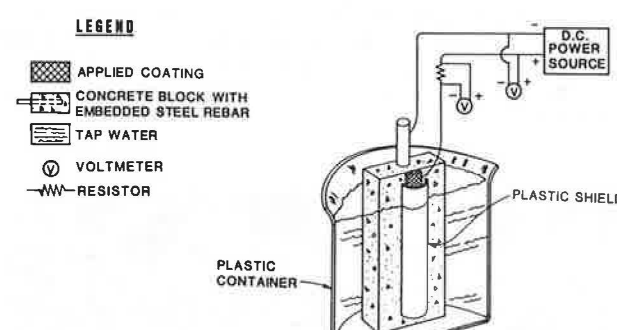

FIGURE 2 Schematic–CP current delivery to reinforced-concrete specimen.

The concrete specimens measured 2.25 x 4.5 x 15.0 in. and each contained a 0.5-in.-diameter embedded reinforcing bar. Because most real-structure CP applications would be retrofitted on already salt-contaminated structures, the reinforced-concrete specimens were selected from a stockpile that had been previously exposed to months of immersion in saturated salt water.

Coating was performed after a light sandblasting to remove any laitance and provide surface roughness, or tooth, for mechanical bonding.

The reinforced-concrete specimens were immersed in a container of tap water. As water was absorbed into the concrete, it reactivated the salt within and thus provided resistance values that were closer to real-life structures during wet periods.

To ensure that CP current would be discharged directly from the conductive coatings to the concrete, the exposed surface of the coatings had to remain dry. This was accomplished by a plastic shield epoxied around the conductive material and sealed at the bottom. Being "in the dry," the coatings could not discharge current into the water, but acted in a manner that simulated real-life conditions.

An external power supply created a constant potential of 12 V between the conductive material and the embedded steel. This caused the coating to discharge current into the concrete and thus consume itself. In most cases the current delivered to the steel was considerably in excess of that needed to provide full cathodic protection; the aim of the test was to consume the coating at a rapid rate.

Testing was ended after approximately 500 hr. For some specimens, the circuit resistance became so high that testing was ended sooner; for others, it appeared that they could have continued to discharge current for a longer time period.

It was found that, in most cases, circuit resistance increased with time as current was being delivered, which indicates a consumption of conductive material and a gradual buildup of an oxide layer, but the effect was not severe. No disbonding was noted on the coatings that had satisfactory original bond.

Adhesion to Concrete

A critical property of conductive coatings is their ability to adhere well to concrete surfaces, both clean and salt contaminated, and to maintain their adhesion over many years while delivering CP current.

Pullout bond tests were conducted by using a 0.75-in.-diameter aluminum dolly epoxied to the coating surface. The epoxy is allowed to cure, and the dolly is then pulled with a calibrated device until bond failure occurs (Figure 3). The tensile stress at failure, in pounds per square inch, is directly read from the device (an Elcometer Adhesion Tester Model 106).

FIGURE 3 Adhesion tester and dollies on coated concrete.

Bond of Newly Applied Coats

Soundings of the entire surface and pullout tests were conducted at six different locations on each coating after it was placed on a reinforced-concrete specimen and allowed to cure. All materials bonded well, with test values ranging from 125 to 525 lb/in.^{2}. On average, the initial bond for both paints and metals was 300 lb/in.^{2}. Most disbonding occurred at the concrete and coat interface, although some paints failed within their layer, and some metals pulled concrete with them.

Bond Versus Coating Thickness

Although not all materials were tested, it was found that some materials, while offering satisfactory bond when applied in thin coats, would readily disbond when thicker coats were attempted. Aluminum curled and peeled-off readily, whereas Sprababbitt A and zinc remained well-bonded after being applied to a maximum thickness (to date) of 24 and 35 mils, respectively.

Weatherability

All paints and metals were applied to lightly sandblasted cement mortar plates (3 x 12 x 0.375 in.). A set of plates was then exposed outdoors, and a duplicate set was subjected to testing in an accelerated weathering chamber. The principal aim of these tests was to visually detect any obvious deterioration or change in appearance due strictly to weathering.

Outdoor Exposure

Specimens were mounted on wooden racks facing south and mounted vertically. The location was the roof of a building in Sacramento, California, which has a semirural, noncorrosive atmosphere, with air temperature extremes from 28° to 106°F and total rainfall of 37 in. during the test period. To date (January 1984), the specimens have been exposed for 1.3 years. The last inspection, at 0.9 year, indicated that all specimens were adhering well and had no major structural defects such as cracking.

Weathering Chamber

Specimens were mounted in an accelerated weathering chamber conforming to ASTM G53-77. This chamber subjected the specimens to cyclic conditions consisting of alternate 4 hr of ultraviolet light at 140°F, and 4 hr of moisture condensation at 104°F. Inspection of the specimens was conducted at 1,000 hr and at 2,000 hr, at which time the test was ended. These inspections indicated that all specimens were adhering well and had no major structural defects.

The paints remained in satisfactory condition, with a slight chalking noted in some, and the metals exhibited a slight darkening in color. The only exceptions were the 405 Bond and Metcoloy #2, which developed rust-colored stains. Results from the outdoor exposure were compatible with the weathering chamber.

Environmental

Inquiries to the various paint and metal wire suppliers provided information on the environmental aspects of their products (Table 2). In addition, environmental and health hazards from sandblasting should also be considered.

With the exception of the E-Kote paints and Metcoloy #2, all materials tested were apparently either nonhazardous or required that the operator wear a respirator. In practice, a mask delivering bleed air from an air compressor is used.

TABLE 2 Environmental Aspects of Materials Tested

Material	Environmental Aspects
Cho-Shield 4130	Water-based solvent; no hazards listed
E-Kote 3062	Solvent-based cellosolve acetate and methyl cellosolve, 25 percent; note that the state of California issued a hazard alert (May 1982) on glycol ethers (cellosolve solvents); they list harm to reproductive systems of test animals
E-Kote 3063	Same solvents and warning as E-Kote 3062
Konductokure	Can be several formulations under ASTM C 309 type 1 for concrete curing compounds; no hazards assumed
Con-Deck W-0731	Water-based solvent; no hazards listed
Con-Deck W-0735	Water-based solvent; no hazards listed
Aluminum SF	No solvents; excessive fume concentration requires respiratory protection
Aluminum 1100	No solvents; excessive fume concentration requires respiratory protection
405 Bond	No solvents; excessive fume concentration requires respiratory protection
Metcoloy #2	No solvents; alloy contains 13 percent chromium and requires complete respiratory protection in the fume area; fumes are extremely hazardous
Sprababbitt A	No solvents; alloy contains 0.25 percent lead and requires respiratory protection
Zinc	No solvents; fumes are toxic; respiratory protection should be provided wherever the fume concentration is sufficiently high to warrant it

Aesthetics

Many reinforced-concrete structures are exposed to public view. This necessitates consideration of the aesthetic qualities of each conductive coating.

All conductive paints tested were either black in color or very dark grays, approaching black. All metals tested were light silvery gray in color, although each material had its own characteristic shade.

After discharging considerable CP current, oxides leached to the surface of the coatings. Each had its own visual characteristics, with most paints showing some gray, except for E-Kote 3063, which showed some bright green. Each metal provided its own characteristic oxide--the aluminum being black or white, Metcoloy #2 being rusty, and the rest being a whitish color.

Economics

Pertinent data and cost estimates (in 1983 dollars) of the materials in raw form and applied in-place are given in Table 3. Because paints can be applied at a considerably faster rate than metals, this is reflected in lower labor costs. In addition to the costs presented in Table 3, a light sandblast (at \$0.50/ft^2) would be necessary to provide adequate bond on all coatings, and is especially critical for the metallic coatings.

The final economic analysis must include data on the efficiency of each material: How many ampere-years will a given weight (or thickness) of coating deliver under real-life conditions, and what is the maximum useful quantity that can be applied? The continuing study is addressing these questions, but it is not completed as of this date. Initial indications suggest that the efficiency of flame-sprayed zinc is at the 50 percent range, which, if confirmed, is a highly acceptable figure from the economics standpoint.

Evaluation of Test Results

Following the laboratory phase of testing, a selection was made of the more suitable materials for further larger-scale testing. The evaluation and selection was conducted, essentially, by noting the undesirable characteristics of the materials, as follows:

1. Environmental hazards: E-Kote 3062, E-Kote 3063, and Metcoloy #2;
2. Poor conductivity: Con-Deck W-0731;
3. Poor bond: Aluminum SF and Aluminum 1100;
4. Poor resistance to weathering: none;
5. Poor aesthetics (assuming black is acceptable): Metcoloy #2 and 405 Bond; and
6. High cost: Cho-Shield 4130, Konductokure, Con-Deck W-0735, 405 Bond, and Sprababbitt A.

This initial evaluation pointed to zinc as the superior candidate for further testing. It appears to be an inexpensive material with excellent conductivity and bond to concrete. It was decided to study the performance of some of the most promising materials on a larger-scale test under outdoor exposure

TABLE 3 Estimated Economics of Materials Tested

	Material Cost		Weight					Cost of Coating (\$/lb)	
Material	Dollars per Gallon	Dollars per Pound	Pounds per Gallon	Pounds per Foot[a]	Spray Rate (lb/hr)	Percent Solids	Percent Loss[b]	Material Only	Material In-Place
Cho-Shield 4130	22.00		6.7		27	37	25	15	21
E-Kote 3062	25.20		19		76	75	25	2	3
E-Kote 3063	70.80		16		64	63	25	9	11
Electrodag 112	41.40		9.7		39	34	25	15	19
Konductokure	14.75		11.5		46	65	25	3	5
Con-Deck W-0731	32.00		10		40	55	25	8	10
Con-Deck W-0735	27.50		9		36	29	25	10	14
Aluminum SF		2.34		0.0142	12	100	25	3	12
Aluminum 1100		2.30		0.0141	12	100	25	3	12
405 Bond		24.53		0.0274	5	100	25	33	54
Metcoloy #2		2.66		0.0417	13	100	25	4	12
Sprababbitt A		9.86		0.0396	50	100	45	18	21
Zinc		1.18		0.0376	32	100	50	2	8

[a] Weight for 1/8 in. diameter wire.
[b] Measured for Sprababbitt A and zinc; estimated for the rest.

on a simulated real structure. The materials selected were E-Kote 3063 (its environmental hazard was unknown at that time), Metcoloy #2, with a thin overcoat layer of Aluminum 1100; Sprababbitt A; and zinc.

SIMULATED FIELD TESTING

Four selected materials were applied in an outdoor exposure to a 12-year-old reinforced-concrete slab. This slab (6 ft x 7 ft x 5.625 in.) was cast on March 19, 1971, in connection with a previous project and was heavily contaminated with salt.

For this test the slab was sandblasted and mounted vertically, thus simulating a wall. Vertical stripes (4 x 60 in.) of conductive materials were applied to the smooth (formed) face of the slab. Smaller stripes (4 x 20 in.) were also applied as reserves (Figure 4).

Before the coating application, electrical connection devices (Figure 5) were fastened flush with the concrete surface by using epoxy. These connectors consisted of a 2 x 2 x 0.03-in. copper plate, which received a coating along with the concrete, and a binding post to which the conductor carrying the CP current was connected. The epoxy (a dielectric) prevents the current from being discharged directly from the copper plate to the concrete. Instead, the current flows to the conductive coating and is distributed over the entire coated surface.

FIGURE 4 Reinforced-concrete slab with coated stripes.

In order to bring the extremely dry condition of the slab to a more normal stage, a mist sprinkler system was installed and operated for 2 sec every 10 min, keeping the surface slightly damp. The coatings were subjected to two basic tests: bond to concrete and delivery of CP current and subsequent consumption.

Adhesion to Concrete

Three 0.75-in.-diameter aluminum dollies were epoxied to each material at different locations on the stripe. In addition, the stripes were sounded for disbonded areas. The results of the adhesion tests are given in Table 4.

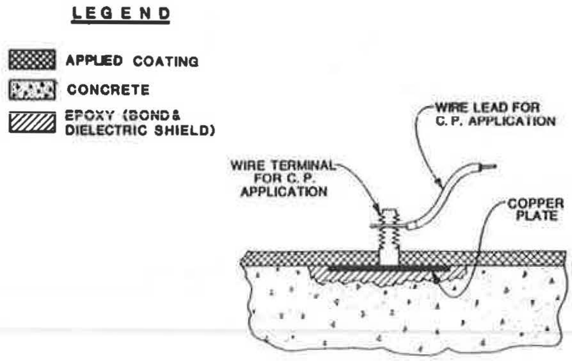

FIGURE 5 Schematic—electrical connectors.

TABLE 4 Bond Tests on Reinforced-Concrete Slab

Material	Disbonded Area (%)	Bond Strength[a] (lb/in.^{2})
E-Kote 3063	–[b]	175
Metcoloy #2/aluminum	10	100
Sprababbitt A	–[b]	150
Zinc	–[b]	200

[a] Average of three tests.
[b] None.

Coating Consumption

All four materials were tested in the circuit shown in Figure 6. The external dc power supplies were adjusted to deliver a constant current of 0.050 amperes (30 milliamperes per square foot of coating) up to the point where the circuit resistance required a maximum of 30 V. Current and voltage were continuously monitored with automatic data-recording devices. It should be noted that the current density being applied was considerably higher than the expected value in an operational system. This was done to obtain useful data in a period of months, rather than years. Figure 7 presents the test record to

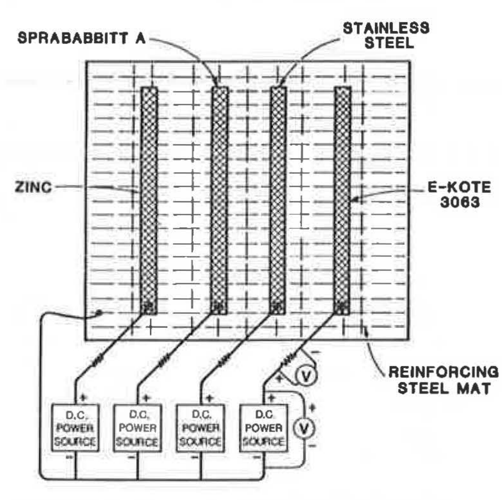

FIGURE 6 Schematic—CP current delivery to reinforced-concrete slab.

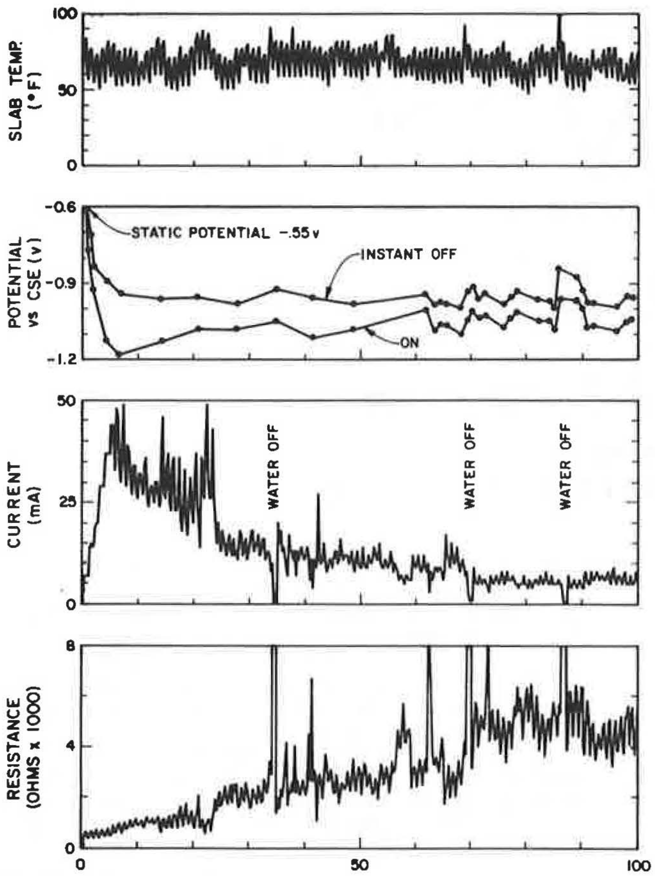

FIGURE 7 Record of zinc strip data for reinforced-concrete slab.

date for the zinc stripe, along with the polarized potentials taken of the reinforcing steel (on and instant-off potentials) versus copper-copper sulfate.

FIELD APPLICATION ON A REAL STRUCTURE

A reinforced-concrete pier of a major structure was selected for application and testing of flame-sprayed zinc. In addition, flame-sprayed Sprababbitt A was also selected because of its bond, conductivity, and aesthetics (although its current cost would not make it economical).

The structure is pier 4 of the Richmond-San Rafael Bridge, located in the northern half of San Francisco Bay. Each pier consists of two reinforced-concrete columns (3.5 x 3.5-ft cross section) of varying height. Pier 4 columns are 20 ft high and their base is cast monolithically onto 6-ft-diameter solid reinforced-concrete shafts. The column bases are about 10 ft above high tide and are subject to a combination of salt air, fog, rain, and wave action. The resulting corrosion distress has been severe enough to necessitate replacement of entire columns in nearby piers.

One column was coated with zinc and the other with Sprababbitt A. Before coating, the concrete was sandblasted and copper and stainless-steel electrical connections (Figure 5) were epoxied onto the concrete surface. To study the distribution of current, the metals were applied in four horizontal bands on each column, with 6-in. bare gaps between them, as shown in Figure 8. The bare gaps were used as locations for taking electrical potential measurements.

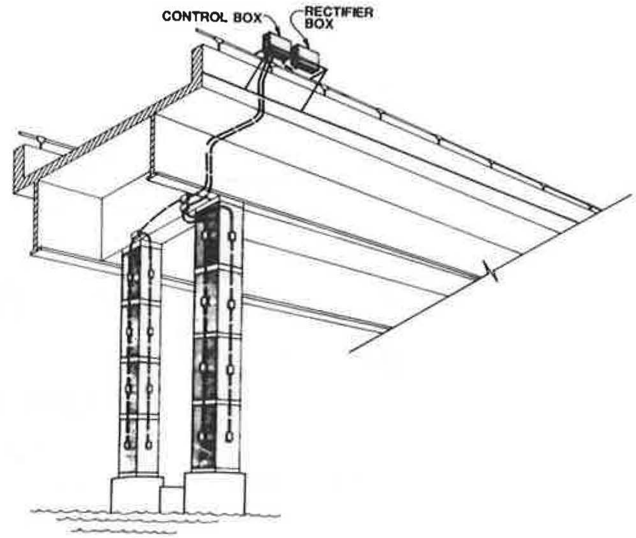

FIGURE 8 Pier 4, Richmond-San Rafael Bridge.

Adhesion to Concrete

Four 0.75-in.-diameter aluminum dollies were epoxied to each band, one to each face of the column. In addition, the coated areas were sounded for disbonded areas. The results of the adhesion tests are given in the following table (note that the bond-strength measurements are from an average of 14 tests):

Material	Disbonded Area (%)	Bond Strength (lb/in.^{2})
Sprababbitt A	None	225
Zinc	None	330

Coating Consumption

Each column was connected to its own CP power supply, which consisted of a commercial ac to dc rectifier capable of delivering 50 V and 5 amperes. Connections to each coated band were made as in the circuit used previously on the concrete slab. CP current was applied by adjusting these constant-voltage-type rectifiers initially to 3 V nominal output, and allowing the current to vary, depending on the concrete resistance.

Because of the changing environment (temperature, wind, tides, fog, rain, and so forth), the current densities varied, as expected, averaging to date 0.98 and 0.84 milliamperes per square foot of steel for Sprababbitt A and zinc, respectively, with peaks approaching, and at times exceeding, 2 milliamperes per square foot during wet weather (Figure 9).

CONCLUSIONS

It is too early to evaluate the results on the pier. At this time, both coatings are performing well. It is estimated that, at the present average current densities, the coatings will theoretically last 17 years for Sprababbitt A (estimated coating = 0.29 lb/ft^2) and 21 years for zinc (estimated coating = 0.30 lb/ft^2). Allowing an efficiency factor (estimated at this time to be 50 percent) the Sprababbitt A should provide CP for about 9 years and the zinc for about 10 years.

Currently, cathodic protection of reinforced concrete by using flame-sprayed zinc appears to be a viable and economic method of controlling corrosion.

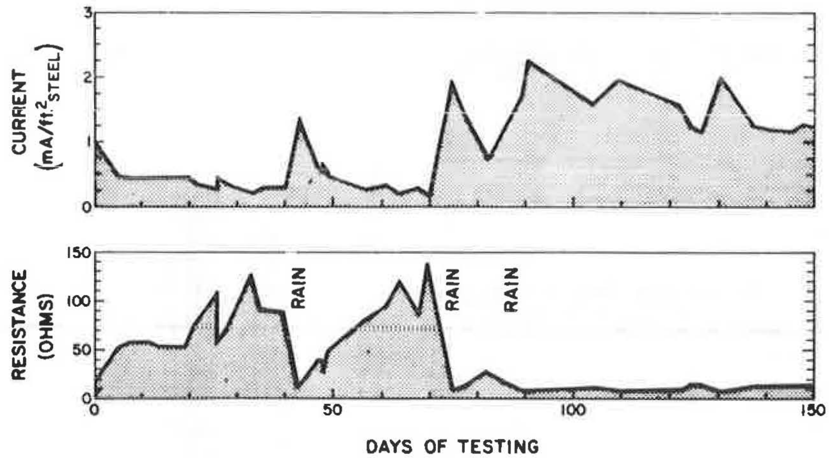

FIGURE 9 Record of zinc-coated column—pier 4, Richmond-San Rafael Bridge.

The technique offers a significant breakthrough in the technology, leading the state of California to apply for a pertinent U.S. patent. Of the materials tested, zinc appears to be superior in several areas, including bond to concrete, environmental hazards, and cost.

Based on the findings to date, the estimated total cost of applying CP to a 10,000 ft^2 bridge deck by using zinc and including an asphaltic-concrete overlay or wearing course would be $4.20 to $5.20 per square foot for a 10-year design life. This contrasts with $30 or more per square foot for a deck replacement.

Further study is recommended to develop nonhazardous formulations for the more promising conductive paints and to test other metals and alloys, such as aluminum-zinc or mild steel. Arc spraying and plasma spraying should also be investigated for suitability in field applications.

ACKNOWLEDGMENT

Presented in this paper were findings of research sponsored by the state of California and the FHWA under the Highway Planning and Research program.

Participating in the work were Donald L. Spellman, Richard A. Carello, Forrest Myhres, Kerri M. Howell, Galen C. Yeaw, and Robert Bridwell.

REFERENCES

1. R.F. Stratfull. Progress Report on Inhibiting the Corrosion of Steel in a Reinforced Concrete Bridge. Corrosion, Vol. 15, No. 6, 1959, p. 65.
2. R.F. Stratfull. Cathodic Protection of a Bridge Deck; Preliminary Investigation. Materials Performance, Vol. 13, No. 4, 1974, p. 4.
3. W.J. Ellis and R.L. Bianchetti. State-of-the-Art Report--Corrosion Control and Repair of Concrete Bridge Structures. NCHRP Project 12-19. TRB, National Research Council, Washington, D.C., 1979.
4. R.E. Colson and W.J. Ellis. Cathodic Protection of Concrete Bridge Structures. NCHRP Project 12-19. TRB, National Research Council, Washington, D.C., Sept. 1980.
5. G.C. Chang, J.A. Apostolos, and F.A. Myhres. Cathodic Protection studies on Reinforced Concrete. Report FHWA/CA/TL-81/02. California Department of Transportation, Sacramento, 1981.
6. P.J. Jurach. An Evaluation of the Effectiveness of Cathodic Protection on Seven Bridge Decks. Report FHWA/CA/SD-80/1. California Department of Transportation, Sacramento, 1980.
7. J.P. Nicholson. New Approach to Cathodic Protection of Bridge Decks and Concrete Structures. In Transportation Research Record 762, TRB, National Research Council, Washington, D.C., 1980, pp. 13-17.
8. H.J. Fromm. Cathodic Protection for Concrete Bridge Decks. Paper 40. Presented at National Association of Corrosion Engineers Conference Corrosion 81, Toronto, Ontario, Canada, April 6-10, 1981.
9. J.B. Vrable. Cathodic Protection for Reinforced Concrete Bridge Decks: Laboratory Phase. NCHRP Report 180. TRB, National Research Council, Washington, D.C., 1977, 135 pp.
10. J.A. Apostolos. Cathodic Protection of Reinforced Concrete Using Flame Sprayed Zinc. Paper 180. Presented at National Association of Corrosion Engineers Conference Corrosion 83, Anaheim, Calif., April 18-22, 1983.
11. R.P. Brown and R.J. Kessler. A New Concept in Cathodic Protection of Steel in Concrete--The Use of Conductive Materials. Paper 179. Presented at National Association of Corrosion Engineers Conference Corrosion 83, Anaheim, Calif., April 18-22, 1983.
12. J.S. Tinnea. In Situ Analysis of Saw Slot Installed Bridge Deck Cathodic Protection. Paper 181. Presented at National Association of Corrosion Engineers Conference Corrosion 83, Anaheim, Calif., April 18-22, 1983.
13. H.S. Ingham and A.P. Shepard. Flame Spray Handbook--Volume 1: Wire Process, 8th ed. METCO Inc., Westbury, Long Island, N.Y., 1969.
14. The Flame Spraying Processes. Bull. 136C. METCO Inc., Westbury, Long Island, N.Y., 1967.

---

document and as convenient identification labels. (It is not practical to refer to paints by their formulations throughout the text.)

It should be noted that the products mentioned in this study have not been used in the manner intended by their manufacturers, but in a novel manner. Success or failure in this project should not reflect on their performance when used in normal service.

Publication of this paper sponsored by Committee on Corrosion and Committee on Performance of Concrete.

Cathodic Protection of Bridge Substructures: Burlington Bay Skyway Test Site, Design and Construction Phases

D. G. MANNING, K. C. CLEAR, and H. C. SCHELL

ABSTRACT

The design and construction phases of a research program to develop an effective cathodic protection system for use on bridge substructures are described. Construction of four experimental systems on columns of the Burlington Bay Skyway Bridge was completed in 1982. One sacrificial anode system and three impressed-current systems were installed, each covering approximately 38 m^2 of column surface. The sacrificial anode system used zinc ribbon anodes with a shotcrete overcoat. A conductive polymer concrete was used as the primary anode in all the impressed-current systems. In System 1 the anodes were used with a shotcrete overcoat. System 2 consisted of the primary anodes with an exposed secondary anode of conductive paint. System 3 employed a secondary anode network of multifilament carbon strand, also with a shotcrete overcoat. A range of instrumentation was designed and installed to determine the effectiveness and efficiency of the four systems.

Considerable efforts have been expended in recent years to develop methods for the rehabilitation of highway bridges that have deteriorated as a result of the corrosion of embedded reinforcement. Most of this work has concentrated on bridge decks (1,2), but similar deterioration is present in substructure elements where it is more difficult and expensive to repair.

Of all the methods available for the repair of structures, only cathodic protection positively arrests the corrosion process. A system of cathodic protection has been used for the rehabilitation of bridge decks in Ontario since 1974 (3,4). Although the principles of this treatment are applicable, the materials and methods of construction used for bridge decks cannot be used on substructures.

OBJECTIVES OF RESEARCH PROGRAM

The overall objective of the research program initiated by the Ontario Ministry of Transportation and Communications in 1981 was to develop a method for the permanent repair of bridge substructures.

Cathodic protection was selected as the most promising method of achieving this goal. A number of projects were begun in support of the program objective. These included laboratory and exposure-plot studies of the various components of cathodic protection systems. The major project in the program involved the design, installation, and evaluation of four experimental systems. Each system consisted of a small-scale section applied to a real structure such that data could be collected to be used in the design of a full-scale demonstration of cathodic protection on a bridge substructure. The specific objectives of this project were to

1. Determine the effectiveness and efficiency of each system in stopping corrosion,
2. Make a technical and economic comparison of the systems, and
3. Identify potential long-term deficiencies.

The design and construction phases of this project are described in this paper.

GENERAL REQUIREMENTS OF A CATHODIC PROTECTION SYSTEM

Cathodic protection is a process that prevents the anodic corrosion reaction by creating an electric field at the surface of the metal so that current flows into the metal (5). This sets up a potential gradient at the metal surface that prevents the release of metal ions as the product of corrosion.

The source of the electric field that opposes the corrosion reaction may be a direct current power supply (usually a transformer rectifier) connected to a network of anodes; this technique is called impressed-current cathodic protection. Alternatively, the current may be supplied from the preferential corrosion of a metal anode that has a stronger anodic reaction than does the structure. This technique is known as sacrificial anode or galvanic cathodic protection.

The requirements for a cathodic protection system for bridge substructures are given in the following list. They are based on requirements for coating systems identified by Apostolos (6):

1. Effectiveness: A low resistance between the anode system and the reinforcement throughout the area to be protected is needed to ensure an even distribution of current and low power consumption;
2. Durability: System materials must be resistant to electrical and structural breakdown within the service environment of salt-contaminated concrete; they must also remain bonded to the protected surface and be resistant to degradation from factors in the external environment, including weathering;
3. Availability, simplicity, and ease of installation: System components must be readily available, must be able to be installed with a minimum of special training, and must be tolerant of a variable quality of workmanship;
4. Minimum maintenance: Systems should be stable with respect to changes in the environment (temperature and humidity) and not require periodic manual adjustment of the power settings;
5. Low cost;
6. Acceptable appearance;
7. Versatility: The system should be capable of application to a variety of substructure sizes and geometries; and
8. Lightweight: The system should add a minimum of dead load to the structure.

SITE SELECTION

The Burlington Bay Skyway Bridge, which is a multiple-span, high-level structure over the entrance to Hamilton Harbour in southern Ontario, was selected for the installation of the test systems. The rectangular columns of the structure are exposed to surface run-off from leaking expansion joints and roadway drains. Salt-staining is frequently visible in the winter months, as shown in Figure 1. The condition of the columns is a function of the exposure to salt and therefore varies from column to column and from area to area on the same column.

FIGURE 1 Salt straining on pier bents, Burlington Bay Skyway.

The site was selected for the following reasons.

1. Columns could be chosen that were exhibiting active corrosion while showing a minimum of physical distress. This means the test conditions were realistic, both in terms of the condition of the structure and the exposure, but repair work was kept to a minimum.
2. The structure is scheduled for major rehabilitation in the near future, and the data collected will be used in designing the rehabilitation scheme.
3. The substructure was readily accessible for construction and monitoring activities without the need for traffic control measures.
4. Electrical power was available.

As can be seen in Figure 1, the height of the columns varies, reaching a maximum of 24 m. A characteristic feature of all the columns is the presence of rustication strips at 1.22-m centers. Where reference is made to a panel elsewhere in this paper, this is the area of one face between adjacent rustication strips. The section of the columns at the location of the test sites was approximately 2.1 x 4.0 m.

All the systems were installed in the same configuration: three panels high on the south face and two panels high on the remaining faces. This was done to determine if the third panel on the south face influenced the corrosion activity over the adjacent unprotected faces. The total concrete surface area in each system was approximately 38 m^2.

DESIGN OF CATHODIC PROTECTION SYSTEMS

System 1

The design was an impressed-current system that consisted of primary anodes of a conductive polymer composite spaced vertically at 450-mm centers with a shotcrete overcoat. The design drawing is shown in Figure 2.

The conductive polymer composite was developed by the FHWA laboratories and consisted of a vinyl ester binder with the addition of spherical carbon particles that provided a specified resistivity of less than 10 ohm•cm. The polymer was supplied as a two-component material, and anodes 25 x 12 mm in section were cast before system construction. Two strands of 30,000 filament carbon fiber were embedded the full length of each anode to increase anode conductivity. The fiber used had an extremely low resistivity (18 x 10^{-4} ohm•cm), high tensile strength (2.7 GPa), and is made from a polyacrylonitrile (PAN) base. One hundred-millimeter lengths of platinized niobium copper core wire, 0.79 mm in diameter, were embedded a length of 50 mm in the ends of the anodes to facilitate connection of electrical supply lines. The anodes were 2.4 m long on the faces that had two panels. Two anodes were used on the south face, each 1.8 m long, for ease of handling.

A separate feeder line was extended from the terminal box to the anodes on each face so that the faces could be activated independently if desired. Switch boxes were provided for the connections from the feeder line to the anodes on the east face so that individual anodes could be disconnected to optimize anode spacing.

A separate constant current rectifier was used to power each of the three impressed-current systems. They were connected to system anodes and ground at the individual system terminal boxes.

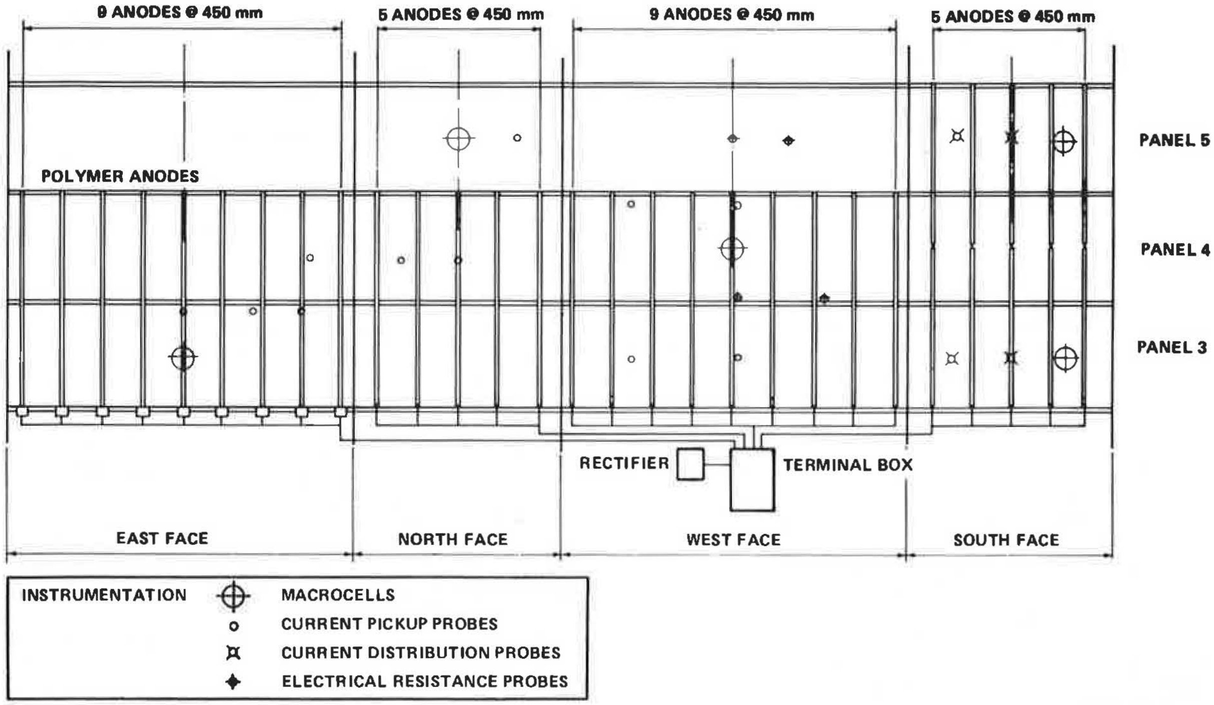

FIGURE 2 System 1: anode and instrumentation placement.

A 40-mm-thick layer of conventional portland cement shotcrete was applied over the entire system.

System 2

The primary anodes were the same as in System 1, except that a single strand of platinized wire was embedded the full length of the anode, rather than carbon strand, to reduce the resistivity of the anodes.

The system was designed with the anodes placed horizontally on the column and connected at the corners to form three rings around the column at the level of the rustication strips, as shown in Figure 3. Power was supplied to the open southwest corner of each ring. Switch boxes were placed in each anode line at the northeast corner so that half of each anode could be disconnected to investigate current distribution in the system. A single anode was placed at the top of the third panel on the south face and provided with its own power supply line. The four supply lines were connected to a rectifier through a terminal box with switches in each line so that the anodes could be powered individually or in groups.

A secondary anode of graphite-pigmented conductive paint was placed on the surface of the panels

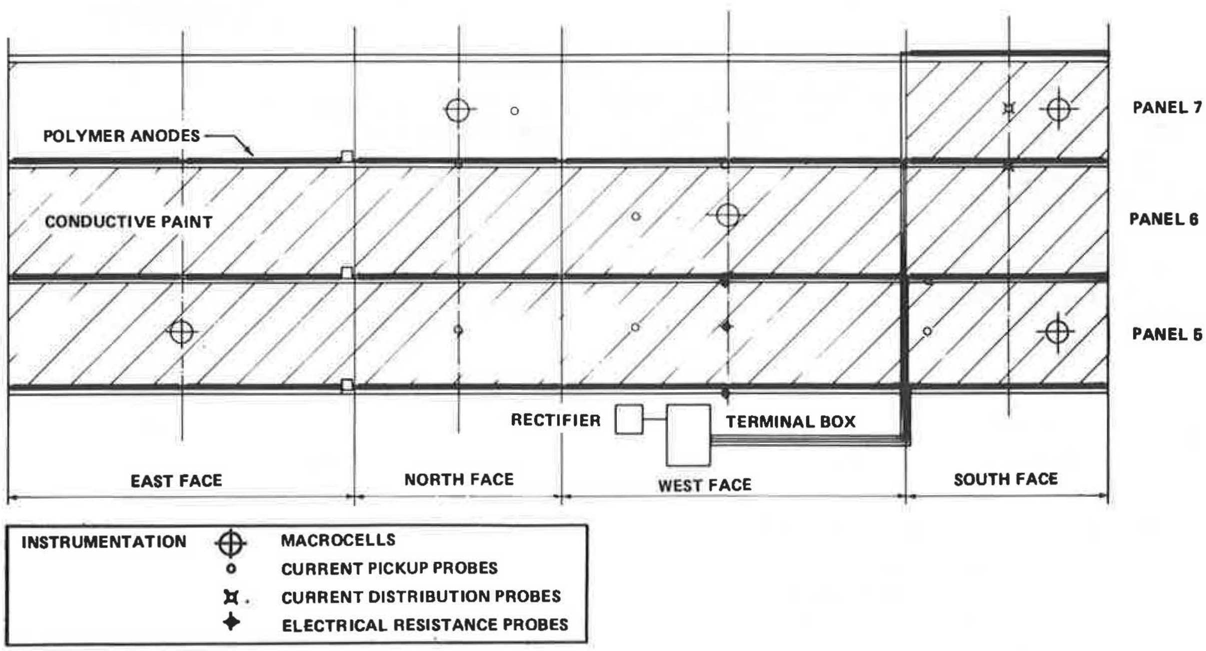

FIGURE 3 System 2: anode and instrumentation placement.

bordered by the anodes to lower resistance between the anodes and the reinforcement. The product used was selected because of its low resistance and promising durability characteristics determined in an earlier investigation (7).

System 3

This design was also an impressed-current system that used the same anodes used in System 2. The anodes were placed vertically, with two anodes at the third points of the long faces and one anode at the center of the short faces, as shown in Figure 4. Each anode was connected to a separate supply line from the terminal box, with a switch in each line to permit individual control. A secondary anode of carbon fiber was applied to form a network on the concrete surfaces. Anchors were placed 100 mm from the edge of each face at points spaced 100 mm apart vertically. The fiber was connected by zig-zagging between the anchor points using a single length of fiber. In this way the fiber on each face was continuous, but there was no connection between adjacent faces. Two types of fiber were used. The south and west faces used a double strand of the 30,000 filament PAN fiber described in System 1. A 20,000 filament pitch-based fiber overbraided with dacron was used on the north and east faces. The resistance per unit length of the 20,000 filament pitch fiber was approximately equivalent to 60,000 filaments of the PAN fiber. The carbon content of the pitch fiber exceeds 99 percent compared with 93 percent for the PAN fiber.

The entire system was covered with 40 mm of conventional portland cement shotcrete.

System 4

This was the only sacrificial anode or galvanic system. Work elsewhere (8,9) had shown that various configurations of zinc anodes could provide adequate protection to steel reinforcement in concrete. The anodes used were in the form of a continuous diamond-shaped (9 x 12 mm) zinc ribbon with a 2.5-mm steel core by which connections to the anode could be made. The anodes were placed vertically on 150-mm centers, as shown in Figure 5. All the anodes on each face were connected to a single feeder cable. The four feeder cables were extended to the terminal box where each was connected through a switch to leads attached to the reinforcement on the corresponding faces.

Because the driving voltage of the system is limited to the potential difference between the zinc anode and the steel reinforcement, it is essential that the circuit resistance be kept to a minimum. Salt was therefore added to the shotcrete to reduce its resistance and also to ensure that the potential of the zinc was active. In long-term installations it would be desirable to use an overcoat material with a high air content so that corrosion products formed on the surface of the anodes are dissipated without cracking the overcoat. However, the overcoat cannot be too porous because it would then be vulnerable to drying, which would greatly increase circuit resistance. Because System 4 was designed only as a short-term experimental installation, no provision for a high air content shotcrete was made. The specified salt content was 0.5 percent Cl^- by mass of shotcrete.

Instrumentation

Instrumentation was needed to determine the effectiveness and permit a comparison of the four cathodic protection systems. Information was required specifically on the current distribution and density within each system over time. There was a lack of commercially available instrumentation to satisfy these needs and, after reviewing the experience of others (10,11), the following instrumentation was developed and fabricated. The specific locations of the various probes are shown in Figures 2-5.

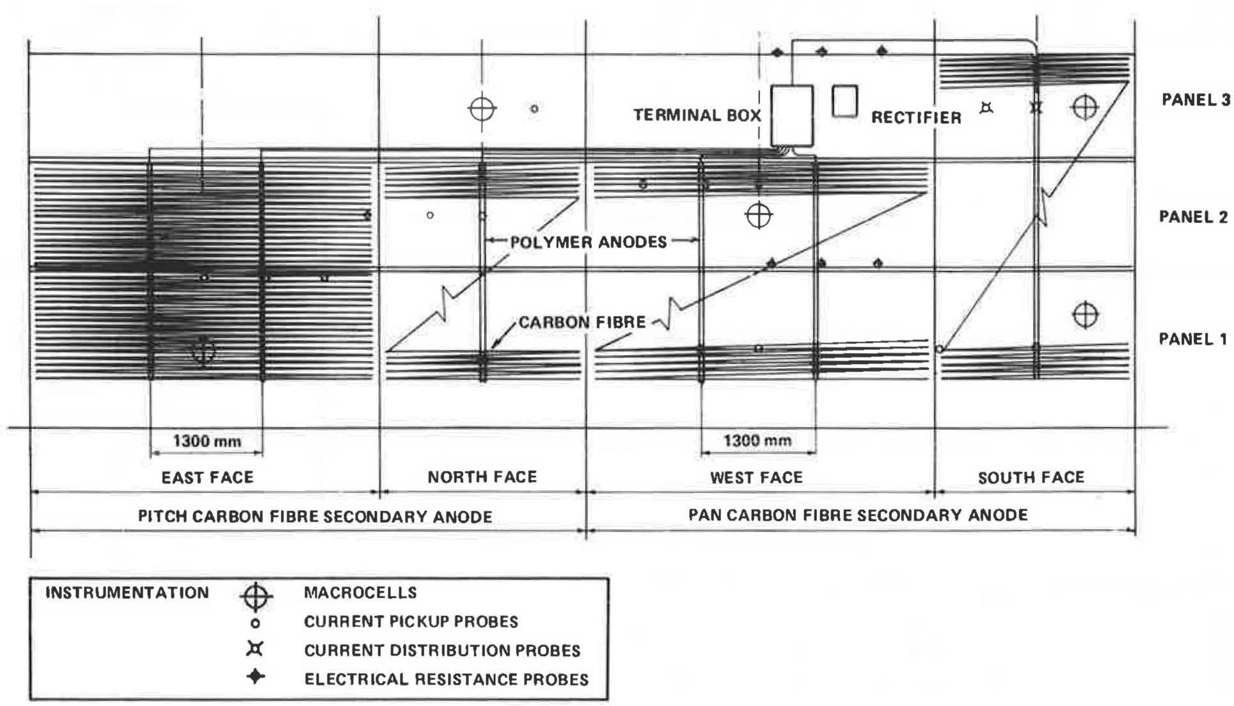

FIGURE 4 System 3: anode and instrumentation placement.

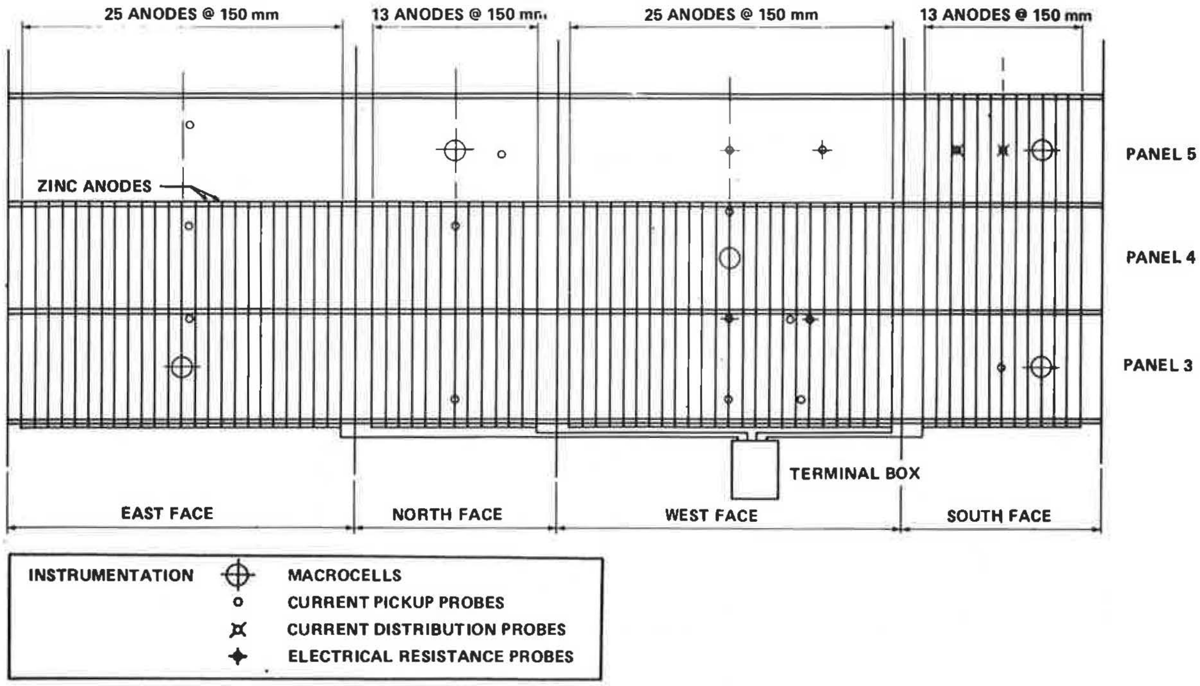

FIGURE 5 System 4: anode and instrumentation placement.

Macrocells

The principle of the macrocell is to create a strong natural corrosion cell. This is done by forcing a portion of the reinforcement to act as a cathode with respect to an anode implanted adjacent to the reinforcement. (It is important to distinguish between this anode, which is a natural half cell, and the anodes that are applied to the surface of the concrete and act as a current distribution system.) The macrocell anode consisted of a short length of reinforcing steel encased in mortar of a high chloride content. Leads extending from the anode and cathode can be connected externally at the terminal box to measure the magnitude and direction of current flow in the cell. It was intended that the current flow in the macrocell would be at least equal to corrosion currents elsewhere in the structure. Consequently, if the application of cathodic protection reverses the direction of current flow in the macrocell, this is an indication that all other corrosion cell activity has been arrested. The applied current necessary to reverse the macrocell is also a measure of the effectiveness of the system.

A thermocouple and a zinc-zinc sulfate reference cell, used for potential measurements at the level of the reinforcement, were also embedded in the macrocell, as shown schematically in Figure 6.

Macrocells were located directly under anode lines, midway between them, and in unprotected areas of the structure. The cells in the unprotected areas were designed to act as controls as well as to measure the effect of any stray currents.

Current Pick-Up Probes

Current pick-up probes provide another means of examining current distribution in the structure. Each probe consists of a short piece of rebar embedded at the level of main reinforcement and connected by a lead wire to the instrumentation panel in the terminal box. By measuring current flow between the probes and ground, the current density at various points in the structure can be calculated. Unlike the macrocells, the probes are free to act as either cathodes or anodes, depending on whether the current flow is to or from the probe.

The current pick-up probes are inexpensive to fabricate and relatively easy to install, as they require little concrete removal. Several probes were installed in each system at locations both beneath and remote from the anode lines.

Current Distribution Probes

The current distribution probes consist of three current pick-up probes installed in a line at different depths from the concrete surface, as shown in Figure 7. The probes are used to measure the variation of current density with depth at different locations in the structure.

Electrical Resistance Probes

The probes were fabricated from thin steel sections that comprise two arms of a bridge circuit. The probes are embedded at the level of the steel, and as one arm corrodes (the other being protected) the resistance increases. By monitoring the probe with a suitably calibrated meter, the rate of corrosion can be expressed in terms of metal loss per year. Similar commercial probes have been used successfully to monitor cathodic protection circuits in bridge decks (4).

Construction

Systems 2 and 3 were placed on the same column, separated by an unprotected area one panel high. System 1 was placed on the second column of the same bent. This was done so that the rectifiers for the three impressed-current systems could be serviced by

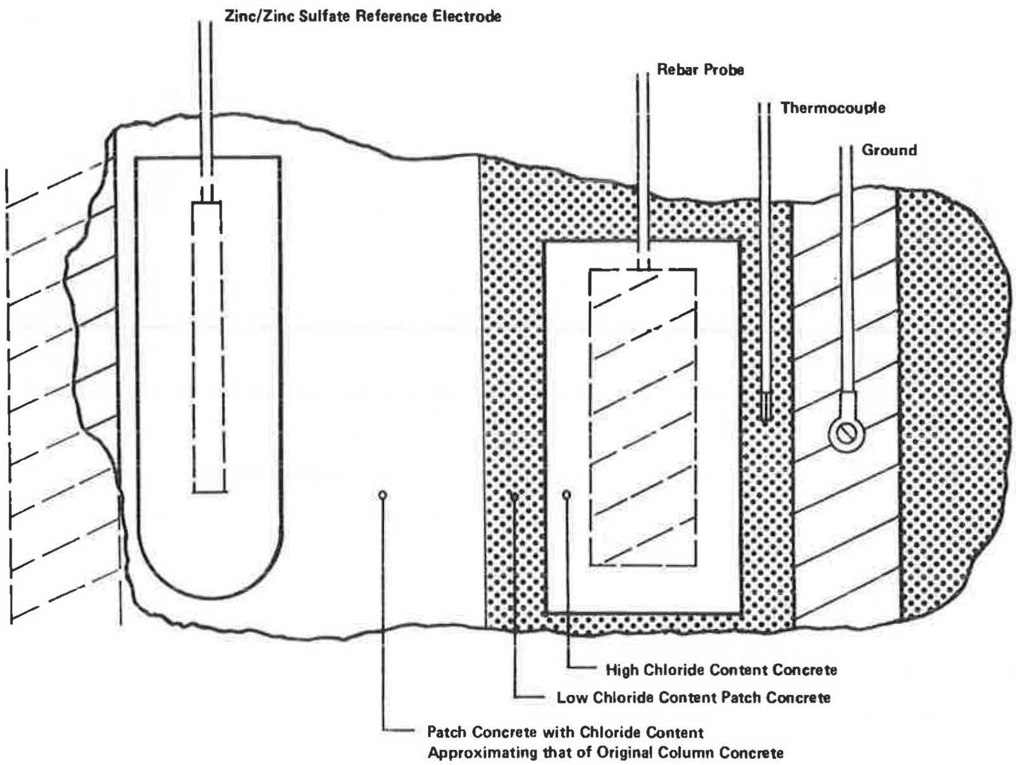

FIGURE 6 Schematic drawing of a macrocell.

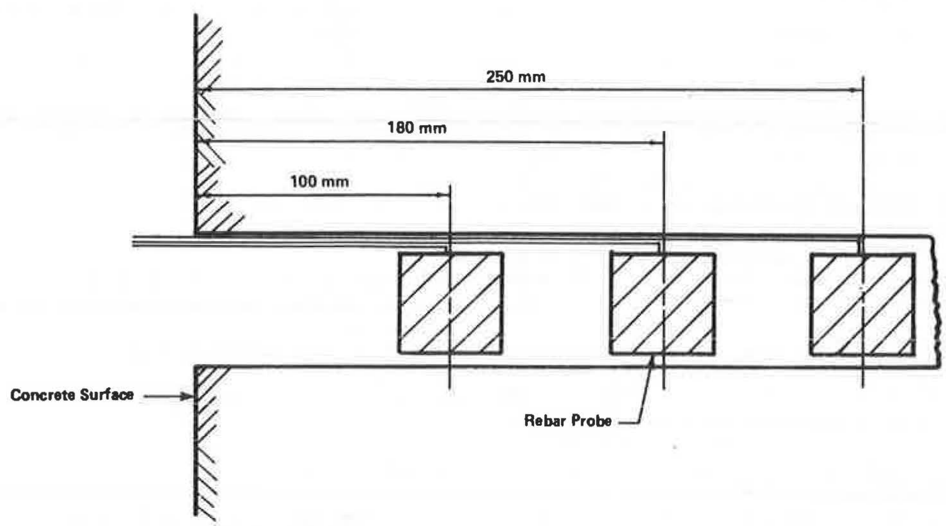

FIGURE 7 Current distribution probes.

a single power supply line. System 4 was placed on the adjacent bent.

The construction of the four systems was completed by Ministry personnel, with the exception of the shotcreting. The reasons for this were threefold:

1. The materials and installation techniques were unproven, so that specifications could not be prepared to enable the work to be done by contract;
2. Design modifications could be readily made as practical difficulties were identified; and
3. A more thorough assessment of technical feasibility could be made by obtaining hands-on experience.

Condition Survey

Before installation of the cathodic protection systems, the condition of each column was documented by a visual survey, measurement of corrosion potentials, detection of delaminated areas by sounding, and determination of chloride content by using cores.

The corrosion potential data (measured in accordance with ASTM C876-77) are given in Table 1, and the total chloride contents (measured in accordance with AASHTO T260) are given in Table 2. The chloride measurements indicate that, after allowing for background chloride levels, the chloride content at the depth of the steel (75 to 100 mm) is greater than

TABLE 1 Half-Cell Potentials

System	Column Face	Half-Cell Potentials > −0.20 V (%)	< −0.20 V > −0.35 V (%)	< 0.35 V (%)
1	North	0	88	12
	South	0	87	13
	East	0	84	16
	West	0	73	27
	Total	0	82	18
2	North	0	96	4
	South	0	88	12
	East	0	84	16
	West	16	73	11
	Total	5	84	11
3	North	0	100	0
	South	0	100	0
	East	0	96	4
	West	2	87	11
	Total	1	94	5
4	North	0	80	20
	South	0	75	25
	East	1	91	8
	West	0	78	22
	Total	1	81	18

the normally accepted threshold value for corrosion at some, but not all, locations. The background chloride levels in the concrete are unusually high because of the high chloride content of the limestone aggregate (12). The half-cell potentials also varied from panel to panel, but active corrosion potentials were included within each system.

Sequence of Construction Activities

The sequence of construction and details of the procedures on each of the four systems are as follows.

1. Repair of delaminated areas with concrete patches.
2. Concrete removal for placement of instrumentation: The instrumentation took much longer to install than anticipated. This was because all the drilling and coring had to be done from a bucket truck, the concrete was of a high quality, and the depth of cover was in the range of 75 to 100 mm. Locating the probes precisely with respect to the reinforcement and the position of the surface anodes also proved to be time consuming.
3. Sandblasting: All the concrete surfaces to be cathodically protected were sandblasted.
4. Installation of instrumentation: After placement of the probes the lead wires were bundled, wrapped, and anchored in place to prevent damage during shotcreting.
5. Epoxy coating of exposed metal: All of the exposed form ties were covered with two coats of epoxy resin to prevent a system short circuit.
6. Installation of primary and secondary anodes: The primary anodes of conductive polymer were precast. All the anodes were attached to the concrete surface by using plastic straps. Completed anode systems are shown in Figures 8 and 9. A close contact between the anode and the concrete was particularly important in System 3, where the carbon fiber was sandwiched between the primary anode and the column surface. This mechanical contact was the only connection between the primary and secondary anodes in this system. The design of the connections of the feeder lines to the anodes in Systems 1 and 4 was modified to ensure that all the connections would be accessible after shotcreting to allow individual anodes to be disconnected. Two coats of conductive paint were applied by hand in System 2. (The finished system is shown in Figure 10.) Because of susceptibility of the carbon fiber network in System 3 to vandalism, it was installed just before shotcreting.
7. Shotcreting (except System 2): The shotcreting was uneventful except for a slight sagging of the PAN carbon fiber on System 3, as shown in Figure 8. The measured chloride content of the shotcrete in System 4 was 0.47 percent Cl by mass as compared with 0.048 percent Cl by mass of the shotcrete in Systems 1 and 3.
8. Connection of instrumentation and control panels: A terminal box was provided for each system that contained a panel on which all instrumentation and anode leads were terminated.
9. Hook-up of rectifiers (Systems 1, 2, and 3): Unfiltered, full-wave rectifiers with a maximum output of 16 V, 12 A were installed adjacent to the terminal boxes. The size of the rectifiers was based on polarization tests conducted after the anodes were installed. Rectifiers that had less capacity would have been adequate but were not available locally. Constant-current rectifiers were used rather than potential control because the latter require the use of a reference cell. The long-term stability of reference cells embedded in concrete is unproven. The use of constant-current rectifiers also offers the advantage of allowing the current passed by the anodes over a given time period to be calculated.

Costs

An estimate of the costs of the four trial systems is given in Table 3. These costs are approximate, calculated only to give an indication of the relative costs of the four systems, and of the costs of substructure repair in general.

Although it was not possible to divide accurately the total time spent among the individual systems, it is believed that the figures reliably reflect the relative costs of the systems. It should be noted that more than half the time spent on this project

TABLE 2 Chloride Content Determinations, Burlington Skyway Cores

Cathodic Protection Installation	Percentage of Total Chlorides (by mass of concrete) by Depth Below Surface (mm) 0-12	12-25	25-50	50-75	75-100	100-125	125-150	150-175
System 1: east face	0.3318	0.2691	0.1368	0.0826	0.0794	0.0755	0.0806	0.0785
System 3								
East face	0.2962	0.3216	0.2172	0.0657	0.0746	0.0781	0.0689	0.0789
West face	0.2416	0.3027	0.1703	0.1051	0.0870	0.0747	0.0823	0.0795
System 4								
East face	0.2223	0.4263	0.3663	0.2201	0.1536	0.1104	0.0936	0.0781
North face	0.1755	0.3895	0.2460	0.1565	0.1195	0.0930	0.0890	0.0754

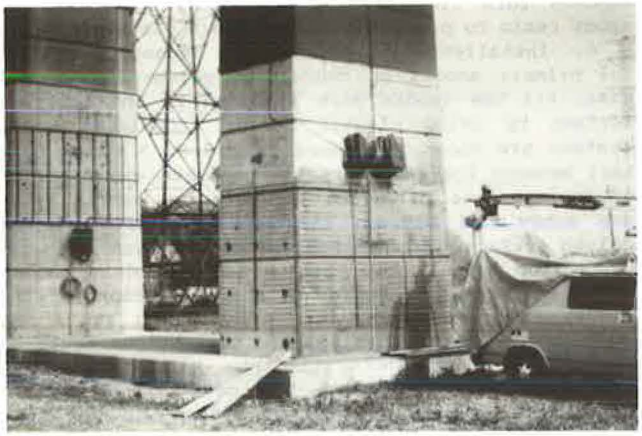

Note: The relative positions of the three impressed-current systems are seen here; System 1 on the far column, and Systems 2 (upper) and 3 (lower) on the near column. Note the system terminal boxes and the extension of anode and instrumentation lines to them. Rectifiers were later placed adjacent to each box. Note the sagging of the PAN carbon fiber during shotcrete application.

FIGURE 8 Systems 1, 2, and 3.

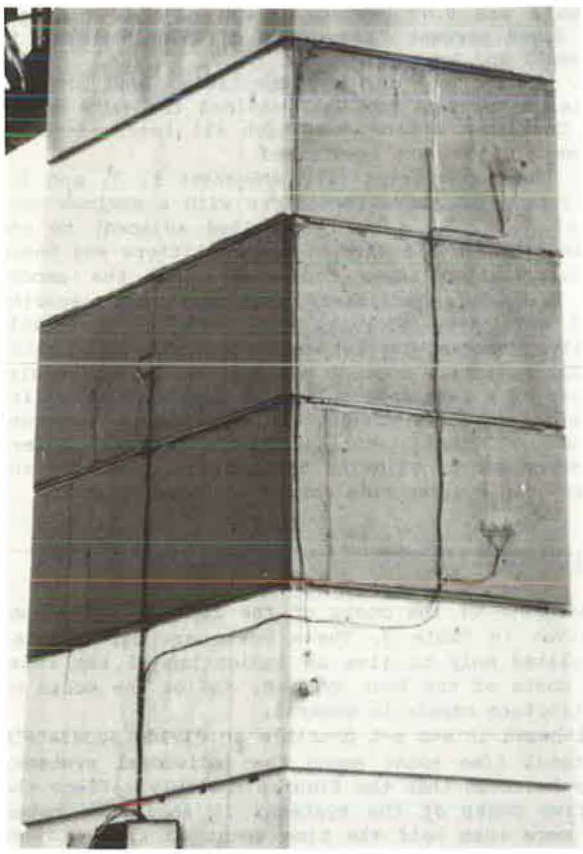

Note: Polymer concrete anodes can be seen at the level of the rustication strips, with black conductive paint covering the protected surface. Macrocell leads (from two cells on the south face and one on the west face) are anchored to the concrete and extended to the system terminal box.

FIGURE 9 System 2, south and west faces.

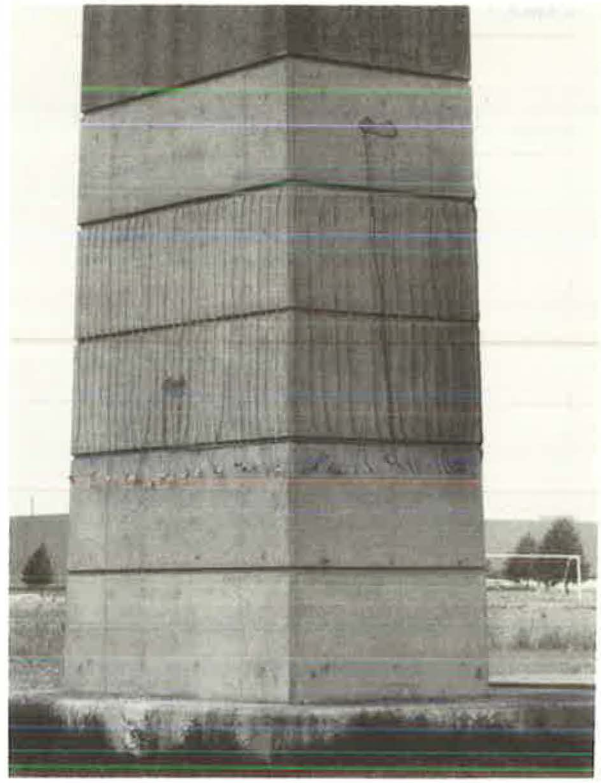

Note: The system is shown before shotcreting, with instrumentation and anode lines in place. Connection cables extend from each anode, ready for connection to feeder cables.

FIGURE 10 System 4, north and east faces.

TABLE 3 Cost of Experimental Cathodic Protection Systems

Item	Cost ($) System 1	System 2	System 3	System 4
Anode materials				
Conductive polymer (including fabrication)	1,830	1,040	570	
Conductive paint		150		
Carbon fiber			70	
Zinc ribbon				890
Shotcrete	2,660		2,660	2,660
Instrumentation (materials only)	1,800	1,800	1,800	1,800
Rectifiers (including connection)	1,380	1,380	1,380	
Other[a]	15,500	16,500	16,500	18,200
Total	23,170	20,870	22,980	23,550
Cost per m^2	610	549	605	620

[a]Includes labor, vehicle and equipment rental, travel expenses, and consulting fees.

was devoted to fabrication and installation of instrumentation. This level of instrumentation would not be employed in a full-scale system. The high construction costs also reflect the fact that many materials and procedures were being used for the first time. The small scale of the project also led to high unit costs for shotcreting, power hook-ups, and purchase of rectifiers.

Nevertheless, even with greater experience and economies of scale, substructure rehabilitation will be expensive. The figures reported in Table 3 are approximately 5 times greater than typical costs for deck rehabilitation (13).

Discussion of Results

Although all four systems were activated in November 1982 and the initial indications are that they are functioning satisfactorily, a number of practical difficulties must be overcome before full-scale applications of similar systems can be made routinely.

The casting and the handling of the polymer concrete anodes was especially difficult. Problems were encountered in maintaining a uniform mixture throughout the casting sequence and in adjusting to the variations in working time, which resulted from changes in ambient temperature. It was also difficult to release the anodes from the molds, and several breakages occurred. The hardened anodes were brittle and required careful handling. The purchase of anodes, commercially made under controlled conditions, is a much more attractive proposition to the user, and such anodes are expected to become available in the marketplace.

The electrical connections to the anodes were the weak link in all of the systems. The platinum wire tails on the polymer concrete anodes were particularly vulnerable to damage and breakage. Most of the connections to the anodes were in fact made outside the concrete because of concern for the performance of connections embedded in concrete. The point-to-point connection between the carbon fiber and polymer anodes in System 3 may be vulnerable to degradation and might be expected to exhibit durability problems.

The PAN-type carbon fiber was difficult to handle to prevent fraying and breakage. It could not be installed under windy conditions, as it tended to snag on the structure. The overbraided fiber was easier to handle, but care was required to avoid sharp bends to prevent breakage. The large number of anchorage points required for the zig-zag network was a disadvantage of the system. A woven fabric or mesh may overcome most of these objections.

The main disadvantage of System 4 was also the large number of anchors required to prevent the zinc ribbon from twisting, as can be seen in Figure 10. An alternative would be to apply the zinc in sheet or strip form. The use of flame-applied zinc is also being investigated (6).

The field of cathodic protection of reinforced- and prestressed-concrete structures is developing rapidly, and alternative anode materials are being identified. A project has been initiated recently at the Ministry to develop screening tests for anodes to evaluate the performance of candidate materials under both laboratory and exposure plot conditions.

The time required for the installation of the instrumentation was grossly underestimated. The macrocells were especially time consuming to install because of the amount of concrete removal required. Although a large amount of instrumentation was required to provide a rapid assessment of the effectiveness of each system, there is a need to define the type of instrumentation and the minimum amount that must be installed in full-scale systems to ensure that their operation is satisfactory.

Initial polarization studies raised questions regarding the long-term stability of the zinc-zinc sulfate reference cells. This has led to the development of a laboratory program to investigate alternative reference cells with the goal of identifying a cell that can be permanently embedded in concrete.

FUTURE WORK

The four systems are being monitored regularly for power consumption, current distribution, and half-cell potentials. Resistivity and temperature measurements are made at the same time. In addition, the systems are carefully inspected for evidence of degradation of the materials. Changes will be made in the configuration of the systems by disconnecting anodes, and measurements will be made to determine optimum anode spacing.

Future work will concentrate on monitoring the existing systems; solving some of the problems that have been identified, including connection details; and developing second-generation experimental systems that will lead to a system suitable for full-scale application.

REFERENCES

1. D.G. Manning and J. Ryell. Durable Bridge Decks. Report RR203. Ontario Ministry of Transportation and Communications, Downsview, Ontario, Canada, 1976, 67 pp.
2. Durability of Concrete Bridge Decks. NCHRP Synthesis of Highway Practice 57. TRB, National Research Council, Washington, D.C., 1979, 61 pp.
3. H.J. Fromm and G.P. Wilson. Cathodic Protection of Bridge Decks: A Study of Three Ontario Bridges. In Transportation Research Record 604, TRB, National Research Council, Washington, D.C., 1976, pp. 38-47.
4. H.J. Fromm. Cathodic Protection of Rebar in Concrete Bridge Decks. Materials Performance, National Association of Corrosion Engineers, Vol. 16, No. 11, 1977, pp. 21-29.
5. Cathodic Protection--Thumbnail Sketch. Materials Performance, National Association of Corrosion Engineers, Vol. 21, No. 1, 1982, p. 50.
6. J.A. Apostolos. Cathodic Protection of Reinforced Concrete Using Flame-Sprayed Zinc. Paper 180. Presented at National Association of Corrosion Engineers Conference Corrosion 83, Anaheim, Calif., April 1983.
7. W.J. Ellis and R.E. Colson. Cathodic Protection of Concrete Bridge Structures, Final Report. NCHRP Project 12-19. TRB, National Research Council, Washington, D.C., 1980.
8. J.B. Vrable. Cathodic Protection for Reinforced Concrete Bridge Decks: Laboratory Phase. NCHRP Report 180. TRB, National Research Council, Washington, D.C., 1977, 135 pp.
9. D. Whiting and D. Stark. Galvanic Cathodic Protection for Reinforced Concrete Bridge Decks: Field Evaluation. NCHRP Report 234. TRB, National Research Council, Washington, D.C., 1981, 63 pp.
10. K.C. Clear. FCP Annual Progress Report--Year Ending September 30, 1980, on Project 4K, "Cost Effective Rigid Concrete Construction and Rehabilitation in Adverse Environments." FHWA, U.S. Department of Transportation, 1980.
11. C.E. Locke and C. Dehghanian. Embeddable Reference Electrodes and Chloride-Contaminated Concrete. Materials Performance, National Association of Corrosion Engineers, Vol. 18, No. 2, 1979, pp. 70-73.
12. C. Rogers and G. Woda. The Chloride Ion Content of Concrete Aggregates from Southern Ontario. Report EM-17. Ontario Ministry of Transportation and Communications, Downsview, Ontario, Canada, 1977.
13. D.G. Manning and R.P. Northwood. The Rehabilitation of Structures on an Urban Freeway: A Case Study. In Proc., Bridge Maintenance and Rehabilitation Conference, West Virginia University, Morgantown, Aug. 1980, pp. 644-668.

Publication of this paper sponsored by Committee on Corrosion and Committee on Performance of Concrete.

Cathodic Protection of Bridge Substructures: Burlington Bay Skyway Test Site, Initial Performance of Systems 1 to 4

H. C. SCHELL, D. G. MANNING, and K. C. CLEAR

ABSTRACT

The performance of four experimental cathodic protection systems during the first 8 months of operation is described. The systems were installed on the columns of the Burlington Bay Skyway Bridge in 1982. The method of data collection and the essential features of the performance of each system are described. Macrocells and current pick-up probes were found to be the most useful tools for monitoring cathodic protection systems. The three impressed-current systems were all effective in stopping corrosion. Insufficient power was available from the galvanic system for it to be practical. The durability of some system components needs to be improved. The future work required to develop a full-scale operational cathodic protection system for bridge substructures is discussed.

Four experimental cathodic protection systems were installed on the columns of Burlington Bay Skyway Bridge in 1982. The methods of data collection and analysis and the performance of the systems during the first 8 months of operation are described.

DESCRIPTION OF SYSTEMS AND INSTRUMENTATION

Although the four systems have been described in detail elsewhere (see paper by Manning et al. elsewhere in this Record), the salient features of each are repeated for reference purposes. Systems 1, 2, and 3 were powered by impressed current, and the primary anode in all cases was a conductive polymer concrete. In System 1 the anodes were used with a shotcrete overcoat. System 2 consisted of the primary anodes with an exposed secondary anode of conductive paint. System 3 employed a secondary anode network of multifilament carbon strand and a shotcrete overcoat. System 4 was a sacrificial anode system that used zinc ribbon anodes and a shotcrete overcoat. Each system was applied to the four faces of a rectangular column and covered approximately 38 m^2 of concrete area.

The instrumentation that was designed and installed to measure the performance of the cathodic protection systems has also been described elsewhere (see paper by Manning et al.). It consisted of macrocells, current pick-up probes, current distribution probes, and electrical resistance probes. The macrocell is a strong natural corrosion cell in which current flow can be measured. The amount of current that must be applied to reverse the direction of current flow in the macrocells is a measure of the effectiveness of the cathodic protection. A zinc-zinc sulfate reference cell was embedded in each macrocell. The current pick-up probes were short pieces of rebar embedded at the level of the reinforcing steel at various points in the structure. They are used to measure current density. The current distribution probes consisted of three current pick-up probes installed in a line at different depths from the concrete surface. They are used to measure the variation in current density with depth. The electrical resistance probes were designed to give a quantitative measurement of corrosion in terms of metal loss per year. Figures 1-4 show the number, location, and identification of the instrumentation in the four systems.

The instrumentation and anode leads were terminated in a single junction box for each system. A schematic diagram of a typical box is shown in Figure 5. All the measurements were made at the box. The control panel within each junction box was designed to allow connections to be changed readily, thus allowing maximum flexibility to investigate parameters such anode spacing.

The three impressed-current systems were each powered by a separate, unfiltered full-wave rectifier that had a maximum output of 16 V and 12 A. The positive terminal of the rectifier was connected to the anode lines and the negative terminal was connected to a ground on the reinforcing steel. This ground connection was not used for any measurements other than rectifier output voltage.

METHOD OF DATA COLLECTION

Current Measurements

Anode Feeder Lines

The anodes in Systems 2 and 3 were supplied by individual feeder lines. In Systems 1 and 4 the anodes on each face of the column were connected so that a separate anode feeder line supplied all the anodes on one face. These connections are shown in Figures 1-4. A switch was placed in each line. In System 4 the anode feeder lines were connected to a ground on the corresponding face of the column. Current measurements were made by measuring voltage drop across a high wattage resistor placed in each line.

Macrocell Rebar Probes

The leads from the macrocell rebar probes were connected through a resistor to the ground connection within the same macrocell. The resistor size was chosen to be approximately 10 percent of the open circuit alternating current (ac) resistance between the probe and ground. The magnitude and direction of the current flow between the probe and the reinforcing steel was determined by measuring the voltage drop across the resistor.

Throughout this study the convention used was to

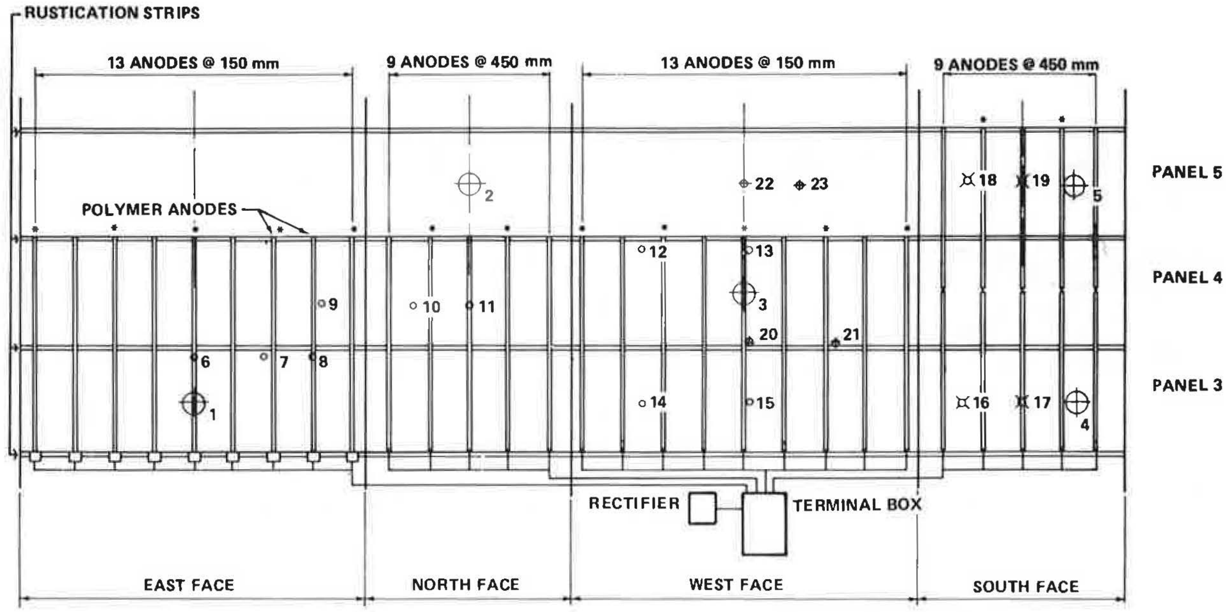

INSTRUMENTATION	1 – 5	MACROCELLS
	6 – 15	CURRENT PICKUP PROBES
	16 – 19	CURRENT DISTRIBUTION PROBES
	20 – 23	ELECTRICAL RESISTANCE PROBES

* ANODES DISCONNECTED APRIL 13 - JUNE 14

FIGURE 1 System 1: anode and instrumentation placement.

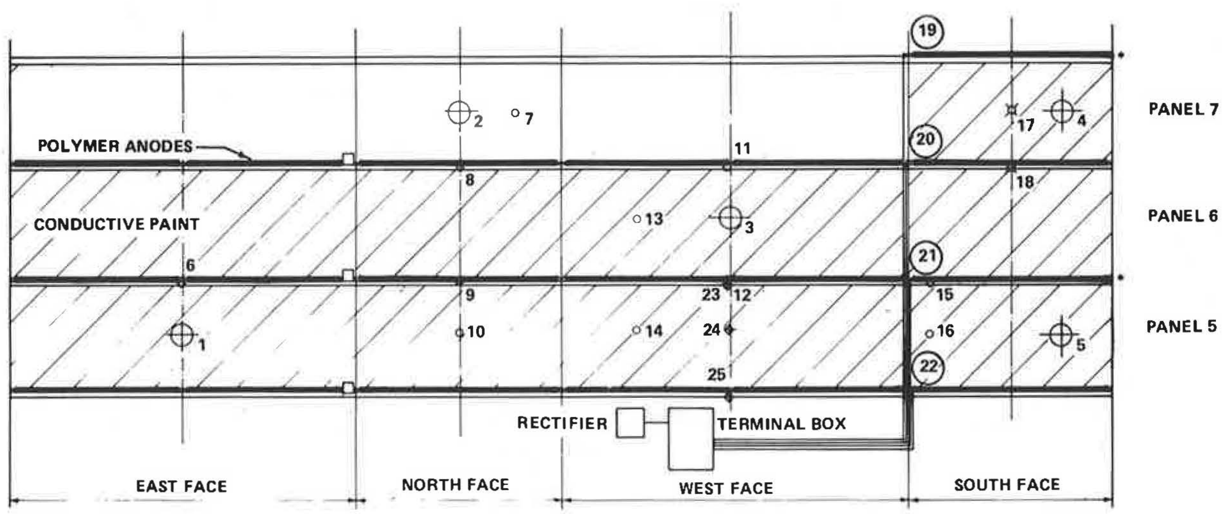

INSTRUMENTATION	1 – 5	MACROCELLS
	6 – 16	CURRENT PICKUP PROBES
	17, 18	CURRENT DISTRIBUTION PROBES
	19 – 22	ANODE LINES
	23 – 25	ELECTRICAL RESISTANCE PROBES

* ANODES DISCONNECTED APRIL 13 - MAY 31

FIGURE 2 System 2: anode and instrumentation placement.

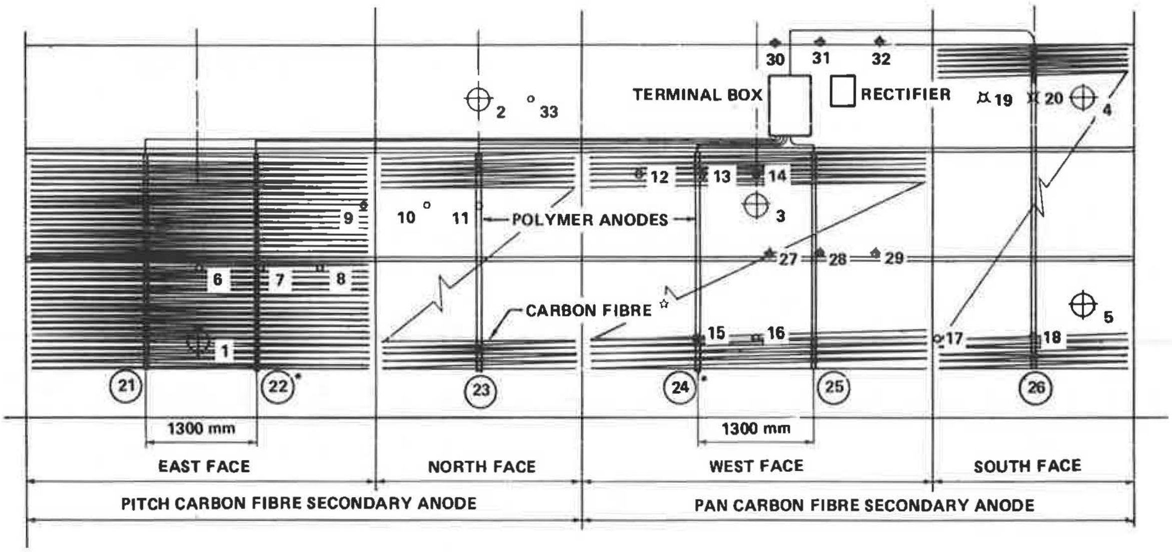

INSTRUMENTATION	1 – 5	MACROCELLS
	6–18, 33	CURRENT PICKUP PROBES
	19 , 20	CURRENT DISTRIBUTION PROBES
	21 – 26	ANODE LINES
	27 – 32	ELECTRICAL RESISTANCE PROBES

* ANODES DISCONNECTED APRIL 13 - JUNE 6

☆ CARBON FIBRE APPLIED TO ALL FACES AS SHOWN FOR EAST FACE

FIGURE 3 System 3: anode and instrumentation placement.

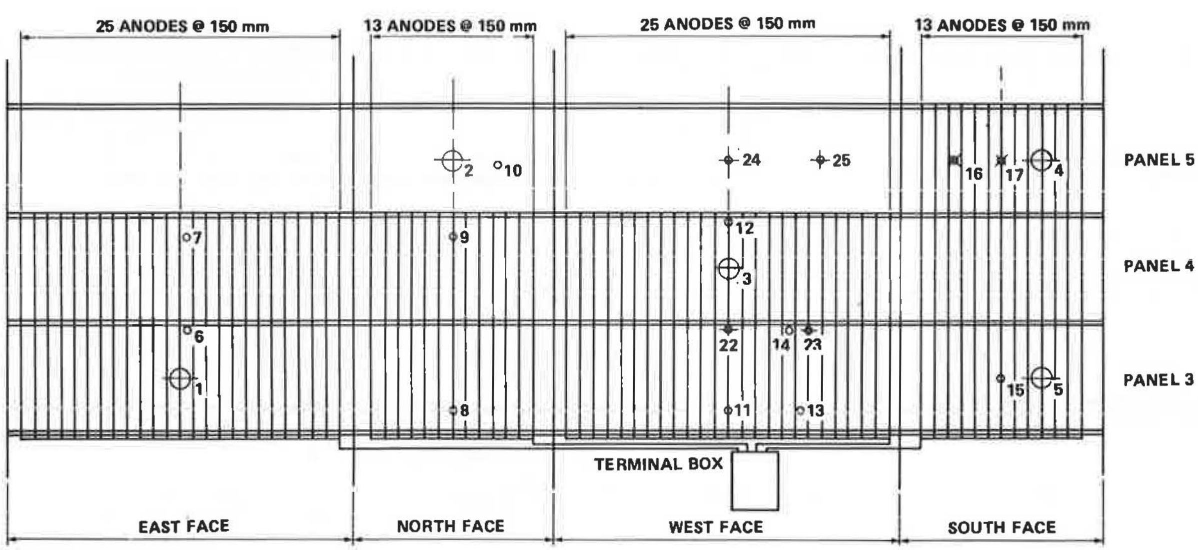

INSTRUMENTATION	1 – 5	MACROCELLS
	6 – 15	CURRENT PICKUP PROBES
	16 , 17	CURRENT DISTRIBUTION PROBES
	22 – 25	ELECTRICAL RESISTANCE PROBES

FIGURE 4 System 4: anode and instrumentation placement.

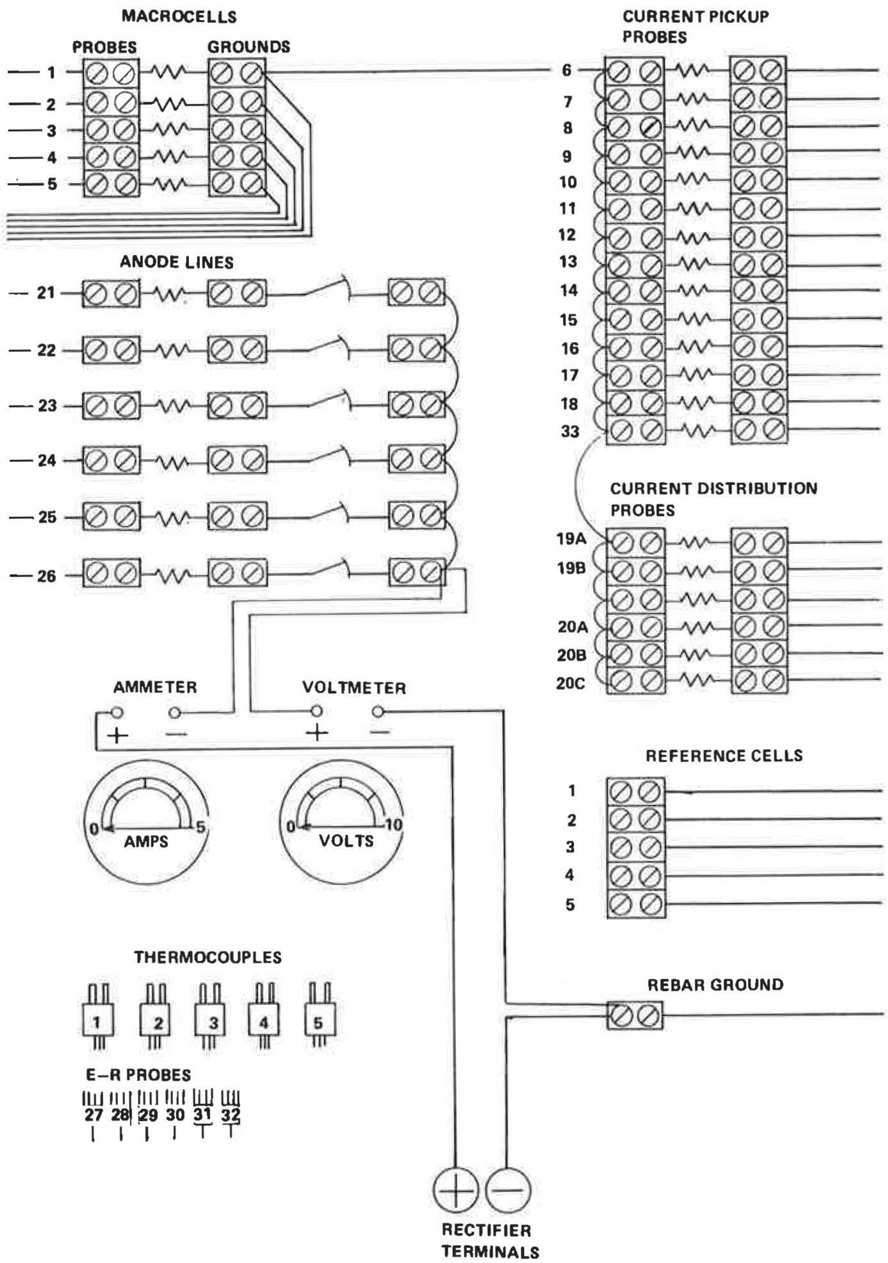

FIGURE 5 Terminal box layout (System 3).

attach the positive lead of the voltmeter to ground. By using this system a positive meter reading indicates the probe is anodic (i.e., corroding). In other words, electron flow is from the probe to the reinforcing steel. Conversely, negative readings indicate that the probe is cathodic (i.e., noncorroding). The readings are expressed in terms of current density on the probe surface in the units $\mu A/cm^2$. It is convenient that the numerical value of current density is almost the same in $\mu A/cm^2$ and mA/ft^2 (the actual conversion is 1 $\mu A/cm^2$ = 0.93 mA/ft^2).

Current Pick-Up Probes and Current Distribution Probes

Unlike the macrocell probes, the current pick-up and distribution probes were connected to a common ground. Resistors were placed in each line and the voltage drop was measured as described in the previous subsection. The magnitude and direction of current flow between each probe and ground was calculated.

Voltage and Potential Measurements

System Voltage

The system voltage in Systems 1, 2, and 3 was measured by connecting a voltmeter across the terminals of the rectifier. In System 4 the instant-off voltages between the anode feeder lines and ground were measured.

Macrocell Reference Cells

The potential of the zinc-zinc sulfate half-cells was measured with respect to the corresponding macrocell ground. Both a voltmeter and an oscilloscope were used to record on and instant-off cell potentials during the operation of Systems 1, 2, and 3. Potential measurements were also made before activating the systems and during periods of depolarization.

Resistance

The resistance between the anode lines and ground was measured whenever current and voltage measurements were made. A 60-Hz ac resistance meter was used. The electrical resistance probes designed to measure corrosion rates were found to be outside the operating range of the measuring instrument, and no useful data were recorded.

Temperature

The temperature in the concrete at the level of the first layer of reinforcing steel was measured whenever data were collected by using the thermocouples embedded in the macrocells.

PRELIMINARY SYSTEM TESTING

Initial measurements were made before system activation (i.e., no anode-to-ground connections) to ensure that all probes were functioning properly and to obtain system-off unpolarized readings.

E-log I polarization tests were conducted on the four systems to determine the magnitude of corrosion currents in the test columns and to define protection current levels. This test involves application of closely controlled direct current (dc) in a series of increasing increments while monitoring the polarization level of reference cells placed at selected structure points. In this case the anode systems were used to apply the current, and the embedded macrocell reference cells were monitored. Polarization [instant-off potential (E)] of the cells was plotted against the logarithm of the applied current (log I). The test is described in detail elsewhere (1,2). Tests were conducted as described by Stratfull (1), with minor variations:

1. Current increments, rather than reference cell off potential increments, controlled the progression of the test;
2. Reference cells monitored were not necessarily at the most anodic points of the structure; and
3. Actual current recorded, rather than current density, was plotted.

For each test the following parameters were determined:

1. Static half-cell potential for each cell monitored (Estat),
2. Corrosion current (Icorr),
3. Minimum current required for cathodic protection (Icp),
4. Minimum potential required for cathodic protection (Ecp), and
5. Cathodic Tafel slope (βc).

A diagram of the test circuit is shown in Figure 6. A plot prepared from a typical test is shown in Figure 7, with the parameter values labeled.

Initial tests on the three impressed-current systems yielded curves with Icp values ranging from 250 to 780 mA and averaging 418 mA. For purposes of comparison, and to develop data on relative anode consumption rates, all three systems were set at a constant current of 500 mA. This level was maintained throughout the monitoring period described in this paper. System 4 was powered by closing the switches between anodes and corresponding ground leads.

All four systems were activated in November 1982, and monitoring was carried out on a regular basis during the period November 1982 to July 1983. The systems were switched off occasionally and allowed to depolarize so that depolarization rates could be

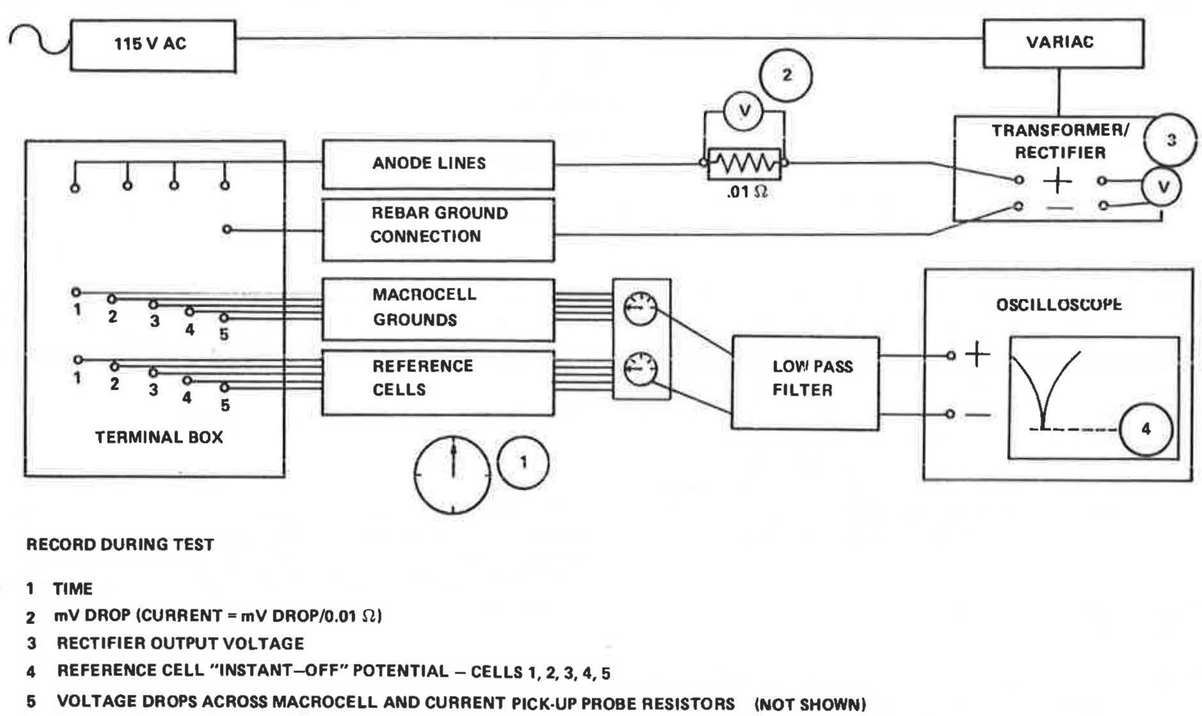

FIGURE 6 Schematic diagram of instrumentation for E-log I test.

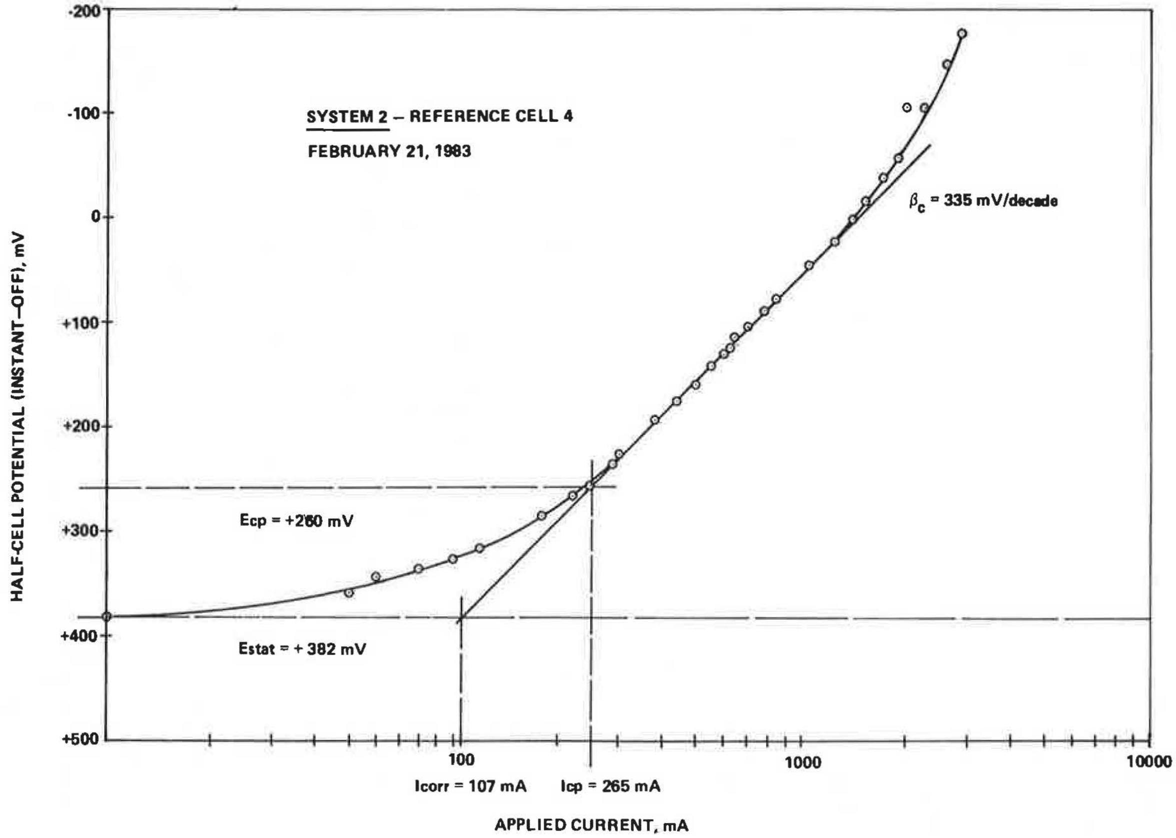

FIGURE 7 E-log I test plot.

monitored and system off conditions examined. E-log I tests were repeated at intervals during these off periods. Later curves yielded values similar to those found in initial tests. As in all E-log I curves, determination of the cathodic Tafel stopes was difficult and subject to interpretation. Additional work is under way to further quantify analysis of these data.

RESULTS OF MONITORING PROGRAM: IMPRESSED-CURRENT SYSTEMS

Current Flow, Density, and Distribution

Anodes and Column Surfaces

A specified applied current of 500 mA resulted in a current density of 13 mA/m^2 on the protected concrete surface of Systems 1, 2, and 3. The actual current levels were slightly less than 500 mA. The surface area of column reinforcing steel lying beneath the protected portion of each system was estimated to be approximately 17.7 m^2, which resulted in an average current density on the steel surface of 28.2 mA/m^2 (2.8 μA/cm^2).

Current densities on the anodes and the separate column faces varied from one system to another because of the different anode configurations. In System 1 there was 5.67 m^2 primary anode surface. It was initially assumed that all anode surfaces would dissipate current, resulting in a current density of 81 mA/m^2 of anode surface. Coring has shown that voids exist between the rear anode face and the column concrete, which indicates that the two were not in intimate contact at the time of shotcrete application. Therefore, the three anode faces in contact with the shotcrete were probably dissipating most of the system current. If this was the case, average current density was increased to 122 mA/m^2 of anode surface.

In Systems 2 and 3 the presence of a secondary anode increased the effective anode area, thereby lowering current densities in the primary anode systems. In System 2 the conductive paint surface anode covered the entire system area, yielding an overall anode current density of 13 mA/m^2. In System 3, 20 m of carbon strand anode were used per square meter of concrete surface. Thus each meter of carbon strand, on average, was required to dissipate 0.66 mA of current.

The surface area of the multifilament strand is difficult to calculate, but assuming a diameter of 2 mm for the overbraided pitch fiber yields a calculated current density of 105 mA/m^2 of fiber surface. Current density on the polyacrylonitrile (PAN) fiber would be somewhat less because of the tendency of this fiber to spread and therefore increase the anode surface area.

Detailed current flow data for the three systems are summarized in Table 1. The values given are the average values during the 8-month period when the systems were operating with all anodes powered. The more significant features of each system are discussed individually.

In System 1 the current densities on the south, east, and west faces were similar. The proportion of current flowing to the north face was less than the other faces because the resistance of the anode line was higher and exhibited greater fluctuations.

In System 2 the resistance of the three anode rings to ground were similar in value but varied over time with fluctuations in temperature and humidity. The percentage of current flowing to each

TABLE 1 Percentage of Total System Current Flowing to Each Anode Line, Corresponding Anode-to-Ground AC Resistance and System Current Densities

System	Anode or Face	Portion of Total Current (%)	AC Resistance (anode to ground) (Ω)	Current Density on Concrete (mA/m^2)
1	North	12.3	26.5	10.4
	South	25.5	16.5	14.3
	East	35.4	11.7	18.3
	West	26.8	15.4	13.9
2	20	34.8	10.4	–
	21	44.6	9.3	–
	22	20.6	11.5	–
3	East face			11.9
	21	6.5	34.3	
	22	17.6	24.1	
	North face: 23	17.0	22.7	14.1
	West face			16.6
	24	20.6	15.7	
	25	11.8	19.6	
	South face: 26	26.5	15.7	14.7
	Pitch anode (north, east)	41.1	–	13.0
	PAN anode (south, west)	58.9	–	15.7

face remained constant. After 7 months of operation the current flowing through anode 20 dropped by considerably more than would be predicted by the change in resistance. The anode will be monitored closely for evidence of deterioration. The current density on each face could not be calculated because the anode system (polymer concrete and paint) is continuous around the column. Anode 19 was installed as shown in Figure 2, but not powered.

The current densities on the four faces of System 3 have remained relatively constant during the monitoring period. However, current flowing to anode 21 has gradually decreased as the resistance has increased.

Macrocells

The five macrocells in each system were placed in the same positions, with one cell outside the protected surface area of each. Before activation of the systems all cells showed positive readings, which indicated anodic current flow on the probe surface. Typical off corrosion current flow to the macrocell probes was on the order of 10 $\mu A/cm^2$. All probes showed initial fluctuations in current level. In all macrocells within the protected areas of the four systems, current flow between the probe and main reinforcing was reversed by application of a 500 mA cathodic protection current, which indicates that the corroding anodes had been eliminated (i.e., had become cathodes). These cells remained cathodic, when the cathodic protection systems were on, throughout the test period.

Measurements made during E-log I tests indicated that the probes became cathodic at current levels much lower than Icp. Macrocells in all systems outside the protected region showed negligible effects from current application and remained anodic throughout the test period. As the systems were repeatedly polarized and depolarized, macrocell corrosion currents measured during system off periods decreased. However, this effect was also seen on some probes outside protected areas, and thus the reduction in corrosion rate cannot at this time be attributed solely to cathodic protection. Macrocell 3 in System 2 was unstable and showed signs of physical distress. Readings from this cell have therefore been omitted.

Current Pick-Up and Distribution Probes

Average current densities on the probes (including the macrocell rebar probes) have been calculated for the time periods when the systems were activated. The density is calculated by dividing the current flow to or from the probe by the surface area of the probe. These figures are given in Table 2. Values for pick-up and distribution probes when the systems were switched off were essentially zero, showing negligible anodic or cathodic current flow. These off values exhibited no significant variations with time when measured during periods of system depolarization. The probe locations vary from system to system and are shown in Figures 1-4.

The current distribution throughout System 1 was satisfactory, with average probe current densities in the range of 1 to 3 $\mu A/cm^2$. The distance of the probe from the anode had little effect on the current density received, probably because of the relatively close anode spacing and the presence of the shotcrete overcoat. A slight decrease in current densities was observed as the distance from the power input end of the anodes increased. Probe 9 showed extremely high current densities, although the reason for this in unclear. The probe outside the protected area (in macrocell 2) showed no change when the power was switched on. The average current densities on the distribution probes were 1.93, 0.79, and 0.56 $\mu A/cm^2$ for probes 100, 180, and 250 mm from the concrete surface, respectively. Thus the probe at the 250-mm depth received 29 percent of the current reaching the probe at the 100-mm depth. A comparison of the average current density on the

TABLE 2 Average Current Densities on Instrumentation Probes

Probe Type and Number	Current Densities ($\mu A/cm^2$) System 1	System 2	System 3
Macrocell rebar probes			
1	-4.93	-2.47	-2.42
2	+0.79	+0.47	-2.94
3	-3.24	–	-4.92
4	-2.19	-0.48	-2.93
5	-0.16	-5.09	-1.63
Current pick-up probes			
6	-2.53	-4.26	-4.64
7	-2.34	-0.03	-10.41
8	-2.69	-2.08	-4.12
9	-18.57	-2.22	-1.90
10	-0.67	-3.86	-4.25
11	-1.13	-2.96	-6.55
12	-1.40	–	-4.36
13	-0.53	-2.61	-8.07
14	-3.94	-1.26	-4.61
15	-2.41	-4.95	-8.89
16	–	-11.91	-7.94
17	–	–	-4.75
18	–		-6.30
33	–	–	-0.09
Current distribution probes			
16a	-1.41	–	–
16b	-0.74	–	–
16c	-0.66	–	–
17a	-2.61	-1.19	–
17b	-0.84	-1.10	–
17c	-0.51	-0.40	–
18a	-1.79	-3.43	–
18b	-0.53	-1.44	–
18c	-0.49	-0.52	–
19a	-0.24	–	-4.91
19b	-1.04	–	-0.65
19c	-0.59	–	-0.35
20a	–	–	-6.34
20b	–	–	-0.97
20c	–	–	-0.42

distribution probes beneath anodes and remote from the anode lines is shown for all three impressed-current systems in Figure 8.

The current distribution in System 2 was even, with current densities in the range of 2 to 4 μA/cm². There was no apparent decrease in protection levels as the distance from the power input end of the anodes increased, which indicates that the paint provided good current distribution. There is no obvious explanation for the abnormally high current level received by probe 16. Probe 7 was located outside the protected area. As with System 1, the current distribution probes showed a significant proportion of the current reaches the 150-mm depth.

The magnitude of current densities measured in System 3 was consistently greater than seen in Systems 1 and 2, generally ranging from 4 to 8 μA/cm² for the current pick-up and distribution probes. On all faces the highest current densities were seen directly beneath primary anodes (at probes 7, 11, 13, 15, and 18 the average density was 8.0 μA/cm²), decreasing midway between anodes (at probes 6, 11, and 16 the average density was 5.7 μA/cm²), and at a minimum midway between anodes and column edges (at probes 8, 10, 12, and 17 the average density was 4.4 μA/cm²). However, such a decrease is probably tolerable. The relationship between the distance of the probe from the primary anode lines and current density is shown in Figure 9. Probe 33, as shown in the figure, is outside the protected area.

Voltage and Potential Measurements

System Voltage

With rectifiers set to maintain a constant current, system voltage levels rise and fall with changes in environmental conditions. Both Systems 1 and 3, with shotcrete overcoats, tended to show stable voltage levels over time with no sudden drops or increases. They showed little variation with short-term temperature changes. System 1 ranged between 3 and 6 V. The lowest voltages occurred during the summer months and the highest voltages occurred during cold winter periods, which corresponds to periods of lower and higher anode-to-ground resistance, respectively. System 3 voltages were in the range of 2.5 to 3.5 V during initial operation, rising to 5 to 7 V during the first winter and remaining near that level (4.5 to 5 V) during the spring and summer of 1983. The ac resistances measured between anodes

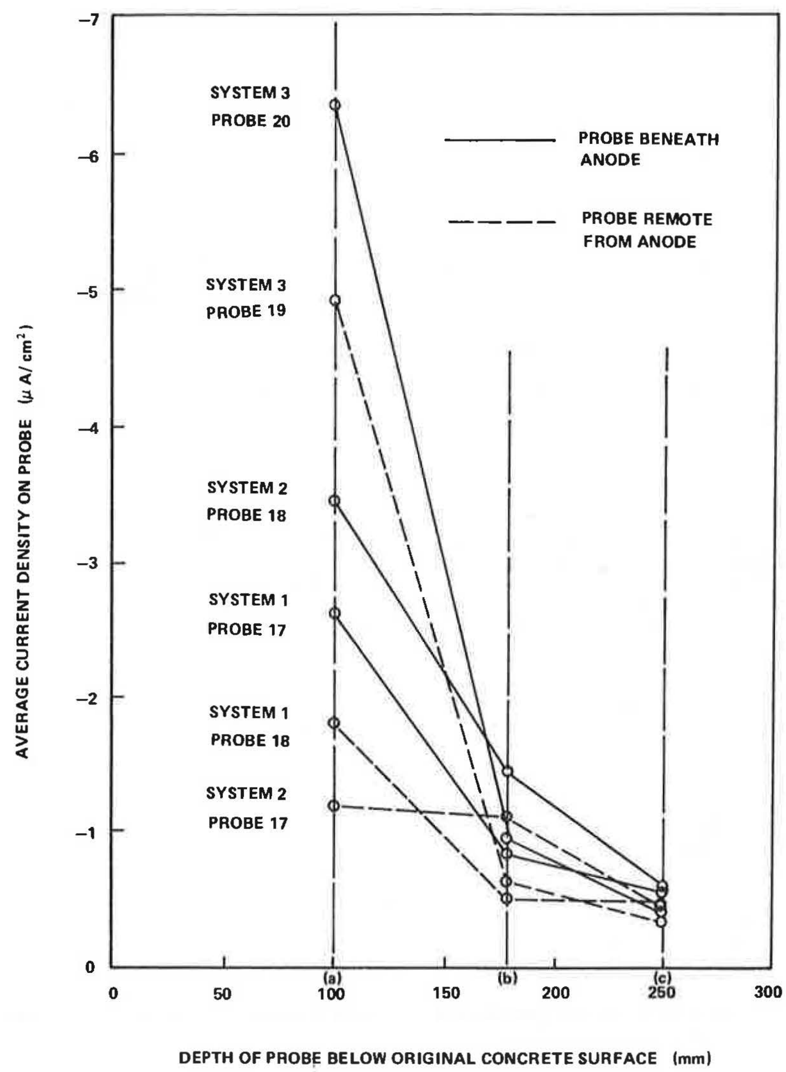

FIGURE 8 Typical variation of average current densities on current pick-up probes with depth and position relative to system primary anodes.

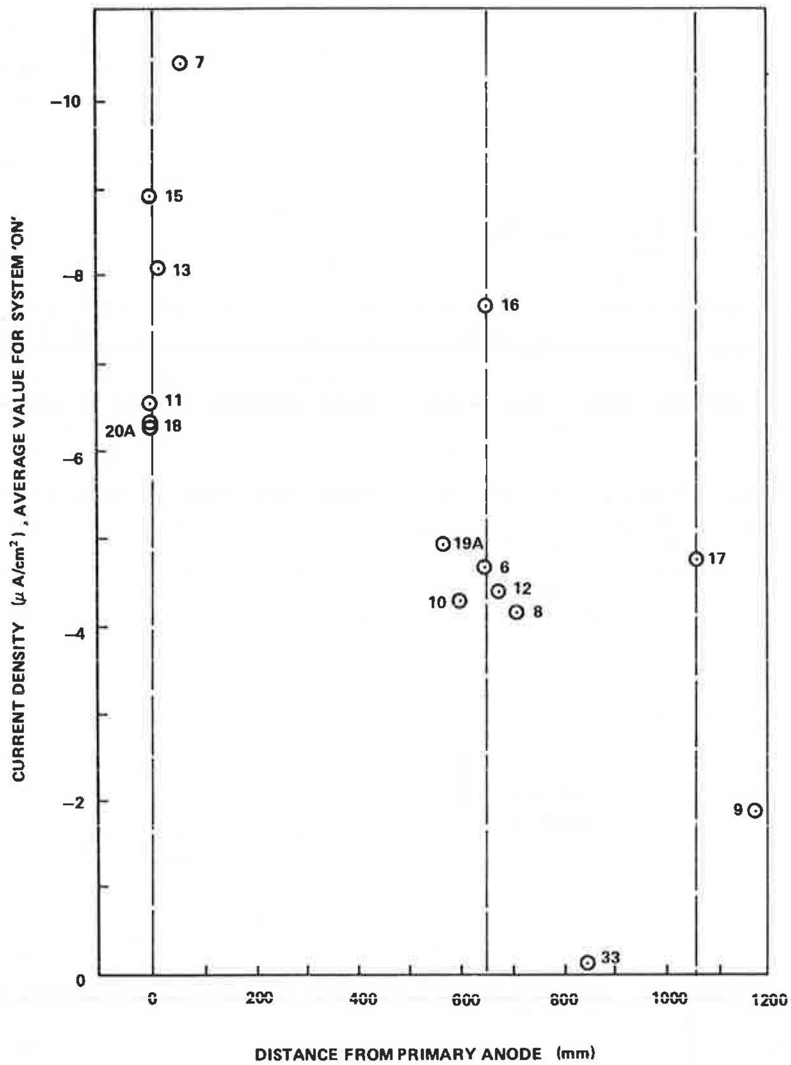

FIGURE 9 System 3: variation of probe current densities with distance of probe from primary anode.

and ground in this system have remained relatively constant. In contrast, System 2 showed rapid and extreme responses to changing temperature and, particularly, humidity conditions. Substantial increases in voltage corresponding to hot dry summer weather occurred and the system was unable to maintain the constant specified current because maximum rectifier output voltage was reached. These high system voltages (13 to 14 V) can be related to increasing anode-to-ground resistance. The resistance readings in July were approximately 4 times those recorded in February. Two factors appear to contribute to this increase in resistance: (a) poor mechanical contact between anode and paint, and (b) drying of the concrete beneath the paint layer.

Examination showed that warping of the anodes between anchoring points had occurred, thus reducing the contact area with the paint. Soaking of the paint on a day when high voltages were recorded caused a drastic drop in voltage, with a threefold increase in system current.

Typical system voltages for the three impressed-current systems are given in Table 3. The dates have been selected to be representative of the conditions experienced during the full 8 months of operation. The temperatures reported are the average concrete temperatures approximately 100 mm below the original concrete surface.

Reference Cells

Reference cell potentials can be interpreted with

TABLE 3 Typical System Voltages, Selected Dates

Date	Temperature (°C)	System Volts System 1	System 2	System 3
November 17, 1982	4.8	4.2	3.6	2.8
November 22, 1982	8.7	4.2	3.0	3.0
January 26, 1983	0.3	5.8	3.9	5.6
March 24, 1983	3.3	5.3	4.3	5.3
April 7, 1983	6.0	6.2	3.1	5.5
April 13, 1983	8.8	4.6	3.8	4.7
April 14, 1983	8.6	6.5[a]	3.4[a]	6.4[a]
April 26, 1983	12.7	6.2[a]	12.0[a]	6.6[a]
June 7, 1983	15.0	6.1[a]	5.3	5.5
June 16, 1983	27.0	3.2	10.7	5.0
June 21, 1983	26.3	3.3	13.6	5.3
July 8, 1983	24.0	3.3	13.4	4.5

[a]Anode arrangement altered.

respect to a number of protection criteria (1,3), including absolute potential values (-850 mV or less with respect to a copper-copper sulfate reference electrode) and potential shifts (-300 mV between static and instant-off potentials, or -100 mV between instant-off potential and steady-state potential of the steel with cathodic protection currents off). Because cell potentials in the test systems varied over a wide range, from cell to cell, while the response of individual cells to current application was generally consistent, a polarization criteria rather than consideration of absolute cell values was most meaningful.

The shift between instant-off potentials and static potential was examined and compared with the specified value of -100 mV. The applied current of 500 mA appears to be more than sufficient to meet this protection criteria for all three systems. The average polarization for the systems over the operating period was -230 mV, based on 10 cells, with cell averages ranging from -187 to -301 mV. The polarization was calculated by subtracting from each instant-off reading the static cell potential measured during the preceding period when the current was switched off. Although static potentials recorded during periods of system depolarization were generally similar, some cells showed a negative shift in static potential with time. This often resulted in a decrease in polarization. For example, the polarization of cell 4 in System 2 decreased from -277 to -134 mV during the monitoring period. This decrease is difficult to interpret. It may be caused by the long-term effects of the application of the cathodic protection, seasonal variations, or changes in the cell itself.

Control cells (cell 2 in all systems) outside the protected area did not all respond the same way and some showed evidence of instability. In System 3 the potential of the cell remained constant, in System 1 the cell showed a steadily increasing negative polarization, and in System 2 cell 2 behaved erratically.

Alteration of Anode Configurations

Some of the anodes were disconnected during the period April to June 1983 to investigate the effects of different anode spacings. In System 1 alternate anodes were disconnected so that the anode spacing was increased to 900 mm. Anode 21 was switched off in System 2 so that the system was powered by two anode rings 2.4 m apart. In System 3 anodes 22 and 24 were switched off so that the east and west faces were powered by a single anode. The maximum distance from a primary anode was then 2.6 m.

The effects of the changed anode spacings were most noticeable in Systems 1 and 3, where the system voltages increased by approximately 30 percent. In System 1 the polarization shift measured by the reference cell directly below an impowered anode decreased by 50 percent and dropped below 100 mV. Current densities on probes adjacent to unpowered anodes also decreased appreciably in both systems. In System 3 the effect was greater on the east than on the west face, which may indicate less-efficient current distribution on this face. The results indicate that the anode spacings in Systems 1 and 3 cannot be increased significantly unless circuit resistance can be lowered through the use of a more conductive overcoat.

In System 2 there was little change in the potential shift recorded by the reference cells or in the current densities on the pick-up probes, although the current density on two of the macrocell rebar probes decreased. System voltage remained the same immediately after anode 21 was switched off. It increased later, although this coincided with a period of higher temperature. The test indicated that System 2 distributes current efficiently and primary anode spacing could be increased from 1.2 m to up to 2.4 m.

Effect of Differential Wetting

A short soaking test was carried out on Systems 1 and 2 to determine the effect of wetting part of each system. The south faces of both systems were soaked by hosing for a period of 20 min. The probes were monitored before soaking, 10 min after soaking began, immediately after soaking, and several hours later the same day. A sunny day was chosen so that the temperatures on the south face were high and the concrete surface was dry.

The short soaking period had no effect on any of the current or voltage measurements in System 1. This indicates that the shotcrete insulates the cathodic protection system from sudden environmental changes.

In System 2 the effects of the soaking were immediate. The system voltage required to maintain the 500-mA current dropped from 9.0 to 4.4 V. Reference cells in the the south face showed an average polarization of -135 mV with respect to the initial reading. Cells in the other faces became slightly (40 to 70 mV) more positive. The current flowing to the probes in the wetted face more than doubled, whereas all other probes showed a substantial reduction in current density. The effect of the soaking was reflected in a change in current density on the probes at the 250-mm depth. The change in current distribution in the system was temporary, and within an hour after soaking the readings began shifting to the values observed before soaking. The results illustrate the sensitivity of conductive paint systems to changes in the environment and point to a skin effect (the tendency of the surface concrete to dry), which significantly increases the circuit resistance of paint systems in a dry environment.

Durability

Cores were removed from Systems 1 and 3 after 8 months of operation to examine the anodes and the concrete surrounding the anodes. At the same time, all systems were inspected visually and sounded to detect delamination. This 8-month period represented approximately 2,050 amp-hr of operation for Systems 1 and 3, and 2,270 amp-hr for System 2.

Extensive areas of delamination were found on the north, south, and west faces of System 1, with lesser areas on the east face. The areas of delamination are shown in Figure 10. The delaminations do not correspond to the location of anodes or other physical features. A network of fine cracks was visible in the shotcrete. The cracks were not visible shortly after construction. Cores were taken from the top of an anode on the west face. A strong odor of chlorine gas was evident after the core was removed. The shotcrete was debonded in this area, and a small gap behind the anode indicated it had not been held tightly against the column face during shotcreting. Concrete adjacent to the anode was discolored and deteriorated. Application of pH paper showed acid levels of pH2 on the back of the anode to pH6 on the concrete surrounding the anode. The anode itself showed no deterioration.

In System 2 the paint was found to be adhering well except in areas where new concrete was placed in the macrocells and the rustication strips. The

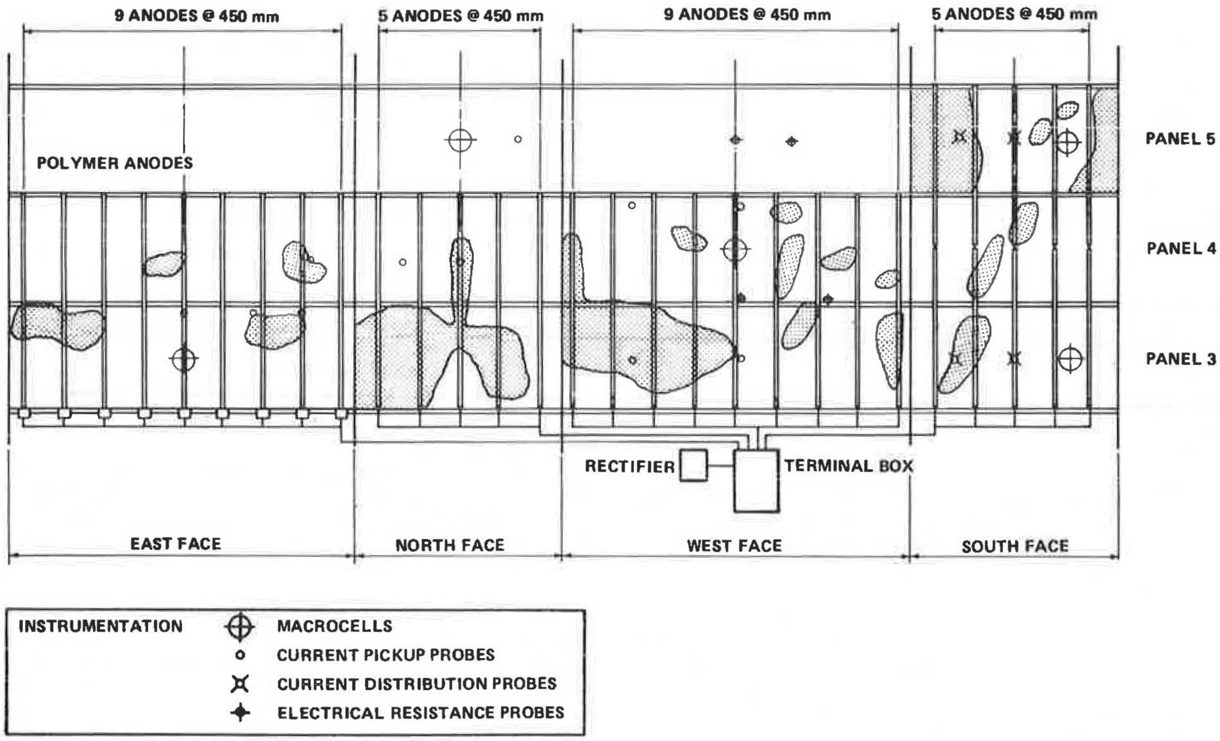

FIGURE 10 System 1: areas of delamination (July 1983).

contact between the anodes and the paint was unsatisfactory, as the anodes had buckled, leaving noticeable gaps between the anodes and the column face. The platinum wire connections appeared brittle and could be easily damaged. There was considerable staining of the paint surface around macrocell 3 by backfill material from the reference cell, which had become unstable. Sounding indicated a small delamination on the top edge of the south face. The shotcrete in System 3 exhibited widespread cracking and extensive delamination in much the same manner as System 1. Coring indicated the delaminations were the result of lack of bond between the shotcrete and the column. The time at which the shotcrete debonded is not known because the shotcrete had not previously been sounded. Cores were also taken about 75 mm from the bottom ends of primary anodes 21 and 22. The core from anode 21 contained cracks that originated from the corners of the anode. The concrete in contact with the anode showed a slight discoloration. Phenolpthalein applied to the core surface indicated that the concrete adhering to the anode remained alkaline, but the material on the debonded face had a pH less than 9.

The core containing anode 22 also showed that the outer surface of the anode was alkaline while the back face was acidic. Both cores showed the embedded platinum wire and carbon strand to be in excellent condition, and there was firm physical contact between the primary and secondary anodes. The presence of the carbon fiber resulted in a gap between the primary anodes and the concrete surface, and this may have been beneficial in dissipating gases formed on the anode surface.

TABLE 4 System 4 Current Distribution

	11/9/82	1/26/83	4/21/83	6/4/83
Temperature (°C)	6	-1	6	27
Total current flow (mA)	154	55	56	100
Current flowing to each column face (%)				
North face	24	22	25	16
South face	25	24	23	19
East face	30	36	29	22
West face	21	18	23	43
Current density on column face (mA/m²)				
North face	6.2	2.0	2.4	2.7
South face	4.3	1.5	1.5	2.1
East face	4.8	2.1	1.7	2.3
West face	3.4	1.0	1.3	4.5

RESULTS OF MONITORING PROGRAM: SACRIFICIAL ANODE SYSTEM

Current Flow, Density, and Distribution

Anodes and Column Surfaces

The currents and current densities in System 4 were much lower than in the impressed-current systems, typically in the range 1 to 4 mA/m^2 of concrete surface. The overall current levels fluctuated between a low of 31 mA in April and a high of 141 mA in July, although a slightly higher current was recorded immediately after the system was activated. In general, anode currents were lowest in the winter months. However, currents varied more than would be expected from the changes in anode-to-ground resistance. The resistances showed little consistent seasonal variation but fluctuated considerably from day to day. The distribution of current among the column faces also varied in an unpredictable manner. The data in Table 4 give typical values of current distribution and density throughout the monitoring period. The average current density on the column reinforcing steel during the period was calculated to be 3.7 mA/m^2 (0.37 $\mu A/cm^2$) of rebar surface.

Macrocells

Macrocell current flow was not permanently reversed by the cathodic protection currents. The cells became increasingly positive (i.e., more active) with time, particularly during the summer. The only brief period of current reversal occurred immediately after the system was activated. The behavior of macrocell 4 throughout the monitoring period is shown in Figure 11. By July 1983 all the macrocells were approaching the prepolarization levels of August 1982.

Current Pick-Up and Distribution Probes

The current densities recorded were extremely low, typically 1 $\mu A/cm^2$ and less for the pick-up probes, and 0.2 $\mu A/cm^2$ and less for the distribution probes. Slightly higher values were recorded immediately after system activation.

The effect of seasonal variation on the current densities on the pick-up probes is shown in Figure 11. As would be expected, temperature effects were much more significant in System 4 than in the impressed-current systems. There was little difference between the response of the individual probes because of the close (150-mm) spacing of the zinc anodes. Although current was detected on the probes 250 mm below the concrete surface, the levels were extremely low and remained sensibly constant.

Voltage and Potential Measurements

System Voltage

The maximum driving voltage of the system is the potential difference between the zinc and steel, which is theoretically 323 mV. The potential difference measured before coupling the anodes to the reinforcement was approximately 300 mV. The polarized driving voltage during system operation was much lower, typically 70 to 140 mV.

Reference Cells

Before activating the cathodic protection, the potentials of the zinc-zinc sulfate reference cells ranged between +241 and +467 mV. After 8 months of operation the instant-off potentials were between +260 and +338 mV, with an average of +300 mV. Three cells, in macrocells 3, 4, and 5, showed a negative (cathodic) polarization of 70 mV or less based on the difference between the average cell readups before activation and the instant-off potentials after 8 months. Cell 1 showed a slight positive shift. Cell 2, outside the protected region, showed -170 mV (cathodic) polarization. Consequently, in this system the variation of the reference cells with time may mask the true effects of the cathodic protection.

Durability

No cracking or surface damage was observed during the visual examination of the shotcrete in System 4. There was only one small delamination, which was located near the top of the west face adjacent to an unprotected panel.

Cores were taken through an anode on the west face, approximately 150 mm from the anode tip. The appearance of the anode was unchanged from the time of construction and there was no evidence of corrosion of the anode surface. At the time the cores were taken, the quantity of electricity passed was approximately 378 amp-hr. This corresponds to a consumption of 368 g of zinc or 0.50 percent of the total mass of anode.

SUMMARY

All three impressed-current systems were effective from the electrical standpoint of stopping steel corrosion. Operating voltages for the three systems typically lay in the range of 3 to 6 V with systems operating at 500 mA. This resulted in 13 mA/m^2

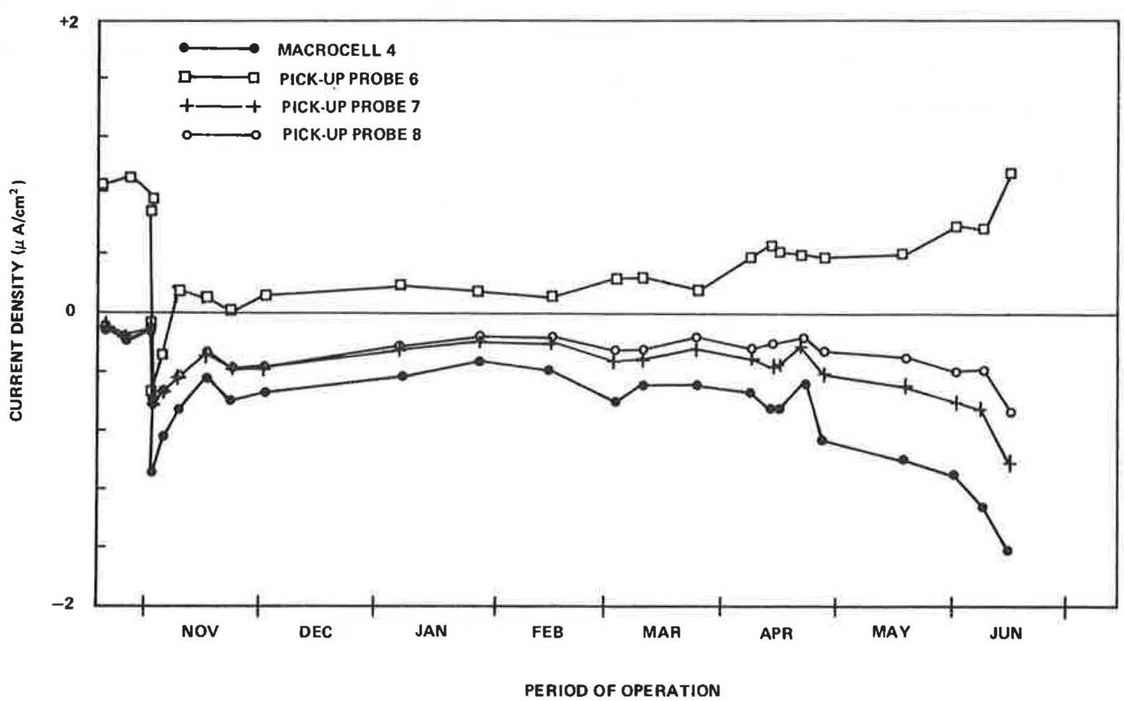

FIGURE 11 System 4: sample macrocell and current pick-up probe current densities during monitoring period.

overall current density on the concrete surface, for all systems, which corresponds to an estimated rebar surface current density of 28.2 mA/m^2. Pick-up and distribution probe current densities were typically 2 to 6 $\mu A/cm^2$, with probes at a 250-mm depth receiving significant current. Zinc-zinc sulfate reference cells indicated an average cathodic polarization of approximately 200 mV, with several cells indicating a decrease in rebar polarization as time passed. Three cells showed evidence of instability with time. Probes outside protected areas showed negligible effects due to cathodic protection currents.

Improvements are needed in System 2 where unsatisfactory contact between the primary anodes and the painted concrete surface, coupled with surface drying effects, resulted in high system voltages. The effect of moisture and temperature was much greater in this system than either System 1 or 3. Tests conducted with different anode configurations indicated that the distance between the primary anodes could be doubled to approximately 2.4 m without significantly affecting current distribution.

The anode spacings in Systems 1 and 3 were found to be adequate, but current density calculations and acid attack observed in the core specimens indicated that an increased anode surface will be required. The debonding of the shotcrete has not been adequately explained. The possibility of the cathodic protection currents having an adverse effect requires further investigation, especially in view of results elsewhere with a similar system on a horizontal surface with overlay, which showed no debonding after 18 months at similar anode current densities (4).

The sacrificial anode system offered insufficient protection to the reinforcing steel. Current levels were low, with an average system current of only 65 mA during the 8-month period of evaluation. The system lacked any means of control and exhibited substantial fluctuations in current distribution. The only practical method of increasing current density is to cover the concrete surface with zinc, but a sacrificial system is unlikely to become practicable unless the criteria now assumed to be necessary for adequate protection are found to be unduly conservative.

In all four systems the anode materials showed no degradation after more than 2,000 amp-hr operation on the impressed-current systems and approximately 400 amp-hr on System 4.

All the embedded instrumentation, other than the electrical resistance probes, functioned satisfactorily. The pick-up probes, which were inexpensive to fabricate and install, were found to be particularly useful in determining the distribution of current over the surface of the reinforcing steel and its variation with depth. The macrocells were useful in determining the effectiveness of the cathodic protection systems. Zinc-zinc sulfate reference cells were found to be unstable, and this simply points to the already well-established need for a reference cell that will be stable when embedded in salt-contaminated concrete.

FUTURE WORK

Although the impressed-current systems stopped corrosion, the durability of the systems must be improved substantially before they would be suitable for a full-scale operational system on bridge substructures. Monitoring of the existing systems will continue and further experimental systems will be constructed at the test site as improved materials are identified. Supporting laboratory and exposure plot studies will concentrate on anode consumption rates, connection details, reference cells, and the effect of cathodic protection on the bond of overcoat materials.

REFERENCES

1. R.F. Stratfull. Criteria for the Cathodic Protection of Bridge Decks. In Corrosion of Reinforcement in Concrete Construction (A.P. Crane, ed.), Society of Chemical Industry, London, England, 1983, pp. 287-332.
2. D. Whiting and D. Stark. Galvanic Cathodic Protection for Reinforced Concrete Bridge Decks: Field Evaluation. NCHRP Report 234. TRB, National Research Council, Washington, D.C., 1981, 63 pp.
3. Recommended Practice: Control of External Corrosion on Underground or Submerged Metallic Piping Systems. Standard RP-01-69. National Association of Corrosion Engineers, Houston, 1972.
4. Y.P. Virmani. FCP Annual Progress Report--Year Ending September 30, 1982, Project 4K, "Cost Effective Rigid Concrete Construction and Rehabilitation in Adverse Environments." FHWA, U.S. Department of Transportation, 1982, p. 40.

Publication of this paper sponsored by Committee on Corrosion and Committee on Performance of Concrete.

Bridge Heating Using Ground-Source Heat Pipes

RON C. LEE, JOHN T. SACKOS, JOHN E. NYDAHL, and KYNRIC M. PELL

ABSTRACT

An experimental bridge deck heating system has been constructed and monitored that uses field-assembled heat pipes to transfer energy from 100-ft vertical evaporators in the ground. Measurements indicate that the heated surface was from 2° to 14°C warmer than the unheated portion of the bridge during heating events. This heating was sufficient to prevent the preferential freezing of the bridge deck surface relative to the adjacent road and provided some snow melting. A computer model that simulates the performance of ground heat pipe systems has been developed and verified by using data from two experimental facilities. This model is being used in conjunction with experimental results to prepare a general design procedure for these types of systems.

Pavement heating systems to control snow and ice accumulation on bridges and ramps have been incorporated at certain critical locations as an alternative to the more traditional methods of plowing or using deicing chemicals. These systems have typically been either embedded electrical resistive heaters or pipes circulating a fluid. The circulating fluid systems generally use fossil fuel energy sources, although several low-grade renewable thermal energy sources such as geothermal water (1) and the warm ground below the frost line (2) have also been tested. The efficiency with which low-grade energy can be transported to the road surface is an area where improvement can be made.

The use of gravity-operated heat pipes to transport thermal energy to a road surface was investigated and developed during the 1970s (3-8). The gravity-operated heat pipe consists of a sealed enclosure that contains a fluid in the liquid-vapor state over its operating temperature range. The lower end of the pipe is the evaporator section, whereas the upper portion is the condenser section. When the evaporator section is warmer than the condenser section, a portion of the liquid vaporizes and travels to the condenser section, where it condenses with the release of its latent heat of vaporization. The evaporation and condensation process creates the driving potential to transport the vapor upward, while gravity returns the condensate to the evaporator. This makes the gravity-operated heat pipe an attractive heat exchanger because it is a completely passive system that does not require any mechanical or electrical parts. Ammonia has been used as the working fluid in these heat pipes, which has the advantage over water-based systems in that it is not susceptible to freezing.

Because the thermal energy is transported in the form of latent heat of vaporization, the heat pipe can transport large amounts of energy over relatively long distances ($\sim$55 m at two installations) with only a small temperature difference. For this reason, low-grade thermal energy sources that might otherwise be totally inadequate for the heating of road surfaces may be feasible energy sources in some situations. The ground heat pipe concept is particularly attractive because of the availability of its renewable energy source.

The average ground temperature several meters below the surface is typically a few degrees greater than the yearly average air temperature. This means that a large media at a temperature on the order of 10°C is theoretically available for use at most U.S. locations. However, the extraction rate of this ground energy is limited by the surface area of the heat pipe, the thermal conductivity of the deck and the ground, and the heat capacitance of the ground. The cost of the ground heat pipe system is obviously also directly related to its surface area, especially the length of the evaporator pipes. Approximately 40 percent of the cost of the ground heat pipe systems that have been installed has been directly attributable to drilling and grouting the evaporator holes. These costs are extremely site specific and are therefore a significant design consideration.

EARLY GROUND HEAT PIPE SYSTEM RESEARCH

Experimental testing of ground heat pipes was initiated in 1970 at the FHWA Fairbanks Highway Research Station (4). The tests, which were conducted by the Dynatherm Corporation, successfully demonstrated the concept as well as pointing out necessary construction precautions. It confirmed, for example, that proper internal cleaning of the heat pipe was extremely important to prevent the generation of noncondensable gases that subsequently block the condenser. The results of this experiment were sufficiently promising to justify the heating of a highway ramp (5) in Oak Hill, West Virginia, by heat pipes. This system was constructed in 1975 and uses 1,213 ground heat pipes extending 60 ft (18.3 m) into the ground. This system was generally successful in preventing snow and ice accumulation, except when snow drifting occurred. The far-field ground temperature in this case averaged around 13°C.

To further develop ground heat pipe technology, the University of Wyoming, under the sponsorship of the Wyoming Highway Department and FHWA, has designed and operated two experimental facilities in southeastern Wyoming. The goals of these projects have been to experimentally investigate the performance of ground heat pipe systems for bridge decks as well as to develop the analytical framework to extend these experimental results into a general design procedure. A schematic of the ground heat exchangers used at these two facilities is shown in Figure 1.

The Sybille Canyon facility (6) was constructed in 1976. A small section of this bridge was heated by 15 heat pipes with ground evaporator lengths that averaged around 40 ft (12.2 m). This experimental site was heavily instrumented to monitor the thermal response at various locations in the deck and roadway and the environmental conditions. At the conclusion of the study, 22 months of essentially continuous data had been collected at 10-min intervals.

The heat pipe system proved to be capable of eliminating any preferential freezing of the heated bridge relative to the adjacent road. The reductions in some of the other freezing parameters that can be

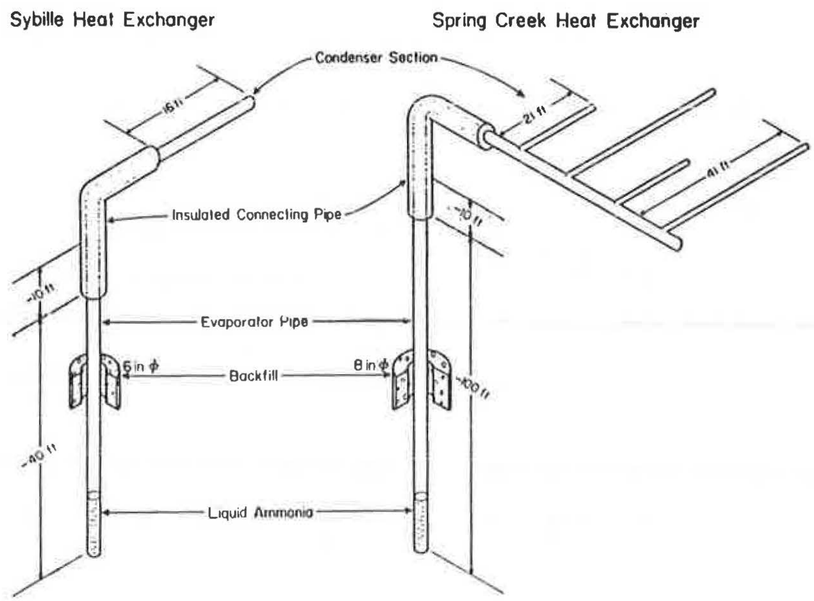

FIGURE 1 Schematic illustration of Sybille Canyon and Spring Creek heat exchangers.

used to characterize the performance of the system are as follows:

Heated Surface Parameters	Percent Reduction 1977-1978	1978-1979
Snow cover time	48	37
Time frozen	72	57
Integrated temperature below freezing (°C days)	90	79

The time-temperature below freezing is the area under the freeze line (0°C) on a surface temperature versus time plot. This parameter provides a measure of the severity of a freeze period.

This was a fairly impressive performance, considering that this was a bridge exposed to the severe Wyoming climate (the second winter being unusually severe), whereas the West Virginia test was performed on a ramp at grade. The far-field ground temperature at Sybille Canyon averaged around 10°C.

SPRING CREEK EXPERIMENTAL FACILITY

The Spring Creek facility (7) was constructed in 1981 in Laramie, Wyoming. An overview of this site is shown in Figure 2. The entire bridge deck, except for a small control section, is heated with 60 evaporator pipes using the manifold ground heat exchanger design shown in Figure 1. In addition, the bottom surface of the heated deck was insulated.

The evaporator sections were constructed from 2-in. (5.08-cm) schedule 80 steel pipe. The sections extend 100 ft (30.5 m) into the ground on 10-ft (3.05-m) centers. A high thermal conductivity grout was backfilled around the evaporator pipes to improve their thermal contact with the ground. Each evaporator pipe supplies four condenser pipes embedded in the deck on 6-in. (0.152-m) spacing through a manifold. The condenser pipes were constructed from 1-in. (2.54-cm) schedule 40 pipe. The pipes were alternatively 21 and 41 ft (16.4 and 12.5 m) long.

The construction of this heat pipe system was obviously much more complex than the previous systems, which consisted of a single tube that was totally assembled in the factory, except for a single field bend. The assembly of the large Spring Creek heat pipes each involved several welds, leak tests, and charging that had to be performed in the field without contaminating the system.

This experimental site was also heavily instrumented to record environmental conditions and system performance. Data acquisition was initiated on January 1, 1982.

The following reductions in heated surface freezing parameters relative to the unheated deck surface (nontraffic lanes) is again used to quantify the system performance:

Heated Surface Parameters	Percent Reduction 1/82-5/82	10/82-5/83
Snow cover time	46	47
Time frozen	46	34
Integrated temperature below freezing (°C days)	72	68

These results are not as impressive as those obtained at Sybille Canyon, but the far-field ground temperature at Laramie is only 8°C, which represents a 20 percent drop in ground temperature relative to freezing as compared to the Sybille Canyon site.

Figure 3 presents a plot of weekly averaged temperatures on the top surfaces of the heated and control sections, as well as the remote ground temperature at the 60-ft (18.3-m) depth. Because heating events are of present interest, only events where the heated surface temperature was below that of the remote ground were considered. The remote ground temperature represents the maximum temperature that the heated surface can approach during such events, whereas the difference between the heated and control temperatures corresponds to the amount of heating that actually occurred. Maximum temperature increases on the order of 10°C were achieved during the coldest periods.

Although the remote ground temperature represents the theoretical temperature potential of the system, the local temperature surrounding the evaporator pipes is depressed because of energy extraction. This depression can degrade the performance of the system with time, and it is a complicated function

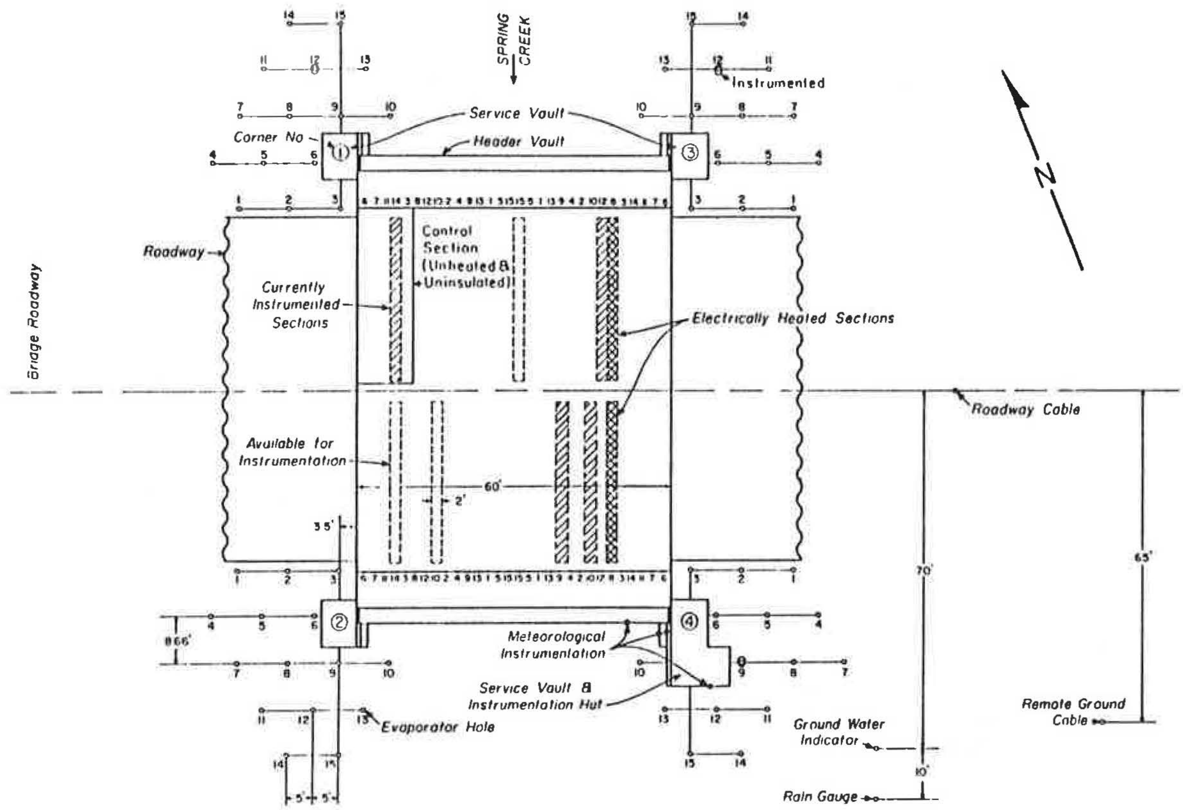

FIGURE 2 Schematic of the Spring Creek facility.

of the amount and rate of energy extraction as well as the thermal recovery of the evaporator field over the summer. The evaporator pipe and remote ground temperature histories are shown in Figure 4. The data in this figure indicate that the temperature of the ground in proximity to an evaporator was depressed by as much as 10°C, with recovery after the first two heating seasons being within 1°C of the far-field ground temperature. The system is to be monitored for 2 more years (until September 1985), which should provide sufficient experimental evidence concerning whether there will be any progres-

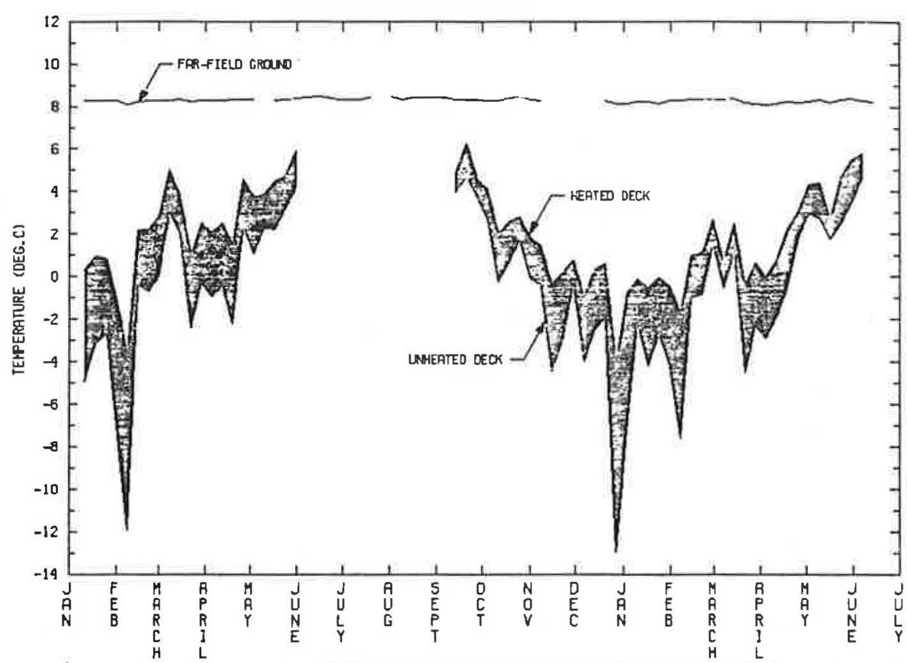

FIGURE 3 Weekly averaged heated and unheated deck surface temperatures during heating events.

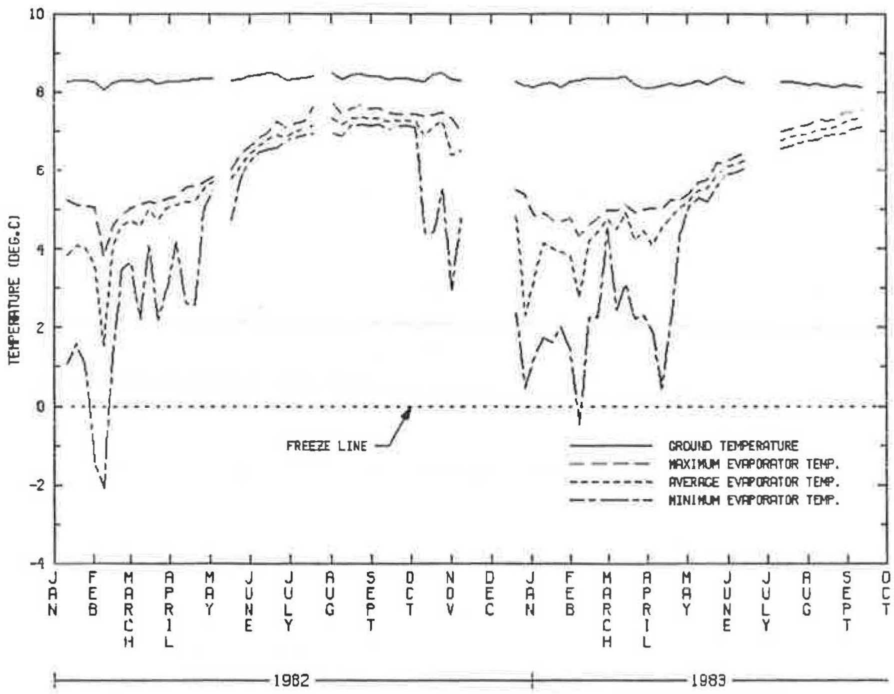

FIGURE 4 Weekly averaged evaporator pipe and far-field ground temperatures at 60 ft (18.3 m).

sive thermal depression of the ground surrounding the evaporator pipes.

The results of the Spring Creek and Sybille Canyon systems were sufficiently successful and provided the necessary expertise to encourage the incorporation of 177 ground heat pipes in the design of an overpass in Cheyenne, Wyoming (8).

ANALYTICAL MODELING

The results of the Spring Creek project, as well as those of the Sybille Canyon facility, provided valuable quantitative performance data for ground heat pipe systems. However, to extend these results into a general design procedure, it was necessary to construct a model that is capable of accurately predicting system performance. A schematic of the heat transfer system that formed the basis of this model is shown in Figure 5.

The model accounts for time-dependent heat transfer in the ground and bridge deck, and the necessary coupling to the environment. Snow melting was not included in the model because only the long-term system performance was of major concern in the design model. There are three types of bottom sur-

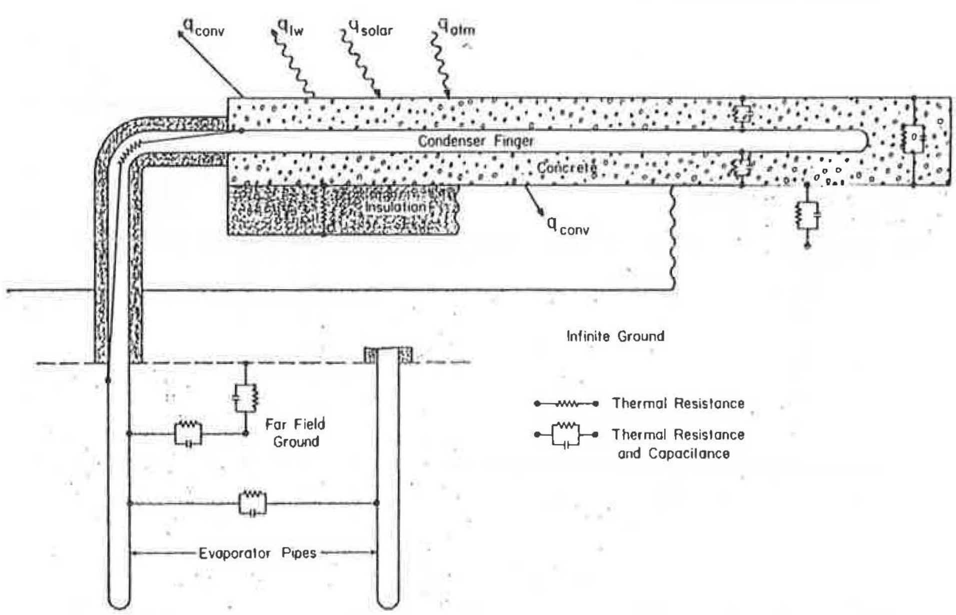

FIGURE 5 Heat transfer system.

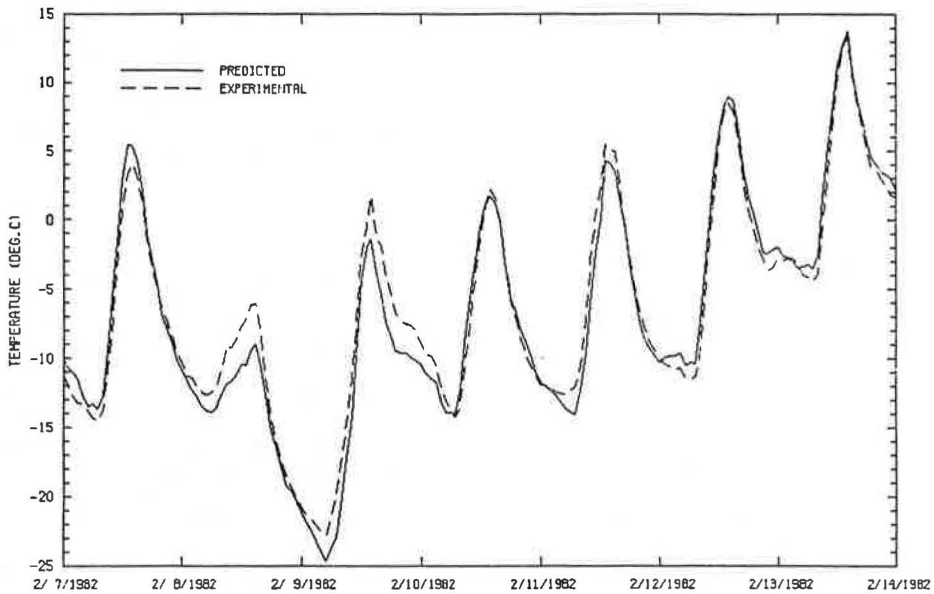

FIGURE 6 Top surface temperatures of unheated deck.

face conditions that can be accounted for: insulated, uninsulated, and ground coupled. Even though standard hourly weather tapes are used as part of the input data base, multiyear simulations can be performed with little computer time because the heat transfer equations are formulated in terms of response functions. The details of the heat transfer model are presented elsewhere (8,9).

To test the validity of the model, a comparison between the predicted and measured performance of the Spring Creek system was performed. The results from 1 week (February 7-14, 1982) of this simulation for the top surface of the unheated and heated decks are presented in Figures 6 and 7. This time period was chosen as being representative of a period of significant deck heating. Figure 6 shows that there is consistent agreement between experimental and predicted unheated top surface temperatures. The corresponding results for the heated top surface (Figure 7) also indicate satisfactory agreement, with minimum temperatures being as much as 14°C higher than the control surface. Similar results were obtained for the remainder of the Spring Creek data base and also for the Sybille Canyon system. The accurate simulations of these two different systems indicate that the analytical model can be used with some confidence as a design tool.

A preliminary parametric study has been undertaken by using the model to predict the performance of the Spring Creek system as a function of certain significant thermal and geometric parameters. The measure of performance that was chosen was the total energy extracted by the heat pipe system over one heating season (September 1982-May 1983). Figure 8 presents the results of this parametric study, where the percent of base heat extraction is plotted as a function of percent change of a system parameter. Energy extraction is seen to be a reasonably strong

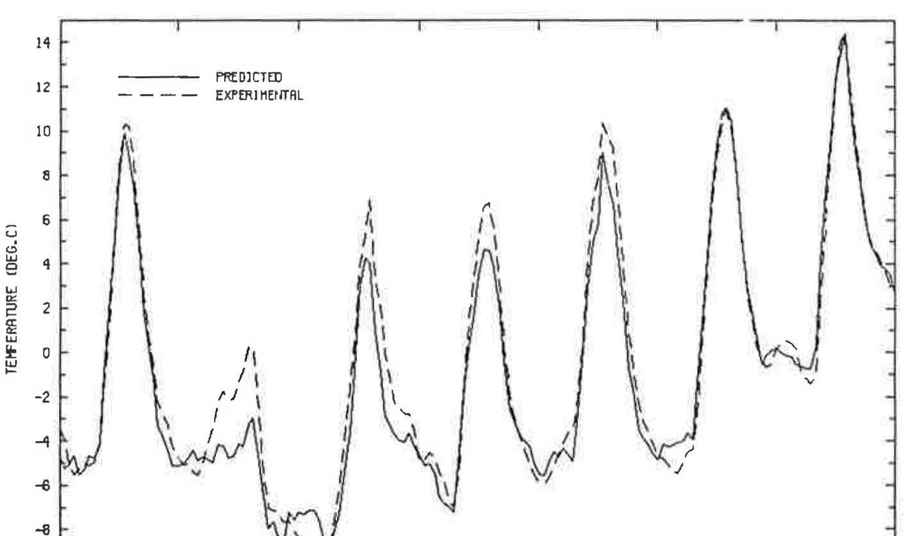

FIGURE 7 Top surface temperatures of heated deck.

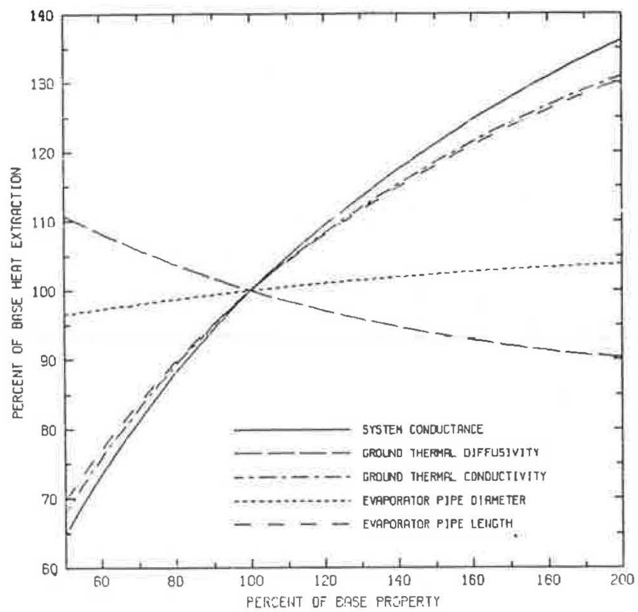

FIGURE 8 Percent change of base energy extraction at Spring Creek as a function of various parameters.

function of the length of the evaporator pipe, the thermal conductivity of the ground, and the thermal conductance of the system from the heat pipe to the air. A somewhat weaker dependence on the thermal diffusivity of the ground is exhibited, and it was found that there is essentially no dependence on the diameter of the evaporator pipe.

CONCLUSIONS

The experimental results for the two bridge heat pipe systems that have been recorded to date indicate that these systems have prevented preferential icing conditions on the bridges as well as providing a significant amount of snow- and ice-melting capability. Further monitoring of the Spring Creek facility will address the long-term characteristics of the system.

The experimental data bases generated at the Sybille Canyon and Spring Creek facilities have been used to verify an analytical model that predicts the transient performance of ground heat pipe systems. This model, in conjunction with experimental results, is being used to prepare a general design procedure for ground heat pipe systems.

REFERENCES

1. M. Sekioka et al. Thermal Considerations on Snow Melting System with Natural Thermal Water at Jozankei Spa, Sapporo, Japan. Journal of Japan Geothermal Energy Association, Vol. 16, No. 2, 1979.
2. F. Winters and S.R. Sasor. Pavement Heating--Executive Summary. Report 77-003a-7722. New Jersey Department of Transportation, Trenton, 1977.
3. J. Nydahl et al. Data Collection and Analysis for Geothermal Research. Final Report. Colorado Department of Highways, Denver, 1981.
4. W.B. Bienert et al. Snow and Ice Removal from Pavements Using Stored Earth Energy. Report FHWA-RD-75-6. FHWA, U.S. Department of Transportation, 1974.
5. D.C. Long and J.S. Baldwin. Snow and Ice Removal from Pavement Using Stored Earth Energy. Report FHWA-TS-80-227. FHWA, U.S. Department of Transportation, 1980.
6. V.A. Cundy. Transmission of Earth Energy by Heat Pipes for Thermal Control of Bridge Decks. Ph.D. dissertation. University of Wyoming, Laramie, 1979.
7. J.T. Sackos. Bridge Deck Heating Using Earth Coupled Heat Pipes. Thesis. University of Wyoming, Laramie, 1983.
8. J. Nydahl et al. Thermal Design of the Earth Heat Pipe System for the U.P. Railroad Overpass. SETA Corporation, Laramie, Wyo., 1981.
9. R.C. Lee. Heat Transfer Analysis of Geothermally Heated Road Structures. Thesis. University of Wyoming, Laramie, 1983.

Publication of this paper sponsored by Committee on Winter Maintenance.

Field Performance of Experimental Bridge Deck Membrane Systems in Vermont

RONALD I. FRASCOIA

ABSTRACT

The Vermont Agency of Transportation Bridge Deck Membrane Evaluation Program begun in 1971 is reviewed, and the field performance of 33 membrane systems over exposure periods of up to 11 years is discussed. Applications of deicing chemicals (sodium chloride) during the evaluation period have averaged 29.5 tons per two-lane mile per year, with accumulations totaling up to 123 lb of chloride (Cl^-) per linear foot of structure. Performance results are based on the presence or absence of Cl^- above base levels as determined by chemical analysis of more than 1,600 recovered concrete samples. The results indicate that, almost without exception, the experimental systems have outperformed the Agency's original standard treatment of tar emulsion. When grouped by general type, the best performance has been provided by the standard preformed sheet membranes and thermoplastic systems. Although somewhat less successful, satisfactory performance has been provided by the polyurethanes, the NCHRP Project 12-11 recommended systems, and miscellaneous preformed systems. In general, the epoxy and tar emulsion systems were not considered successful, although they have allowed only an average of 0.35 lb of Cl^- per cubic yard of concrete more than base levels in the top inch of concrete as compared to an average of 6.97 lb/yd^3 on exposed bridge decks over a similar evaluation period. Chloride contamination was detected in one sample or less on 33 percent of the 63 bridge decks under evaluation. Projections based on performance results to date suggest a significant number of the membrane systems will provide protection from serious Cl^- contamination for 50 years or longer.

Before the period in the early 1970s when bridge deck deterioration was recognized as a serious problem, a number of Snow Belt states commonly treated concrete bridge decks with a seal or membrane system and covered it with a bituminous pavement. The most common systems consisted of coal tar emulsions and roofing grade asphalts often used in conjunction with woven cloth or glass fabric designed to reinforce the system.

In the late 1950s the Vermont Agency of Transportation placed bituminous pavements over several portland cement concrete decks without first attempting to seal the concrete surface with a waterproofing system. In subsequent years inspections of such structures disclosed the presence of severe concrete deterioration beneath the pavement. The condition was always most prevalent along curb lines and adjacent to expansion dams where ponding action increased the level of chloride (Cl^-) contamination. In a number of cases the concrete was removed to a point below the top mat of reinforcing steel with hand shovels or low pressure water. Often the rebars were found to be completely free of corrosion. Such conditions suggest that the severe concrete deterioration was the result of high Cl^- contamination, numerous freeze-thaw cycles, and the retention of high moisture levels in the concrete caused by the presence of the bituminous overlay. This supposition is supported by studies (1,2) that point out the potential for damage to concrete because of salt crystal growth.

During the period 1960-1971 Vermont specified two coats of tar emulsion and two 1-in. courses of bituminous pavement as the standard treatment for bridge decks. In the late 1960s, Agency personnel recognized that the tar emulsion was not able to prevent Cl^- contamination and the subsequent concrete deterioration and rebar corrosion that was occurring along poorly drained areas. Faced with such information, the Agency chose to participate in the FHWA-sponsored National Experimental and Evaluation Program No. 12: Bridge Deck Protective Systems.

The program was established to encourage the states to try various new products and construction techniques designed to extend the service life of bridge decks. Vermont's participation took the form of a membrane evaluation program that began in 1971 with the application of two experimental systems on four new bridge decks. From that point to 1978, 33 different systems were applied in the field on 69 new concrete bridge decks. The products included 15 preformed systems, 7 epoxies, 5 thermoplastic materials, 4 polyurethanes, and 2 tar emulsion systems. Because the membrane systems were considered experimental, the applications were closely monitored and documented with reports. The information in the reports included background data on deck construction, concrete test results, condition of the decks, membrane product data, laboratory test results, observations made during the membrane applications, cost information, preliminary field test results, and discussions on the applications. Summaries of each membrane system were concluded with recommendations on further use.

The information presented in this paper summarizes the performance of the various membrane systems based on field samples taken through the period 1971-1982.

FIELD EVALUATION PROCEDURE

Follow-up field evaluations of the membrane systems began in 1975 on products that were exposed to a minimum of two winters of deicing chemical applications. Field testing in 1976, 1977, and 1978 included 37, 34, and 47 structures, respectively. Through the current date, field performance results have been obtained on all 33 experimental systems.

Field testing the first 2 years included electrical resistivity readings, electrical half-cell potential readings, and the recovery of concrete samples for the determination of Cl^- content by wet chemical analysis. Comparisons were made between the resistivity readings and the Cl^- levels detected at specific resistivity test locations. When correlation between the two test methods was found to be less than 60 percent, resistivity testing was deleted from the evaluation program in the following years.

For the past 7 years (1977-1983), the performance of the various membrane systems has been considered only in relation to the presence or absence of Cl^- more than base levels as determined by chemical analysis of recovered concrete samples. Such samples were taken at points 1, 5, and 15 ft off the curb line. The 1-ft offset was selected because of the potential for leakage at the curb line area, whereas the 15-ft offset establishes membrane performance in the wheel path area that is subject to aggregate puncture under continuous traffic. The 5-ft offset is located in the breakdown lane, where satisfactory performance would be expected if the membrane was not damaged during paving or lateral leakage did not occur. In most cases the test areas were located on the low end of the decks where Cl^- concentrations would be heaviest. Where superelevations resulted in drainage away from the breakdown lane, concrete samples were obtained from the opposite curb line. The pulverized concrete samples were obtained from 0- to 1-in. and 1- to 2-in. depths with the aid of a rotary hammer and a 3/4-in. carbide-tipped twist drill. The overlying bituminous pavement was removed by the same procedure followed by cleaning with compressed air. A depth gauge attached to the drill was used to obtain the proper depth. Sample holes were patched with a quick-set cement.

Before 1982 total Cl^- content in the recovered concrete samples was analyzed following California Test Method 404-C (1972). The method involved an indirect Volhard titration. In 1982 total Cl^- content was analyzed by using a colorimetric procedure based on American Public Health Association Standard Methods for the Examination of Water and Wastewater, Method 602 (1975). The results were randomly checked with a specific ion electrode by using AASHTO test method T 260-82.

FIELD CONDITIONS

Approximately 80 percent of the experimental membrane systems are located on Interstate 91 in the northeastern portion of Vermont where the annual freezing index averages 1,400, 80 to 115 freeze-thaw cycles occur, and snowfall ranges up to 140 in. With the exception of two installations in central Vermont, the remaining systems are located in southwestern areas, where the annual freezing index ranges from 950 to 1,100, 75 to 115 freeze-thaw cycles occur, and snowfall ranges from 70 to 100 in.

Through the spring of 1982 the test sites had been exposed to an average of eight winters of deicing chemical applications. The applications of road salt have been continuously monitored by the Agency's Maintenance Division, and the records indicate that yearly applications ranged from 8.5 to 38.3 tons per two-lane mile, with an average of 29.5 tons. During the evaluation period, the applications have totaled up to a maximum of 123 lb of Cl^- per linear foot of structure, or approximately 3 lb/ft² of deck surface.

Average daily traffic (ADT) volumes on the experimental systems have ranged from 370 to 1,990 vehicles. Total vehicle passes average 3,336,000 passes per structure. The average total passes are equivalent to approximately 3,000 18-kip equivalent axle loads (EALs).

MEMBRANE PERFORMANCE

In this study membrane performance results are considered in regard to the percent of contaminated samples and the level of Cl^- contamination. Chloride contents are expressed in parts per million (ppm) chloride ion by weight of concrete. For a simple and approximate conversion of ppm to pounds of Cl^- per cubic yard of concrete, divide by 250.

For the purpose of the study, concrete samples are considered contaminated when the Cl^- content is 50 ppm more than the base Cl^- levels recorded on the specific bridge decks following construction. Several important facts should be kept in mind as contamination results are reviewed. The presence of Cl^- contamination does not mean a complete failure has occurred. It does indicate the membrane is not 100 percent effective, and the level of contamination must be considered to determine the seriousness of the failure. With regard to rebar corrosion, Cl^- contamination does not become a serious threat until the Cl^- migrates down to the level of the reinforcing steel and the build-up at that level approaches or exceeds 325 ppm or approximately 1.3 lb/yd³ of concrete (3,4). The level of Cl^- contamination that results in severe deterioration to concrete has not been established. However, it is believed that the critical level is much higher than the 325-ppm level that will initiate corrosion of the reinforcing steel.

The following subsections describe the performance of the seven general groups or types of membrane treatment under evaluation, plus information on six exposed bridge decks for comparison purposes. The data in Tables 1-8 provide performance data on individual products and the averages for each group. The Cl^- values recorded in Tables 1-8 and Table 10 include base Cl^- levels. The average Cl^- content of all samples and a summary of membrane performance is given in Tables 9 and 10. The location of Cl^- contamination is given in Table 11, a summary of membrane characteristics and performance is given in Table 12, and proprietary products may be identified by referring to Table 13.

Standard Preformed Sheet Systems: Status--3 Systems on 21 Bridges Averaging 7 Winters of Exposure

The standard preformed sheet membrane systems have

TABLE 1 Field Performance of Standard Preformed Systems

System	No. of Bridges	Avg Winters Salted	Samples Contaminated (%) 0-1 in.	Samples Contaminated (%) 1-2 in.	Avg Cl^- in Contaminated Samples (ppm) 0-1 in.	Avg Cl^- in Contaminated Samples (ppm) 1-2 in.
70-mil preformed sheet	7	8.1	14	4	111	80
65-mil preformed sheet	5	8.4	19	12	111	79
75-mil preformed sheet	9	6.1	25	5	140	103
Class averages		7.3	19	7	125	86

TABLE 2 Field Performance of Thermoplastic Systems

System	No. of Bridges	Avg Winters Salted	Samples Contaminated (%)		Avg Cl⁻ in Contaminated Samples (ppm)	
			0–1 in.	1–2 in.	0–1 in.	1–2 in.
Rubberized asphalt	2	11	9	0	73	0
Polypropylene fabric and asphalt concrete (AC)	1	6	11	0	70	0
Polyvinal chloride (PVC) polymer	2	7	12	12	393	128
Hot asphalt and glass fabric	2	9	28	14	208	131
Class averages		8.6	17	8	209	130

TABLE 3 Field Performance of Polyurethane Systems

System	No. of Bridges	Avg Winters Salted	Samples Contaminated (%)		Avg Cl⁻ in Contaminated Samples (ppm)	
			0–1 in.	1–2 in.	0–1 in.	1–2 in.
100 percent solids (69 mils)	1	8	0	0	0	0
Asphalt modified (100 mils)	1	6	0	0	0	0
Asphalt modified (38 mils)	2	9.5	31	22	88	69
Tar modified (39 mils)	1	10	50	28	77	70
Class averages		8.6	26	17	83	70

TABLE 4 Field Performance of NCHRP Project 12-11 Preformed Systems

System	No. of Bridges	Avg Winters Salted	Samples Contaminated (%)		Avg Cl⁻ in Contaminated Samples (ppm)	
			0–1 in.	1–2 in.	0–1 in.	1–2 in.
Pitch and PVC polymer	1	8	7	7	298	150
Neoprene rubber	1	8	27	13	180	84
Butyl rubber	1	8	27	27	114	89
Ethylene-propylene-diene monomer (EPDM) rubber	1	8	33	7	82	72
Butyl rubber and felt	1	8	47	20	90	150
Class averages		8	28	15	120	109

TABLE 5 Field Performance of Miscellaneous Preformed Systems

System	No. of Bridges	Avg Winters Salted	Samples Contaminated (%)		Avg Cl⁻ in Contaminated Samples (ppm)	
			0–1 in.	1–2 in.	0–1 in.	1–2 in.
165-mil panel	1	4	0	0	0	0
60-mil tar resin	1	4	0	0	0	0
PVC-butyl rubber	1	6	11	0	68	0
75-mil vented	2	4.5	27	20	118	82
Hydrocarbon rubber	1	8	40	20	77	68
60-mil vented	2	4.5	40	13	108	98
Butyl-neoprene	2	4.5	47	20	193	111
Class averages		4.9	30	12	125	91

TABLE 6 Field Performance of Epoxy Systems

System	No. of Bridges	Avg Winters Salted	Samples Contaminated (%)		Avg Cl⁻ in Contaminated Samples (ppm)	
			0–1 in.	1–2 in.	0–1 in.	1–2 in.
90-mil 100 percent solids	1	8	0	0	0	0
13-mil polyamide	1	8	44	17	70	58
Coal tar modified	2	9.5	47	31	100	74
12-mil polyamide	1	8	60	13	108	67
48-mil 100 percent solids	1	9	61	17	138	68
52-mil 100 percent solids	1	9	67	17	100	54
12-mil solvent cut	1	10	89	67	201	69
Class averages		8.9	50	22	116	68

TABLE 7 Field Performance of Tar Emulsion Systems

System	No. of Bridges	Avg Winters Salted	Samples Contaminated (%)		Avg Cl^- in Contaminated Samples (ppm)	
			0–1 in.	1–2 in.	0–1 in.	1–2 in.
Tar emulsion and glass fabric, 7-layer system	5	9.8	58	31	111	84
Tar emulsion, 2 coats	2	11	64	44	270	182
Class averages		10.1	60	35	163	122

TABLE 8 Chloride Contamination Levels on Exposed Bridge Decks

System	No. of Bridges	Avg Winters Salted	Samples Contaminated (%)		Avg Cl^- in Contaminated Samples (ppm)	
			0–1 in.	1–2 in.	0–1 in.	1–2 in.
No treatment	3	7.3	95	65	1,559	791
Linseed oil and mineral spirits	3	11.7	100	98	1,855	945
Class averages		9.5	97	82	1,743	887

TABLE 9 Average Cl^- Content of All Samples

System	No. of Decks	Avg Winters Salted	No. of Samples	Avg Base Cl^- Level (ppm)	Avg Cl^- Content Above Base Levels (ppm)	
					0–1 in.	1–2 in.
Standard preformed	21	7	458	47	38	15
Thermoplastic	7	9	208	39	53	25
Polyurethane	5	9	155	47	32	18
NCHRP Project 12-11 preformed	5	8	150	65	39	15
Miscellaneous preformed	10	5	162	53	46	20
Epoxy	8	9	258	34	70	31
Tar emulsion	7	10	234	30	108	58
Avg, all systems	9	8	226	45	55	26

TABLE 10 Summary of Membrane Performance by Type

System	Samples Contaminated (%)		Avg Cl^- in Contaminated Samples (ppm)	
	0–1 in.	1–2 in.	0–1 in.	1–2 in.
Standard preformed	19	7	125	86
Thermoplastic	17	8	209	130
Polyurethane	26	17	83	70
NCHRP Project 12-11 preformed	28	15	120	109
Miscellaneous preformed	30	12	125	91
Epoxy	50	22	116	68
Tar emulsion	60	35	163	122
Exposed bridge decks	97	82	1,743	887

TABLE 11 Location of Cl^- Contamination and Percent of Samples Over Corrosion Threshold Level of 325 ppm

	Samples Contaminated (%)						Samples Greater Than 325 ppm (%)					
	1 ft Offset		5 ft Offset		Wheel Path		1 ft Offset		5 ft Offset		Wheel Path	
System	0–1 in.	1–2 in.	0–1 in.	1–2 in.	0–1 in.	1–2 in.	0–1 in.	1–2 in.	0–1 in.	1–2 in.	0–1 in.	1–2 in.
Standard preformed	34	10	14	5	15	4	3	0	1	0	0	0
Thermoplastic	18	9	17	6	17	9	3	0	6	3	3	0
Polyurethane	31	27	15	8	31	16	0	0	0	0	0	0
NCHRP Project 12-11 preformed	52	32	16	8	16	4	8	0	0	0	4	0
Miscellaneous preformed	37	11	26	11	26	15	0	0	0	0	7	0
Epoxy	71	32	41	18	41	16	0	0	4	0	2	0
Tar emulsion	82	64	51	18	46	21	15	3	0	0	3	0
Avg, all systems	46	25	26	10	26	11	4	0	2	1	2	0

TABLE 12 Summary of Membrane Characteristics and Performance

						Bond Between					
System	Ease of Application	Flexibility	Bond and Seal at Curb	Blisters	Pinholes	Membrane and Concrete	Pavement and Membrane	Problems with Pavement Application	Applied Cost[a] per yd^2 ($)	Overall Performance	Recommendation
Standard preformed	Easy	Good	Fair	Yes	No	Fair	Good	Occasionally	4.50	Good	Continue use
Thermoplastic	Hard	Poor to good	Fair	No	Yes	Good	Good	Occasionally	6.00	Good	Consider selective use
Polyurethane	Easy	Good	Excellent	No	Yes	Good	Poor	Occasionally	5.25	Fair to good	Consider selective use
NCHRP Project 12-11 preformed	Hard	Very good	Fair	Yes	No	Good	Good with protection boards	Yes	10.65	Fair to good	Not recommended; application too difficult
Miscellaneous preformed	Easy	Good	Poor	Yes	No	Fair	Fair	Yes	5.00	Fair to good	Consider selective use
Epoxy	Easy	Poor	Fair	No	Yes	Good	Poor	No	9.50	Poor	Not recommended for use
Tar emulsion	Very easy	Poor	Poor	No	No	Good	Good	No	1.35–3.50	Poor	Not recommended for use

[a]Cost covers period 1971-1978. Cost does not include bituminous overlay. Estimate $3.00/$yd^2$ for 2-in. overlay when bituminous mix is bid at $27/ton in-place.

TABLE 13 Description of Systems Applied

Fifteen preformed systems on 38 bridges
Heavy-duty bituthene: 65-mil reinforced rubberized asphalt
Protecto Wrap M 400: 70-mil reinforced tar and synthetic resin modified
Royston No. 10: 75-mil reinforced bituminous
Royston No. 10 P.V.: 75-mil pre-vented reinforced bituminous
Royston No. 15: 60-mil pre-vented reinforced bituminous
Nordel: 65-mil reinforced noncured hydrocarbon rubber
Hyload 125: 125-mil pitch and PVC polymer
Gacoflex N-35: 0.0625-in. cured and buffed neoprene rubber
Sure-Seal Butyl: 65-mil vulcanized butyl rubber
Sure-Seal EPDM: 65-mil cured EPDM rubber
Butylfelt: 60-mil butyl rubber and felt laminate
Hydro-Ban RVN-45: 45-mil reinforced PVC and butyl rubber
Tri-Ply: 62-mil butyl neoprene rubber
Polyguard 860: 60-mil reinforced tar resin
Melnar 8: 165-mil reinforced rubberized asphalt in 4 x 8-ft panels
Five thermoplastic systems on 9 bridges
Uniroyal 6125: 195-mil hot-applied rubberized asphalt
Hot asphalt and glass fabric: 5-layer built-up system
NEA 4000: 90-mil single component PVC polymer
Petromat: nonwoven polyporpylene fabric and asphalt cement
Gussaphalt: 2-in. mastic-type paving mixture
Four polyurethane systems on 7 bridges
Polytak 165: asphalt-modified polyurethane, 38-mil application
Bon-Lastic Membrane: tar-modified polyurethane, 39-mil application
Duraseal 3100: 100 percent solids polyurethane, 69-mil application
Chevron Bridge Membrane: asphalt-modified polyurethane, 100-mil application
Seven epoxy systems on 8 bridges
Duralkote 304: solvent-cut epoxy, 12-mil application
Duralkote 306: coal tar modified, 46- and 65-mil applications
Duralbond 102: 100 percent solids, 48-mil application
Rambond 620-S: 100 percent solids, 52-mil application
Rambond 223: 100 percent solids, 90-mil application
Ramcoat Epoxy Paint: polyamide, 12-mil application
Polyastics: polyamide epoxy, 13-mil application
Two tar emulsion systems on 7 bridges
Tar emulsion: 2 coats at 0.1-0.2 gal per coat
Tar emulsion and glass fabric: 7-layer built-up system

provided the best overall performance to date, with only 7 percent of the samples revealing contamination at the 1- to 2-in. depth and total Cl^- levels averaging 86 ppm in contaminated samples (Tables 1 and 10). All three products feature controlled membrane thickness, satisfactory cold temperature flexibility, and relatively easy application. The materials have been used on nearly all nonexperimental bridges in Vermont since 1973, when a specification was written that allowed the contractor the option of selecting one of the three proprietary systems.

Two potential problems recognized with the use of preformed membranes are the curb line seal and the formation of blisters in the pavement-membrane system. It is believed that the curb seal problem has been alleviated by modifying the specification to include the use of a compatible liquid polyurethane sealant along the membrane perimeter and the vertical curb face.

The problem of blister formations remains to be solved. Blisters that occur in the bituminous mix during paving are often caused by concentrations of air that were trapped beneath the membrane during installation. In many cases such blister formations can be prevented by puncturing the larger air bubbles and then bonding the membrane to the deck after the air has been forced out the vent hole. Blisters are also caused by small concentrations of moisture that collect beneath the membrane because of outgassing of moisture vapor from the concrete. Such moisture may subsequently turn to a vapor when exposed to the high temperature of the bituminous overlay. The blistering can often be reduced by requiring that the overlay be placed shortly after the membrane application is completed.

Post-construction blistering is also believed to be the result of moisture vapor pressures outgassing from the concrete. The occurrence of such blisters can be reduced by improving membrane adhesion to the concrete and by increasing the thickness of the bituminous overlay. Initial and post-construction blistering has been noted on a number of preformed membrane installations made in Vermont, but the occurrences have never become serious problems. In most cases the blisters have been noted only after the pavement has become slightly polished by snowplow wear on the high spots.

Thermoplastic Systems: Status--4 Systems on 7 Bridges Averaging 9 Winters of Exposure

Performance of the thermoplastic systems has also been satisfactory, with 8 percent of the samples revealing contamination at the 1- to 2- in. depth and total Cl^- levels averaging 130 ppm in contaminated samples (Tables 2 and 10). Test results suggest that at least two of the systems could be recommended for further use. The best performance has been obtained from a hot rubberized asphalt, although it should be noted that the system is not recommended for structures on grades or superelevations in excess of 3 percent because of the potential for membrane-pavement stability problems under traffic. Protection boards were not included on the two decks under evaluation, but would be specified on any future applications of the system.

An application of Gussaphalt, a mastic-type paving mixture commonly used in Europe, resulted in a failure that required removal of the system after

330 linear feet of full-depth cracks occurred during the second winter. The failure was believed due to stresses caused by rapid temperature changes.

Polyurethane Systems: Status--4 Systems on 5 Bridges Averaging 9 Winters of Exposure

The polyurethane systems rate third with regard to the percent of contaminated samples, but the level of contamination is the lowest of all classes of material, averaging only 83 ppm total Cl^- in the top inch and 70 ppm at the 1- to 2-in. depth (Tables 3 and 10). The permeability may be caused by the development of pinholes and bubbles in the liquid-applied materials during application. The problems, caused by outgassing of moisture vapors from the concrete, can be alleviated by applying the polyurethane after midday when air temperatures are declining and by applying multiple coats. Advantages offered by the polyurethanes include ease of application, satisfactory cold temperature flexibility, and excellent bond and seal along curb lines. The systems should include protection boards or roll roofing to ensure adequate bond between membrane and pavement. Two of the individual polyurethane systems have remained free of detectible Cl^- contamination for up to 8 years of exposure.

NCHRP Project 12-11 Preformed Systems: Status--5 Systems on 5 Bridges Averaging 8 Winters of Exposure

The five vulcanized, cured, or cross-linked preformed elastomer systems selected as the most promising membrane materials under Phase I of NCHRP Project 12-11 were well-designed and displayed excellent physical characteristics. However, the application of the systems in Vermont under Phase II of the project was difficult, thus making it appear doubtful that the systems could be placed properly under typical field conditions. The overall performance of the systems has been satisfactory (Tables 4 and 10), except for curb line areas where 52 percent of the samples have been contaminated (Table 12). A pitch and polyvinal chloride (PVC) polymer system has performed best, with Cl^- contamination limited to a single sample.

Miscellaneous Preformed Systems: Status--7 Systems on 10 Bridges Averaging 5 Winters of Exposure

Most of the systems included in this group are similar to the three standard preformed sheet systems but have had less widespread use. Four of the systems have performed well, including two products that have remained free of detectible Cl^- contamination (Table 5). Two of the products were manufactured with 0.0625-in. prepunched vent holes designed to prevent initial and post-construction blistering by allowing vapors to escape from beneath the membrane following installation. Both products were basically successful in reducing the amount of air entrapped beneath the materials, but Cl^- contamination found in 27 to 40 percent of the field samples suggests that some of the holes did not reseal on application of heat and pressure during the paving operation.

Epoxy Systems: Status--7 Systems on 8 Bridges Averaging 9 Winters of Exposure

With the exception of one product, the epoxy systems have performed poorly when compared with the other experimental membranes (Tables 6 and 10). Exactly 50 percent of the samples revealed Cl^- contamination at the 0 to 1-in. depth, although the levels are still low, averaging less than 0.5 lb/yd^3 over base Cl^- levels.

Advantages of the epoxy systems include relative ease of application, generally satisfactory bond to the concrete, and avoidance of problems with pavement applications. Disadvantages include unsatisfactory cold temperature flexibility and a tendency to pinhole or bubble during application.

Tar Emulsion: Status--2 Systems on 7 Bridges Averaging 10 Winters of Exposure

Test results indicate that both the two-coat standard treatment and the glass fabric reinforced system performed poorly when compared with all other classes of material. Contamination was identified in 60 percent of the samples taken at the 0 to 1-in. depth (Table 7). Based on all samples taken, the tar emulsion systems have allowed an average of 0.43 lb/yd^3 of Cl^- contamination above base levels in the top inch of concrete. When such contamination levels are compared with the average of 6.97 lb/yd^3 of Cl^- recorded on exposed concrete decks (Table 8), the results suggest that tar emulsion does offer a substantial level of protection to the concrete. The highest levels of Cl^- contamination were recorded on two 11-year-old structures treated with two coats of tar emulsion. Copper-copper sulfate half-cell potential measurements taken on the two structures in 1982 indicated the presence of active corrosion on 1 percent of the deck areas.

Exposed Bridge Decks: Status--6 Bridges Averaging 10 Winters of Exposure

For comparison purposes, three exposed bridge decks and three decks treated with an initial application of linseed oil and mineral spirits have been monitored for Cl^- contamination levels over a similar evaluation period. The results reveal Cl^- contamination in all samples taken from the top inch of concrete, with levels averaging 1,743 ppm or 6.97 lb/yd^3 (Table 8). Contamination was found in 98 percent of the samples from the 1- to 2-in. depth, with levels averaging 887 ppm or 3.55 lb/yd^3. In general, the decks appear to be in satisfactory condition; however, the most recent copper-copper sulfate half-cell potential measurements indicate the presence of active corrosion on an average of 30 percent of the deck areas. Concrete delamination was noted on one structure where it totaled 13 percent of the deck surface.

DISCUSSION OF PERFORMANCE

The test results given in Tables 1-7 disclose that 12 of the decks under evaluation were free of Cl^- contamination. Contamination was limited to a single sample on nine additional decks. The combined decks treated with 15 different membrane systems make up 33 percent of the decks under evaluation.

A number of the membrane systems did not provide adequate provisions for preventing Cl^- penetration along curb lines. As shown in Table 11, 46 percent of the curb line samples were contaminated at the 0 to 1-in. depth. Furthermore, such samples made up 47 percent of all the contaminated samples recorded in the top inch of concrete. The data in Table 11 also disclose that the number of Cl^- contaminated samples found at the 5-ft offset from the curb line and in the wheel path were approximately equal. Such results suggest aggregate puncture under traffic loading is probably not a significant factor contributing to membrane permeability in Vermont.

Attempts to project future performance of the membrane systems may be seen in Figures 1 and 2. All projections are based on a statistical analysis by using the method of least squares.

Figure 1 shows the number of samples contaminated with Cl^- is increasing at a rate of 1.3 percent per year. If the present rate continues, the top inch of concrete will become contaminated with Cl^- after 64 years of service. All samples at the 1- to 2-in. depth will be contaminated after 73 years of service.

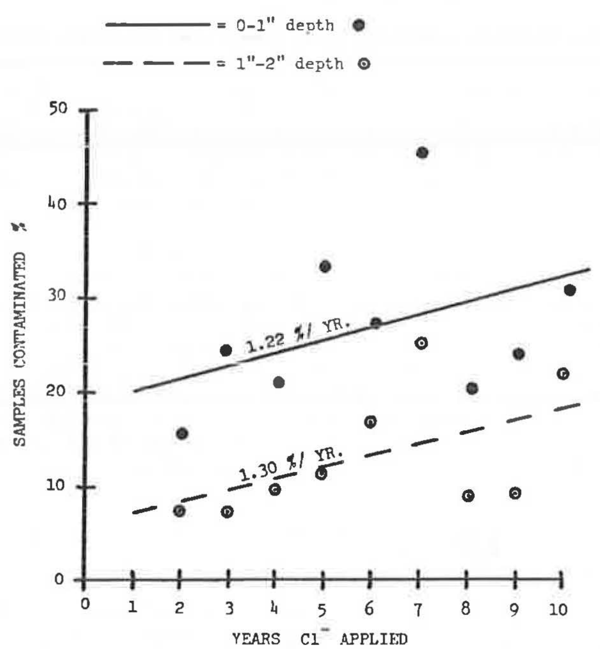

FIGURE 1 Rate of increase in percentage of samples contaminated with Cl^-.

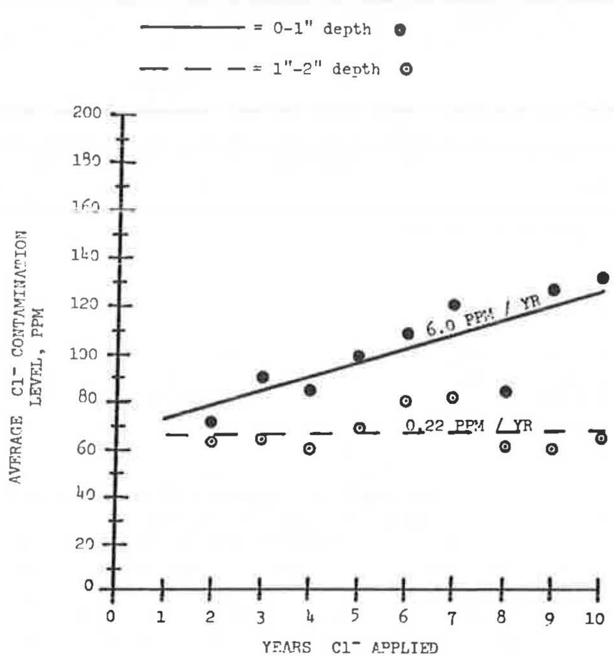

FIGURE 2 Rate of increase in Cl^- contamination levels.

The level of contamination is an important factor that must be considered when attempting to project the service life of the membrane systems and the service life of the bridge decks. Figure 2 projects the rate of increase in contamination levels at approximately 6 ppm per year in the top inch of concrete. If the 6-ppm rate of increase continues, the contamination will reach the 325-ppm corrosion threshold level in the top inch of concrete after 43 years of service. The rate of increase in contamination levels at the 1- to 2-in. depth is less than 1 ppm per year. Although all projections point toward a long service life, it is recognized that at some point in time the various membrane materials will begin to deteriorate and the performance life will decrease accordingly.

Currently, only 25 of 1,625 samples tested have Cl^- contamination greater than the corrosion threshold level of 325 ppm (Table 11). When the tar emulsion and epoxy-treated decks are not included, the number drops to 13, or 1 percent of the samples, with all but 1 occurring in the top inch of concrete. When all samples are taken into consideration, the average Cl^- content greater than base levels is 55 ppm in the top inch and 26 ppm at the 1- to 2- in. depth (Table 9). Because the decks were constructed with 2 in. of concrete cover, additional corrosion-free life can be expected before the 325-ppm Cl^- level is reached at the 2- to 3-in. depth.

The test results indicate that most of the membrane systems have performed well for up to 11 years of exposure. Based on the experiences gained during the membrane installations, it is believed that overall membrane performance would have been even better if the following conditions had been met:

1. Systems not well suited for the intended purpose had been eliminated through better preliminary laboratory testing;
2. Difficulties with certain facets of some applications had been anticipated and avoided; this would be possible with future applications of the same materials;
3. Certain construction procedures had been modified to suit the particular needs of a system;
4. Additional safeguards had been taken to prevent leakage along curb line areas;
5. Protection board had been placed over some membrane systems to improve stability during the paving process and under continuous traffic;
6. Construction traffic had not been allowed to travel on the membrane and first course of pavement; and
7. Pavement overlay thickness was increased to 2.5 in., with a minimum of 2 in. maintained.

CONCLUSIONS

Many conditions such as weather, winter maintenance practices, traffic volumes, and design and construction practices are known to vary in different regions. Accordingly, it is recognized that membrane systems that extend the service life of bridge decks in Vermont may not necessarily perform with the same results at other locations. Nevertheless, based on performance data obtained to date, the following conclusions are considered significant.

1. Performance results based on more than 1,600 field samples indicate that, almost without exception, the experimental membrane systems have outperformed the Agency's original standard treatment of tar emulsion.

2. When grouped by general type, the best performance has been provided by the standard preformed sheet membranes and thermoplastic systems, closely followed by the polyurethanes, the NCHRP Project 12-11 recommended systems, and miscellaneous preformed systems.

3. In general, the epoxy and tar emulsion systems were not considered successful, although they have allowed only an average of 0.35 lb of Cl^- per cubic yard of concrete more than base levels in the top inch of concrete as compared with an average of 6.97 lb/yd^3 on exposed bridge decks during a similar evaluation period.

4. Chloride contamination was detected in one sample or less on 33 percent of the 63 bridge decks under evaluation. Protective systems on the 21 decks included 15 of the 33 different membrane systems tried.

5. Less than 2 percent of the more than 1,600 field samples disclosed Cl^- levels greater than 325 ppm, the level considered sufficient to initiate corrosion of the reinforcing steel. All but three of the greater than 325-ppm samples were located in the top inch of concrete.

6. Although curb line samples made up only 33 percent of those taken, they accounted for 47 percent of all contaminated samples, pointing out the difficulty of sealing that area of the bridge deck.

7. The number of Cl^- contaminated samples found at the 5-ft offset from the curb line and in the wheel path (±15-ft offset) were approximately equal. Such results suggest aggregate puncture under traffic loading is probably not a major contributor to membrane permeability.

8. Projections based on performance results to date suggest that a significant number of the membrane systems will provide protection from serious Cl^- contamination for 50 years or longer.

RECOMMENDATIONS

1. Before initiating action to replace deteriorated bituminous pavements on membrane-treated bridge decks, field testing for Cl^- contamination should be undertaken on the respective structures. If the performance survey results indicate a membrane system is still providing the desired protection, only the upper ±75 percent of the bituminous pavement should be removed with cold planing equipment, thereby retaining the functional membrane system.

2. Long-term field performance results indicate that a variety of membrane systems can be made to work if adequate time and effort are spent in selection, design, and installation. However, the potential for improper placement and other related problems with individual applications should be sufficient to discourage membrane use in areas where a lack of sufficient care and attention might be anticipated.

3. Promising new membrane systems that have become available in the past 5 years or so should be applied in the field in a new test program to determine their effectiveness in relation to current acceptable materials.

4. This research project should be continued as planned for a minimum of 3 additional years through fiscal year 1987.

ACKNOWLEDGMENT

The findings in this paper were made possible through funding of a Highway Planning and Research Program (HPR) Part II Research Project by the FHWA and the Vermont Agency of Transportation.

The contributions of Agency employees and coworkers in the Materials and Research Division are gratefully acknowledged. Special appreciation is expressed to the following Research and Development personnel who significantly contributed to this research project: Paul E. Corti, John L. Bullard, and Ned C. Houston.

REFERENCES

1. E.M. Winkler and P.E. Singer. Crystallization Pressures of Salts in Stone and Concrete. Geological Society of America Bulletin, Vol. 83, 1972, pp. 3509-3514.
2. C.F. Crumption and F.P. Jayaprakash. Scanning Rust Crystals and Salt Crystals with Electron Microscope. In Transportation Research Record 860, TRB, National Research Council, Washington, D.C., 1982, pp. 45-49.
3. D.A. Lewis. Some Aspects of the Corrosion of Steel in Concrete. Proc., 1st International Congress on Metallic Corrosion, London, England, 1962, pp. 547-555.
4. K.C. Clear. Time to Corrosion of Reinforcing Steel in Concrete Slabs. In Transportation Research Record 500, TRB, National Research Council, Washington, D.C., 1974, pp. 16-24.

Publication of this paper sponsored by Committee on Corrosion and Committee on Performance of Concrete.

Abridgment

Kansas' Experience with Interlayer Membranes on Salt-Contaminated Bridge Decks

JOHN E. BUKOVATZ and CARL F. CRUMPTON

ABSTRACT

Nearly 12,000 yd^2 of interlayer membranes were installed on salt-contaminated decks in Kansas between 1967 and 1974. The decks were from 6 to 50 years old when the membranes were placed. All of the membranes are performing well after 12 to 16 years. Traffic over the membranes during that time ranged from 3 to 160 million vehicles. The majority of resistivity readings taken in 1982 were greater than 500,000 $ohms/ft^2$. The asphalt wearing surfaces over the membranes were judged satisfactory to excellent. The 16-year-old membrane covered only part of a deck, but that part is in far superior condition than the remaining bare deck. In 1926 an asphalt-cotton fabric membraneous waterproofing system was placed over 1,437 yd^2 of a new Kansas bridge deck. The membrane was covered with a cement-sand mortar layer that was topped with paving bricks. After 56 years of service and about 50 million vehicle passes the concrete below the membrane contained less than 0.75 lb of chloride ion per cubic yard of concrete. In Kansas the evaporation rate is higher than the precipitation rate. This may be one reason why membranes work well on salt-contaminated decks in Kansas.

A Kansas Bridge Deck Deterioration Study (1) of the early 1960s considered protection of the bridge deck surfaces from salt intrusion in some phases of the study. Hot-mix overlays were unsatisfactory and were not recommended unless they were placed over a membrane (1,2).

The formal study of interlayer membrane performance in Kansas began with an installation in 1967 on a 6-year-old, salted, rural Interstate interchange bridge. The first installation (membrane system 52a; see Tables 1 and 2) was also the first installation of this proprietary membrane on a bridge deck anywhere in the world. The material, a polypropylene fabric, was placed on one quadrant of the bridge deck. The installation was about 72 ft long and one lane wide. The remaining deck was left bare. The membrane was covered with a wearing surface consisting of 0.7 to 0.8 gal/yd^2 of a cationic emulsified asphalt and hand-placed crushed-chert-type chat aggregate. A 20 percent excess of aggregate was applied to assure a good heavy coverage. By 1970 the performance was satisfactory enough that Kansas decided to evaluate other membranes on old decks.

From 1970 to 1974 four different types of mem-

TABLE 1 Interlayer Membrane Systems Used on Old Decks in Kansas

NCHRP 165 System No.[a]	System Type	Description
12	Preformed	A pliable sheeting construction from polypropylene and coal tar placed over a primer; a hot-mix overlay covers the membrane
52a	Liquid/preformed	An applied in-place nonwoven polypropylene fabric with cationic emulsified asphalt; chat (chert) aggregate was rolled into RS-2K emulsion for the wearing course
52b	Liquid/preformed	Same as 52a, except that the fabric was placed over a thin coat of AC-5 and covered with a hot-mixed asphalt-concrete (AC) overlay
67	Liquid	A cold-applied, coal-tar modified, elastomeric polyurethane with a 55-lb grade asphalt-impregnated roofing sheet over it; all overlaid with 2.5 in. of hot-mix AC
80	Liquid	A coal-tar modified polyurethane elastomer cold-applied with catalyst (curing agent) added before application; the material was covered with no. 40 asphalt roofing sheet, which was topped with a hot-mix overlay

[a]See Table 9 of NCHRP Report 165 *(2)*.

TABLE 2 Membrane Installation Data

Bridge ID	Type of Membrane System[a]	Date Membrane Installed	Date Bridge Constructed	Material Installed (yd^2)	Overlay Thickness (in.)	Bridge Type[b]
A	52a	1967	1961	112	0.125	RBGC
B	12	1970	1936	700	1.5	Cont. I-Beam
C	80	1971	1958	283	1.5	Cont. RC slab
D	80	1971	1959	404	1.5	Cont. RCDG
E	52b	1971	1953	254	2	Cont. RC slab
F	52b	1971	1936[c]	1,035	2	RCDG
G	80	1971	1936[c]	1,313	1.5	Steel I-beam
H	67	1974	1924[d]	7,700	2.5	RC slab and Cont.
I	-	1926	1926	1,437	3.5	SBMS/SSGC

[a]See Table 1 for description (2, Table 9).
[b]Bridge types are as follows: RBGC = reinforced box-girder continuous; RCDG = reinforced-concrete deck girder; RC = reinforced concrete; Cont. = continuous; and SBMS/SSGC = steel beam simple/steel girder, stringer floor beam continuous.
[c]Widened in 1971.
[d]Widened in 1974.

branes totaling nearly 12,000 yd^2 were placed on seven more salt-contaminated bridge decks that were 12 to 50 years old when the membranes were installed. All seven decks had typical salt-related damage, such as hollow planes, shallow spalls, and patched areas. The shallow spalls were not patched before installing the membranes. The data in Table 1 describe the membranes used, and the data in Table 2 provide pertinent information about the installations.

PERFORMANCE

All of the test bridges with membranes were observed in 1982 or 1983. Resistivity measurements were made on bridges A through F (Table 2). Bridges G and H are in high traffic urban areas, and the accident risk outweighed the value of the resistivity measurements; therefore, measurements were not taken.

The 1967 membrane test section, membrane type 52a (Tables 1 and 2), showed a great contrast in condition between the covered and uncovered parts of the deck in 1983 (see Figure 1). (Note in Figure 1 that the deck under the membrane is in far better condition than the bare deck on the left.) All of the corrosion potentials on the uncovered deck measured more negative than -0.35 V. No measurements were made through the membrane. One-third of the resistivity readings on the membrane were more than 500,000 ohms/ft^2. Patches, spalls, and hollow planes were present on 91 percent of the uncovered deck area. Only 6.5 percent of the deck in the membrane area experienced delaminations, and they were all at the edges of the membrane adjacent to the uncovered deck or along the curb. There were no spalls or patches in the membrane area. The uncovered part of the deck contained from 6 to 16 lb of chloride per cubic yard of concrete, whereas the concrete under the membrane contained only 1.5 to 3 lb Cl^-/yd^3. The bridge had been salted for 6 years before the membrane was placed. It is possible the deck already had as much as 3 lb of chloride per cubic yard of concrete in 1967 when the membrane was placed. The salt content was not determined at that time, however. Total traffic over the membrane had been about 3 million vehicles up to the time of the 1983 evaluation.

FIGURE 1 A 16-year-old polypropylene fabric membrane covering part of the deck in right foreground.

The membranes on bridges B through G (Table 2) were 12 and 13 years old in 1983; the membrane on bridge H was then 9 years old. In that time they have been subjected to numerous salt applications for snow and ice control as well as from 6.5 million to 160 million vehicles. Trucks made up from 1.4 to 19 percent of the total vehicle traffic. Skid resistance on the overlays that were subjected to traffic of from 76 million to 160 million vehicle passes was from the mid to upper 20s. At lower traffic, the skid number ranged from the upper 30s to low 50s.

The only membrane that has partly failed was the 9-year-old membrane. Failure was caused by the membrane being placed on too steep a downhill slope with a stop light at the bottom end of the bridge and an average of 8 million vehicle passes annually. Only part of the membrane failed. The membrane and its overlay farther away from the light on a flatter slope is still in place after more than 76 million vehicle passes over the bridge.

Resistivity measurements made in 1982 on five of the bridges, then 11 and 12 years old, indicated that two of them had all readings greater than 500,000 ohms/ft^2. Two others had more than 90 percent of the readings greater than 500,000 ohms/ft^2. The fifth one had only 36 percent of the readings greater than 500,000 ohms/ft^2.

The appearance of the asphalt riding surface in each installation was from satisfactory with some cracking to excellent. Surface cracking after 11 and 12 years ranged from 0.8 to 1.8 lineal inches per square foot of area. The overlays exhibited unbonding from 2 to 22 percent of the deck areas. In spite of this, little maintenance has been performed on any of the overlays (other than the 9-year-old one) since the membranes were placed.

Before the installation of the membrane some of the bridges had considerable seepage of water from the bottom of the deck during rainy or snowy seasons. This condition did not recur after the membranes were placed.

Salt or corrosion studies below the membranes have not been made because the researchers did not want to puncture them. Furthermore these membranes were installed before those studies began; therefore, there was no base point control. It should be remembered that all of the decks had been routinely salted during snow and ice storms and exhibited typical salt damage to the reinforced concrete before the membranes were placed.

A 56-year-old Kansas membrane installation was investigated in 1982. It was about 0.25 in. thick and was made up of asphalt with two layers of cotton fabric. The plans merely referred to it as membraneous waterproofing. No data concerning makeup or mode of placement were given; hence it is not described in Table 1, although it is included in Table 2 as bridge I. The membrane was installed over a 6.75-in.-thick concrete deck at the time of construction in 1926. The membrane was covered with a cement-sand mortar layer 0.5 in. thick. A riding surface layer of 3-in.-thick pavement bricks was embedded in the top of the mortar layer. Sometime during the 1960s an asphalt overlay was added because the deck was getting rough from the loss of some bricks.

In 1982 a condition survey of this structure was made and 41 samples of the concrete were taken from below the membrane. Tests for chloride showed that none of the samples taken contained even 0.75 lb of chloride per cubic yard, and 81 percent contained less than 0.4 lb/yd^3. Copper-copper sulfate half-cell corrosion potential measurements were made in core holes. Only 10 percent of the readings were more negative than -0.35 V. That corrosion may have begun when the cores were taken.

Damage to the concrete bridge deck was limited essentially to the unprotected sidewalks and the areas adjacent to the edge of the membrane where water had penetrated. It is obvious that the membraneous waterproofing has served its purpose well for those 56 years. During that time the bridge carried an estimated 50,000,000 vehicles. About 15 percent of them were trucks.

The performance of membranes on new decks is covered by Frascoia in a paper elsewhere in this Record. The 56 years of satisfactory performance of a membrane in Kansas supports his long-term projections for membrane performance.

SOME PERTINENT POINTS ABOUT KANSAS CLIMATE

Kansas sometimes is referred to as the mixing pot for the weather. Most Kansas bridges undergo an average of 60 or more freeze-thaw cycles each year. They are subjected to an average of five or six winter snowstorms and one to three ice or sleet storms each year. The snow and ice are usually removed by snowplows and deicing salts. Kansas bridge decks receive about 20 applications of salt per year at the rate of 1,300 lb per 2-lane mile (3).

Bridges in Kansas may be subjected to air temperatures as low as -40°F in the winter and as high as 120°F in the summer. Winter wind-chill factors may reach -65°F in the winter, whereas the summer temperature of asphalt overlays often reaches 160°F. Rapid changes in temperature are not uncommon. Parts of Kansas average about 7,000 degree hours greater than 85°F. Precipitation ranges from more than 40 in. in the southeast part of the state to about 16 in. in the southwest. The evaporation rate is higher than the precipitation rate all across the state. The greatest differential is in southwestern Kansas, where lake evaporation is as high as 62 in. per year and precipitation is as low as 16 in. per year, on average. It is believed that if the membranes can retard the downward movement of water and chlorides, evaporation will soon take over and keep them near the surface.

SUMMARY AND CONCLUSIONS

Nearly 12,000 yd² of interlayer membranes have been installed on old salt-contaminated decks in Kansas. They have served quite well with little maintenance for 12 to 16 years. If the 16-year-old membrane had covered the entire deck, it is probable there would have been one less Kansas bridge that needed extensive deck repair. One 1,437-yd² membrane placed on a new deck has served well for 56 years.

In Kansas the evaporation rate is higher than the precipitation rate. This probably influenced the satisfactory performance. Care in installation and proper timing of all procedures is also necessary to give the membranes a chance to work. Sealing the overlay-hubguard contact would be beneficial.

ACKNOWLEDGMENT

The membranes were installed with state funds, but the evaluations were made under the Highway Planning and Research Program as part of NEEP-12. The support from the Kansas Department of Transportation and the FHWA is highly appreciated.

REFERENCES

1. J.E. Bukovatz, C.F. Crumpton, and H.E. Worley. Bridge Deck Deterioration Study. Final Report. State Highway Commission of Kansas and FHWA, U.S. Department of Transportation, 1973.
2. C.J. Van Til, B.J. Carr, and B.A. Vallegra. Waterproof Membranes for Protection of Concrete Bridge Decks: Laboratory Phase. NCHRP Report 165. TRB, National Research Council, Washington, D.C., 1976, 70 pp.
3. B.F. McCollom. Design and Construction of Conventional Bridge Decks That Are Resistant to Spalling. In Transportation Research Record 604, TRB, National Research Council, Washington, D.C., 1976, pp. 1-5.

Publication of this paper sponsored by Committee on Corrosion and Committee on Performance of Concrete.

Determination of In-Place Timber Piling Strength

M. S. AGGOUR, A. M. RAGAB, and E. J. WHITE, JR.

ABSTRACT

A nondestructive inspection procedure that uses the ultrasonic technique to determine the material properties of timber piles above and below water is described, and the equipment developed is presented. The technique is suitable primarily for piles such as those on the Denton Bridge (that collapsed in Maryland in 1976) and others that are immersed in fresh water for long periods of time and sustain damage to the wood microstructure, which can reduce pile capacity by actually changing material parameters, such as strength and density, without a loss of cross-sectional area. This type of destructive action cannot be detected by any existing inspection technique. Laboratory testing of a large number of new and old piles from four different bridges in the state of Maryland were used to establish relationships between the pulse velocity from the ultrasonic testing and the crushing strength of the timber piles. Variables that affect the relationships, such as type of wood, degree of decay, moisture content, and treatment of the wood, were also studied. The relationships developed were verified by determining the pulse velocity of in-place piling in a fifth bridge, then removing the piles, cutting them into sections, and axial load testing the sections to determine the strength of the piles. It has been concluded from the favorable comparison of the calculated and the experimentally determined strength that the technique and equipment developed could be confidently used in timber pile inspection. The quantitative determination of the remaining strength of timber piles in service will lead to appropriate judgments as to the ability of the piles to further support the loads imposed on them.

Federal and state legislation requires periodic inspection and evaluation of highway and railroad bridges and requires that they be rated as to their safe load-carrying capacity. It has been pointed out that 70 percent of the highway bridges in the United States were built before 1935 (1) and that almost 4 out every 10 are defective. Therefore, it is vital that these bridges be effectively inspected in order to predict their remaining life and verify their structural integrity. One aspect of the problem is the existence of a large number of timber piling structures that are old and rapidly deteriorating. Thus their periodic inspection is necessary to ensure the early detection of damage or deterioration and to prevent structural failure. Inspection is also essential for an economical decision with regard to bridge replacement or rehabilitation.

Despite a recent underwater inspection of the piling, an unanticipated failure occurred to a timber-supported bridge at Denton, Maryland, in early 1976. The underwater inspection had indicated reasonable soundness of the timber, but later laboratory tests indicated substantial reduction in material strength during the life of the piling. These deficiencies were undetected by current inspection techniques and were only determined after failure of the bridge. Because wood is a biological material, it is subject to decay fungi, checking, abrasion, insect attack, and other factors that reduce strength with time in service. In addition, below water a variety of marine borers invade the wooden piles and cause loss in wood volume on the surface, or erode away the piling interior. Also, impact, fatigue, and overloading by traffic on bridges cause additional pile damage. Thus it is to be expected that bridge timber pile structural integrity and resistance decrease with time in service.

A research project supported by the Maryland State Highway Administration and FHWA is being conducted by the University of Maryland, the main objective of which has been to develop a nondestructive test for determining the in-place strength of bridge timber piling that has sustained damage to the wood microstructure with or without a loss of area of the pile section (2). Piles such as those in the Denton Bridge and others that are immersed in fresh water for long periods of time can sustain damage to the wood microstructure. This type of damage can reduce pile capacity by actually changing material parameters, such as strength and density, without a loss of cross-sectional area. This type of destructive action cannot be detected by a sonic instrument developed in the early 1960s (3) for inspection of marine piling or by any other method.

The project can be divided into four major tasks:

1. Develop an in-place nondestructive testing (NDT) technique and equipment;
2. Develop a data bank for new and old piles by NDT of pile sections and then determine their strength through testing to failure, thereby allowing the strength of timber piles to be evaluated throughout their service life;
3. Develop relationships between the NDT data and the strength of timber piles (factors that influence the test interpretation, such as type of wood, treatment, moisture content, and so on, were considered); and
4. Develop analytical methods to determine the effect of decay on the stress distribution and on the load-carrying capacity of single piles.

To limit the size of this paper, the fourth task has not been included and is presented elsewhere (4).

In this paper the ultrasonic pulse velocity technique used in characterizing the material properties of timber piles is presented. The equipment developed for above-water and underwater testing of piles are briefly described. The relationships between the wave velocity and the remaining strength, developed through extensive testing, are presented. The technique was further verified by NDT of in-place piling, then removing the piles, cutting them into sections, and axial load testing the sections to determine their strength.

It is concluded that although wood is a natural material with a relatively high variation in inherent strength, the equipment and relationships developed can be used confidently to determine the remaining strength of the pile in-place.

CAUSES AND EFFECTS OF DETERIORATION

Because of the organic composition of wood and the harsh environment in which they are usually located, bridge timber piles are subject to deterioration. The principal causes of deterioration of piles in service are bacteria, fungi, insect attack, fire, mechanical wear, and marine borers. Of primary concern in this work are the determination of the physical and engineering properties of decayed wood. The effects of decay include (a) loss of density--although still retaining its outward appearance, decayed wood generally becomes extremely light in weight; (b) increase in permeability--decayed wood absorbs liquid and becomes waterlogged much more readily than does sound wood; and (c) loss in strength--caused by enzymatic degradation of the wood cellulose and lignin. It has been observed that the toughness or capacity of decayed wood to withstand loading is reduced rapidly. Other strength properties, such as resistance to bending and crushing, are also reduced.

The extent of decay is difficult to assess by visual inspection. This is because the timber pile may be completely decayed internally while the external appearance indicates soundness of material.

METHODS OF INSPECTION

Because the causes of timber pile deterioration are many and varied, and because the protective measures used to guard against this deterioration (although extremely useful in some cases) are no guarantee that deterioration will not occur, it is therefore necessary to periodically inspect timber piles. The inspection procedures are to determine if damage is occurring and to what extent the stability and safety of the piles have been affected. The availability of this valuable information would assist the engineer in establishing a schedule for the replacement of any unsafe piles. There are two basic groups of testing--destructive and nondestructive methods. Destructive testing (DT), as the name implies, increases the loss of cross-sectional area of the tested pile. Some of the destructive testing methods in use are probing and core sampling. In general, all destructive tests have been known to impose undue strain on the tested pile, and they imply a sampling process in which the tested pieces are assumed to represent the entire population not tested. Nondestructive testing is the name given to all test methods that permit inspection of material without impairing its usefulness. The methods include visual inspection, sounding, radiography, resonance methods, and ultrasonic methods.

ULTRASONIC TESTING OF WOOD

In the NDT of wood-based materials and structures various pulse-measuring instruments have been developed, producing varying degrees of success as a means of evaluating the soundness of wood structures in service. Lee (5) used the ultrasonic test technique for the examination of decayed timbers forming the roof structure of an 18th century mansion. Muenow (6) also used the ultrasonic test for inspecting 11 sections of wooden utility poles from the Commonwealth Edison Company. McDonald et al. (7) and McDonald (8) used ultrasonics to determine the quality of lumber for automated production of clear cuttings for better use of timber resources. Pellerin (9) indicated that the wave velocity in wood gave a good indication of the quality of the interior of the wood, because the progress of a wave is slowed by an increasing number and size of defects. Vanderbilt et al. (10) used the ultrasonic test technique for evaluating the strength and stiffness of large timber piles. Lanius et al. (11) presented a procedure for examining wood joists in an existing structure. In the procedure the stress-wave technique was performed to determine the allowable working stresses for the joists.

For timber piles, studies were initiated in 1955 at B.C. Research in Vancouver, British Columbia, Canada, that developed an underwater sonic-probe as a nondestructive method of testing in-place underwater piling (3). The instruments are used to locate marine borer damage and to evaluate the extent of cross-sectional loss of wood. It should be mentioned here that this sonic testing method, as developed, deals with the gross dimensions of the pile and changes caused by marine borers or mechanical damage in these dimensions. However, Scheffer et al. (12) have shown that a pile immersed in fresh water for long periods of time can sustain damage to the wood microstructure. This type of damage can reduce pile capacity by actually changing material parameters such as modulus of elasticity. This type of destructive action is not detected by the sonic instrument developed and is the primary concern of the equipment developed in this work (as in the case of the Denton Bridge collapse).

WAVE PROPAGATION IN WOOD

It can be shown that the velocity of propagation of the waves parallel to the grain V_L and in the radial direction V_N (normal to the grain) in an orthotropic material with a Poisson's ratio for transverse strain in the longitudinal direction when stress is applied in the radial direction in the range of 0.02 to 0.04 is approximately

$$V_L = (E_L/\rho)^{1/2} \quad (1)$$

and

$$V_N = (E_N/\rho)^{1/2} \quad (2)$$

where

E_L = dynamic modulus of elasticity in the longitudinal direction,
E_N = dynamic modulus of elasticity in the radial direction (normal to grain), and
ρ = material mass density.

Hearmon (13) and others showed that these equations are reasonably true for wood. The equations made it possible to calculate the dynamic modulus of elasticity of a material if the velocity of the stress wave and the material mass density are known.

EQUIPMENT DEVELOPED

Ultrasonic waves, particularly pulsed waves, were used for the quantitative inspection of timber piles. A commercial testing apparatus constitutes the basic instrument, which provides a means of generating and transmitting pulses of ultrasonic sound through the pile and electronically measures the time of transmission of the sound from the face of the transmitter to that of the receiver. From the measured transit time for the pulse to traverse a known path length, the propagation velocity can be determined.

A short description of the equipment developed for the in-place testing of timber bridge piling is presented. A detailed description of the equipment and the field procedures for testing are presented elsewhere (14,15).

Two pieces of equipment were developed, one to be used above-water and the other underwater, to determine the pulse velocities in sections along the in-place timber pile. Two basic measurements are obtained at regular depth intervals: transit time and path length. The transit time is obtained in digital form. The distance between the two faces of the transducers (path length) is determined either by direct reading on a scale as in the case with the above-water equipment or by measuring the distance the transducers travel as in the case of the below-water equipment. The above-water equipment is simply a scissors-type piece of equipment that is used to hold the transducers in place and measure the distance between them, as shown in Figure 1. The underwater equipment is composed of a sensing unit that is mounted on a special gear to lower and raise it along the length of the pile for the inspection. The measurements are collected through a monitoring unit at the surface. The equipment developed can be used without the aid of a scuba diver. Figure 2 shows a side view of the equipment during testing in a tank that was built to study the operation of the equipment underwater.

EXPERIMENTAL TESTS FOR DATA BANK

In this study the ultrasonic testing technique is used in characterizing the material properties of wooden piles. The results of the ultrasonic testing are correlated with the strength values from the compression parallel to grain test. The developed relationships can then be used for establishing the in-place strength of bridge timber piling. To accomplish such an objective, a data bank is needed that encompasses all variables that affect the strength of timber piles.

Various combinations of the following factors were considered in the testing program, including type of wood, effect of treatment, direction of grain, density of wood, degree of decay, moisture content, and the effect of testing above and below water. The results of some of the tests performed are summarized here but are presented in detail elsewhere (4,14).

FIGURE 1 Above-water equipment.

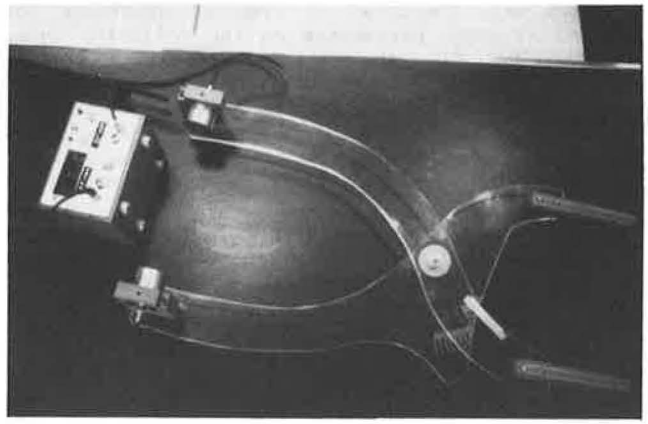

FIGURE 2 Side view of underwater equipment in laboratory testing.

Scope of Testing

Tests on specimens prepared from sections of piles and tests on sections themselves were comprehensive and complete in scope. The statistical evaluations for the test results were based on a 95 percent confidence limit. The tests included different types of new and old wood piles. In all cases, NDT was performed first, followed by either a compression strength test or a bending test.

Sections Tested

Tests were conducted on sections from new and old piles. The new piles were both treated and untreated Southern Yellow Pine. For the old piles, sections were obtained from the following bridges.

1. Bridge No. 0404 on Sandyfield Road, crossing Nine Pin Branch (Worcester County, Maryland): Twenty-one sections of treated Southern Yellow Pine, submerged 25 years in water and taken from three different piles of the bridge, were obtained. Creosote treatment of 16 lb/ft^3 was used.
2. Bridge No. 9015 on MD-392 over Marshyhope Creek (Dorchester County): Thirty-four sections of treated Southern Yellow Pine were obtained from 12 different piles removed after 25 to 30 years of service. Creosote treatment was 12 lb/ft^3.
3. Denton Bridge at Denton, Maryland (Caroline County): This bridge collapsed in 1976. Laboratory tests by the Maryland Highway Department indicated substantial reduction in strength of the piles during their service life. For this study, 32 sections of Red Pine were taken from four different piles after a service life of 60 years.
4. Piles from relieving platform at Fort McHenry Tunnel Project: This platform, being removed for the purpose of constructing a tunnel, is located in Baltimore. Thirty-four sections of untreated Southern Pine from piles from the platform were obtained. The platform is about 18 years old.

Specimens Tested

Tests were conducted on prepared specimens for crushing strength parameters on the following types of wood: Douglas Fir (50 specimens), Red Oak (30 specimens), new untreated Pine (30 specimens), new treated Pine (30 specimens), and old treated Pine (395 specimens).

Tests were conducted on prepared specimens for bending strength parameters on the following types of wood: Red Oak (40 specimens), untreated Yellow Pine (25 specimens), treated Yellow Pine (25 specimens), and Yellow Pine from Marshyhope Bridge sections (42 specimens). As in the case of the crushing strength testing, the ultrasonic tests were followed by the bending strength test on the same specimens.

Sample Preparation and Testing Methods

New pine piles were selected in accordance with ASTM D25-79. Specimens were cut from the sections of piles in accordance with ASTM D143. The size of the specimens prepared for compression parallel to grain testing was 1 x 1 x 4 in. This was in compliance with ASTM D143, Part II. For static bending tests the procedure followed was ASTM D143-79, Part II, Sections 245-252. For the compression parallel to grain tests the procedure followed was identical to ASTM D143-79, Part II, Sections 253-259, with the exception that load compression curves were not taken because only the maximum crushing strength was of interest.

For the ultrasonic tests, time readings were taken across the grain in three directions and parallel to the grain in three locations: at the pith, in the middle of the section, and on the outer rings of the section. The wave velocities were calculated, and the dynamic modulus was then determined.

Correlation Between Specimen and Section Results

The ultrasonic test was conducted on sections to measure the wave velocity parallel to grain (V_L). Sections with height-to-diameter ratios between 1 and 3 were tested. The test was also conducted on specimens prepared from the same sections. The dimensions of the specimens were 1 x 1 in. in cross section and had a length of either 4 or 16 in. The results indicate that the average wave velocity parallel to grain for the sections is about 0.885 of the specimen, and for the crushing strength the ratio between the crushing strength of sections of piles to small specimens at 12 percent moisture content for Southern Pine was found to be 0.92. [Wilkinson (16) showed that this ratio is 0.90 at the pile tip and 0.97 at the butt of the pile.] Thus the wave velocity and crushing strength for sections can be determined if only small specimens are tested. However, this is only true for new piles.

Relation Between Dynamic and Static Modulus

The modulus determined from ultrasonic testing is referred to as the dynamic modulus. Most of the data reported indicated that the dynamic modulus of elasticity is higher than the modulus of elasticity evaluated in the static bending test E_s by 5 to 15 percent (17). It has been suggested that the difference is caused by the rate of loading. Figure 3 shows the relationship determined for Red Oak specimens.

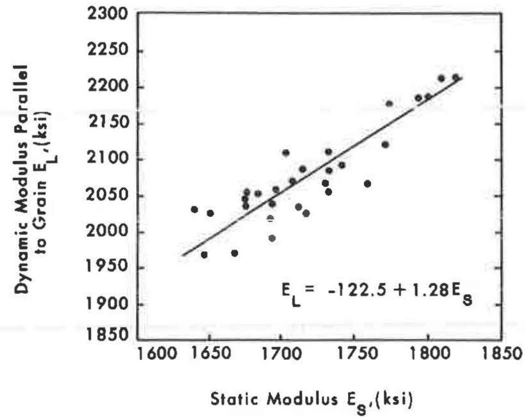

FIGURE 3 Static and dynamic moduli for Red Oak specimens.

are the more popular species used for timber piles. The properties from all test results at air dry are presented elsewhere (14).

Variables Considered

The following variables were considered in the testing program because of their influence on the reliability of the assessment of the inspected piles.

Type of Wood

The species selected in this study--Douglas Fir, Southern Pine, and Red Oak--were chosen because they are the more popular species used for timber piles. The properties from all test results at air dry are presented elsewhere (14).

Effect of Treatment

Various procedures have been developed to help ensure lasting protection of timber piles by preventing the growth of deterioration agents around and within the piles. The basic protective barrier method for wood piling is impregnation by chemical preservatives. Creosote is the most widespread preservative in use on timber piles. Processes associated with the treatment can lead to reduction in strength of the wood. The primary strength reduction appears to be controlled by the conditioning process used before pressure treatment (18).

To study the effect of treatment on piles used in the state of Maryland, untreated Southern Yellow Pine sections were tested ultrasonically and then sent to a company for creosote treatment, after which the sections were retested. The treatment applied was the same as for other piles used in the state; thus the effect of treatment was studied on the same sections. In addition, both treated and untreated sections were tested for strength determination. The data in Table 1 give the average properties of crushing strength, wave velocity, density, and dynamic modulus for sections of treated and untreated Pine. It can be concluded that treatment reduced the crushing strength by 20 percent.

Direction of Grain

Wood is characterized by three mutually perpendicular axes of symmetry, corresponding to the longitudinal, radial, and tangential directions of the wood structure. The strength and elastic properties of wood differ in these three different directions. In

TABLE 1 Properties of Treated and Untreated Pile Sections

Type of Wood	Crushing Strength, σ_{cr} (psi)	Wave Velocity (ft/sec) V_L	V_N	Density, γ (lb/ft^3)	Dynamic Modulus, E_L (ksi)
Untreated Yellow Pine	6,227	15,740	6,340	34.9	1,880
Treated Yellow Pine	5,005	14,435	6,010	43.2	1,980

most properties, however, the major differences are denoted by strength and elastic values parallel and perpendicular to the grain, as the differences between these properties of wood in the tangential and radial directions are, in general, relatively small.

To study this factor, specimens and sections were prepared for ultrasonic testing in the tangential and radial direction for the following types of wood: Douglas Fir, untreated Pine, treated Pine, and Red Oak. The results indicated that the velocity in the radial direction is higher by about 10 percent than the velocity in the tangential direction. In addition, for all types of wood, it was found that the wave velocity parallel to grain (V_L) is 2 to 3 times the wave velocity normal to grain (V_N). However, for old piles the relation between V_L and V_N no longer varies from 2 to 3 and is as shown in Figure 4. It was also found that the ratio between the longitudinal and normal to grain velocities is a function of the wood unit weight, as is shown in Figure 5.

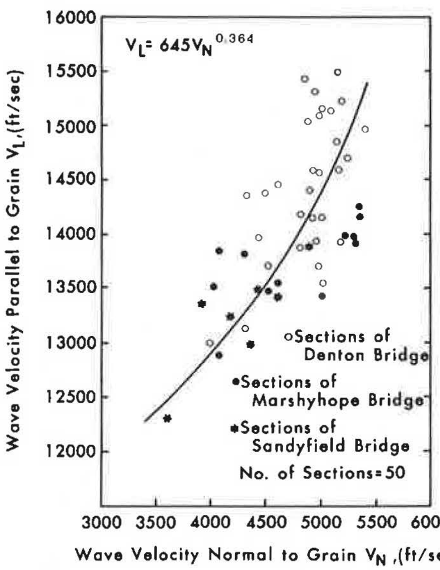

FIGURE 4 Relationship between V_L and V_N for old piles.

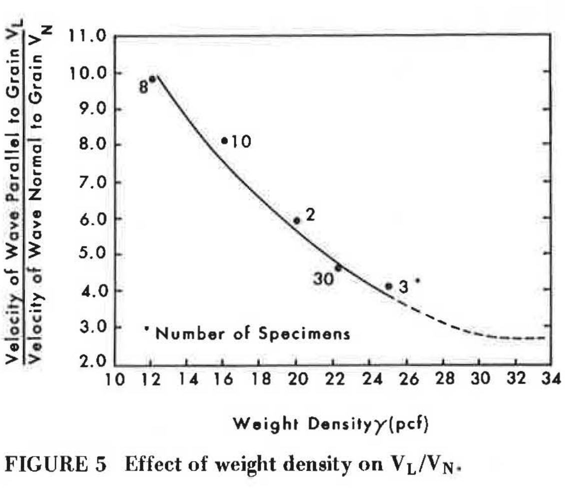

FIGURE 5 Effect of weight density on V_L/V_N.

Effect of Density on Wave Velocity

The air-dry weight density (γ) for sections of old piles obtained from different bridges are plotted with the wave velocity (V_N) in Figure 6. The data in the figure indicate that the relationship is strongly dependent on the amount of treatment the pile received when it was new. The figure could be used to estimate an approximate value of γ when the velocity (V_N) is known; however, it should only be used if there is no other means of determining the air-dry unit weight.

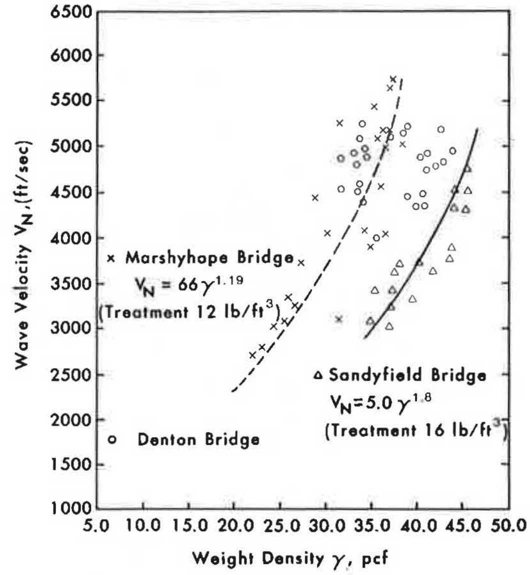

FIGURE 6 Relationships between wave velocity and weight density.

Effect of Degree of Decay

Scheffer et al. (12) noted from studying piles removed from the Potomac River in Washington, D.C., after 62 years of service that the crushing strength of small specimens prepared from the pile above the mudline has been reduced by 60 percent and of that below the mudline by 20 percent. In a similar study of bridge piles after 85 years in the Milwaukee River, Bendtsen (19) reported that the average modulus of rupture of the Red Pine was 32 percent, the modulus of elasticity 27 percent, and the specific gravity 12 percent lower, respectively, than the published values in ASTM.

To study the effect of the degree of decay on the ultrasonic and crushing strength tests, piles from four different bridges of different service lives were used. Both sections and specimens were tested.

For the specimens, the results of ultrasonic tests and compression tests for small specimens prepared from sections above and below water level indicated the following reduction in comparison to specimens prepared from new treated piles:

Properties	Avg Reduction (%)
Crushing strength, σ_{cr}	69
Dynamic modulus, E_L	60
Wave velocity, V_N	55
Density	55

For sections in which cavities were present, the dynamic modulus in the longitudinal direction was corrected for such loss in area. The reduction in the engineering properties in all bridges (no sections from the platform at the Fort McHenry Tunnel

TABLE 2 Reduction in Engineering Properties of Pile Sections

Pile Sections From	Avg Reduction (%) Crushing Strength, σ_{cr} (psi)	Dynamic Modulus, E_L (ksi)	Wave Velocity, V_N (ft/sec)	Density (lb/ft^3)
Sandyfield Bridge	40	22	37	16
Marshyhope Bridge	73	67	59	43
Denton Bridge	36	16	20	18

were tested) caused by decay are summarized in Table 2.

Figure 7 shows the relationship between the dynamic modulus (E_L) and the crushing strength for one of the bridges, and Figure 8 shows this single variable relationship for all the bridges. Figure 9 presents the correlation between crushing strength and wave velocity normal to grain, and weight density (i.e., a multivariables relationship). In the multivariables equation, the first parameter represents the effect of the velocity across the pile section, whereas the second term represents the contribution of the average weight density. The predicted crushing strength from the single-variable model is higher by about 8 percent than that of the multivariables model for the same unit weight.

Effect of Moisture Content

The moisture content of air-dry wood in most wood represents an average of about 12 percent. In using the green strength values, it is important to use the value that corresponds to the fiber saturation point, above which the strength is the smallest and is approximately constant. This moisture content value is assumed to be about 24 percent. For NDT, James (20), Burmester (21), and Gerhards (22) all studied the effect of moisture content on the longitudinal wave velocity.

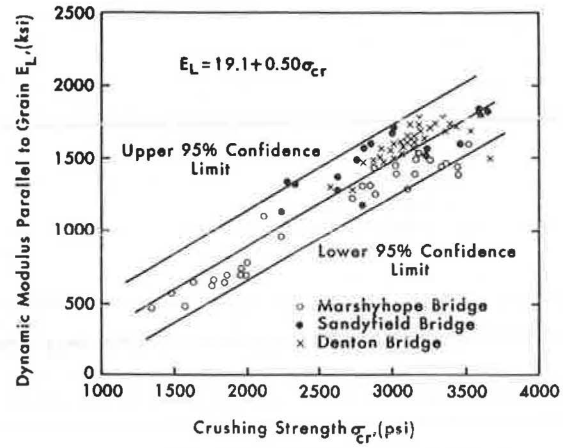

FIGURE 8 Relationship between E_L and σ_{cr} for all bridges.

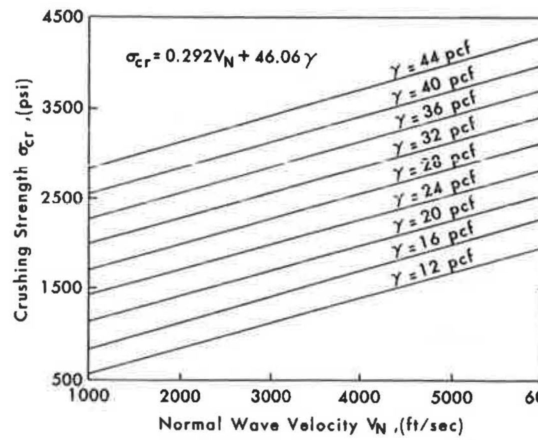

FIGURE 9 Crushing strength and normal wave velocity as a function of weight density.

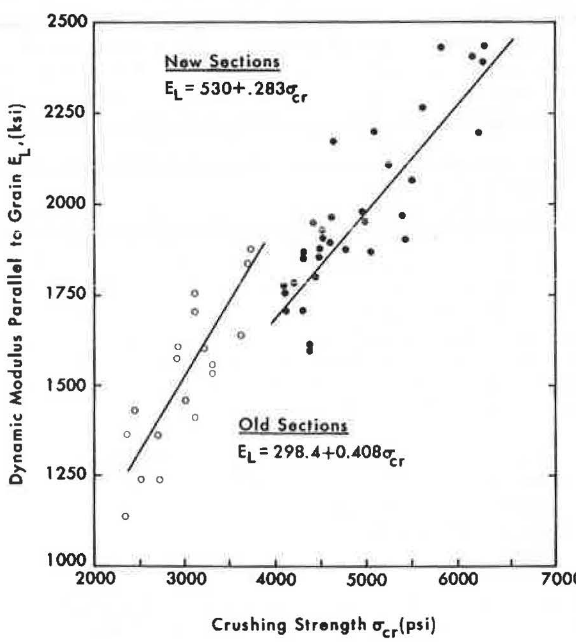

FIGURE 7 Relationships between E_L and σ_{cr} for Sandyfield Bridge.

In this study the effect of moisture content on the wave velocity has been determined for Red Oak, and untreated and treated Pine. Figure 10 shows the effect of the moisture content on the wave velocity parallel to grain. The figure shows that the wave velocity decreased by about 9 percent between the moisture content at air-dry condition and at the fiber saturation point.

The compression test parallel to grain was also conducted on sections of treated Pine obtained from different piles. Two sets of sections were prepared from the same pile for the purpose of testing one set at air-dry condition and the other set at wet

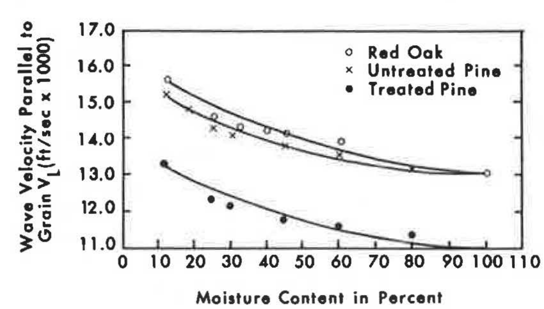

FIGURE 10 Effect of moisture content on V_L.

condition. It was found that the crushing strength of the sections at air-dry condition is 1.48 times that of the sections at wet condition (i.e., a pile underwater loses about 33 percent of its strength).

Tests Above and Below Water

Ultrasonic tests were conducted on treated and untreated solid sections of new Yellow Pine piles in air and in water at different moisture contents. The results indicated that the difference between the ultrasonic velocities for solid sections tested in air or in water at the same moisture content are small and may be neglected. In the case of treated sections of old Yellow Pine piles that were tested in air and also in water at air-dry and at wet conditions, again no difference existed between the values measured in the air or water at the same moisture content.

Figure 11 presents the relationship between the ratio (RA) of the velocity at air-dry condition to wet condition, and the weight density γ in pounds per cubic foot for good and decayed pile sections. Because the greater the decay in the wood the more water it will absorb, the ratio RA will therefore be higher for those values of small γ and lower for high values of γ, as shown in Figure 11.

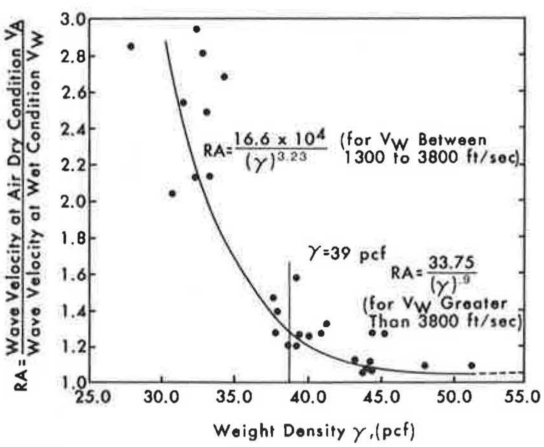

FIGURE 11 Ratio RA as a function of weight density.

Summary

From knowledge of the wave velocity that is obtained from field inspection, the dynamic modulus and the crushing strength can be determined. It should be noted here that the values obtained for the crushing strength have to be corrected for any of the factors that were discussed previously, such as treatment, whether the reading was taken above or below water, and so on.

CONDITION OF PILES IN-PLACE

Ultrasonic testing was performed on sections from piles from all bridges, followed by compression testing of the sections, except for Bridge No. 9015 on MD-392 over Marshyhope Creek, where ultrasonic testing was also performed in-place before the pilings were removed. By using the ultrasonic data, the correlation curves for some sections, and the crushing strength determined from testing of other sections, the crushing strength distribution along the length of the piles was plotted. Figure 12 shows an example of such a plot. The data from all the piles indicated that along the pile length a reduction in strength between 10 to 40 percent had occurred; however, at the water line (between high and low tide) a larger reduction took place in two of the bridges (up to 80 percent reduction in strength in one of the piles tested). This means that there existed a severely decayed part at the water line in some piles and the degree of decay decreased going either up or down along the pile.

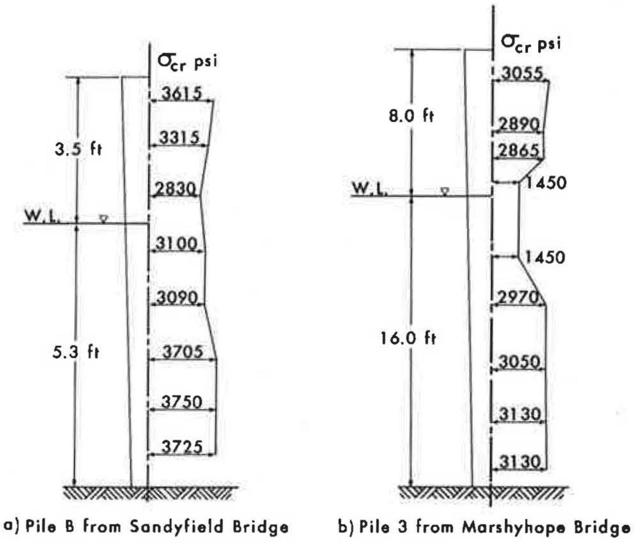

FIGURE 12 Crushing strength along length of pile.

It is interesting to note that in some cases, piling whose external appearance suggested no damage and appeared to be in satisfactory condition indicated no wave transmitted by the equipment developed. When these piles were removed it was found that a large decay pocket was present at the center, surrounded by extensive internal decay with a shell of sound wood 2 to 3 in. thick remaining in the pile. In general, it was found that decay had occurred at the pith of the section while the treated outer ring was in a better condition.

VERIFICATION OF CORRELATION CURVES

The correlation curves developed were verified and checked by comparing the crushing strength calculated by using those curves and those that were determined experimentally. The ultrasonic tests were first conducted on piles from a highway bridge on MD-715 over US-40. The bridge had the advantage in that it included two sets of piles, one original and the other added later to strengthen the bridge. When the bridge was removed to be replaced by a larger bridge, 9 piles were taken to obtain 32 sections. The results of the ultrasonic tests were substituted in the developed correlation curves to determine the crushing strength of the pile sections. These values were then compared with the crushing strength obtained from the compression parallel to grain tests on the same sections. The results of these tests and the comparison are presented elsewhere (4).

The results indicated that the calculated average crushing strength is different by only about ±11 percent from the actual measured strength. This percentage is close to the acceptable limit (7 percent) of the probable variation in the crushing strength in random trees of the same type.

SUMMARY AND DISCUSSION OF RESULTS

The testing technique employed was that of the ultrasonic wave propagation method. It used the relationship between the wave velocity in a material and its properties. In ultrasonic testing, pile sections were subjected to rapidly alternating stress waves of low amplitudes. Undamaged wood is an excellent transmitter of these waves, whereas damaged and decayed wood delays transmission. The method, therefore, required accurate measurements of the velocity of the propagated stress wave.

The NDT was followed by extensive axial load testing of pile sections and a correlation was then established between the wave velocity or dynamic modulus and the strength of new piles. In addition, old piles from four different bridges in the state of Maryland were obtained to provide the opportunity to follow the NDT procedures through from field in-place measurements in one bridge (before they were removed from service) to laboratory NDT and finally to tests to failure for strength determination in all bridges. The results of the ultrasonic tests were correlated with the strength values from the destructive tests. In addition, small specimens were cut from new and old piles and both NDT and DT were conducted to determine the mechanical properties of wood and the correlation between NDT and DT. In both testing programs all variables that influence the results were considered. The relationships developed were verified and checked by comparing the crushing strength calculated by using these curves and those determined experimentally from a fifth bridge. It has been concluded from the favorable comparison that the relationships can be used successfully to predict the remaining strength of a pile in-place.

Following the inspection of the piles, an analysis should be undertaken by using the existing condition of the pile to determine if the pile can still perform as intended in its original design. A preliminary study, where the decay was represented by assuming a loss in the cross-sectional area or a reduction in the modulus of elasticity, indicated that the additional stresses developed in decayed piles caused by static and dynamic loading are substantial and should be considered (4).

CONCLUSION

Equipment was developed for the NDT of in-place timber piling below and above water. A testing program was used to develop a correlation between the NDT results (wave velocity) and the remaining strength of in-place timber piles. Verification of the correlation was carried out by testing in-place piling by using NDT then removing the piles, cutting them into sections, and axial load testing the sections to determine the remaining strength of the pile.

The technique is suitable primarily for piles that sustain damage to the wood microstructure, such as those immersed in fresh water for long periods of time. From the substantial reduction of strength obtained, it can be concluded that the use of equipment such as developed here are not merely sophisticated techniques for pile inspection but are essential ones.

The study provided an adequate inspection procedure to determine if damage is occurring or has occurred and to what extent, thus predicting the true performance of the pile. The quantitative determination of the remaining strength of timber piles in service with any degree of decay will enable the engineer to make appropriate judgments as to the ability of the pile to further support the loads imposed on it. It will also provide information on which to base a maintenance plan to meet the current or anticipated loading demands, affect decisions on new installations, and aid in projecting the service life of the bridge based on a predictable safety level.

ACKNOWLEDGMENT

The research reported herein was sponsored by the Maryland State Highway Administration in cooperation with the FHWA. The authors are grateful for the guidance and contributions made during the course of the project by the Technical Advisory Committee: A. Scott Parrish, R.J. Heard, M.M. Ytkin, H.B. Policelli, R. Nickerson, and Charles McGagney. Thanks also to Earle S. Freedman, chief engineer, Maryland State Highway Administration, for his support of the project.

REFERENCES

1. P. Nye. The Wearing Out of Urban America. Nation's Cities, Oct. 1977, pp. 8-12.
2. M.S. Aggour, E.J. White, Jr., and A. Ragab. Ultrasonic Testing of Underwater Timber Piles. ASNT Spring Conference Paper Summary. American Society for Nondestructive Testing, Columbus, Ohio, March 1982.
3. J.J. Agi. Nondestructive Testing of Marine Piling. Proc., 4th Nondestructive Testing of Wood Symposium, Vancouver, Wash., 1978, p. 187.
4. A. Ragab. Residual Strength Determination of Timber Bridge Piling. Ph.D. dissertation. University of Maryland, College Park, 1983.
5. I.D.G. Lee. Ultrasonic Pulse Velocity Testing Considered as a Safety Measure for Timber Structures. Proc., 2nd Symposium of Nondestructive Testing of Wood, Spokane, Wash., 1965, pp. 185-203.
6. R.A. Muenow. The Ultrasonic Nondestructive Evaluation of Wood Utility Poles, Wood and Concrete Railway Ties and Trestles, and Other Similar Structures. Tech. Paper V-117. James Electronics, Inc., Chicago, 1966, pp. 1-6.
7. K.A. McDonald, R.G. Cox, and E.H. Bulgrin. Locating Lumber Defects by Ultrasonics. Res. Paper FPL 120. Forest Service, U.S. Department of Agriculture, Madison, Wis., 1969.
8. K.A. McDonald. Lumber Defect Detection by Ultrasonics. Res. Paper FPL 311. Forest Service, U.S. Department of Agriculture, Madison, Wis., 1978.
9. R.F. Pellerin. Nondestructive Testing of Wood--A Possible Method for Timber Piling. Proc., 4th Nondestructive Testing of Wood Symposium, Vancouver, Wash., 1978, pp. 169-174.
10. M.D. Vanderbilt, J.R. Goodman, and J.A. Puckett. Testing of Large Timber Poles. Paper A-43. Presented at Society for Experimental Stress Analysis Spring Meeting, San Francisco, 1979.
11. R.M. Lanius, Jr., R. Tichy, and W.M. Bulleit. Strength of Old Wood Joists. ASCE, Journal of the Structural Division, Vol. 107, No. ST12, 1981, pp. 2349-2363.
12. T.C. Scheffer, C.G. Duncan, and T. Wilkinson. Condition of Pine Piling Submerged 62 Years in River Water. Wood Preserving, Vol. 47, No. 1, 1969, pp. 22-24.
13. R.F.S. Hearmon. Elasticity of Wood and Plywood. Forest Products Research Special Report 7. Her

Majesty's Stationery Office, London, England, 1948.
14. M.S. Aggour and A. Ragab. Safety and Soundness of Submerged Timber Bridge Piling. FHWA/MD Interim Report AW082-231-046. FHWA, U.S. Department of Transportation, June 1982.
15. B.O. Orogbemi. Equipment for Determining the Dynamic Modulus of Submerged Bridge Timber Piling. Master's thesis. University of Maryland, College Park, 1980.
16. T.L. Wilkinson. Strength Evaluation of Round Timber Piles. Res. Note FPL-101. Forest Service, U.S. Department of Agriculture, Madison, Wis., 1968.
17. J. Bodig and B.A. Jayne. Mechanics of Wood and Wood Composites. Van Nostrand, New York, 1982.
18. R.M. Armstrong. Structural Properties of Timber Piles, Behavior of Deep Foundations. Report STP-670. ASTM, Philadelphia, 1979, pp. 118-152.
19. B.A. Bendtsen. Bending Strength and Stiffness of Bridge Piles After 85 Years in the Milwaukee River. Res. Note FPL-0229. Forest Service, U.S. Department of Agriculture, Madison, Wis., 1974.
20. W.L. James. Effect of Temperature and Moisture Content on Internal Friction and Speed of Sound in Douglas Fir. Forest Product Journal, Vol. 11, No. 9, 1961, pp. 383-390.
21. A. Burmester. Relationship Between Sound Velocity and Morphological, Physical, and Mechanical Properties of Wood. Holz als Roh und Werstoff, Vol. 23, No. 6, 1965, pp. 227-236 (in German).
22. C.C. Gerhards. Stress Wave Speed and MOE of Weetgum Ranging from 150 to 15 Percent MC. Forest Product Journal, Vol. 25, No. 4, 1975, pp. 51-57.

Publication of this paper sponsored by Committee on Structures Maintenance.

Production and Testing of Calcium Magnesium Acetate in Maine

MARTHA T. HSU

ABSTRACT

The search for an effective substitute for the deicing agent sodium chloride has led to the development of calcium magnesium acetate (CMA). However, CMA is not commercially available. A project for the production of CMA using resources in Maine was carried out at the Maine Department of Transportation. After the product was made, other physical and chemical tests were also performed. The results indicated that CMA can be made in Maine from an apparent abundant source of high magnesium limestone and acetic acid (cider vinegar). A 10 percent solution of acetic acid with 10 min of agitation with the magnesium limestone coarse aggregate provides the best production of CMA for this grade. A commercial production of CMA should consider the constant reflux method with constant monitoring of the pH. Evaporation of the solution by solar energy is not effective because of the large amount of rainfall in Maine. Bituminous concrete batch plants have waste heat, which might be able to aid in this evaporation need. The field trial of CMA as a deicing agent demonstrated both advantages and disadvantages. A major concern is its dustiness. Outdoor uncovered storage of CMA is not practical. The corrosion effect of CMA solution toward metal or concrete needs further study.

The use of sodium chloride (NaCl) as a deicing agent on highways has been under scrutiny for some time. The chief concern is environmental compatibility. Sodium chloride is corrosive in nature and it affects the water-absorbing capability of soil (1,2).

Many research agencies have been searching for an effective substitute for sodium chloride. In March 1980, Dunn and Schenk (3) of Bjorkste Research Lab, Inc., published their findings on their study for a salt substitute. Their project was sponsored by FHWA. The results indicated that calcium magnesium acetate (CMA) was a promising alternative for NaCl. This new deicing agent would react at about the same melting rate as NaCl in the temperature range of common activity, but CMA also had the advantage of being a corrosion inhibitor. The run-off from melting action would be beneficial to most soils, and there is an insignificant effect to water supplies.

Realizing the potential of CMA use and the knowledge that CMA is not produced commercially, FHWA initiated a pooled fund project for CMA in May 1981 to find an efficient manufacturing process and to establish an evaluation procedure for the product. Ultimately a production contract was awarded to SRI International, and an environmental study contract was awarded to the California Department of Transportation. Both research programs began in October 1981, and many interim reports have been published since then. The work undertaken at SRI International has been to produce acetic acid by using Clostridium Thermoaceticum to ferment biomass-derived sugars. The acetic acid was then combined with dolomitic lime to produce CMA.

In the winter of 1981-1982 the Iowa Department of Transportation also undertook studies for the manufacture of CMA (4,5). The application of CMA was tested in the field in April 1982, as well as in the winter of 1982-1983. Their production method was to mix glacial acetic acid with a mixture of hydrated lime and dry concrete sand. This resulted in a product of CMA coated sand in a ratio of 3:1 (sand/CMA).

There are three major processes to produce CMA: (a) high magnesium quick lime (CaO + MgO) reacting with acetic acid, (b) high magnesium hydrated lime [$Ca(OH)_2$ + $Mg(OH)_2$] reacting with acetic acid, and (c) dolomitic limestone (or dolomite, $CaCO_3$ + $MgCO_3$) reacting with acetic acid. Because there is an abundant resource of dolomitic limestone in Maine, as well as possible waste of acetic acid (vinegar) in the apple orchard industry, a research effort was proposed to study the possible reaction process, the available raw materials, the by-products, and the ability to produce CMA from these waste products. The present study is the result of such an undertaking supported by the FHWA, U.S. Department of Transportation, as part of the Maine Department of Transportation Work Plan TQX HPR-PL-1(19).

EXPERIMENTAL PROCEDURES

Dolomitic limestone, calcium carbonate ($CaCO_3$) and magnesium carbonate ($MgCO_3$), was chosen instead of quick lime or hydrated lime because it is a natural resource in Maine. The chemical reactions are as follows:

$$CaCO_3 + 2HAc \rightleftarrows CaAc_2 + H_2CO_3 \quad \llcorner\!\!\rightarrow H_2O + CO_2 \tag{1}$$

where

$HAc = CH_3COOH$, acetic acid

$$MgCO_3 + 2HAc \rightleftarrows MgAc_2 + H_2CO_3 \quad \llcorner\!\!\rightarrow H_2O + CO_2 \tag{2}$$

The dolomitic limestone was supplied by Lime Products Corp., Union, Maine, and was produced in two sizes: coarse and fine. The acetic acid was supplied by W.H. Shurtleff Chemical Company. Both products were provided to the Maine Department of Transportation (MeDOT) at no cost.

Preliminary Laboratory Screening of Reaction Process

There were two types (coarse and fine) of dolomitic limestone used in this study. The fineness modulus (FM) values of the coarse and fine grade material were 3.2 and 0.78, respectively. The mole ratio of calcium and magnesium was 0.7.

Preliminary experiments indicated that concentrated (glacial) acetic acid does not react with the dolomite. Moreover, acetic acid has an extremely pungent odor. Therefore, concentrations of acetic acid of 20, 10, and 5 percent (by volume) were chosen for screening. Ultimately, a 10 percent solution was used. It was also apparent that the best yield of the reaction between coarse limestone and 10 percent acetic acid was around 20 percent. However, the unreacted limestone could be used as an abrasive agent or recycled for further reaction.

Laboratory Pilot Study

On June 24, 1982, 10 lb of the coarse limestone were mixed with 10 gal of 10 percent acetic acid in a concrete mixer for about 10 min. This batch was repeated five times, and all the mixtures were poured into a 3-ft 11-in. x 4-ft 2-in. container that was lined with a heavy plastic sheet. The depth of the original solution was 5 in. The entire operation was situated adjacent to the Materials and Research building in Bangor.

The evaporation of this solution was constantly monitored. By July 16, 22 days after the mixing date, the CMA was dry. The product was analyzed and showed a mole ratio of Ca/Mg = 2.5.

Batch Trial Production Using Coarse Grade Limestone

The first large-scale production was carried out on July 30, 1982, in Warren, Maine. The Lime Products Corp. had constructed an evaporation site under a dome structure that was covered with heavy plastic sheets.

The mixing process used a commercial readi-mix concrete mixer. This truck was filled with, in sequence, water, glacial acetic acid, and coarse dolomite. The mixture was then agitated for 10 min and was poured into a 40 x 10.5-ft reservoir that was lined with a heavy plastic sheet. This operation was repeated several times. Because of a defective water meter, the concentration of the acetic acid solution was 2 percent instead of the intended 10 percent. The entire process used 100 gal of glacial acetic acid and 1,440 lb of dolomitic limestone. The latter was increased to a total of 4,000 lb to ensure excess limestone and alkalinity.

The summer of 1982 was cooler than normal. The plastic covering, while minimizing rainwater from entering the solution, greatly reduced the evaporation process. To hasten the evaporation, additional heating lamps and aeration devices were installed. By the end of November most of the surface was dry, with the exception of a few puddles of liquid. The pH of the liquid was 6.5. The liquid was transferred into another container. The remaining wet sludge was neutralized further to a pH of 9 with high magnesium quick lime. The final product was then transferred to five 55-gal drums for storage. The total weight of the wet material was 3,320 lb.

Batch Trial Production Using Fine Grade Limestone

On August 11, 1982, a second batch production was carried out by using the fine grade dolomite as the starting material instead of the coarse grade. The acetic acid was 10 percent by volume. The entire production consisted of 200 gal of glacial acetic acid, 1,800 gal of water, and 8,000 lb of fine dolomitic limestone. The dimension of the second evaporating basin was 10 x 20 ft, half of the previous structure, and it was also enclosed in plastic sheeting. Heating lamps and aeration equipment were later installed as before to speed up evaporation.

By the end of October the solution began to congeal. The liquid showed a pH of 5.2. When a small amount of semisolid material was dried and analyzed, it resulted in a product containing calcium acetate and magnesium acetate of a 4:1 mole ratio.

At the same time the bottom of the basin became impermeable and claylike. Therefore, the liquid-semisolid portion of the product was transferred to four 55-gal drums. Quick lime was added to bring the pH to 12, and finally the pH was adjusted to 9 or 10 with acetic acid. The drums of this semisolid were brought to the Materials and Research Laboratory in Bangor for further drying. The resultant CMA powder material contained unreacted limestone and quick lime. The total weight was 1,180 lb.

Analysis of a few batches of this CMA product revealed the CMA content to be around 75 percent. Test data also indicated that nearly all of the product was calcium acetate.

Field Trial on Deicing Power of CMA

On January 6, 1983, a snowy day with the temperatures around 30°F, a field trial was conducted on the driveway of the Materials and Research parking lot. Forty-five pounds of sodium chloride (NaCl) were applied on one part of the driveway (50 ft long) and an equal amount of CMA powder was applied on another area (also 50 ft long). A 30-ft untreated area was left in the middle. The general impression was that CMA reacted slower than NaCl, but it remained on the road for a longer period; the evidence was its apparent effectiveness the next day when fresh snow fell on the pavement again. However, because of the unreacted limestone and lime, tracking into the building by laboratory personnel was considered an annoyance.

Runoff and Leaching of CMA-Sand Stockpile

A CMA-sand stockpile was prepared by mixing 3 yd^3 of sand with 500 lb of CMA powder on December 29, 1982. The CMA was noted to be extremely light and there was a considerable amount of dust as it was being mixed. A trench was dug around the pile, which allowed the water to run off the stockpile into a container recessed in the trench. The concentration of CMA in the runoff was monitored weekly. At the same time samples of the CMA-sand mixture were obtained weekly to be analyzed for calcium acetate and magnesium acetate content. The same type of leaching test was conducted also for a NaCl-sand pile for comparison.

Corrosion Test of CMA Solutions

Calcium magnesium acetate solutions of various concentrations were prepared in which steel test strips (1 x 6 x 0.015 in.) were immersed for 2 weeks. All strips were prepared with the same types of cutting edges. The test strip was suspended in a 400-mL beaker filled with 300 mL of the desired solution. The solution was then covered with a plastic bag and sealed with a rubber band around the beaker. By using a magnetic stirrer, the solution was agitated at a slow, uniform rate for the entire duration.

The MeDOT CMA solutions used in the testing were prepared by first making a saturated solution of this material. Later testing of this solution on the atomic absorption spectrophotometer indicated this saturated solution to be a 13.2 weight percent CMA solution. Solutions of other concentrations were prepared by simple dilution of this saturated solution.

A corrosion test was also performed with solutions of CMA that was produced under the SRI contract with FHWA (6). The concentrations were expressed in weight percent also. Two more corrosion tests were carried out, one on deionized water for control and one on 10 percent NaCl for comparison. In addition to the experiments previously mentioned, 7 percent solutions of pure calcium acetate and magnesium acetate were also tested for their corrosion property.

Ponding Test--Corrosion of Rebars in Concrete

A ponding test was performed on concrete blocks according to AASHTO Designation T259-80. Steel rebars were placed within the slabs at a depth of 2.5 in. from the surface. The dimension of the blocks was 21 x 12 x 3.25 in. A confinement of the dimension of 18 x 9.5 x 1 in. was made on top of each block with the use of wooden frames and wax seals. The solutions tested were 3 percent CMA produced by MeDOT, 3 percent CMA supplied by SRI, 3 percent NaCl, and water.

The solutions were maintained at a depth of at least 0.5 in. during the test. At the end of 90 days the solutions were removed from the slabs. The slabs were allowed to dry, and subsequently sawed near a rebar so as to expose the rebar for examination.

Electrical half-cell potential measurements of the reinforcing steel were taken (7). In addition, a small portion of the slab was sawed off from each block. The small pieces were then polished and examined for penetration. A powdered sample of each slab was also prepared according to the depths of the slab, 0 to 1.75 in. and 1.75 to 3.5 in. These samples were then tested for either chloride content in the case of NaCl or for acetate in the case of CMA materials.

Relative Slipperiness of CMA Solution Compared with Other Deicing Chemicals

Testing was carried out on four deicing chemicals in terms of their relative slipperiness. Water was used as a standard for the comparison. Each of the four chemicals was mixed with water to produce a saturated solution. The chemicals used and the resultant specific gravities were as follows: sodium chloride (1.193), calcium chloride (1.420), calcium magnesium acetate (1.106), and urea (1.135).

The instrument used for determining the relative slipperiness was a British portable tester. Testing was performed in accordance with ASTM E-303. The results are in British pendulum numbers (BPN) and do not necessarily agree or correlate with other slipperiness measuring equipment.

The surfaces of bituminous concrete pavement and portland cement concrete were used for the comparison. The five lubricants (water plus the saturated solutions) were applied separately to each of the two surfaces. A total of 10 (BPN) values were obtained for each lubricant on each surface. The mean value was considered representative for each of the respective lubricants.

The testing surfaces were flushed with water and dried between the testing of each lubricant.

RESULTS AND DISCUSSION

Production of CMA Using Dolomite

The method used in this project possessed the following advantages:

1. The price per pound of limestone was about one-hundredth of that of lime,
2. Solar energy was used instead of electricity or fuel, and
3. The minimum amount of machinery and physical facilities were employed.

However, from the experience gained so far, it appears that many obstacles do exist. The following are among the important ones.

1. The reaction of limestone with acetic acid involves the formation of carbonic acid, and subsequently the evolution of the carbon dioxide (reac-

tions 1 and 2). Theoretically, these reactions could be driven to completion by constant reflux, but in reality this is difficult to achieve. However, the reaction between quick lime (calcium oxide and magnesium oxide) and acetic acid involves only combination of the two reactants; thus it would be more efficient:

$$CaO + 2HAc \rightleftarrows CaAc_2 + H_2O \quad (3)$$

$$MgO + 2HAc \rightleftarrows MgAc_2 + H_2O \quad (4)$$

2. Calcium carbonate and magnesium carbonate react with acetic acid at different rates, which also vary as the pH of the solution changes. This also holds true for calcium oxide and magnesium oxide. Thus the products from this project had a Ca/Mg mole ratio of 2.5 in the preliminary coarse material trial. The ratio was 4.0 for the product with the fine grade trial batch when the pH of the original solution was 5.2. However, when the pH was adjusted to 9 or 10, the final product was nearly devoid of magnesium acetate. Recognizing that magnesium acetate has a lower eutectic point than calcium acetate, the deicing effectiveness of the final product would be somewhat diminished.

3. The dependence on solar energy is not realistic for Maine's climate. During summer months overcast or rain is a common occurrence ($\geq$ 40 in. of average precipitation per year). A method to evaporate the solution economically is needed. (The addition of more ventilation to the covered plastic evaporation pits would have greatly accelerated the evaporation rate).

Field Application of CMA

Although only one application was made in the use of CMA for deicing, it was apparent that the CMA produced from this project (mainly calcium acetate) initially reacted slower than NaCl, but persisted for a longer period of time. The easily detected tracking problem may be caused by the unreacted limestone and the lime that could be avoided if the reaction was carried to completion.

Storage of CMA Outdoors and Uncovered--Leaching Effect and Runoff

The results of the calcium acetate and magnesium acetate contents in the CMA-sand stockpile that was left uncovered outdoors were plotted in Figure 1. The data in this figure show that the content of calcium acetate and magnesium acetate diminished gradually with time. The fluctuation of these data is the result of uneven mixing and random sampling sites. Allowing for these imperfections, it is apparent that CMA was leached out by rain or snow when stored outdoors and uncovered.

The results of analysis for the runoff from the CMA-sand stockpile are shown in Figure 2. There were considerable fluctuations for the Ca^{++} and Mg^{++} content in the runoff. This is mainly the consequence of the weather change in the precipitation occurrence. A heavy rainfall or snowstorm followed by melting gave rise to high Ca^{++} and Mg^{++} content. The opposite was true for low precipitation. On one occasion (January 19, 1983) there was no runoff in the collection vessel because of freezing conditions.

Corrosion Test of CMA Solutions

The results of the corrosion test for CMA solutions, prepared from the material produced by MeDOT and by SRI, are given on Table 1. The results on water and 10 percent NaCl solution are also given as a comparison. In an attempt to compare the corrosion effect of the two individual ingredients in CMA, 7 percent solution of magnesium acetate ($MgAc_2 \cdot 4H_2O$) and 7 percent solution of calcium acetate ($CaAc_2 \cdot H_2O$) were also tested. The results are also given in Table 1.

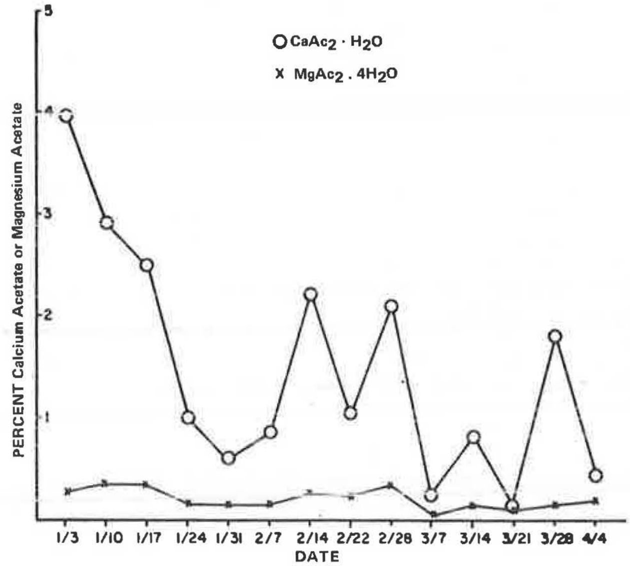

FIGURE 1 Calcium acetate and magnesium acetate contents in the CMA-sand stockpile as a function of time (stored outdoors uncovered).

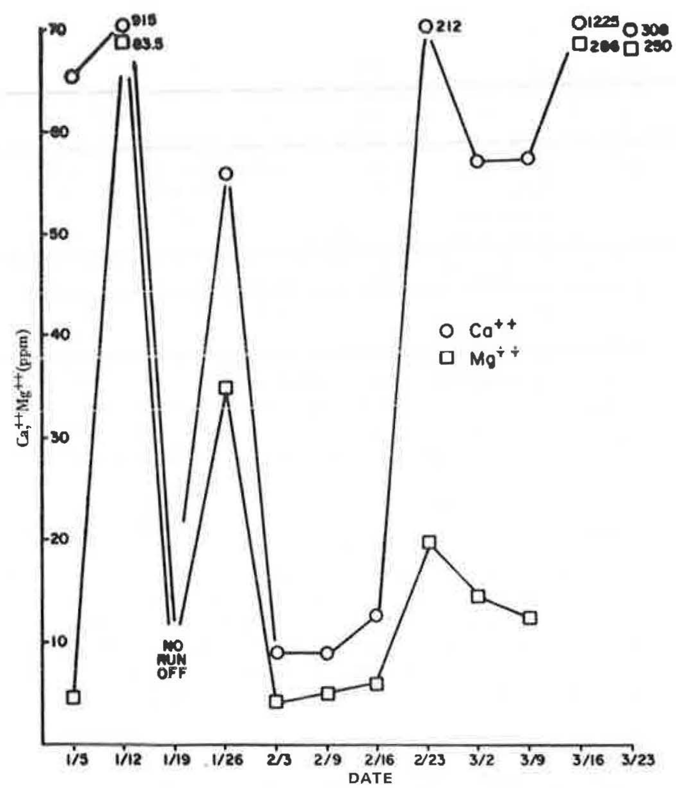

FIGURE 2 Ca^{++} and Mg^{++} content in runoff from the CMA-sand stockpile as a function of time (stored outdoors uncovered).

TABLE 1 Corrosion Test Results of CMA Solutions after Two-Week Immersion Period

Solution Description	Concentration (weight percent)	Initial pH	Final pH	Percent Weight Loss of Test Strip
CMA (MeDOT)	13.2	11.2	9.8	0.28
	9.6	11.1	7.3	0.33
	6.8	11.1	7.6	1.05
	4.1	11.1	7.4	0.69
	1.4	10.7	7.4	0.03
CMA (SRI)	14.0	9.2	8.8	0.26
	10.0	9.7	8.6	0.30
	5.0	9.5	8.5	0.22
H_2O		4.9	5.4	0
NaCl	10	7.9	5.5	0.98
$CaAc_2 \cdot H_2O$	7	7.7	7.2	0
$MgAc_2 \cdot 4H_2O$	7	7.2	7.2	0.14

The corrosion effect of an electrolyte has been well established (8). In a corrosion process the predominent reactions at the anode and cathode are as follows:

$$\text{Anode (oxidation)} \quad Fe \rightleftarrows Fe^{2+} + 2e \tag{5}$$

$$\text{Cathode (reduction)} \quad H^+ + e \rightleftarrows \tfrac{1}{2}H_2 \tag{6}$$

or

$$2H^+ + \tfrac{1}{2}O_2 + 2e \rightleftarrows H_2O \tag{7}$$

These oxidation-reduction reactions could be viewed as an electron transfer process. Therefore, a highly ionic medium would facilitate the transfer, thus the corrosion.

Another important factor would be the pH of the solution. High pH (basic) means that the concentration of H is low; reactions 6 and 7 will have less tendency to move to the right, thus less corrosion.

Sodium chloride is considered a neutral salt; theoretically, the pH of a NaCl solution is 7. On the other hand, both calcium acetate and magnesium acetate are considered basic salt, which yields a solution of pH higher than 7 when dissolved. This is the predominant factor that contributed to the corrosion-inhibition character of CMA. This can be substantiated qualitatively from the results given in Table 1. (However, the high percent weight loss exhibited by the 6.8 percent MeDOT CMA is difficult to explain.) Realizing that the starting material for the production of CMA at MeDOT contained many other ingredients in the limestone while the production process for SRI CMA enabled the removal of all other impurities, further analysis is needed to explain this abnormality.

Ponding Test--Corrosion of Rebars in Concrete

Because of the limited time of testing (90 days), the rebars in the concrete did not appear to be corroded. Closer examination of the electrical half-cell potential measured against copper-copper sulfate half-cell indicated voltages as follows: 0.08 V and 0.09 V for H_2O ponding test slabs; 0.18 V and 0.18 V for NaCl; 0.11 V and 0.10 V for MeDOT CMA, and 0.07 V and 0.30 V for the two SRI CMA slabs. With the exception of the last value, it is apparent that CMA does have less corrosion effect than NaCl. A major reason is that Ca^{++} and Mg^{++} undergo hydrolysis in water:

$$Ca^{++} + 2H_2O \rightleftarrows Ca(OH)_2 + 2H^+ \tag{8}$$

$$Mg^{++} + 2H_2O \rightleftarrows Mg(OH)_2 + 2H^+ \tag{9}$$

and produce calcium hydroxide, $Ca(OH)_2$, and magnesium hydroxide, $Mg(OH)_2$. The solubilities of these hydroxides in water are extremely low, with $Mg(OH)_2$ being considered insoluble. A thin white film that formed on the MeDOT CMA slabs was evident. Therefore, it is not surprising that the CMA slabs showed little penetration, whereas analysis of the chloride in the NaCl slabs gave an average chloride content of 5.6 and 2.6 lb/yd for the 0 to 1.75-in. and 1.75- to 3.5-in. layers, respectively.

Relative Slipperiness of CMA Solution Compared with Other Deicing Chemicals

The friction results are given in Table 2. The data indicate that calcium chloride created a significant reduction in the frictional characteristics of both surface types. This is not unusual, because calcium chloride is a hygroscopic water absorber. It also poses a problem to the driver because it forms, particularly on the windshield, a thin film that is difficult to flush off.

TABLE 2 Surface Frictional Properties of Deicing Chemicals Measured with British Pendulum Skid-Resistance Tester

	Bituminous Concrete		Portland Cement Concrete	
Lubricant	BPN (avg)	Reduction[a] (%)	BPN (avg)	Reduction[a] (%)
Water	78.2	–	37.1	–
Sodium chloride	70.9	9	32.2	13
Calcium chloride	60.3	23	24.6	34
CMA	70.1	10	28.4	28
Urea	71.1	9	34.4	7

[a]Based on water as a standard.

The CMA performed nearly the same as the other lubricants on the bituminous surface but indicated a significant reduction of BPN on the dense concrete. It should be noted that all deicing agents reduced the frictional resistance when compared to water.

CONCLUSIONS

1. CMA can be made in Maine from an apparent abundant source of high magnesium limestone and acetic acid (cider vinegar).
2. A 10 percent solution of acetic acid with 10 min of agitation with the magnesium limestone coarse aggregate provides the best production of CMA for this grade.
3. A commercial production of CMA should consider the constant reflux method with constant monitoring of the pH.
4. Evaporation of the solution by solar energy is not effective because of the large amount of rainfall ($\geq$ 40 in.) in Maine. Bituminous concrete batch plants have waste heat that might be able to aid in this evaporation need.
5. The field trial of CMA as a deicing agent indicated both advantages and disadvantages. A major concern is its dustiness.
6. Outdoors uncovered storage of CMA is not practical.
7. The corrosion effect of CMA solution toward metal or concrete needs further study.

REFERENCES

1. R.E. Hanes, L.W. Zelazny, K.G. Verghese, R.P. Bosshart, E.W. Carson, Jr., R.E. Blasser, and D.D. Wolf. Effect of Deicing Salt on Plant Biota and Soil: Experimental Phase. NCHRP Report 170. TRB, National Research Council, Washington, D.C., 1976, 88 pp.
2. M.T. Hsu. Roadside Deicing Chemical Accumulation After Ten Years Application. Tech. Paper 82-10. Materials and Research Division, Maine Department of Transportation, Bangor, 1982.
3. S.A. Dunn and R.U. Schenk. Alternate Highway Deicing Chemicals. Report FHWA-RD-79-109. FHWA, U.S. Department of Transportation, March 1980.
4. M. Sheeler and W. Rippie. Production and Evaluation of Calcium Magnesium Acetate. Final Report, Project HR-243. Highway Division, Iowa Department of Transportation, Ames, 1982.
5. M. Sheeler. Experimental Use of Calcium Magnesium Acetate. Project HR-253. Iowa Department of Transportation, Ames, 1983.
6. C.W. Marynowski, J.L. Jones, R.L. Boughton, D. Tuse, J.H. Cortopassi, and J.E. Gwinn. Process Development for Production of Calcium Magnesium Acetate (CMA). Report FHWA-RD-82/145. FHWA, U.S. Department of Transportation, March 1983.
7. K.C. Clear. Time-To-Corrosion of Reinforcing Steel in Concrete Slabs--Volume 3: Performance After 830 Days. Report FHWA-RD-76-70. FHWA, U.S. Department of Transportation, 1976.
8. F.L. LaQue. Corrosion of Steel--Simplified Theory. In Steel Structures Painting Manual (Volume 1), Steel Structures Painting Council, Pittsburgh, 1982, pp. 3-8.

Publication of this paper sponsored by Committee on Winter Maintenance.

Corrosion of Galvanized Steel Floor Slab Reinforcement

SAM BHUYAN and ROBERT G. TRACY

ABSTRACT

A 17-year-old parking facility in metropolitan Detroit is experiencing floor slab deterioration. An investigation was performed to determine the nature and extent of deterioration and identify probable restoration alternatives. The investigation involved visual observation, materials testing, a chain drag delamination survey, and determination of concrete cover to slab reinforcement. The structural frame consists of a 12-in.-thick flat plate floor slab system spanning in two directions supported by columns approximately 30 ft on centers. Floor slab reinforcement in the top and bottom slab sections are galvanized reinforcing steel bars. The floor slab and ceiling deteriorated from corrosion-induced spalling. Chain drag and coring surveys indicate that approximately 26 percent of exposed floor surfaces and 5 percent of ceiling surfaces are delaminated or spalled to a depth of about 2 in. Clear concrete cover is generally good, with a low cover of about 1.25 in. and an average cover of about 2.25 in. The chloride content of the concrete, determined within the top 3 in. of the slab, ranged from 25.2 to 8.5 lb/yd^3 of concrete. The average concrete compressive strength of the floor slab is about 5,670 psi. The average air content of the concrete was determined to be 2.3 percent. Slab concrete pH ranges from 9.93 at the deck surface to 10.82 at the 3-in. depth. Reinforcement section loss of upwards to 20 percent was noted at isolated areas.

The objective of this paper is to provide a report on the field performance of a 17-year-old parking structure with galvanized floor slab reinforcement.

The case study is for the Kennedy Square Parking Garage in Detroit. The parking facility, built in 1965, consists of a slab on grade and two supported levels of parking. The parking levels are located directly beneath a pedestrian plaza, complete with plantings and a wading pool. The structural system for the supported level consists of a conventionally reinforced flat slab with drop panels and circular columns. The slab has galvanized steel reinforcing bars in the top and bottom mat of slab reinforcement. Typical slab reinforcement is shown in Figure 1.

Concern with the structure developed because of observed concrete spalling and cracking. An engineering investigation into the physical condition of the parking facility was completed in June 1982. The investigation objective was to determine the physical condition of the structures and to recommend appropriate repair procedures. The scope of the work included evaluating the parking facility through

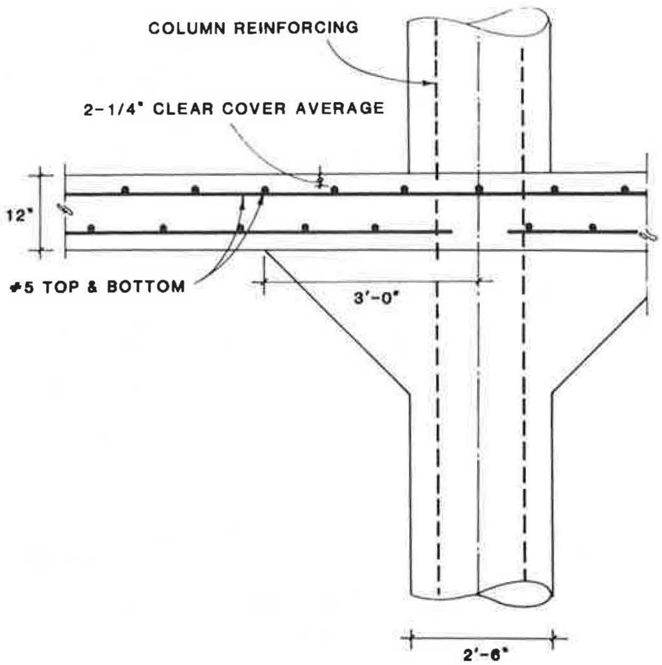

FIGURE 1 Floor slab section at column.

visual examination, nondestructive testing, and materials testing.

CONDITION APPRAISAL AND DISCUSSION

The condition appraisal of the structure was separated into three tasks: a visual examination; field surveys; and materials testing. A complete visual examination of all accessible floor slab surfaces, ramps, columns, and walls was performed. Materials testing involved chloride ion analysis, compressive strength testing, and determination of the air content of concrete. Field surveys consisted of taking pachometer readings and performing chain drag surveys.

Floor Slab Surface

Visual examination indicated that the floor slab was experiencing widespread spalling. A chain drag survey also indicated the presence of floor slab delaminations. Concrete cores were removed at selected locations to verify the chain drag survey results.

Spalls and delaminations were concentrated around columns and along column lines. The extent of surface delaminations determined were observed to range from several to hundreds of square feet and were typically 2 to 3 in. deep. Approximately 31,000 ft^2 (26 percent) of the supported floor surface was determined to be spalled or delaminated (see Figure 2, which is a field survey sheet).

Examination of the cores and open spalls indicated that much of the deterioration was caused by reinforcement corrosion. This corrosion had proceeded to the point of causing humps in the floor surface. Cores removed from the floor slab exhibited fracture planes 2 to 3 in. beneath the exposed surface. At isolated locations, 20 percent section loss of embedded reinforcing steel was observed. The most significant section loss was observed in the column capitol region.

Patterned floor slab cracking was frequently observed throughout the parking facility. The most common cracking was circumferential around the columns and radial extending out from column capitols. Random full-depth slab cracks were also frequently encountered, as were restraint cracks near perimeter walls and elevation breaks. Many of the surface cracks penetrated through the slab and caused significant salt contamination and leaching below.

Ceilings

The ceilings of this structure exhibited frequent full-depth leaking cracks, spalling, and delaminations. Delaminations ranged between 2 and 30 ft^2 in surface area and averaged between 1 and 2 in. in depth. The plaza level ceiling showed the most leaking cracks, as there are sidewalks and soil areas above. Spalls and delaminations frequently coincided with leaking construction joints or cracks.

Floor Slab Control and Construction Joints

Control and construction joints were often observed to be leaking. This contributed to corrosion of the

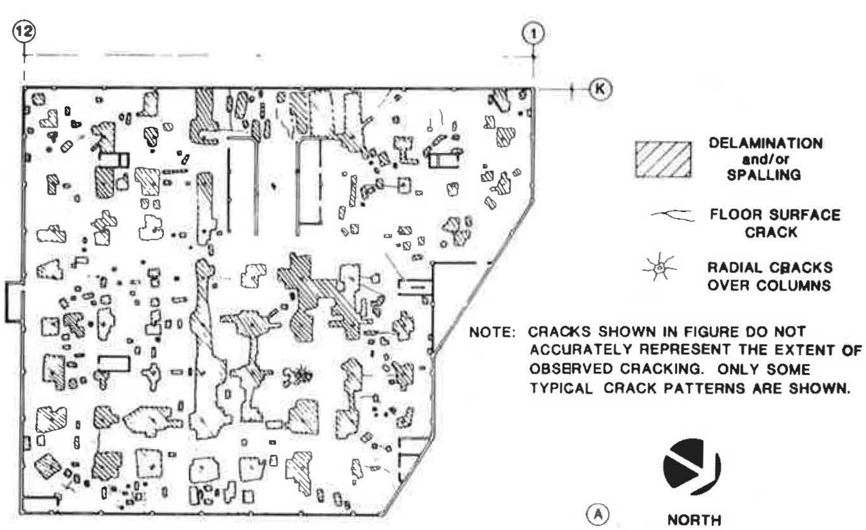

FIGURE 2 Second level plan view.

bottom mat of the floor slab reinforcement and subsequent delamination and spalling of the ceilings below. Ceiling repairs were estimated to be approximately 5 percent of the total surface area. There was no indication that these joints were previously sealed, and it is likely that normal concrete shrinkage and the lack of building expansion joints (coupled with considerable restraint from the perimeter walls) were the principle causes of crack movement and leaking.

Columns

The columns in this structure were in satisfactory condition. Occasional minor spalls and delaminations were noted above the floor surface. The columns did not appear significantly impaired, and observed spalls were usually less then several square feet in surface area and less than 2 in. deep.

RESULTS OF MATERIALS TESTING

Concrete Chloride Ion Analysis

Chloride sampling was performed at 17 locations throughout the structure. Samples were taken from random parking bays and drive lanes by using the dry (Roto hammer) sampling method. Test results indicated high concentrations of chloride within the first 3 in. of the concrete. Concentrations ranged from 25.2 lb/yd³ of concrete in the top 1 in. to 12.4 lb/yd³ of concrete at the 3-in. increment of the first supported tier.

Results from the second supported tier, or upper parking level, had somewhat lower chloride concentrations, ranging from 18.6 lb/yd³ of concrete in the top 1 in. to 8.5 lb/yd³ of concrete at the 3-in. increment. Results of chloride ion content testing are shown in Figure 3, which indicates significant chloride contamination of concrete at the level of reinforcing steel. However, the corrosion threshold level for galvanized reinforcement is not known. For plain black steel the threshold level is indicated to be 1.1 to 1.6 lb/yd³ of concrete (1).

For cover measurements, pachometer readings were taken at 30 locations on each supported tier. Clear cover measured over the top reinforcing steel mat ranged from approximately 1.25 to 4 in. and the average concrete cover was determined to be approximately 2.25 in.

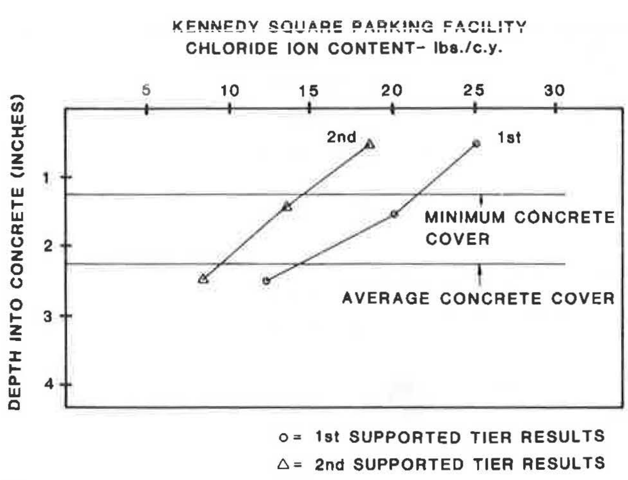

FIGURE 3 Chloride ion content versus depth into concrete.

Concrete Compressive Strength Testing

Compressive strength tests were performed on eight concrete core samples. Core compressive strengths ranged from approximately 4,500 to 6,600 psi. The average compressive strength, approximately 5,700 psi, was greater than the 3,000-psi specified design strength.

Determination of Air Content of Concrete

A microscopic examination of concrete core samples was performed to determine the air void characteristics of the concrete in accordance with ASTM C 457-80. Results of the examination indicated that the average air content of the concrete was approximately 2 to 3 percent. This value is significantly below the acceptable range of 4 to 8 percent, which indicates that the concrete is only marginally durable against freeze-thaw exposure in the presence of deicing agents.

This deck, however, is partly protected from rapid freeze-thaw cycling by its earth containment (underground design). Scaling was not observed to be a significant deterioration mechanism, as the floor surface exhibited only isolated surface erosion from freeze-thaw action.

During the microscopic examination a cursory inspection of the polished section of concrete revealed the presence of a gel formation, which suggested the possibility of alkali-aggregate reactivity. Further tests to confirm the presence of alkali-aggregate reactivity were recommended but have not been performed.

pH Testing

Concrete powder samples were collected from the floor slab and subjected to pH testing. Samples were extracted incrementally beginning at the surface and stopping at 3 in. One-inch increments were obtained to allow pH determination as a function of depth.

Test results indicated the average pH of the concrete to be 9.83 at the surface increment and 10.82 at the third increment. These values are considered lower than would be anticipated for conventional concrete, which is typically 12.5 or more. Values lower than 11.5 are believed to create a corrosive environment, even without the presence of chloride (2). It is further evident that the effect of high chlorides in low pH concrete would cause an unusually harsh and aggressive environment, given the presence of moisture and oxygen (3).

CONDITION APPRAISAL CONCLUSIONS

Based on visual observations, materials testing, and nondestructive tests performed, observed concrete deterioration was determined to be primarily caused by corrosion of embedded steel reinforcement. Materials tests indicated that corrosion of steel could be attributed to the high chloride content of the concrete at the level of embedded steel reinforcement and low concrete pH. It is evident that concrete delamination and subsequent spalling are progressive and will continue to seriously affect the existing structural integrity and serviceability of the parking facility.

Although further recommended petrographic examination was not performed, it is the authors' opinion that the presence of alkali-silica gel was probably caused by localized reactions in the open cracks. Evaluation of crack patterns observed in the structure suggests that cracking is probably a result of restraint and normal concrete shrinkage. Close examination of core crack pattern and characteristics failed to detect evidence of polygonal cracking, which is considered typical when alkali-silica reactions are a predominant deterioration mechanism. Thus it is not believed that alkali-silica reaction is a serious problem in the subject structure.

DISCUSSION OF RESULTS

There is considerable controversy concerning the advantages of using galvanized reinforcement in concrete slabs exposed to harsh environments such as bridges, decks, parking structures, or marine structures. Some researchers have maintained that zinc provides adequate corrosion protection for the reinforcing steel embedded in concrete slabs exposed to periodic deicer or seawater exposure.

Several laboratory and field studies have been performed in connection with galvanized reinforcement in concrete (4-6). The studies frequently contradict one another, and evaluation of data generally results in differing opinions regarding measurable and anticipated performance of galvanized reinforcements. Some studies indicate that under conditions of high chloride concentrations at the embedded steel, substantial corrosion of zinc can occur, followed by corrosion of steel (7,8).

A meaningful estimate of long-term performance can only be obtained by actual field evaluation of structures constructed with galvanized reinforcement. To date, several long-term studies related to bridge decks have been performed (4), but none related to galvanized reinforcement in parking decks has been reported.

During investigations of similar facilities with conventionally reinforced uncoated reinforcing bars, approximately equivalent deterioration was recorded during the 12th year of service. This suggests that the galvanized coating delayed the corrosion initiation by roughly 5 years when compared to black steel.

It is generally agreed that significant study would be required before implementation of remedial actions to restore the structure. Candidate systems identified for study and possible use at the subject facility are special concrete overlays, both conventional and polymeric; polymer impregnation by deep grooving; and traffic bearing membranes.

SUMMARY AND CONCLUSIONS

The condition appraisal of Kennedy Square Parking Garage represents a long-term performance of galvanized reinforcement in parking decks. Results of the evaluation indicate that although galvanized reinforcement was used, floor slab spalling and delamination are widespread. The field condition appraisal consisted of visual examination, chain drag delamination survey, determination of chloride content of concrete, determination of air void characteristics of the concrete, and compressive strength of core samples.

Although various laboratory and field studies elsewhere may suggest the beneficial effects of zinc in reducing reinforcement corrosion, the condition appraisal of the Kennedy Square Parking Garage indicates that concrete slabs under long-term exposure to chloride salts have deteriorated because of corrosion of galvanized reinforcement. Extensive corrosion of zinc has occurred, followed by corrosion of steel. Although chloride concentrations around embedded steel are somewhat higher than may be considered typical for bridge decks, they are not considered abnormally high.

Restoration of the subject parking facility has been delayed because of budget considerations, but interim measures are being taken to maintain structure serviceability. Periodic maintenance is being performed along with regular monitoring, inspections, and testing. The restoration alternatives are being evaluated carefully to ensure that the most cost-effective solution is selected when restoration proceeds.

REFERENCES

1. K.C. Clear. Time-to-Corrosion of Reinforcing Steel in Concrete Slabs--Volume 3: Performance After 830 Daily Salting Applications. Report FHWA-RD-76-70. FHWA, U.S. Department of Transportation, 1976, 59 pp.
2. B. Erlin and G. Verbeck. Corrosion of Metals in Concrete--Needed Research. In Report ACI SP 49, American Concrete Institute, Detroit, 1975, pp. 39-46.
3. G. Verbeck. Mechanism of Corrosion of Steel in Concrete. In Report ACI SP 49, American Concrete Institute, Detroit, 1975, pp. 21-38.
4. D. Stark. Evaluation of the Performance of Galvanized Reinforcement in Concrete Bridge Decks. Final Report, Project ZE-320. International Lead Zinc Research Organization, Inc., New York, May 1982.
5. A.B. Triple, Jr., E.L. White, F.H. Haynie, and W.K. Boyd. Methods for Reducing Corrosion of Reinforcing Steel. NCHRP Report 23. HRB, National Research Council, Washington, D.C., 1966, 22 pp.
6. A.P. Crane. Corrosion of Reinforcement in Concrete Construction. Presented at Meeting on Corrosion of Reinforcement in Concrete Construction, London, England, June 13-15, 1983, pp. 407-418.
7. T.E. Backstrom. Use of Coating on Steel Embedded in Concrete. ACI Publication SP-49-9. American Concrete Institute, Detroit, 1975, pp. 103-110.
8. Durability of Concrete Bridge Decks. NCHRP Synthesis of Highway Practice 57. TRB, National Research Council, Washington, D.C., May 1979, 61 pp.

Publication of this paper sponsored by Committee on Corrosion.

Abridgment

Field Evaluation of Oil- and Gas-Produced Brines as Highway Deicing Agents

RONALD W. ECK and WILLIAM A. SACK

ABSTRACT

Field tests conducted as part of a project to assess the potential of West Virginia waste oil and gas field brines for highway deicing purposes are discussed. Brine characteristics and current disposal practices are reviewed along with published accounts of brine use. A detailed discussion of the field test program is presented, including an analysis of the brine used, descriptions of the high pressure brine applicator unit, the test sites, brine storage, and a description of the methodology used on a typical application run. Results of eight test runs indicated that waste brines were effective deicing agents over a wide variety of weather and pavement conditions. Bare pavement was achieved rapidly with both high pressure and gravity application, even at temperatures as low as 15°F, because of the significant amounts of calcium in the brine. Skid-resistance measurements, made by using a portable tester, showed a substantial increase in pavement skid resistance after brine application. Refreezing was not found to be a significant problem. Study of the impacts of natural brines on construction materials and on the environment as well as the economics of storage and handling is also under way as part of the overall project.

Under the constraints of environmental problems and tight operating budgets, highway agencies are seeking ways to minimize the use of deicing chemicals. One approach is the use of naturally occurring salt brines that are a waste product of oil and gas production. As a liquid, brine has the advantages of being fast acting and does not blow or bounce off the road. Use of natural brine for deicing purposes could solve several problems simultaneously. The oil and gas industry would be able to dispose of an unwanted by-product and highway agencies could acquire a deicing material at minimal cost. Furthermore, the natural brine that is used would be applied at controlled rates rather than discharged directly to the environment, as is currently done in some regions.

Before advocating a major natural brine deicing program, there are a number of issues that should be evaluated. For example, the quantity of brine available for highway deicing in a given geographical region must be assessed. Transportation and storage costs must be estimated. Brine quality from the major producing formations must be determined, including both the major salts and the minor trace elements. It would be desirable to compare brines with commercial deicing agents relative to melting, skid resistance, refreezing of roadway surfaces, and effects on transportation materials. A comprehensive research project is in progress at West Virginia University to address these issues. In this paper the field tests conducted during the winter of 1981-1982 are discussed.

BACKGROUND

Naturally occurring salt brines may be thought of as connate or entrapped sea water. Brines are often associated with oil and gas deposits and are brought to the surface during production as a by-product. The quantity of brine produced or separated from the oil or gas varies greatly with the type of formation, age of the well, and how the field is managed. Production of brine from gas and oil wells may range from negligible amounts to more than 30 gal per thousand cubic feet of gas and to more than 50 gal per barrel (42 gal) of oil.

The major constituents of sea water and some typical brines are given in Table 1 (1). A number of trace constituents such as barium, strontium, lead, and zinc will also be found in most brines. Brines tend to increase in concentration with depth, but a brine taken from a given formation and location will usually be relatively constant in concentration with time.

Brine disposal is a significant and costly problem for oil and gas producers. The high concentration of dissolved salts found in brines and the large volumes involved present the potential for serious and long-term contamination of groundwa-

TABLE 1 Analyses of Natural Brines (mg/L)

State	Formation	Chloride	Sulfate	Bicarbonate	Sodium	Calcium	Magnesium	Total[a]
	Ocean waters (mean)	19,410	2,700	-	10,710	420	1,300	34,540
Michigan	Dundee Limestone	161,200	155	60	66,280	25,740	4,670	258,105
Oklahoma	Wilcox Sand	89,990	515	65	44,020	9,460	1,990	146,040
Oklahoma	Arbuckle Limestone	101,715	120	60	50,345	10,160	2,120	164,520
Kansas	Hunton Limestone	76,797	207	61	40,284	5,440	1,790	124,579
Pennsylvania	Oriskany Sandstone	169,000	0	-	57,100	35,900	3,510	265,510
Ohio	Clinton Sand	154,000	524	23	52,300	37,200	5,090	249,137
West Virginia	Chemung[b]	134,720	-	-	59,800	23,180	3,014	220,715
West Virginia	Oriskany[b]	181,050	-	-	75,860	54,820	3,276	315,006

Note: Data adopted in part from Miller (1).

[a]Total for constituents shown.
[b]Analyzed and used during this study.

ters. The preferred method of brine disposal today is injection into the formation of origin or another formation. However, although underground disposal is quite feasible is some regions, there are significant limitations on the use of this method in many sections of the country.

Natural brines have been used as deicing agents for many years; some of the published accounts date back to the 1950s (2,3). A number of state, county, and local highway agencies (especially in New York, Pennsylvania, and Michigan) have used or are using natural brine deicers; but most experiences have not been reported in the literature. It appears that no comprehensive evaluation has been conducted on the use of natural brines for highway deicing.

FIELD TEST PROGRAM

A portable hydrodynamic brine applicator system designed by the Connecticut Department of Transportation for application of brine at 300 psi was acquired through the FHWA. A complete description of this system has been prepared by Pickett and Carney (4). The unit was mounted on a 9-ton dump-body truck obtained from the West Virginia Department of Highways.

Spraying was carried out on campus roadways designated by the West Virginia University (WVU) Physical Plant. The roads designated initially were low-volume roadways situated away from the main campuses of the University. They are characterized by relatively narrow pavements, sharp horizontal curvature, and short length. All sites had bituminous wearing surfaces. Truck speeds on these roads were extremely low because of the short roadway length and restricted geometry. Low speed, in combination with the starting and stopping associated with the short length, resulted in high brine application rates. As the field study continued and the effectiveness of brine as a deicer and the reliability of the spray unit were demonstrated, the investigators were given responsibility for treating some of the more important campus roads. The higher speeds attainable on these routes resulted in more realistic brine application rates.

Brine used (see Table 1) in the field study was produced from gas wells in West Virginia and was obtained free of charge. Deliveries of brine were made throughout the winter to several types of aboveground closed steel storage tanks located on the WVU campus. All tanks were made of carbon steel and had been previously used for other purposes.

DESCRIPTION OF APPLICATION AND EVALUATION PROTOCOL

Each time snow removal or ice control efforts were initiated, the spray unit was driven to the brine storage facilities on campus for filling. The truck and spray unit were weighed before and after brine application to determine the amount of brine applied. During the runs a passenger in the truck used a stopwatch to measure application times. Another individual was outside the vehicle collecting snow and runoff samples both before and after application, and taking temperature measurements and photographs.

The British portable tester device was used to collect limited skid-resistance data. The British pendulum number (BPN) values obtained on snow-covered pavements in this study were not used as measures of pavement skid resistance but rather were used to indicate whether the deicing agent had been successful in breaking the bond between the pavement and the snowpack (the higher the BPN, the greater the frictional resistance). For this reason, the authors caution that the readings obtained in this study should not be compared with other wet pavement BPN values.

SUMMARY OF RESULTS

As the field testing progressed, it was observed that corrosion products from the steel spray bar tended to plug the spray nozzle openings (0.08-in. diameter), which resulted in reduced sprayer effectiveness and required periodic cleaning of nozzles. In addition, it was believed that the high initial cost of the spray unit coupled with potential maintenance problems associated with the high pressure system might reduce the attractiveness of the unit. Therefore, the unit was converted to essentially a gravity flow unit by removing every other nozzle from the spray bar for the last two runs of the season.

As indicated by the data in Table 2, eight field runs were made. The brines were generally effective in melting snow and ice and achieving bare pavement within a relatively short period of time. Only two test runs (runs 7 and 8) were made by using the

TABLE 2 Summary of Field Test Results of WVU Campus Roadways

Run No.	Date	Temperature (°F)	Snow Depth (in.)	Roadway Cover Type	Mode of Delivery	Brine Source	Sites Treated[a]	Avg Speed (mph)	TDS (lb) per TLM[b]	Comments
1	12/17/81	28-30	1-2	Loose snow	Pressure	Chemung	ER, H, A, L, D	–	697	Produced bare pavement quickly
2	1/9/82	14-17	2	Loose snow	Pressure	Chemung	ER, SB, H, A, D, L	4-10	1,480	Better melt-off than campus roads treated with dry salt; SB road became bare after treatment as it received traffic; temperature fell rapidly throughout period
3	1/16/82	28-31	1.25-2	Loose snow	Pressure	Chemung	ER, FB, H, A	<6	1,693	Rapid melt-off; bare pavement
4	1/25/82	16-22	3-4	Packed snow	Pressure	Chemung	SB, EC, ER, MC, PP	11.5-15	355	Bare pavement achieved; good melt-off
5	2/11/82	17-19	3-4	Packed snow and ice	Pressure	Oriskany	ER	10.6	1,422	Melt-off slower because of low temperature and packed ice
6	2/13/82	21-25	2-2.25	Loose snow	Pressure	Oriskany	ER, FB, EC, PP, C	4-10.3	1,750	Excellent, rapid melt-off, some traffic, partial plowing
7	3/3/82	25	1	Packed snow and ice	Gravity	Oriskany	PP	12.0	534	Rapid melt-off; bare pavement
8	4/6/82	26-30	0.5-1	Packed snow	Gravity	Chemung	EC	7.4	506	Good melt-off

[a] Site key: EC = Evansdale Campus, MC = Medical Center, FB = Facilities Building, ER = Engineering (rear), H = Horticultural Farm, A = Airport, L = Livestock Farm, D = Dairy Farm, SB = Stadium Bypass, PP = Physical Plant (access road), and C = Coliseum.
[b] Pounds of total dissolved solids (TDS) per two lane mile (TLM) of highway.

gravity application. Under the conditions present, gravity application appeared to be as effective as the high-pressure spray in achieving melt-off. A discussion of the runs in which skid-resistance data were collected is presented in the following paragraphs.

No response could be made to a snowstorm on February 9, 1982, because of being temporarily out of brine. Two days later the Engineering Road site was still covered with a slippery ice pack (BPN = 29.2) because Physical Plant crews had not treated the road. It was decided to treat the road (run 5) with two applications of brine.

Skid-resistance data and color photographs were acquired roughly 1, 3, and 24 hr after brine application. Within 0.5 hr, under light traffic conditions, the surface of the ice pack became mealy in texture. One hour after application darkened wheel tracks appeared (BPN = 35.4). At this point the sun came out and speeded up the melting process. Within 3 hr the pavement was basically wet (BPN = 69.4); after 5 hr the pavement was beginning to dry off. The next morning the humidity was high with temperatures in the mid-teens. There were some areas of refreezing in low spots on the pavement, but the main wheel paths were dry (BPN = 90.4).

Another snowstorm 2 days later provided an opportunity to acquire additional data at the Engineering Road site (run 6). Part of the road was left untreated to provide a comparison with the section receiving brine application. BPN values for the before condition were in the low 30s for both sites. One application of brine was made; snow continued to fall for another 1.5 hr. After 3 hr clouds broke up and some solar radiation was noticeable. Under light traffic conditions the wheel paths of the treated section became mainly clear, with a small amount of slush present. The BPN value had almost doubled to 63.8. The untreated section had packed snow in the wheel paths; the BPN value had increased only slightly to 36.6.

Brine application rates for each run are also provided in Table 2. In practice, typical salt (sodium chloride) application rates range from 300 to 700 lb per two-lane mile (TLM). In order to compare the application rate of brine to conventional deicing agents, brine strength may be expressed as total dissolved solids (TDS), which includes all the salts or dissolved solids in the brine. Thus the weight of TDS in natural brines is comparable to the weight of dry salt used in conventional deicing operations. The data in Table 2 indicate that brine application rates during the eight field test runs varied from 355 to 1,750 lb TDS per TLM (203 to 967 gal per TLM).

The high application rates used in some of the runs are not typical of the amount of salt that would be required in a full-scale brine application program. Deicing applications were initially carried out on short, low-volume roadways, which resulted in low average truck speeds. Another factor contributing to high brine use on certain runs was operator inexperience. As the winter progressed, deicing was also carried out on some higher type and longer roadways, thus allowing higher average truck speeds and reduced application rates.

As expected, traffic load and packing of snow also influenced application rates. The runs with the lowest brine application rates (runs 4, 7, and 8) were made principally on roads with higher traffic volumes and packed snow. Loose snow resulting from lack of plowing or little traffic tends to absorb brine, thereby considerably reducing its effectiveness just as would occur with use of rock salt.

CONCLUSIONS AND RECOMMENDATIONS

Results of field testing have demonstrated that waste oil and gas field brines are effective deicing agents over a wide variety of weather and pavement conditions. It was found that visible melting began to occur almost immediately after application, and bare pavement was achieved rapidly, even at temperatures of 15°F on low-volume roadways. The effectiveness of the brines at low temperatures may be attributed to the fact that the brines used contained significant amounts of calcium as well as sodium salts (see Table 1).

Skid-resistance measurements at various times after brine application indicated a substantial increase in pavement skid resistance. Refreezing was not found to be a significant problem. It would be desirable to perform similar tests under comparable conditions by using rock salt as a deicing agent.

Both simple gravity and high-pressure spray application of the brine achieved rapid melt-off and bare pavement. Based on the satisfactory results obtained with gravity application, it is recommended that additional field application of brine be carried out using this method. The increased simplicity and lower equipment and maintenance costs associated with gravity application appear to make this method attractive.

Brine was stored in aboveground steel tanks during the course of this work, as is common in the oil and gas industry. No problems were encountered with this method of storage, although other types of storage containers (such as fiberglass) are being evaluated.

Based on the results of the research thus far, use of by-product brines from the oil and gas industry appears to offer an effective and potentially cost-effective means of highway deicing. It is recommended that additional field testing be carried out on more typical higher type roadways with higher volumes by using the gravity mode of application.

ACKNOWLEDGMENT

The data in this paper are based on research sponsored by the West Virginia Department of Highways in cooperation with the FHWA, U.S. Department of Transportation. Special thanks are extended to Carmen Romano and Ali Atefi for their assistance. The cooperation of West Virginia University Physical Plant personnel is greatly appreciated.

REFERENCES

1. D W. Miller, ed. Waste Disposal Effects on Ground Water. Premier Press, Berkeley, Calif., 1980, pp. 294-321.
2. H.E. Stafseth. Liquid Chemicals for Ice Control. Public Works, Vol. 89, No. 5, May 1958, pp. 91-93.
3. J.O. Kyser. Brine Solution Removes Stubborn Ice. Public Works, Vol. 102, No. 1, Jan. 1971, pp. 67-68, 89.
4. M.A. Pickett and J.F. Carney III. Portable Hydrodynamic Brine Roadway Deicer System. In Transportation Research Record 833, TRB, National Research Council, Washington, D.C., 1981, pp. 30-32.

Publication of this paper sponsored by Committee on Winter Maintenance.